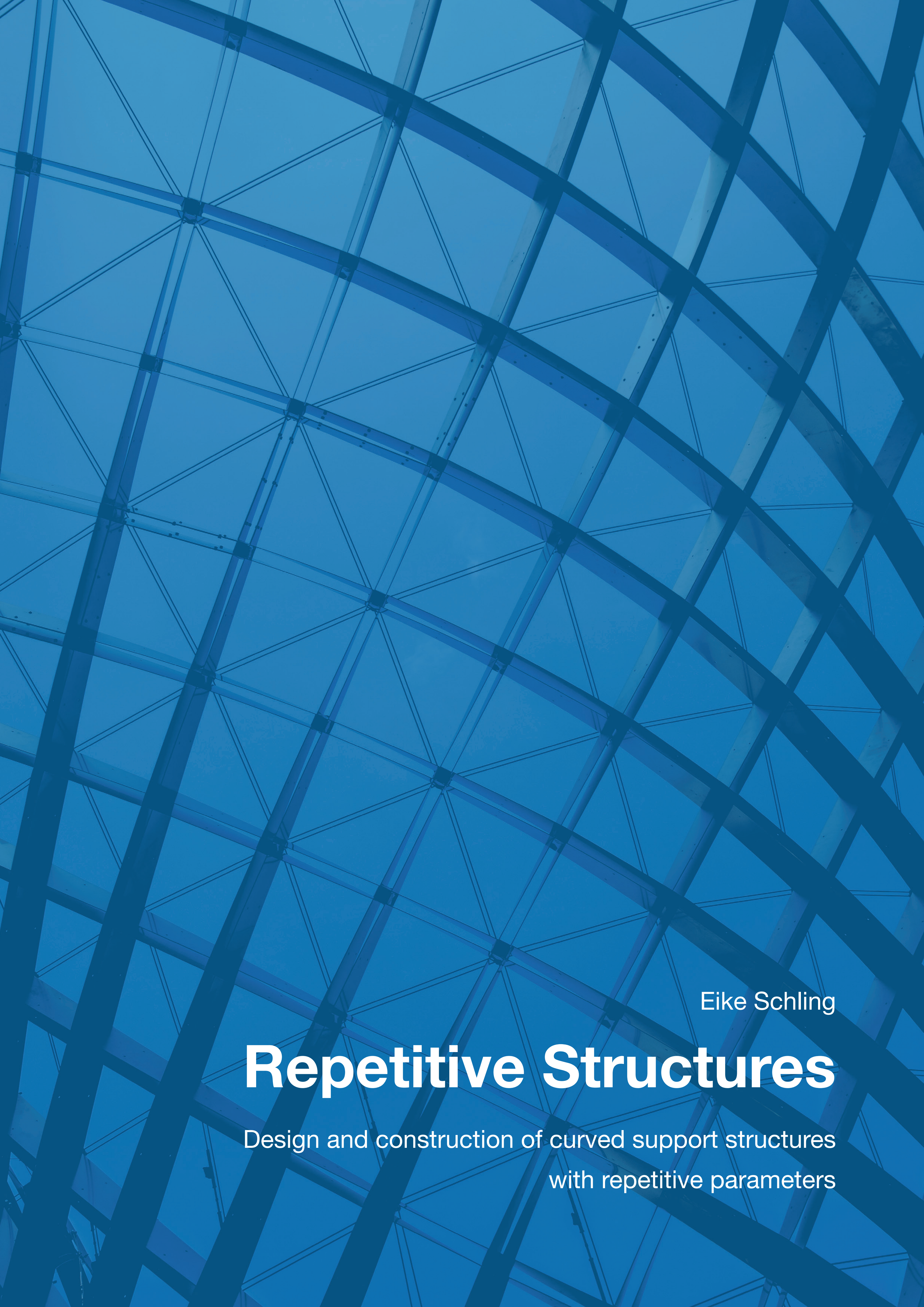

Eike Schling

Repetitive Structures

Design and construction of curved support structures with repetitive parameters

Eike Schling

Repetitive Structures

Design and construction of curved support structures
with repetitive parameters

Technische Universität München
Fakultät für Architektur
Lehrstuhl für Tragwerksplanung
Prof. Dr.-Ing. Rainer Barthel

Arcisstraße 21
80333 München

www.lt.ar.tum.de

Eike Schling
Repetitive Structures
Design and construction of curved support structures with repetitive parameters

München, November 2018

DOI: 10.14459/2018md1449869
ISBN: 978-3-938660-39-3

Cover page
Structural grid of the Asymptotic Gridshell
*Image: **ES 2018** based on **Felix Noe 2017***

Lehrstuhl für Tragwerksplanung
Fakultät für Architektur
Technische Universität München

Eike Schling

Repetitive Structures

Design and construction of curved support structures with repetitive parameters

Vollständiger Abdruck der von der Fakultät für Architektur der Technischen Universität München zur Erlangung des akademischen Grades eines Doktor-Ingenieurs genehmigten Dissertation.

Vorsitzender:
Prof. Dipl.-Ing. Florian Musso

Prüfer der Dissertation:
1. Prof. Dr.-Ing. Rainer Barthel
2. Prof. Dr. Helmut Pottmann

Die Dissertation wurde am 09.08.2018 bei der Technischen Universität München eingereicht
und durch die Fakultät für Architektur am 08.10.2018 angenommen.

Schalen sind auf natürliche Weise schön und effizient, weil die fließende und doppelt gekrümmte Form Lasten ohne Biegung, nur in der Fläche, also nur über Zug- und Druckkräfte fortleiten kann. Sie brauchen daher bedeutend weniger Material als biegebeanspruchte, ebene Tragwerke, beispielsweise Träger oder Platten.

Es besteht aber ein Gegensatz zwischen günstigem Tragverhalten und schwieriger, da doppelt gekrümmter Herstellung. Die Lösung dieses Gegensatzes ist eine wichtige Voraussetzung für den erfolgreichen Schalenbau.

Hans Schober, 2016

Shells are naturally beautiful and efficient. Their continuous, doubly curved shape is able to carry loads without bending, by only using tension and compression forces within the surface. Because of this behaviour, shells need substantially less material than flat structures, such as beams or plates, which require bending.

There is, however, a contradiction between the beneficial load-bearing behaviour and the highly complex fabrication of doubly curved structures. Resolving this contradiction is an important requirement to successfully construct shells.

Hans Schober, 2016

Zusammenfassung

Die vorliegende Arbeit untersucht zweifach gekrümmte Gitterstrukturen, mit dem Ziel deren Herstellung zu vereinfachen. Dafür werden Netzwerke mit konstanten geometrischen Parametern beschrieben, und die damit verbundenen Möglichkeiten für Entwurf und Konstruktion erarbeitet.

Es wird eine ganzheitliche Theorie „Repetitiver Strukturen“ unter Berücksichtigung geometrischer und konstruktiver Kriterien vorgelegt, die es ermöglicht die Verwendung gleicher Bauteile anhand einzelner Parameter zu untersuchen. Auf diese Weise werden Zusammenhänge von Form und Struktur aufgedeckt und eine neue Methode für den Entwurf und die Konstruktion elastisch geformter Gitterschalen entwickelt.
Die Arbeit verbindet Theorien der Differentialgeometrie mit Erfahrungen aus Architektur und Bauingenieurwesen und schafft dadurch neue Erkenntnisse für den modernen Schalenbau.

Auf der Grundlage eines kurzen Überblicks zum Stand der Forschung werden die theoretischen Rahmenbedingungen zur Analyse und Gestaltung Repetitiver Strukturen geschaffen. Diese werden zunächst auf bestehende Konstruktionen angewendet. Hieraus wird eine Übersicht über bestehende und zukünftige Möglichkeiten der Parameterwiederholung abgeleitet. Die Wechselwirkungen zwischen Fläche, Netzwerk und Parametern werden durch induktiven Studien dargestellt. Anhand experimenteller Entwürfe wird dann die elastische Verformung von Bauteilen als Konstruktionsstrategie untersucht.

In einer deduktiven Studie werden die Krümmungseigenschaften von Gitterstrukturen in direkte Beziehung mit der elastischen Verformung der Gitterstäbe gebracht. Auf Basis dieser Abhängigkeiten wird eine Entwurfsmethode entwickelt, die sich die Eigenschaften asymptotischer Kurven auf Minimalflächen zunutze macht. Diese Methode ermöglicht eine Konstruktion zweifach gekrümmter Gitter mit geraden Lamellen und rechtwinkligen Knoten.

Schließlich wird die Theorie in einem architektonischen Projekt angewendet: Anhand des Forschungspavillons „Asymptotic Gridshell“ werden die Herausforderungen und Potentiale repetitiver Strukturen für den Planungsprozess, das Tragverhalten und den Bauablauf einer elastisch geformten Gitterschale aufgezeigt.

Abstract

This thesis investigates doubly curved grid structures with the goal to simplify their fabrication. For this purpose, we examine networks with constant geometric parameters, and describe their potentials for design and construction.

A holistic theory of “repetitive structures” is established, which takes into account both geometric and constructive criteria. This allows us to investigate individual parameters in order to create identical building parts. The theory is used to uncover principles of form and structure, and develop a novel method to design and construct elastically formed gridshells.
The work combines theories from differential geometry with knowledge from architecture and structural engineering and thus gains new insights for modern shell design.

Based on a review of scientific publications and built examples, a theoretical framework is created to analyse and design repetitive structures. First, we apply this theory to existing structures, and generate an overview of current and future possibilities of parameter repetition. Next, we investigate the interdependence between surface, network and parameters within inductive studies. Through the prototypical design and fabrication of experimental structures, we examine the elastic deformation of building parts as a constructive strategy to achieve repetition.

In a deductive study, the parameters of curvature are related to the deformation behaviour of individual beams. Based on this dependency, a design method is developed, which utilizes the properties of asymptotic curves on a minimal surface. This method provides the geometric condition to construct a doubly curved grid from exclusively straight lamellas and orthogonal nodes.

Finally, the method is implemented in an architectural case study:
The practical challenges and advantages of repetitive structures are experienced through the planning process, the construction progress, and the load-bearing behaviour of the “Asymptotic Gridshell”.

Acknowlegements

This thesis was developed between 2015 and 2018 where I was engaged in research and teaching at the Chair of Structural Design at the Technical University of Munich.

To my supervisor, Prof. Dr.-Ing. Rainer Barthel, I would like to express my sincere gratitude for his guidance and critical feedback throughout my research. His experience and openness led to the interdisciplinary character of my work. His generosity and trust have been of substantial importance to the development of the Asymptotic Gridshell and the completion of my thesis.

I also want to extend my genuine appreciation to my co-advisor, Prof. Dr. Helmut Pottmann, for his patience and dedication in answering every last question on differential geometry. His profound knowledge and architectural interest have nourished this fruitful and ongoing collaboration in the field of Architectural Geometry.

To my mentor, Prof. Dr.-Ing. Lars Schiemann, I would like to express thanks for his enthusiasm and conviction. It was he who encouraged me to pursue my interest in repetitive structures and understand its overarching relevance on architectural design and structure.

I would like to acknowledge Prof. Dr. Alain Thierstein for his relevant and positive feedback on methodology which strengthened the scientific foundations of this work.

I thank my colleagues at the Chair of Structural Design for their support and sympathy even during the most unsociable months of my dissertation. I'd specifically like to thank Jonas Schikore and Joram Tutsch for the countless intense and inspiring discussions on the structural behavior of strained gridshells. The FE simulations conducted by Jonas Schikore were crucial in understanding and validating the load-bearing behavior of our prototypical structures. Similarly, I would like to thank Martin Kilian at the Institute for Discrete Mathematics and Geometry in Vienna for his collaboration and support.

I am especially grateful to Denis Hitrec who started as a student in my course on gridshells and continued to be an irreplaceable partner in developing the computational workflow and design of our asymptotic structures. The completion of the Asymptotic Gridshell would not have been possible without him and the additional help of students like Andrea Schmidt, Viktor Späth, Miquel Lloret Garcia and Maximilian Gemsjäger who showed tireless dedication throughout the four weeks of construction.

In this context I would like to thank Thomas Brandl and Harry Siebendritt, and the construction team of the Brandl Steel Construction Company in

Eitensheim. Their enthusiasm for trying out new construction methods and their generous support in assembling the Asymptotic Gridshell have been tremendous. I am similarly grateful to Matthias Müller, metalsmith at the Technisches Zentrum, TUM, whose educational talent and inventions played a substantial role in developing and fabricating this novel steel structure. I would also like to thank André Ihde and his colleagues at Pfeifer in Memmingen for their support in tailoring the steel cables.

Furthermore, I thank the geometry experts at Evolute GmbH in Vienna, especially Alex Schiftner, for supplying their software and technical support. The same appreciation goes to Benedikt Philipp and Anna Bauer from the Chair of Structural Analysis, Prof. Dr.-Ing. K.-U. Bletzinger, who developed and supplied the TeDa Plugin and thus enabled an accurate modelling of NURBS minimal surfaces.

I want to express my deep appreciation of the financial support given to us by the Department of Architecture at the TUM. The Dr. Marschall Stiftung as well as the Leonhard-Lorenz-Stiftung have contributed greatly in financing both prototypes and Gridshell materials. I especially thank Gerhard Schubert and his colleagues at the Architectural Research Incubator / ARI who have continuously promoted my research through media, network and financial support.

I would like to thank Hans Schober, Jürgen Hennicke, Alexander Schiftner and Dieter Ströbel for supplying the geometry of their extraordinary gridshells.

My search for a simplification of freeform structures originated during my time at PLP Architecture in London between 2009 – 2012. I was responsible for the digital planning of complex façade structures, and profited greatly from my close collaboration with Lars Hesselgren, who continously inspired me to take on new challenges.

I would like to thank my parents, especially my mother and stepfather, for their academic consultation and confidence in my work.

Finally, my deepest gratitude goes to my wife, Cat, for her consistent love and encouragement during this endeavor. Beyond her endless patience and family support, she has contributed to my scientific process from the very beginning through intellectual discussions, and has helped to finalize this thesis through nightly editing sessions. Last but not least, I would like to thank my three daughters, Mona, Lucie and Selma, who have been an ever-optimistic part of this journey through their unrivalled excitement for all my built structures.

Eike Schling
Munich, August 2018

Contents

Nomenclature

Geometric

k_1 Maximum principal curvature [m^{-1}]
k_2 Minimum principal curvature [m^{-1}]
K Gaussian curvature: $K = k_1 \cdot k_2$ [m^{-2}]
H Mean curvature: $H = (k_1 + k_2) / 2$ [m^{-1}]

A Area of a face [m^2]
S Qualitative shape of a face

P Planarity of a mesh face [m]
l Length of an edge [m]
c Continuity of a curve [°]
d Proximity of a network to a target surface [m]
d Seam variance measuring the tolerance between panels [m]

k Curvature of a spatial curve [m^{-1}]
τ Torsion of a spatial curve [m^{-1}]
τ_g Geodesic torsion of a surface curve [m^{-1}]
k_n Normal curvature of a surface curve [m^{-1}]
k_g Geodesic curvature of a surface curve [m^{-1}]

ϕ_e Orientation vector of an edge curve

t Tangent vector of a curve
n Normal vector of a surface
u Sideways vector of a surface curve
r Vector of a surface ruling

ω Mesh angle at a node [°]
ι Intersection angle at a node [°]

α Normal angle at a node [°]
β Geodesic angle at a node [°]
γ Torsional angle at a node [°]

μ Angle of deviation from the principal curvature direction [°]

o Offset distance of two parallel surfaces [m]
o_n Node offset [m]
o_e Edge offset [m]
o_f Face offset [m]

Mechanic

t Thickness of a profile [mm]
h Height of a profile [mm]
g Mass density [g/cm³]

x Longitudinal orientation of a beam
y Lateral orientation of a beam
z Vertical orientation of a beam

κ_x Curvature (twist) due to torsion around the x-axis [m^{-1}]
κ_y Curvature due to bending of a beam around the y-axis [m^{-1}]
κ_z Curvature due to bending of a beam around the z-axis [m^{-1}]

θ Angle of rotation of a twisted beam [rad]

M_T Torsional moment around the x-axis [Nmm]
M_y Bending moment around the y-axis [Nmm]
M_z Bending moment around the z-axis [Nmm]

I_T Torsional constant [mm^4]
I_y Moment of inertia with respect to the y-axis [mm^4]
I_z Moment of inertia with respect to the z-axis [mm^4]

i_p Polar radius of gyration [mm^4]

W_T Section modulus of torsion [mm^3]
W_Y Section modulus with respect to the y-axis [mm^3]
W_Z Section modulus with respect to the z-axis [mm^3]

E Young's modulus [N/mm^2]
G Shear modulus [N/mm^2]

f_y Yield strength [N/mm^2]
$\sigma_{y,k}$ Normal yield stress: $\sigma_{y,k} = f_y \cdot 1.0$ [N/mm^2]
$\tau_{y,k}$ Shear yield stress: $\tau_{y,k} = f_y \cdot \sqrt{3}$ [N/mm^2]

ε_H Strain due to Helix Torsion
c_ε Shift of the parabolic distribution of normal stress due to Helix Torsion

Introduction

Objective

Throughout the history of architecture, the use of repetitive building parts has been a key goal to simplify fabrication, ease construction, and save costs and time. This may be achieved by laying identical bricks or using identical ball joints, dividing a sphere into congruent triangles or rationalizing a curved façade to only use planar glass panels. In any case, using repetitive parts inevitably effects the overall shape or layout of a structure.

There is a multitude of scientific studies and built examples which achieve repetition within double-curved structures. In geometry the term “repetitive” is used to describe congruent elements, such as nodes, edges or faces, within a network, while an architectural structure aims at identical building parts. These two perceptions do not always coincide: In practice, adjustable joints, tolerances or deformation allow the use of repetitive parts, even for a geometrically non-repetitive element.

The following work combines insights from mathematics and engineering to create a holistic theory of “repetitive structures” considering both the geometric and constructive parameters. This theory does not only offer an analysis of existing structures and a definition of strategies to achieve repetition. It is also used to systematically investigate the morphology of repetitive networks, define parametric relationships, identify fundamental principles of form and deduce parameter combinations for future designs.

A great potential lies in the use of elastic deformation to achieve a curved geometry from flat and straight building parts. The curvature of surface-curves is analysed and superimposed with the three axes of bending of load-bearing beams. In consequence, specific shapes and networks are identified which allow for a simplified construction of elastically formed grids. This strategy is used to develop a new design method for strained gridshells using asymptotic curves on a minimal surface.
The design and construction of a prototypical structure, the Asymptotic Gridshell, presents insights into the planning, fabrication and construction process, and its load-bearing behaviour.

Motivation

With the technological advances in both 3D modelling and fabrication, it is possible to design and construct any arbitrary shape or structure. Any surface can be subdivided into unique parts, which are then individually manufactured, labelled and assembled.
The question arises: Why bother rationalizing a form or network?
Understanding the complexity of a spatial network not only offers simplification of the construction with substantial cost savings. Foremost, it gives the architect the control over their designs: It opens up a spectrum of solutions to choose from, rather than capitulate to the most advanced fabrication tool. Being aware of the dependencies of shape, segmentation and building part lets us decide what rationalizations are most effective, which topology might be beneficial, and which tool to use for fabrication.
Moreover, combining geometric expertise with the experience in material behaviour helps us find new fabrication-aware[1] designs to create a symbiosis of form and support structure.

Figure 1 *Structural grid of the Asymptotic Gridshell (Photo: **Felix Noe 2017**).*

1 The term “fabrication-aware design” is used to describe computational design methods which take into account the fabrication and construction of a structure. This might entail a simple rationalization of the geometry, or the implementation of specific requirements for manufacturing techniques in the design process (Pottmann 2013).

Methodology and Tools

Methodology

There are three methods used in this thesis to investigate repetition in grid structures:

A deductive approach can be described as a "top-down" process: The theories of differential geometry are used to deduce geometric properties and then applied to design shapes and segmentations with repetitive parameters.

An inductive approach takes the inverse "bottom-up" route: The enforced repetition of specific parameters within a network, triggers a specific behaviour or shape adjustment, which is then documented and classified. The inductive approach is a "naïve" process, and may not display all possible solutions. However, it intuitively illustrates the morphology of repetitive grids and has the potential of uncovering new solutions and dependencies.

Finally, the concept of research by design[2] is used to investigate repetitive structures. This approach relies on physical prototypes to design structures, combining all aspects of geometry, structure, fabrication and aesthetics.

Tools

The thesis heavily relies on both digital and physical modelling to investigate the behaviour of repetitive grids.

The digital tools include simple 2D and 3D modelling software, parametric applications and algorithmic scripting. They are used to create a digital representation of networks, model dependencies to rapidly alter a given geometry, and develop new tools that implement scientific insights. Next to these geometric applications, we conduct digital simulations and optimizations to investigate the morphological behaviour of networks under parameter constraints. Finally, FEM-software was used to analyse the load-bearing behaviour of a prototype structure.

Physical models not only allow us to investigate geometric features, but to – hands on – experience the construction process, the load-bearing behaviour and aesthetic qualities. They are used throughout our studies to verify theoretical findings and trigger further research questions.

---

2 The term "Research by design" was coined at the Faculty of Architecture in Delft (***van Ouwerkerk 2001***) referring to the general concept of producing new knowledge through the act of designing, and has been actively implemented as a tool to investigate scientific questions. A working group under the research committee of the EAAE1 has produced a rather cumbersome definition of this concept in 2011 (***Hauberg 2012***):

- Research by design is any kind of inquiry in which design is a substantial part of the research process.
- In research by design, the architectural design process forms a pathway through which new insights, knowledge, practices or products come into being.
- Research by design generates critical inquiry through design work that may include realized projects, proposals, possible realities or alternatives.
- Research by design produces forms of output and discourse proper to disciplinary practice, verbal and non-verbal, that make it discussable, accessible and useful to peers and others.
- Research by design is validated through peer review by panels of experts who collectively cover the range of disciplinary competencies addressed by the work.

In this thesis, our preliminary motivation to use research by design, is to uncover further design solutions beyond the inducible or deducible results.

Structure

This thesis is written for the designer - architect or engineer - who is responsible for the geometry of a curved building structure. The work is situated in the cross-field of architecture, engineering and mathematics, with a strong focus on geometry.
The work is divided into three parts:

- Part I: 'State of the Art' presents fundamental theories of geometry (*Chapter 1*), and gives a short overview of the most relevant geometric publications and architectural structures that investigate repetition (*Chapter 2*).

- Part II: 'Repetitive Structures' develops a theoretical framework of geometric and constructive parameters for repetitive structures, and defines fundamental geometric dependencies (Chapter 3). This framework is not only used to analyse existing constructions. It draws conclusions on common strategies and sets an impulse for further investigations (*Chapter 4*).
  Chapter 5 presents five independent but constitutive studies which investigate selected sets of parameters to explore the morphological behaviour of repetitive networks. These studies first compare smooth and discrete structures (*Section 5.1*), investigate tolerances and deformation for smooth, rectangular panelizations (*Section 5.2*), create prototypical modular designs (*Section 5.3*), deduce principle relationships of curvature and deformation of networks (*Section 5.4*), and finally develop a novel design method for strained gridshells (*Section 5.5*).

- Part III: 'Case Study' (Chapter 6) implements the novel method in the planning and construction process of a prototypical pavilion, the Asymptotic Gridshell, giving important insights into the design process, construction development and its load-bearing behaviour

Publications

Parts of this thesis are based on research which has already been published in peer reviewed papers or technical reports, and has been conducted in cooperation with co-authors.
Some studies of *Chapter 5* are also found in:

- Eversmann, Philipp; Schling, Eike; Ihde, André; Louter, Christian (2016): Low Cost Double Curvature. Geometrical and Structural Potentials of Rectangular, Cold-bent Glass Construction. In K. Kawaguchi, M. Ohsaki, T. Takeuchi (Eds.): Proceedings of the IASS Annual Symposium 2016. Tokyo
- Schling, Eike; Barthel, Rainer (2017): Experimentelle Studien zur Konstruktion zweifach gekrümmter Gitterstrukturen. Experimental studies on the construction of doubly curved structures: Fachwissen. In Detail structure (01), pp. 52–56.
- Schling, Eike; Barthel, Rainer; Tutsch, Joram (2014): Freie Form - experimentelle Tragstruktur. In Bautechnik 91 (12), pp. 859–868.
- Schling, Eike; Hitrec, Denis; Barthel, Rainer (2017a): Designing Grid Structures using Asymptotic Curve Networks. In Klaas de Rycke et al. (Eds.): Humanizing Digital Reality. Design Modelling Symposium Paris 2017. Singapore: Springer Singapore, pp. 125–140.

Chapter 6 contains further work from:

- Schling, Eike; Hitrec, Denis; Schikore, Jonas; Barthel, Rainer (2017b): Design and Construction of the Asymptotic Pavilion. In K.-U. Bletzinger, Eugenio Oñate, B. Kröplin (Eds.): VIII International Conference on Textile Composites and Inflatable Structures. STRUCTURAL MEMBRANES 2017. pp. 178–189.
- Schling, Eike; Kilian, Martin; Wang, Hui; Schikore, Jonas; Pottmann, Helmut (2018): Design and Construction of Curved Support Structures with Repetitive Parameters. In Lars Hesselgren, Karl-Gunnar Olsson, Axel Kilian, Samar Malek, Olga Sorkine-Hornung, Chris Williams (Eds.): AAG 2018. Advances in Architectural Geometry. Wien: Klein Publishing, pp. 140–165.

PART I
STATE OF THE ART

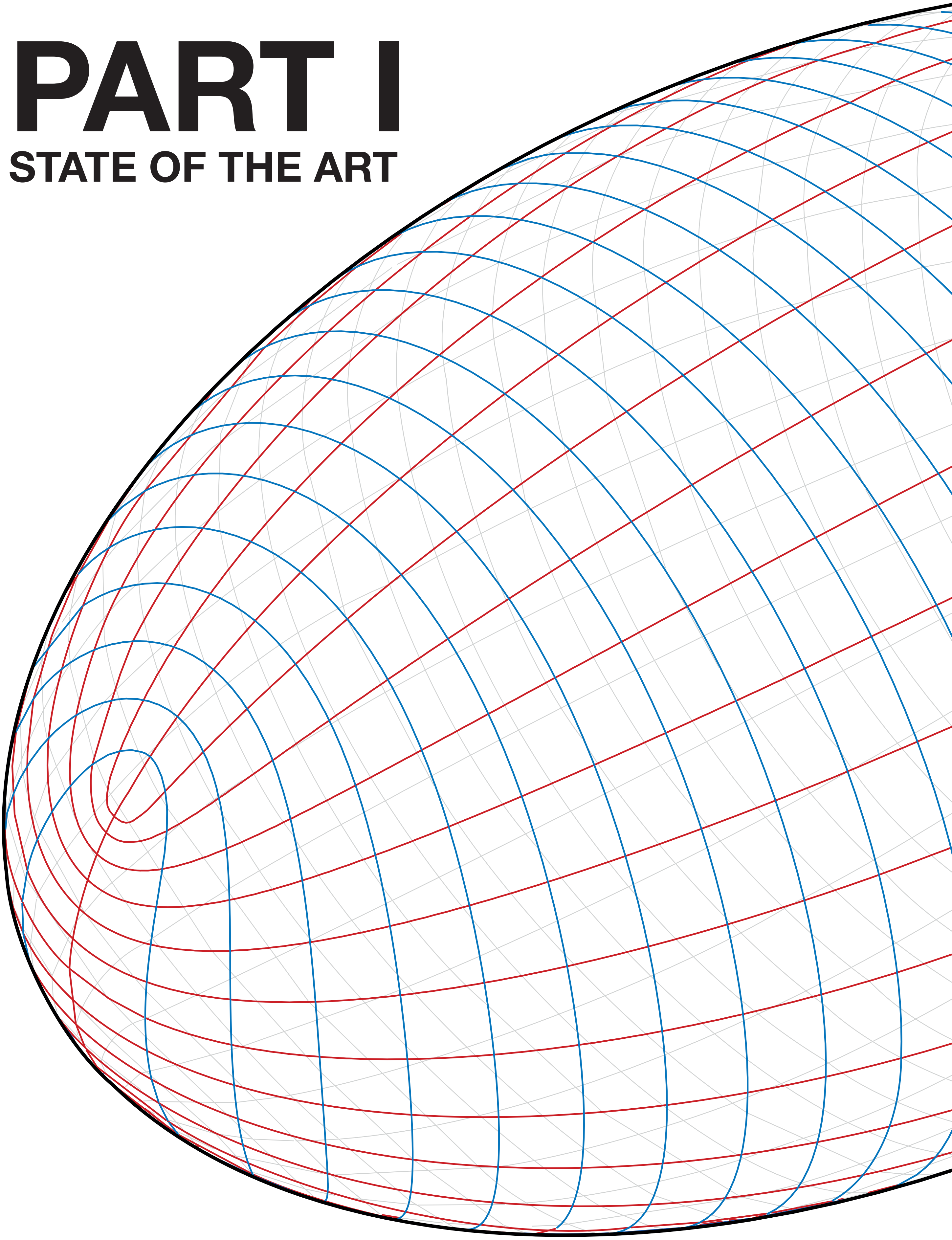

1 Geometric Fundamentals

Designing freeform architectural structures commonly follows a similar workflow. The overall shape is defined by a design surface. The surface is subdivided into smaller segments suitable for fabrication and construction. This segmentation results in a network of faces, edges and nodes. The repetitive nature of these elements is dependent on the curvature of the initial surface, as well as the properties and topology of the network.

- *Section 1.1* outlines the definitions of curvature based on curves and surfaces.

- *Section 1.2* gives an overview of the classification of surfaces and their properties.

- *Section 1.3* introduces the different types of segmentation and presents the geometric and architectural properties of common networks.

- *Section 1.4* introduces network topology, its relationship to curvature and its potential to create repetition.

This fundamental knowledge of geometry is well described in literature on descriptive and differential geometry. The following chapter primarily refers to the educational book, Architectural Geometry (***Pottmann et al. 2007a***). Any further sources will be cited in situ.

Figure 1.1 *Principal curvature lines on an ellipsoid (**ES 2018**).*

1.1 Curvature

Curves and surfaces can be described as one or two-dimensional, smooth[3] arrays of points. Curvature describes the deviation of these continuous geometric elements from a straight or flat state.

1.1.1 Curvature of a Space Curve

A curve is a one-dimensional object. At each point a tangent vector **t** and normal plane define its local direction. The local curvature of a curve is measured at the osculating circle at each point. The **curvature** k is the inversion of the curvature radius r, $k = 1/r$.

The **torsion** τ describes the rotation of the osculating plane[4] about the tangent vector[5]. If k and τ are constant, the curve describes a circle, helix or, if $k = 0$, a straight line. A planar curve displays no torsion, $\tau = 0$.

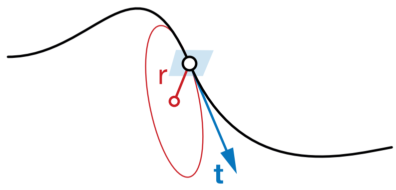

Figure 1.2 *Curvature of a curve. A curve is a one-dimensional, smooth array of points. At each point, the direction is defined by a tangent vector and normal plane. The local curvature is the inverse of the radius of the osculating circle (**ES 2016** based on **Pottmann et al. 2007a, p. 227**).*

1.1.2 Curvature of a Surface

A surface is a two-dimensional object. At each point the normal vector **n** and tangent plane define its local orientation. The local curvature of a surface is calculated at each point individually:

The surface is intersected with the planes through the normal vector. The curvature of the resulting section curve (at that point) is called the normal curvature k_n. There are infinitely many planes (and thus section curves) radial to this normal vector. The two section curves with the highest and lowest normal curvature determine the two **principal curvatures** k_1 and k_2. They are always perpendicular to each other and indicate the two principal curvature directions. From these two principal curvatures, the Gaussian curvature ($K = k_1 \cdot k_2$) and the mean curvature ($H = (k_1 + k_2) / 2$) are calculated.

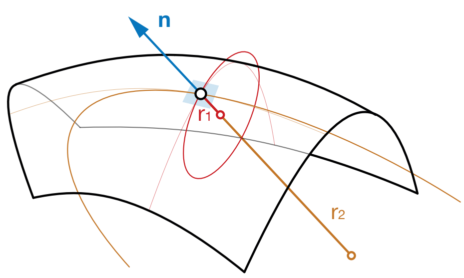

Figure 1.3 *Curvature of a surface. A surface is a two-dimensional smooth array of points. At each point, the orientation is defined by the normal vector and tangent plane. The curvature of a surface is calculated from the two principal curvature radii at this point (**ES 2016** based on **Pottmann et al. 2007a, p. 215**).*

3 without kinks or folds

4 The osculating circle is a tangent circle which best approximates the curve progression at a particular point. It is derived from a limit refinement of three consecutive points. The osculating circle spans the osculating plane, which is tangent to the curve at that same point.

5 The normal plane and the osculating plane intersect along the principal normal of the curve which is the direction of the curvature radius. The normal vector to the osculating plane is called the binormal. The three vectors – curve-tangent, principal normal and binormal – define a coordinate system which is called the Frenet frame. The rotation of this frame around the tangent vector determines the torsion τ of the space curve.

The **Gaussian curvature** K is commonly used to describe the shape and magnitude of surface curvature. If the two principal curvature radii centers lie on the same side of the surface, their product is positive. This is called an elliptical surface point (*Figure 1.4*) with positive (synclastic) Gaussian curvature, as can be seen on an egg or a sphere.
If the two principal curvature radii centers lie on opposite sides of the surface, their product is negative. This is called a hyperbolic surface point (*Figure 1.5*) with negative (anticlastic) Gaussian curvature, as illustrated by the shape of a horse's saddle.
If one of the two principal curvatures are zero, their product is also zero. This is called a parabolic surface point (*Figure 1.6*). Such single curvature can be seen on a cylinder or cone.

The **mean curvature** H indicates the balance of curvature. If the two principal curvature radii have the same absolute value, but opposite orientation, the mean curvature is zero (*Figure 1.7*). Surfaces with a constant mean curvature of zero are called minimal surfaces (*Section 1.2.3*).

To illustrate the curvature behaviour at a surface point, we trace the values of normal curvature k_n in relation to the rotation of section curves (*Figure 1.4* - *Figure 1.7*). This **curvature graph** has two extremes, k_1 and k_2, which indicate the **principal curvature directions**, and two, one or none zero-crossings, which indicate the asymptotic directions.

Scenario. The asymptotic directions can be illustrated by the following scenario: Imagine a ruler standing upright on the saddle of a horse, touching it at one point. When rotating the ruler around this point, it will hit the saddle at two specific directions where the normal curvature is zero. These are the asymptotic direction. Repeating the same exercise on a synclastic surface, like a balloon, will not find a contact-direction. The ruler can be freely rotated, as the normal curvature is never zero.

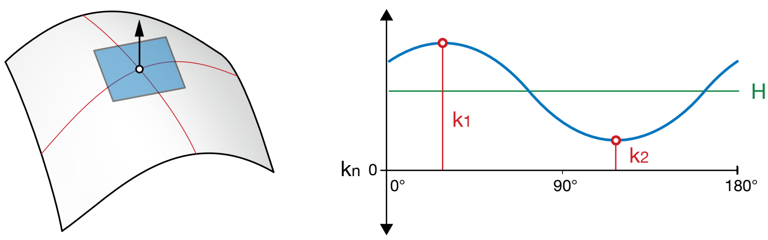

Figure 1.4 *Synclastic curvature. Left: An elliptical surface point indicates positive curvature (**ES 2018** based on **Pottmann et al. 2007a, p. 243**). Right: If k_n is never zero, there are no asymptotic directions (**ES 2018**).*

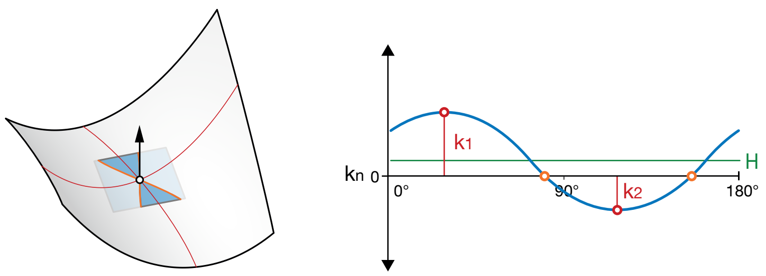

Figure 1.5 *Anticlastic curvature. Left: A hyperbolic surface point indicates negative curvature (**ES 2018** based on **Pottmann et al. 2007a, p. 243**). Right: The curvature graph illustrates the symmetrical occurrence of asymptotic directions in respect to the principal curvature directions (**ES 2018**).*

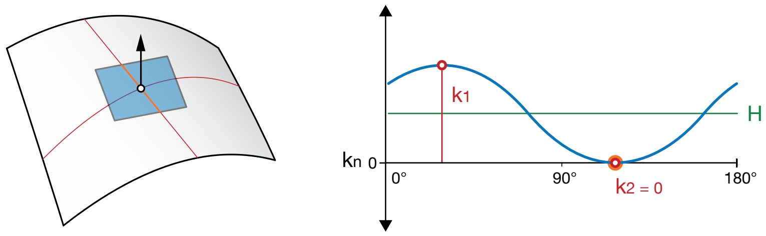

Figure 1.6 *Single curvature. Left: A parabolic surface point indicates single curvature. One of the principal curvatures is zero (**ES 2018** based on **Pottmann et al. 2007a, p. 243**). Right: The curvature graph illustrates the coincidence of principal curvature and asymptotic directions (**ES 2018**).*

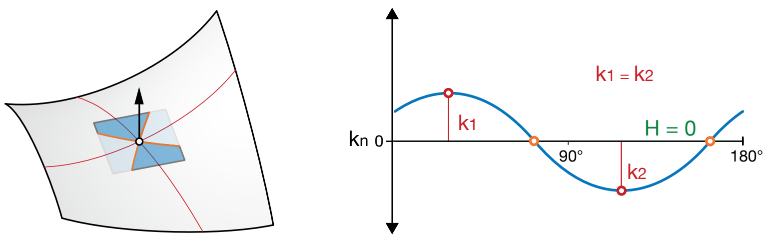

Figure 1.7 *Mean curvature of zero. Left: A hyperbolic surface point of $k_1 = -k_2$ (**ES 2018**). Right: The curvature graph illustrates the regularity/bisecting nature of principal curvature directions and asymptotic directions on a minimal surface (**ES 2018**).*

These two types of directions can be imagined like a magnet field across a surface, indicating the directions of extreme and vanishing normal curvature. The normal curvature of any other direction can be calculated from k_1 and k_2 as a function of the deviation angle μ from the principal curvature direction.

$$k_n(\mu) = k_1(\cos\mu)^2 + k_2(\sin\mu)^2 \tag{1.1}$$

The directions of vanishing normal curvature ($k_n = 0$) are called the **asymptotic directions**. The asymptotic directions can be determined by cutting the surface with its tangent plane. They are the tangent directions of the section curves at that point.

There are two asymptotic directions at any hyperbolic surface point. They lie in symmetry about the principal curvature directions (*Figure 1.5*). At an elliptical surface point, the tangent plane does not intersect with the surface, and the normal curvature is never zero. There are thus no asymptotic directions (*Figure 1.4*). At a parabolic surface point the two asymptotic directions fall together with the principal curvature direction at $k_n = 0$ (*Figure 1.6*). If the mean curvature of a surface is zero, the asymptotic directions bisect the principal curvature directions ($\mu = 45°$) and are perpendicular to each other (*Figure 1.7*).

1.1.3 Curvature of Curves on a Surface

When analysing a curve on a surface, the information of direction (of the curve) and orientation (of the surface) are combined. In this case, the "Darboux frame" (Strubecker 1969), can be constructed from the normal vector **n**, tangent vector **t** and their cross product, the sideways vector **u**.

The rotation about all three vectors of the Darboux frame can be measured. These three specific curvatures are called **geodesic curvature** k_g (around **n**), **geodesic torsion** t_g (around **t**) and **normal curvature** k_n (around **u**). The curvature radii of k_g and k_n can simply be derived from the curvature k, by projecting its curvature-vector into the tangent, or tangent-normal plane.

$$k = \sqrt{{k_n}^2 + {k_g}^2} \tag{1.2}$$

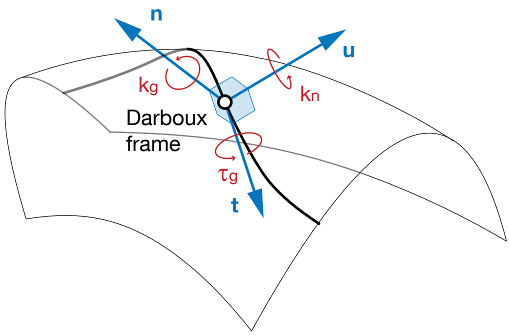

Figure 1.8 *Curvatures of a curve on a surface. The curvature is measured separately for all three axes of the Darboux frame. They are called the geodesic torsion (around* ***t****), the geodesic curvature (around* ***n****) and the normal curvature (around* ***u****) (ES 2016).*

Scenario. The three curvatures of a curve on a surface can be illustrated by using the following scenario: Imagine a car driving through a landscape of rolling hills. Where the road changes its incline - going up or down - the driver experiences normal curvature. If the road changes direction - turning right or left - the driver experiences geodesic curvature. If the road changes its lateral inclination and banks to the side, the car tilts due to geodesic torsion.

1.1.4 Total Curvature and Gaussian Image

The **total curvature of a planar curve** is defined mathematically as the integral of curvature along the curve. This value can be determined graphically by mapping each point of this curve onto a **unit-circle**. This image is generated through the unitized normal vectors of the surface drawn from a common origin.[6] If the normal vector at the start and endpoint are equal, the total curvature is either 0 (for a meandering curve) or $2\cdot\pi$ (for a circular curve). For any closed planar curve (without self-intersection) the total curvature is $2\cdot\pi$.

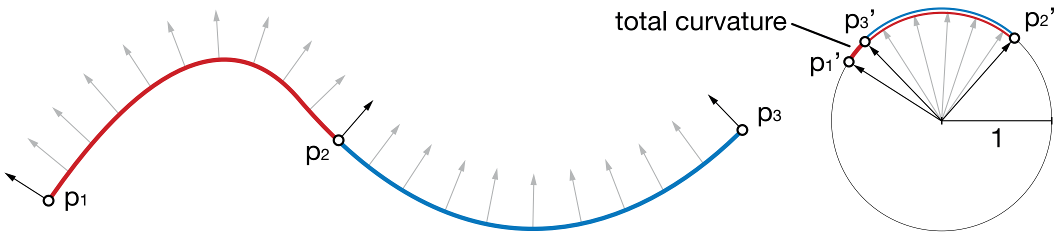

Figure 1.9 *The total curvature of a planar curve can be expressed graphically by the unit circle (ES 2018 based on Pottmann et al. 2007a, p. 494).*

The **total curvature of a surface** is determined in a similar way using the normal vector at each surface point to map an image of the surface onto a **unit-sphere**. This representation is called the Gaussian image. The signed area of the Gaussian image equals the total curvature. This value can be derived solely from its boundaries.

Surfaces which exhibit both positive and negative Gaussian curvature generate a self-intersecting Gaussian image with positive and negative regions overlapping. The total curvature is calculated from the difference of the areas created by the self-intersecting boundary.

6 If the curve changes from positive to negative curvature, the respective parts of the unit-circle are drawn twice by subsequent curve-vectors. These parts are labelled with a positive sign (in the direction of rotation) and negative sign (in the opposite direction), thus cancelling each other out in the calculation of total curvature.

If the normal vector is constant along the boundaries of a surface, the total curvature is zero, because the boundary collapses to a point on the unit-sphere. Any closed surface has a total curvature of a multiple[7] of 4π, the surface area of the unit sphere.

The **total absolute curvature** is the absolute sum of positive and negative Gaussian curvature. It is determined by adding the absolute values of all areas of the Gaussian image.

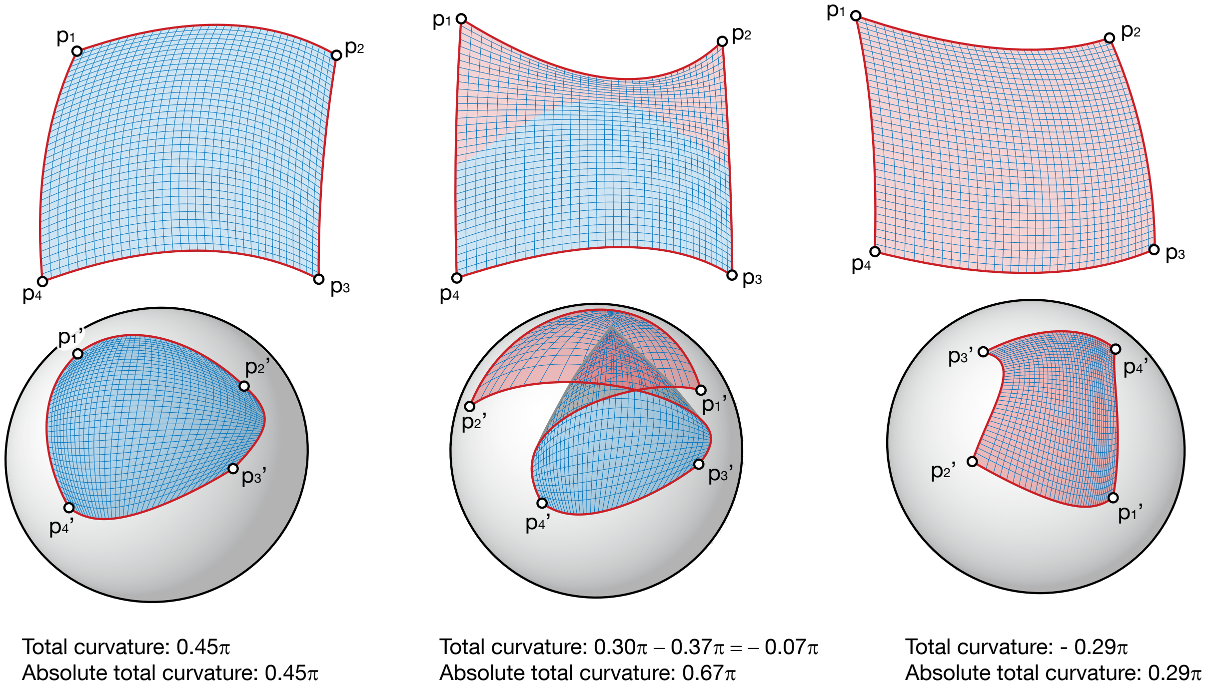

Figure 1.10 *The Gaussian image is a representation of the curvature of a surface created by a spherical mapping. The difference between positive and negative area of the Gaussian image indicates the total curvature. Overlapping boundaries signify a change from positive to negative curvature (**ES 2018** based on **Pottmann et al. 2007a, p. 495**).*

Scenario. The Gaussian image of a surface can be imagined like a bedsheet, whose size is not dependent on the area, but the curvature of the surface. Surface-regions which have the same orientation are folded on top of each other. Here the positive and negative curvature cancel each other out. The total curvature is the difference of positive and negative curvature which can be imagined as the two sides of the folded sheet. In this scenario, the total absolute curvature is the complete area of the unfolded bed-sheet.

7 A sphere has a total curvature of 4π, a torus on the other hand creates a so called "handle", doubling the total curvature to 8π.

1.2 Surfaces

The following section gives a short overview of surfaces based on the categorizations of Pottmann and Barthel (**Pottmann et al. 2007a; Barthel 2015**) in traditional, freeform and physical surfaces/shape optimizations. Apart from these continuously curved surfaces, a final section introduces the notion of polyhedral surfaces as an independent type.

1.2.1 Traditional Surfaces

Traditional surfaces (*Figure 1.12, left*) are classified by how they are constructed geometrically. The three primary families are ruled, translational and rotational surfaces.
The construction of traditional surfaces is based on kinematic operations. They are defined by a profile curve moving along a smooth path. In the case of **ruled surfaces** this profile curve is a straight line (the ruling) moving along two individual path curves. A **translational surface** is described by the parallel movement of one profile curve (the generatrix) along one path curve (the directrix). Finally, a **rotational surface** is generated by rotating a profile curve about a central axis, resulting in a family of radial meridian curves and an orthogonal family of parallel circles.

Further traditional surfaces are a **pipe surface**, described by the movement of a circle perpendicular to a path curve, or a **helical surface** described by the transformation of a profile curve along a helical path.
There are combinations and subsets of these categories. A hyperbolic paraboloid e.g., can be described as a double-ruled surface or a translational surface of parabolas. Similarly, a one-sheet rotational hyperboloid is both a double-ruled and a rotational surface.

A subset of the family of ruled surfaces are **developable surfaces**. They hold the additional geometric property that along any ruling the surface has the same tangential plane. This is true if all rulings are parallel, such as in a cylindrical surface; if all rulings pass through the same point (the apex), such as in a cone or central extrusion; or if all rulings are tangent to a fixed space curve. Such rulings describe a so-called tangent surface.
Developable surfaces are single-curved, i.e., have constant vanishing Gaussian curvature. They are of special importance to this research as they can be unrolled (i.e., developed or mapped isometrically) into the plane without stretching or shearing like a piece of paper. This makes developable design surfaces most receptive to repetitive patterns. Developable geometries of building parts, like panels or lamellas, are favourable for construction.

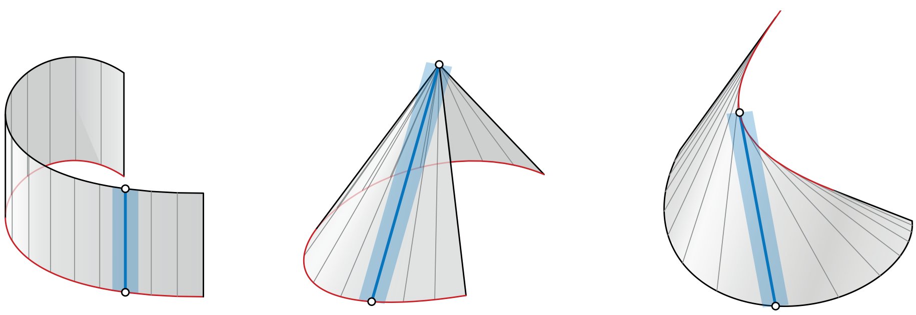

Figure 1.11 *Developable surfaces are either cylindrical, conical or tangential surfaces (**ES 2018** based on **Pottmann et al. 2007a, p. 535**).*

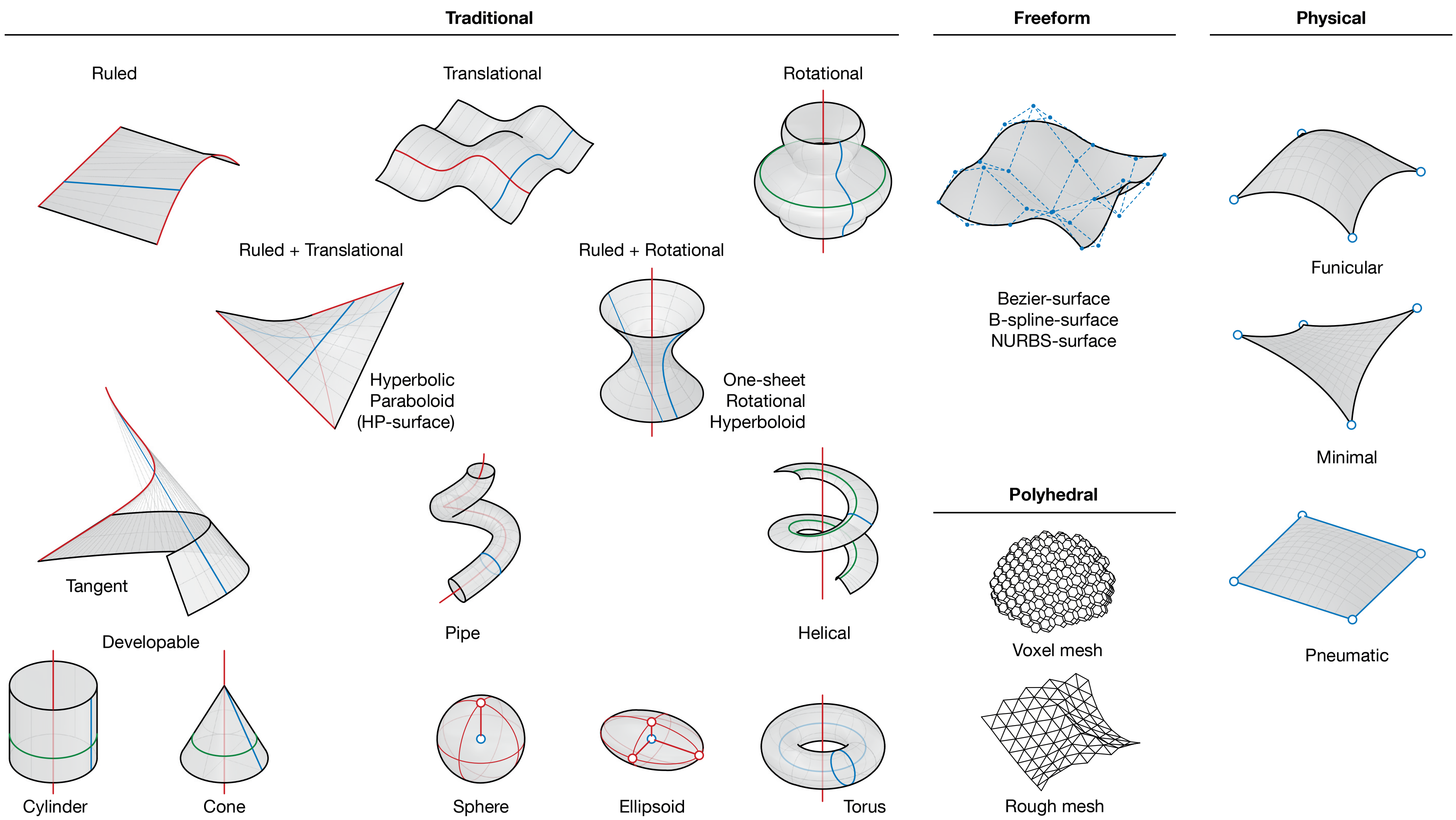

Figure 1.12 *Overview of surface classes (**ES 2016** based on **Pottmann et al. 2007a; Barthel 2015**).*

1.2.2 Freeform Surfaces

Digital freeform surfaces (*Figure 1.12, middle*) are defined via control points. They can assume virtually any smooth shape and can be manipulated locally within a confined region – a powerful tool for designers.

A freeform surface is generated by an algorithm, which approximates a two-dimensional array of control points. The three common types, Bezier surfaces, B-spline surfaces (B stands for "Basis") and NURBS surfaces (Nonuniform rational B-spline curves), are based on the homonymous digital freeform curves. They have increasing control mechanisms:

- Bezier surfaces are constructed via a repeated linear interpolation of control points, invented by Paul De Casteljau in 1959. Changing a control point has a global effect on the shape.
- B-spline surfaces consist of several Bezier-segments of the same degree and thus allow a local shape control within each segment.
- NURBS surfaces have the additional control of "weights" at each control point. The designer is able to pull or release the curve/surface at any control point individually.

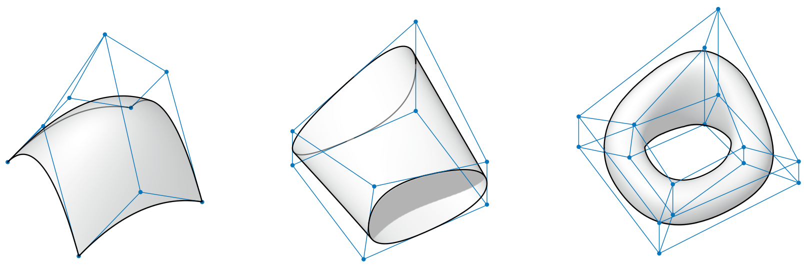

Figure 1.13 *Digital surfaces are defined by a quadrilateral network of control points with open or closed topology (**ES 2018** based on **Pottmann et al. 2007a, p. 361**).*

1.2.3 Physical Surfaces

Physical surfaces (*Figure 1.12, right*) represent a state of equilibrium under given loads or boundary conditions. They are derived from a natural formation process and thus show a high aesthetic quality.

Digital modelling of physical surfaces is achieved through an optimization process, in which either their mechanical or geometrical properties are approximated. Their particular curvature-behaviour makes them susceptible for segmentations with repetitive elements. The most relevant types for subsequent research are minimal surfaces. Other examples are funicular forms, pneumatic (constant mean curvature) surfaces, surfaces with constant negative Gaussian curvature, or hydrostatic shapes.

A **minimal surface** is the surface of minimal area between any given boundaries. Minimal surfaces have a mean curvature of zero. They can be found in nature in the shape of soap films. Their form is found digitally in an iterative process by minimizing the area of a surface or finding the shape of equilibrium of tension.

Some minimal surfaces can be derived from mathematical definitions, such as: the plane (for any planar boundary curve), the catenoid (the rotational surface of a catenary curve), or the Enneper surface.

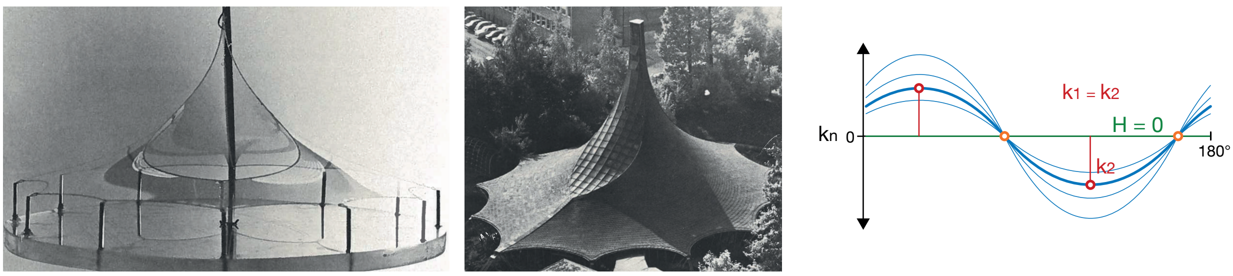

Figure 1.14 *Left / Middle: Soap films naturally form a minimal surfaces. Such shapes are used in tensile structures like the Institute for Lightweight Structures in Stuttgart (**Glaeser 1978**). Right: All points on a minimal surface have a mean curvature of zero and follow a symmetric pattern on the curvature graph (**ES 2018**).*

A **funicular form** is the inverted hanging shape of a given net under a defined set of loads and supports. For a single line or thread under self-weight, this results in a catenary and, when inverted, resembles the thrust line of a double-hinged arch. This shape can be determined graphically through the theory of graphic statics. This method can be extended for three-dimensional structures enabling an intuitive load-based design of compression-only shell structures (***Block 2009***).

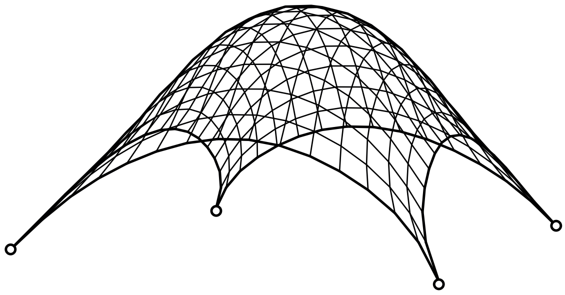

Figure 1.15 *Left: A funicular form is an inverted hanging shape, such as the chain models of the Multihalle in Mannheim (**Barthel 2005**). Right: A funicular network can be found digitally within a physical simulation (**ES 2018**).*

Surfaces with constant mean curvature (CMC) are the mathematical representation of inflated membranes, such as a soap bubble or pneus (from isotropic material). Their curvature behaviour corresponds to the equilibrium shape caused by a pressure difference (***Lobaton and Salamon 2007***). The simplest CMC surface is a sphere, where H = 1/r. Minimal surfaces are a subset of CMC surfaces, in which the pressure difference is zero, resulting in a constant mean curvature of zero.

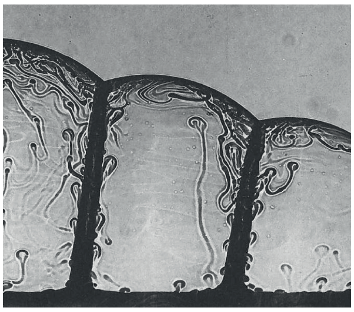

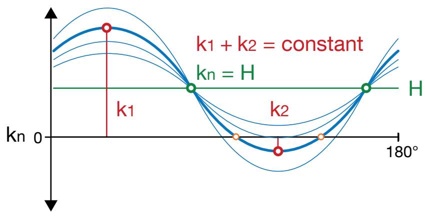

Figure 1.16 *A constant mean curvature (CMC) surface is the mathematical representation of inflated structures. Left: Soap bubbles (**Schaur and Bach 1977, p. 91**). Middle: The pneumatic façade of the National Aquatics Center in Beijing (**AB 2008**). Right: All points on a CMC surface have the same mean curvature, and thus follow a symmetrical pattern on the curvature graph (**ES 2018**).*

A pseudosphere is one example of a **surface with constant negative Gaussian curvature**. The term is used specifically to refer to a tractricoid, the rotational surface of the path of pulling an object under the influence of friction.[8] Pseudospheres are isometric to the hyperbolic plane and display an exponential increase of surface area towards their boundaries. This quality is used e.g., in the design of acoustic horns/speakers.

8 A tractrix is the path of movement of an object which is pulled under the influence of friction. It is created when pulling the object in the horizontal plane by a string of constant length along a straight line perpendicular to its initial position. Rotating this curve around the direction of the pulling force creates the pseudospherical surface called "tractricoid" (***Weisstein 2018b***).

__Figure 1.17__ Left: A pseudosphere is a surface of constant negative Gaussian curvature (__ES 2018__). Middle: Such shapes are used e.g. in the design of acoustic horns (__NA 2015__). Right: All points on such a surface follow a pattern on the curvature graph symmetrical to the function of zero mean curvature (__ES 2018__).

1.2.4 Polyhedral Surfaces

A smooth surface may be approximated by a discrete mesh (*Section 1.3.1*). The proximity of this mesh to the reference surface may vary greatly, and allow for independent geometric qualities. Examples of such independent polyhedral surfaces are **voxel**, **lobel** or **honeycomb meshes** (*Section 2.2.1*).
Assigning these meshes to a smooth surface class might be misleading. They are thus classified separately as polyhedral surfaces.

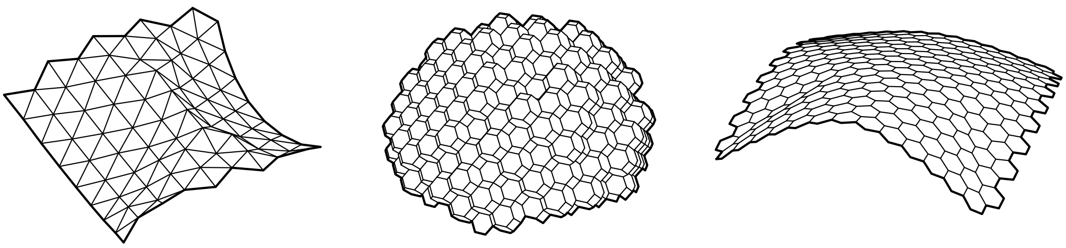

__Figure 1.18__ Examples of polyhedral surfaces (__ES 2018__).

1.3 Segmentation

For the purpose of construction, the design surface is usually divided into smaller segments. This segmentation results in three entities which directly inform the geometry of building parts: The faces, which become the façade panels; the edges, which become structural beams, mullions or transoms; and the nodes, at which the beams are joined. The particular geometry of each element is related to the surface curvature, the type of segmentation and the quality of the network.

1.3.1 Classification

A smooth shape can simply be subdivided by drawing a network of curves on the surface. This **smooth segmentation** creates curved faces and edges, both coinciding with the surface geometry. The nodes are locally planar and traversal[9], connecting continuously smooth curves. This segmentation is used scarcely in building construction as the fabrication of double-curved panels and curved beams are a rare and costly feature.

The most common strategy to segment a curved building envelope is to approximate the smooth edges with straight lines from node to node. This **discrete segmentation** only touches the surface at the nodes. A discretization naturally creates tangential discontinuities[10] at both the edges and faces.
Even though discretization greatly simplifies the geometry of faces and edges, it shifts the complexity to the nodes. “In general no two nodes are congruent and, which is worse, a typical node exhibits torsion, i.e., is a truly spatial object whose manufacturing is challenging” (***Bo et al. 2011***).

There are **hybrid solutions** of smooth and discrete segmentations allowing for some curvature of edges or faces, but discretizing other parts. A common method is to create a curved segmentation of edges in one direction and a discretized segmentation in the other. These “semi-discrete segmentations” result in a series of ruled surfaces strips (***Pottmann et al. 2008***). Another method is to create curved but non-continous edges between nodes (*Section 4.2.2*).

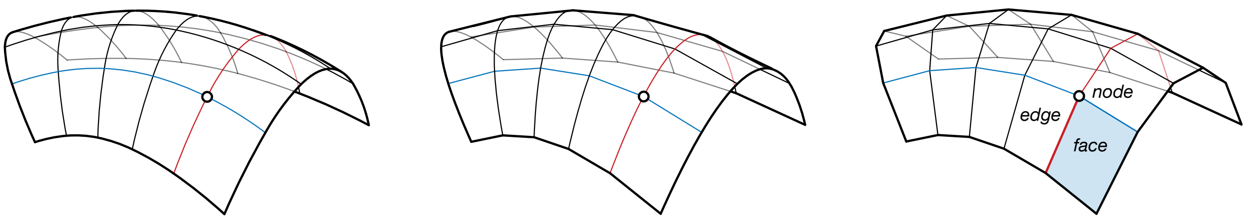

smooth segmentation | **(semi-discrete) hybrid segmentation** | **discrete segmentation**

planar, traversal nodes
curved edges
double-curved faces

single-traversal nodes
linear / curved edges
single / double-curved faces

spatial nodes
linear edges
planar / twisted faces

Figure 1.19 *Classification of discrete, hybrid and smooth segmentation (**ES 2016**).*

9 Nodes are called “traversal” if opposite edges are tangent to each other, i.e., edges run continuously smooth through the node.
10 Schiftner et al. (***2013***) differentiate between “discontinuity in position”, meaning a gap or overlap within a network, and “discontinuity in tangency”, describing a kink between curves or a fold between surfaces.

1.3.2 Networks

Networks are defined by the type of pattern used in a segmentation. Choosing the network (triangular, quadrilateral, hexagonal or others) not only influences the overall appearance, it also effects the stability of the structure, and the shape and complexity of faces and nodes. This section gives an introduction of the most common architectural networks and highlights their geometric and architectural properties.

The most common networks in architecture are based on the three planar regular tesselations: triangles, quadrilaterals and hexagons. Each polygon in these regular tessellations has an incircle touching all edges, and a circumcircle touching all nodes of the polygon.

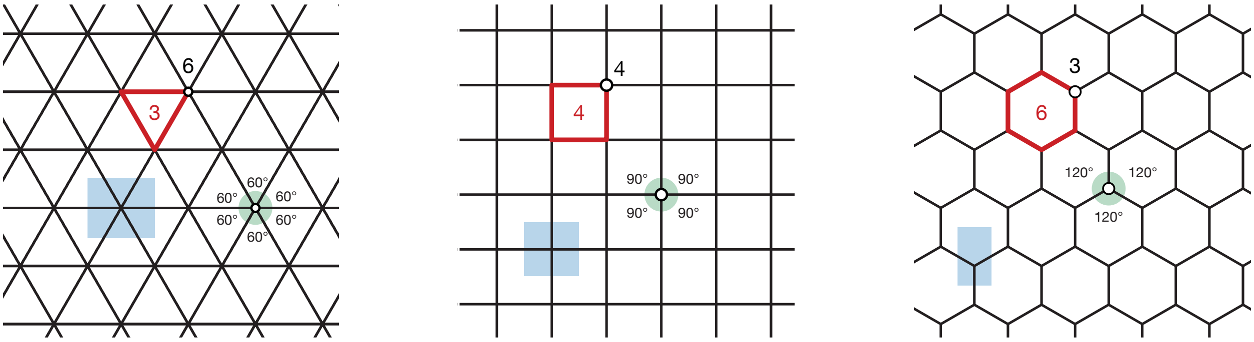

Figure 1.20 *Overview of triangular, quadrilateral and hexagonal networks showing valence, mesh angles and density (**ES 2016**).*

Triangular networks {3,6}[11] are often used in discrete segmentations as they naturally create a rigid structure with planar faces. They consist of three families of continuous edge-curves and are dual[12] to a hexagonal network. Triangular networks are dense (ratio edge/area = 3.22)[13], and result in a high node complexity with six edges meeting at every joint. Moreover, triangular panels are less favourable for fabrication, as their cutting process creates more waste material.

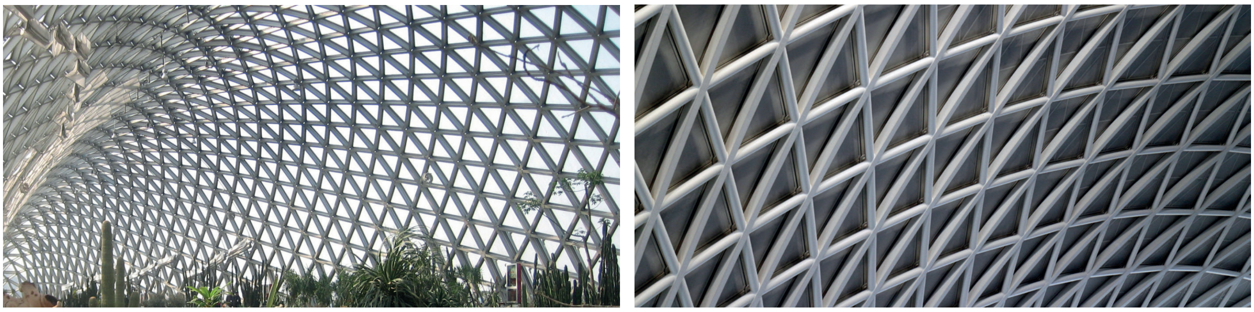

Figure 1.21 *Triangular networks. Left: Botanical Garden in Shanghai (**AWA 2010**). Right: King's Cross Station in London (Photo: **Jonas Schikore 2018**).*

Hexagonal networks {6,3} are dual to triangular networks. They are the least dense (ratio edge/area = 1.32) and are unstable in a hinged assembly. They have three edge directions meeting at each node without creating continuous curves. It is possible to create hexagonal discretization with flat panels, however, for anticlastic surface regions, this results in non-convex panel shapes (*Figure 1.22, right*).

11 Regular tessellations may be labelled with the Schläfli symbol {p,q}, in which p describes the number of vertices (or edges) of the regular polygon and q the number of polygons meeting at each node. The latter is also called the valence.

12 Connecting the face midpoints of a tessellation creates another "dual" tessellation.

13 For the purpose of comparing network density, the edge length within a periodic patch of a network is divided by the area of this patch.

Figure 1.22 *Hexagonal networks. Left: Eden Project in Cornwall (GA 2001). The geodesic dome consists of a hexagonal and a tri-hex network together forming a space frame. Right: Landesgartenschau Exhibition Hall in Schwäbisch Gmünd (ICD 2014). The hexagonal shell consists of convex and non-convex timber plates.*

Quadrilateral networks {4,4} are often preferred in architectural design. They consist of two families of continuous edge curves, are dual to themselves, and have a density ratio of 2.00. Quadrilateral networks are unstable in a hinged assembly, which is commonly restricted by diagonal cables. It is possible to create a discretization with planar quads along conjugate curves. Additionally, quadrilateral panels offer an efficient fabrication with few offcuts.

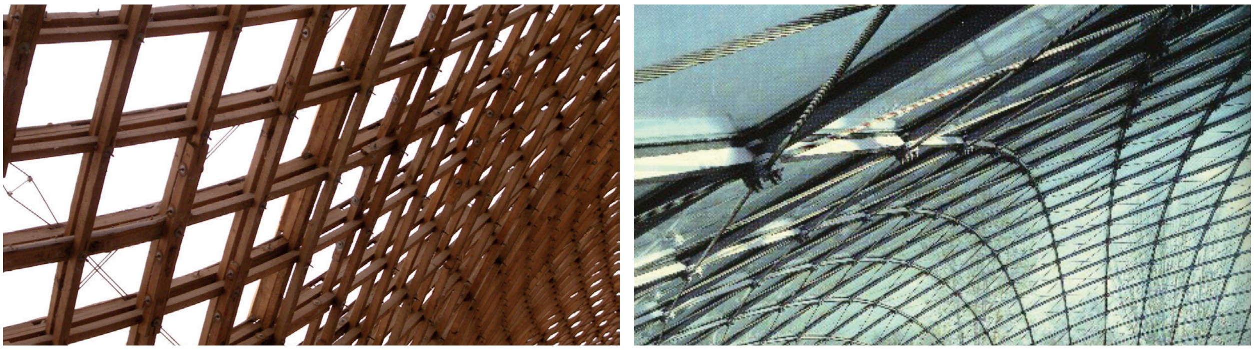

Figure 1.23 *Quadrilateral networks. Left: Multihalle Mannheim, 1972 by Frei Otto (Photo: Rainer Barthel 2007). Right: House for Hippopotamus at the Berlin Zoo (SBP 1996).*

Apart from these common networks, there is a large variety of **hybrid patterns**, which combine several types of polygons, like the tri-hex pattern used for the Centre Pompidou in Metz, the Islamic pattern of the Abu Dhabi Louvre, or the triangle-quad mesh of the Islamic Art Exhibition in the Louvre in Paris, and **bespoke patterns** with irregular combinatorics, like the Dutch National Maritime Museum in Amsterdam.

Figure 1.24 *Hybrid and bespoke networks. A) Hybrid, tri-hex pattern of the timber gridshell, Centre Pompidou in Metz (SBA 2010). B) Hybrid pattern of regular triangles, squares and octagons as roof shading for the Louvre Abu Dhabi (AJN 2017). C) Bespoke pattern of the courtyard gridshell, Dutch National Maritime Museum in Amsterdam (NP 2011). D) Hybrid triangular and quadrilateral tiling of the courtyard roof, Islamic art exhibition in the Louvre in Paris (MBA 2012).*

1.4 Network Topology

The network topology describes the way that faces and edges are connected. Creating nodes with higher or lower valence helps to adjust a network to the surface curvature and thus prevent distortion. The following section explains the relationship between network angles and curvature, introduces the manipulation of valences as an initiator of curvature, and presents singularities as a design feature and their potential for repetitive structures using the examples of platonic solids, geodesic domes and smooth freeform networks.

1.4.1 Discrete Curvature

Any planar tessellation has the property of a constant angle-sum of 360° at each node.[14] If this sum is decreased, the polygons form a vertex-pyramid which is a discrete representation of synclastic curvature. This reduction of the angle-sum is equivalent to a reduction of area from the vertex outward, as ed by the gap which appears when unfolding the same polygons into the plane. If the sum of angles is increased beyond 360°, the surplus of area causes the polygons to fold up and down into a saddle shape resembling an anticlastic curvature.

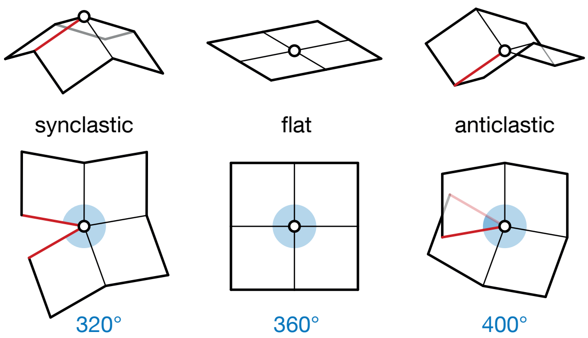

Figure 1.25 *The sum of mesh angles is an indicator of discrete curvature (**ES 2018** based on **Pottmann et al. 2007a, p. 81**).*

Instead of changing the mesh angles of polygons, we can introduce nodes with irregular valence to create curvature. Reducing the valence of a quadrilateral node from 4 to 3 (i.e., subtracting one square from a regular quadrilateral node) reduces the angle sum to 270° and creates a vertex pyramid representing synclastic curvature. Adding two squares to this node increases the valence to six, and the angle sum to 540° degrees, and thus represents anticlastic curvature.

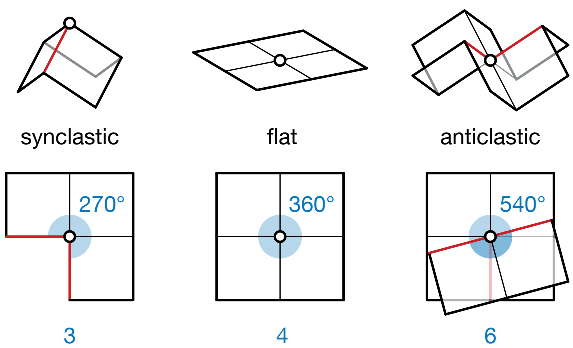

Figure 1.26 *The sum of mesh angles can also be changed by reducing or increasing the valence at a node (**ES 2017**).*

14 This logic is not reversible. A tiling of equilateral triangles with a constant angle sum of 360° may form a roughly folded polyhedral surface or a smooth mesh approximating single curvature. Similarly, a quadrilateral network with constant angle sum 360° may result in a cylindrical mesh. This behaviour is owed to the straight continuous folds that appear in regular triangular and quadrilateral segmentations, making these planar tilings the only geometrically unstable arrangement.

1.4.2 Platonic Solids

If a reduction of valence is applied systematically to a regular tessellation, the vertex-pyramids form a platonic solid: Subtracting one triangle at each vertex of a triangular tessellation {3,6} creates an icosahedron {3,5}. It consists of 20 equilateral triangles meeting with a valence of 5 at every node. The same logic of valence-reduction can be applied two more times to form an octahedron {3,4} and a tetrahedron {3,3}. Similarly, a quad-network {4,4} may form a cube {4,3} if one square is deducted at every node. An assembly of three pentagons per node creates a dodecahedron {5,3}.
These five platonic solids are the closest discrete representation of a double-curved surface (a sphere) that achieve complete geometric repetition, i.e., consist of only congruent faces, edges and nodes.

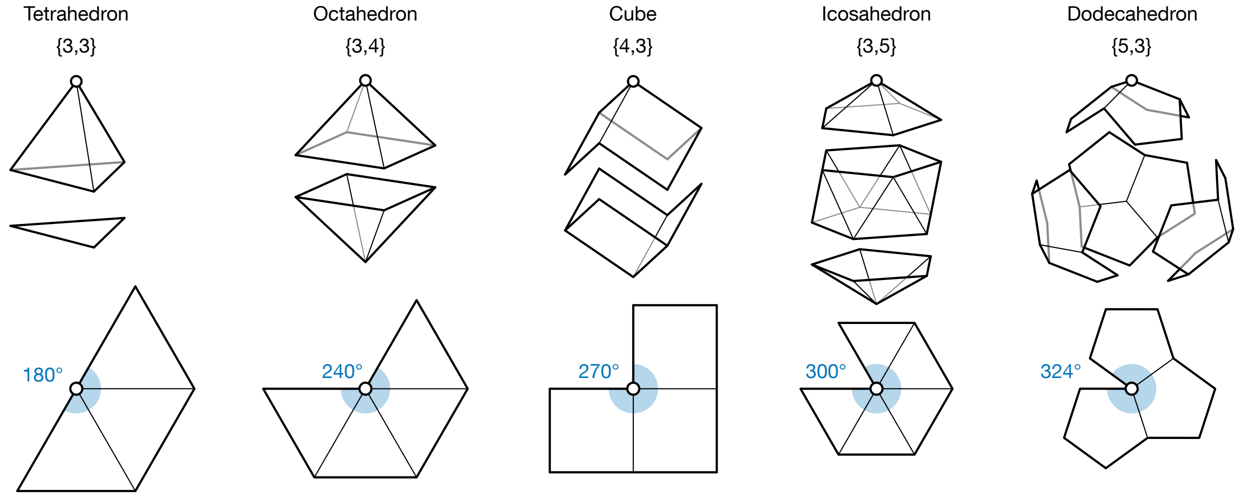

Figure 1.27 *The platonic solids are derived from regular patterns by consistently reducing their valence. Their combinatorics are defined by the Schläfli diagram (**ES 2018** based on **Pottmann et al. 2007a, p. 82**).*

1.4.3 Geodesic Sphere

The geodesic sphere is derived from an icosahedron: Each triangle is subdivided and projected to the circumsphere of the platonic solid. With this method it is possible to achieve a better approximation of the spherical geometry, while only introducing a limited number of individual triangles. This method was used by Walter Bauersfeld and Richard Buckminster Fuller to construct their famous geodesic domes (*Section 2.3*). The network is a triangular {3,6} pattern in which 12 nodes show a reduced valence of 5. They are called **singularities** and are located at the vertices of the initial icosahedron.

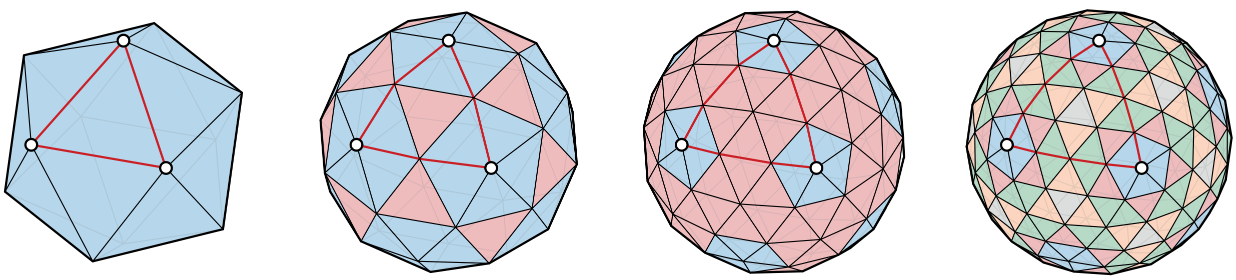

Figure 1.28 *Modelling process of a geodesic sphere. The subdivision of an icosahedron and subsequent projection onto its circumsphere creates a partially repetitive double-curved tiling. A subdivision into 4 and 9 triangles both result in only two unique faces. A further subdivision into 16 triangles creates 5 unique faces (**ES 2018** based on **Pottmann et al. 2007a, p. 98**).*

1.4.4 Singularities

Singularities are the key to realizing a homogeneous network on a double-curved surface. On a synclastic surface this results in a reduction of the valence, on an anticlastic surface, the valence is increased. This topological behaviour of curved meshes not only plays an important role in the optimization of networks, it is also a fundamental part of curvature analysis (visible in the behaviour of principal curvature networks) and can be observed in nature in the forming process of chemicals and crystals.

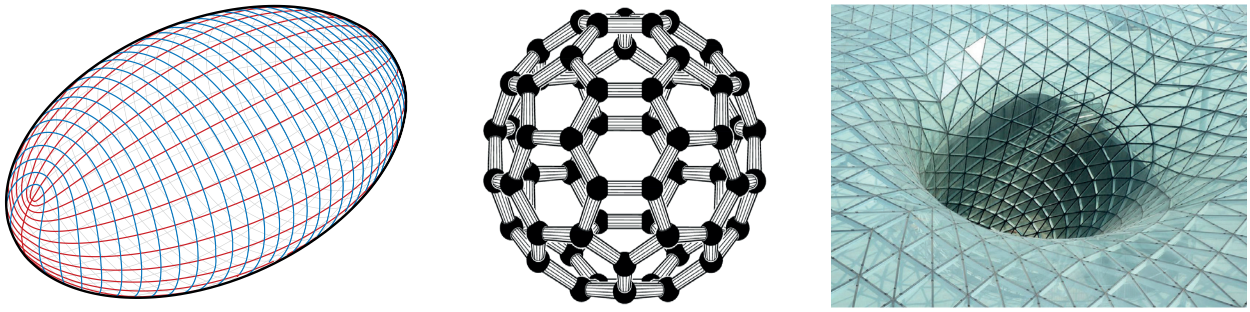

Figure 1.29 *Singularities often occur in curved structures: Left: Principal curvature lines on an ellipsoid (ES 2018). Middle: A carbon molecule (Buckminsterfullerene), named after Buckminster Fuller (WM 2004). Right: Singularities of valence 8 within a triangular network at the New Milan Trade Fair (FA 2005).*

To illustrate the effect of singularities, we modelled an equilateral quad network on a sphere. Due to the double curvature, the network is distorted to the extent that edges start to overlap.
A comparable segmentation with four symmetrical singularities (but no equilateral edges), creates a homogeneous network with little distortion. This is because the topology of the underlying mesh better approximates the shape of the sphere.

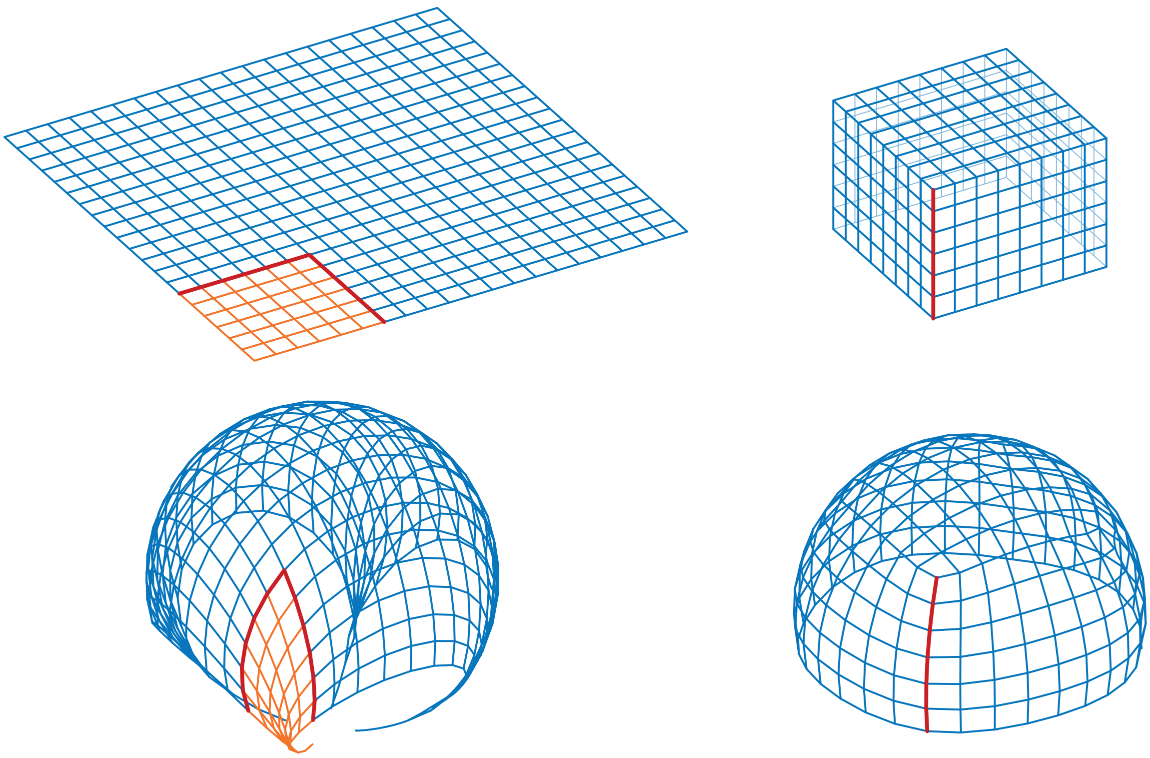

Figure 1.30 *A comparison of two networks with (right) and without (left) singularities. The topology of the network with singularities better approximates the shape of the sphere, and thus creates less distortion (ES 2018).*

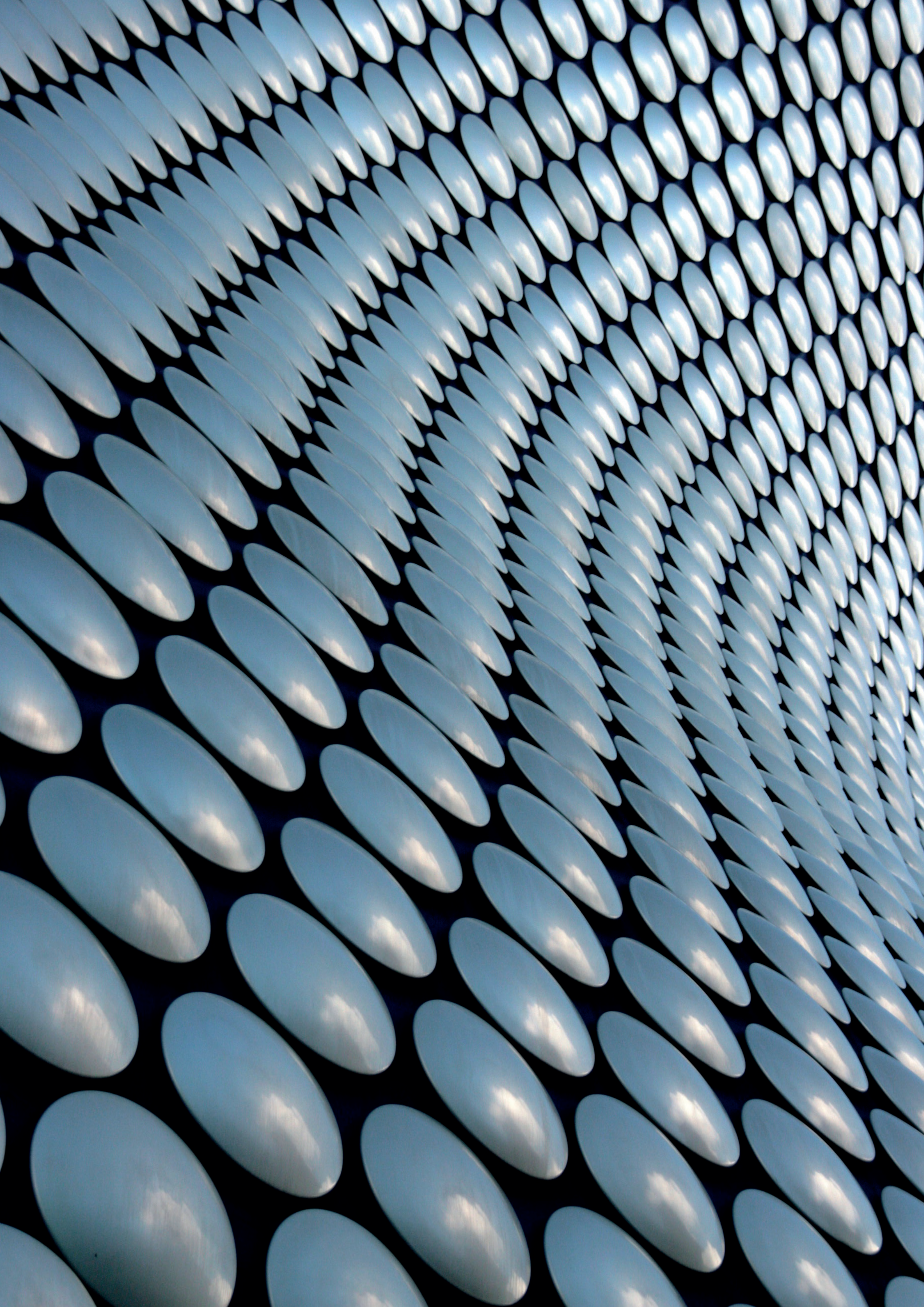

2 Literature Review

The following chapter is divided into three sections which present the constitutive research phases of this thesis:

- *Section 2.1* focuses on the terminology and perception of repetition in geometry and architecture. A fundamental insight of this review was the varying perception of repetitive structures in theory and practice.

- The subsequent review of repetitive structures is therefore separated into geometric investigations (*Section 2.2*) and architectural developments (*Section 2.3*). It resembles the foundation for the theoretical framework (*Chapter 3*) and the subsequent analysis (*Chapter 4*).

- Finally, the constructive properties of one particular reference, the Multihalle in Mannheim, are described in *Section 2.4*. They are the primary reference for the development of the novel construction method presented in *Section 6.2*.

Figure 2.1 *Repetitive circular panels covering the Selfridges building in Birmingham (WM 2010).*

2.1 Terminology and Perception

The following section first reviews common terms used to describe repetitive structures. Thereafter, two publications are compared to clarify the perception of repetitive structures from a geometric and constructive standpoint.

2.1.1 Terminology

The term 'repetitive' is often used interchangeably with the architectural term 'modular', as well as the geometric terms 'congruent' and 'isometric'. The following section will define each term and discuss its relevance to this research.

Repetitive. The term repetition is derived from Latin 'repetere', meaning 'to repeat or to demand back'. The act of repeating is focused on a reproduction, copy, or replica of the initial entity, and does not imply a transformation or manipulation. A repetitive element is understood as having the identical shape and size throughout its use.

Modular. The meaning of the term 'module' has evolved throughout history: Vitruv introduced the term 'modulus' in his Book IV on the rhythmic design of the Parthenon. The module was used as the common denominator of all building parts which defines the subdivisions and proportions of the Doric temple. During the industrialization of the 19th century, the module became the product of a series-production. In the 1950s, Konrad Wachsmann and Richard Buckminister Fuller developed architectural building-systems for space structures made from identical modular parts (***Ludwig and Cook 1998***).
"*In our digital age, CAD/CAM-Planning and fabrication technologies enable a more differentiated notion of the module*" (***Agkathidis 2009***). The module is moving away from identical components towards a "*parametric and associative diagram*" (***Tessmann 2009***).
Today, a module is not necessarily considered identical in scale nor in shape. It merely describes an architype, from steel-joint to cubic housing-cell, which can be modified in each iteration. It is therefore not synonymous with our understanding of a repetitive part.

Figure 2.2 *The modular housing complex, Habitat 67, in Montreal (**WM 2006**).*

Congruent. The term 'congruent' is derived from the Latin 'congruere', meaning 'to correspond, to coincide'. It is used synonymously with the word 'identical', meaning that two elements have the same shape and size. Two elements are congruent if they can be mapped onto each other by applying a congruence transformation or 'isometry', such as rotation or translation. Apart from this direct congruence, an opposite congruence can also be achieved by reflecting an element which preserves the length and angles, but flips the orientation. The term 'congruent' is used in this thesis to describe a repetitive parameter.

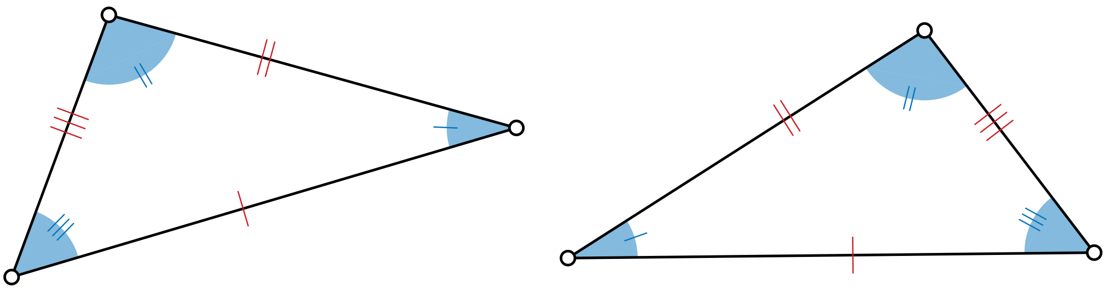

Figure 2.3 *Congruence. The two triangles are oppositely congruent, having the same shape and size, but alternating orientations (**ES 2018** based on **Pottmann et al. 2007a, p. 141**).*

Isometric. The term ‘isometry’ describes a congruence transformation which maps two congruent elements onto each other. An ‘isometric mapping’ extends this notion of congruence: It is the transformation of a point, curve or pattern from one surface to another, preserving length, angles and Gaussian curvature. This means that an isometric mapping is only possible between two surfaces of equal Gaussian curvature. This is the case for all single curved (developable) surfaces which can be mapped isometrically onto the plane.

Isometric mapping corresponds to our definition of ‘developable deformation’, which allow a geometric comparison of elastically bent edges or faces (defined in *Section 3.2.3*).

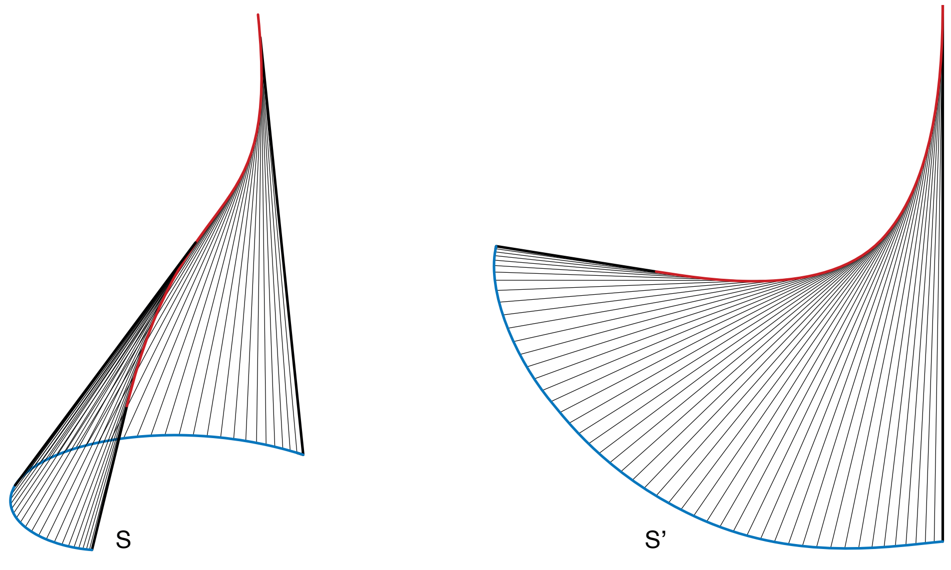

Figure 2.4 *Isometric mapping. A developable surface S is isometric to its unrolled planar image S’. This means that the length, angles, area and Gaussian curvature are preserved (**ES 2018** based on **Pottmann et al. 2007a, p. 496**).*

2.1.2 Perception

Repetition is addressed in geometric and constructive publications, meaning both congruent geometric entities and identical building parts. This might cause confusion when labelling a structure as ‘repetitive’. The following section looks at two exemplary sources, a review on Architectural Geometry (***Pottmann et al. 2015***), and a description of the construction of the Reticulated Dome in Neckarsulm (***Schober 2016***), which illustrate the perception of repetitive elements in theory and practice. At the same time, the publications introduce important criteria for the analysis and classification of repetition.

Geometry

The review on architectural geometry adresses repetition as an autonomous topic of geometric research. Pottmann et al. (***2015***) introduce important strategies and categories of repetition and give a short overview of structures which achieve repetitive elements with respect to nodes, edges and faces.
Within discrete meshes, Pottmann et al. (***2015***) differentiate between “*structures aiming at smoothness*” and “*non-smooth structures*”. The latter is seen as a strategy to achieve repetition: “*Element repetition for meshes is probably best achieved if one thinks of non-smoothness as a design element and intentionally plays with the rough surface, or with no surface at all”* (***p. 158***).
“*Real projects involving repetition*” are introduced as a separate section claiming that: “*In practice the problem of introducing repetition is circumvented rather than solved by not using true freeform structures at all”* (***p. 158***).

Tolerances are seen as a driver for repetition. They are especially relevant for the panelization of a structure rather than the structural grid itself. For smooth double-curved skins, the reuse of moulds is mentioned as a hidden repetivity; “*…hidden repetitive geometry is obviously highly relevant. Unfortunately, it is very difficult to detect in general”* (***p. 153***).

Gridshell construction

In his book on form, topology and structure of shells, Schober (***2010***) describes the principles of the *Netzkuppel* as an equilateral, quadrilateral network with freely rotating joints to form any freeform network with constant edge length. Subsequently, the construction of the Reticulated Dome in Neckarsulm is explained as follows: “The entire cupola, despite its double-curvature, consists of only identical parts: one type of butt-strap, one type of edge beam, and one type of cable clamp” (***p. 42***).

The project is constructed from identical parts despite variable geometric parameters (joint angles). While the repetition of edge beams is owed to the repetitive geometry of the Reticulated Dome (*Netzkuppel)*, the repetition of joints is achieved through an adaptable hinged construction detail.

Conclusion

The articles introduce several fundamental criteria of repetition, such as the separation of faces, edges and nodes, the differentiation between theory and practice, and the understanding of distinct strategies to achieve repetition. They pose the challenge that repetition is partly hard to detect, but propose no method to uncover or quantify it.
In all listed examples repetition is understood with respect to elements, not parameters. The repetition of building parts, however, is not necessarily consistent with that of geometric entities.
To enable a holistic analysis and design of repetitive structures, a differentiation of geometric parameters and constructive criteria will be introduced in *Chapter 3*.
Consequently, the remaining literature review examines both geometric and architectural developments.

2.2 Geometric Investigations

In geometric publications, the term ‘repetition’ is understood as the instalment of identical faces, equilateral edges or congruent nodes, while the investigation of planar faces or torsion-free nodes is considered a simplification rather than a repetition. Nonetheless, all methods are considered in this literature review if they lead to a repetition of geometric parameters.

The section is separated into discrete and smooth segmentations. The examples are roughly sorted by their geometric entity (face, edge and node) or strategy to achieve this repetition.

2.2.1 Discrete Segmentation

Repetitive faces

A common method in computational design is to transform an existing mesh, and optimize it to achieve a high number of identical faces based on a set tolerance. During this process, other geometric properties, such as surface proximity, edge continuity or alignment might be taken into account. By weighting the different optimization goals, the designer can choose how important repetition should be in influencing the overall appearance. The result is a compromise which best fulfils all requirements.

Such an optimization may result in a preferably low number of unique elements called “**equivalence classes**” (***Singh and Schaefer 2010***). Enforcing a reduced number of unique faces has a direct effect on the smoothness and curvature of the resulting mesh. This is well illustrated in the investigation on K-Set tilable surfaces (***Fu et al. 2010***).

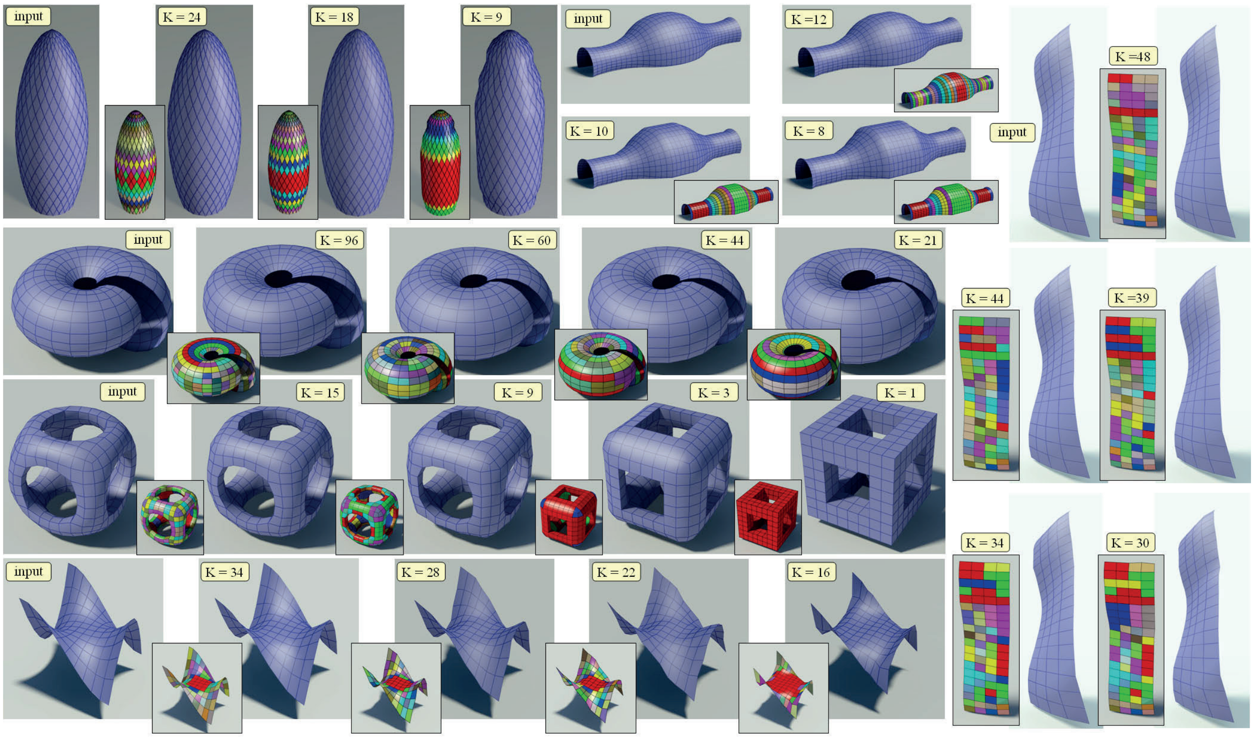

Figure 2.5 *K-Set tilable surfaces. Optimizing a mesh with the goal of reducing the number of unique mesh faces automatically creates a rough surface (**Fu et al. 2010**).*

Tiling an arbitrary shape with a limited number of unique tiles may only be achieved if a rough surface is accepted. Taking this concept to the extreme and generating a full repetition of all entities, one obtains a coarse mesh, as illustrated by a Lego model (***Lipson 2002***). Such a discretization is called a **voxel mesh**. Restricting each face, edge and node to a fixed building block not only results in a rough representation with considerable deviation from the reference surface, but it also restricts the orientation of panels in space. The shape is approximated solely by local changes in the mesh topology.
Huard et al. (***2015***) developed a method to rationalize a surface based on such regular space filling polyhedra, also called voxels. The method finds the intersection of a target surface with a three-dimensional "foam" of voxels and picks the closest faces in each polyhedra to create one continuous polyhedral surface with identical panels.

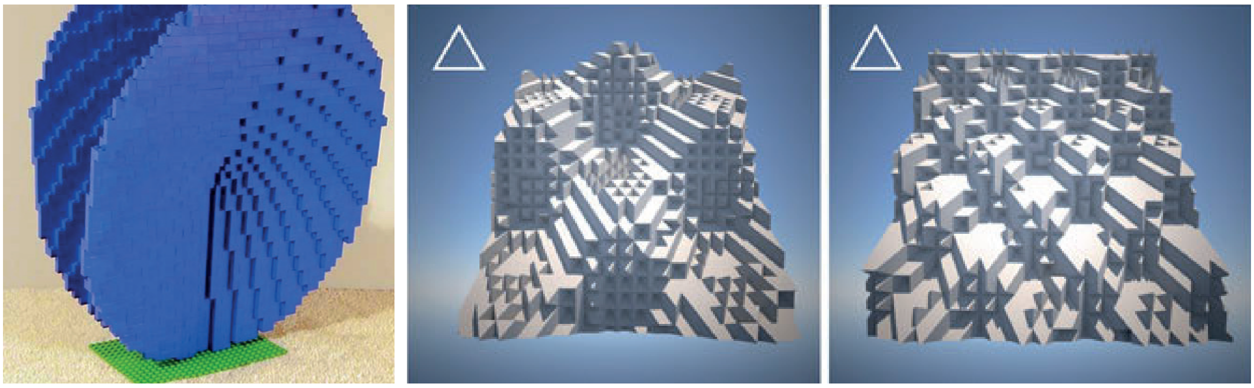

Figure 2.6 *Voxel meshes create polyhedral surfaces with just one repetitive face. Left: Lego model approximating a Catalan minimal surface (**Lipson 2002**). Middle and Right: Two voxel meshes approximating the same freeform surface at different resolutions using only equilateral triangles (**Huard et al. 2015**).*

A more flexible concept of a **rough, polyhedral surface** is illustrated by a crumpled piece of tiled cloth as was created by the designer Lisa Strozyk in the shape of wooden textiles (***Strozyk 2011***). A double-curved shape can be approximated by creating deep folds which account for the change in surface area. This approach creates a full repetition of faces (and thus edges), while accepting a varying kink between each face. The example shown in *Figure 2.7* approximates a semi-sphere creating a rough polyhedral mesh.

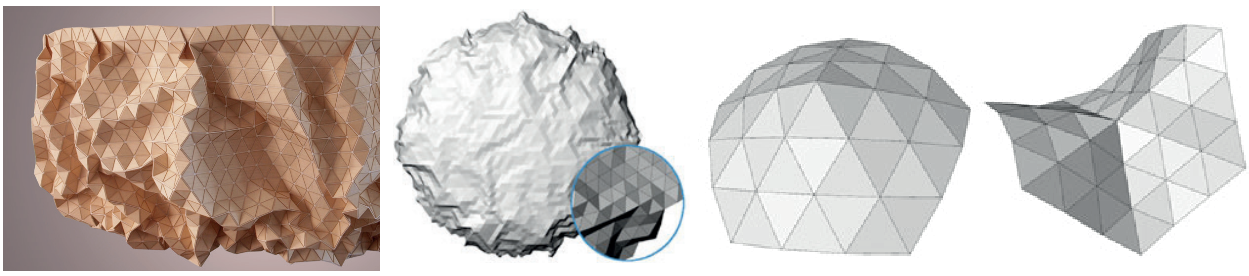

Figure 2.7 *Equilateral triangular meshes can be used to create either rough and "crumpled" polyhedral surfaces (**Strozyk 2011**) or discrete segmentations of developable surfaces (**Huard et al. 2015**).*

Such a network of **repetitive triangular faces** may also assume a smooth curved shape. However, its shape spectrum is restricted to single curved surfaces. French architect Alain Lobel presented a large number of meshes, called Lobel Frames, which are built entirely from equilateral triangles (***Lobel 2005***). By introducing singularities, Lobel creates convex curved shapes with kinks and folds, all of which approximate piecewise developable surfaces. A computational method to model these shapes was presented by Huard et al. (***2015***) illustrating both a rough and smooth tesselation with equilateral triangles.

In their article on **Triangle-Based Point-Folding Structures**, Zimmer et al. (*2012*) rely on standardized pyramidal moulds to produce the panels for a triangulated freeform surface. The same strategy was used for the ArboSkin façade mock-up in Stuttgart (*Köhler-Hammer 2013*).
The double-curved triangulated façade is built from identical pyramidal moulds which are cut individually to fit the varying triangular faces.

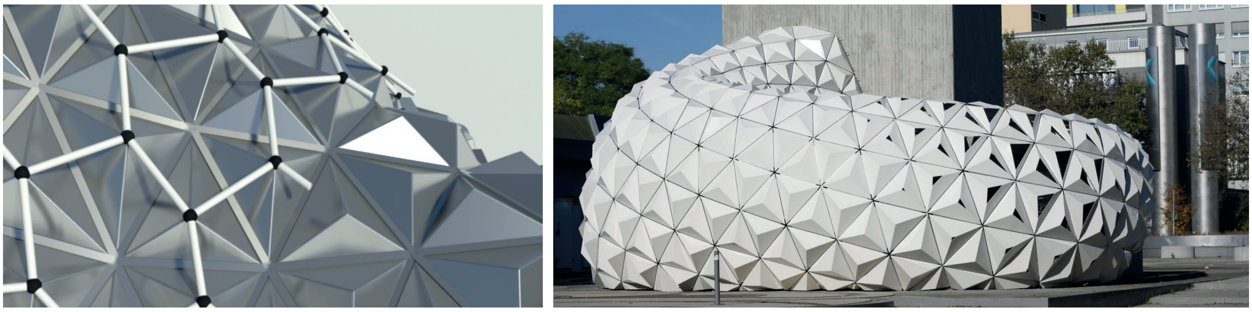

Figure 2.8 *Repetitive moulds: Triangle-Based Point-Folding Structure by (Zimmer et al. 2012) and the ArboSkin Façade mock-up (Köhler-Hammer 2013) both rely on standardized pyramidal moulds to produce panels for a triangulated freeform surface.*

Planar Faces

A less restrictive, but desirable goal is to create planar faces as they have decisive advantages for the fabrication of panels. While discrete triangles always have planar faces, hexagons and quads require systematic rationalization to achieve this property.

It is possible to tile any surface with **planar hexagons**. However, the Gaussian curvature has an effect on the hexagonal shapes. Positive Gaussian curvature creates convex, honeycomb-like hexagons, while negative Gaussian curvature produces non-convex hexagons (*Jiang et al. 2015*).

The design of a hexagonal mesh is usually achieved by means of duality to a triangular mesh (*Pottmann et al. 2015*): Troche (*2008*), for example, uses the nodes of a dual triangular tessellation to intersect a set of planes and thus create a hexagon tiling with planar faces. Another method is triangulating the Gaussian image of the surface and mapping this image back to obtain a planar hexagonal mesh (*Almegaard et al. 2007*).
Both approaches have limited control over the location of the final nodes. They are mostly successful if the initial triangular mesh is aligned with the principal curvature directions. This way, they exhibit the least amount of geodesic torsion, thus creating regular intersection edges, and naturally implementing singularities.

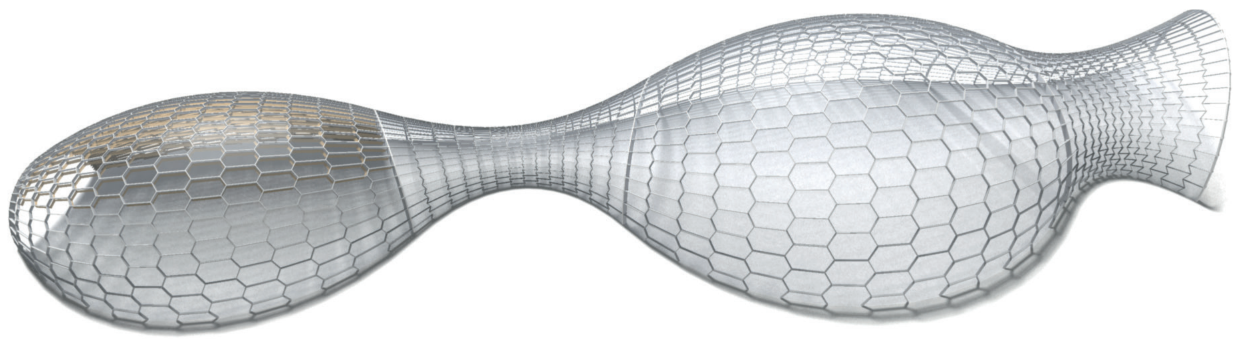

Figure 2.9 *A planar hexagonal network on a freeform surface displays convex hexagons in areas of positive Gaussian curvature and non-convex hexagons in areas of negative Gaussian curvature (Pottmann et al. 2007b).*

There is a large number of publications investigating **planar quad (PQ) meshes** and their geometric properties, computation and optimization in combination with other properties, such as rectangular panels or torsion-free nodes.
PQ meshes are geometrically defined as the discrete representation of conjugate curve networks (***Sauer 1970***). A network is conjugate if the two families of curves are related such that the tangent vectors of one family form the rulings of a developable surface at the intersections with a curve of the other family. For more background we refer to Pottmann et al. (***2007a, pp. 680–684***).

Any surface has an infinite number of conjugate curve networks and thus infinite solutions for a planar quad mesh. However, the closer this network is oriented to the principal curvature directions, the more rectangular the faces become. Conjugate curve networks are formed, e.g., by the meridian curves and circles of a rotational surface (which are at the same time the principal curvature directions) or the profile and path curves of a translational surface.[15]

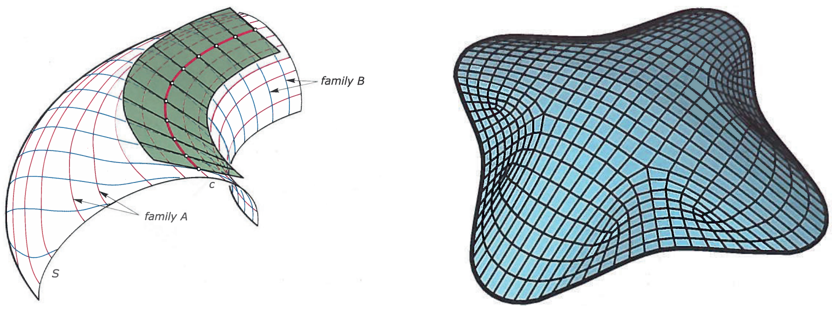

Figure 2.10 *Planar quad meshes. Left: Illustration of a conjugate curve network with tangent vectors as rulings of a developable strip (**Pottmann et al. 2007a, p. 680**). Right: An example of a PQ mesh which is designed towards the principal curvature directions (**Pottmann et al. 2007a, p. 683**).*

Translational meshes are modelled from a profile and a rail-polyline. Each profile-polyline is copied parallel to each vertex of the rail-polyline, creating a quadrilateral network with planar parallelograms.
Similarly, rotating a polyline about a central axis and connecting the vertices with polygonal circles creates a rotational mesh with planar trapezoids. Schober (***2016***) used polylines with equilateral edges to design reticulated shells. He devised more shape variations by linearly scaling and rotating the profile curves, stretching the profile curve from a central focus point or scaling the whole mesh in one, two or three dimensions. These variations are called ‘Scale-Trans-Surface’ and preserve the geometric property of planar faces but not necessarily of equilateral edges.

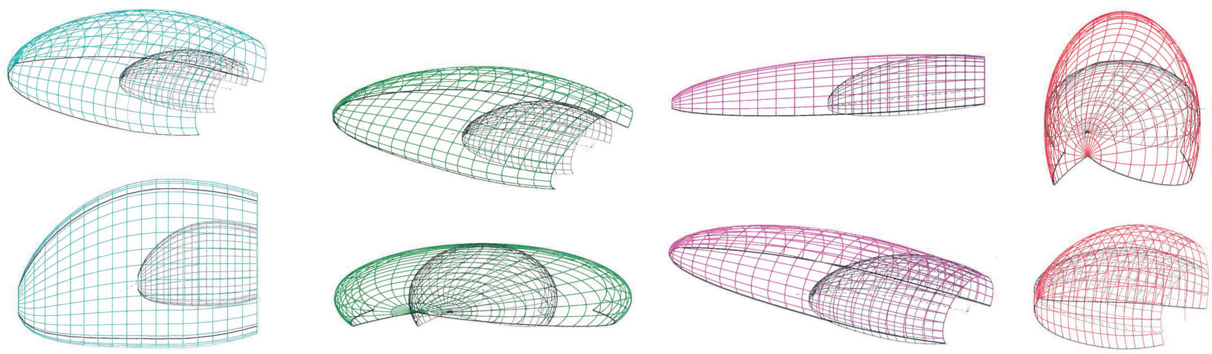

Figure 2.11 *Translational mesh and Scale-Trans-Surfaces. Deforming a translational mesh by scaling it in 3D, 2D or 1D, preserves the property of planar faces (**Schober 2016, p. 138**).*

15 The profile and path curves of a translational surface do not necessarily align with the principal curvature directions. The resulting PQ mesh may thus display extreme oblique angles.

Equilateral Edges

In differential geometry, equilateral, quadrilateral networks are called **Chebyshev nets**, named after the Russian mathematician who first described them in 1878 (***Chebyshev 1878***).

Naturally, equilateral edges are closely related to repetitive faces (as described above). If all faces are regular, all edges are of equal length as well. A constant edge length is also a property of the translational meshes.

An equilateral, quadrilateral net can assume any curved shape through the individual rotation of mesh angles. The initially square faces become rhombuses and thus account for the change in surface area (*Section 1.4.1*). Such a quad mesh does not necessarily have planar faces.

The Institute for Lightweight structures (IL) has conducted a series of experiments on the geometry of "the uniform mesh net with square meshes" to create prestressed or funicular structures (***Hennicke 1974***). A variety of **chain-models** with triangular, quadrilateral, hexagonal, hybrid and non-uniform mesh formats was tested. Only equilateral triangles do not allow for the tolerance in mesh angle. Hence, their shape spectrum is restricted to single curved surfaces or results in discontinuous, slagging edges (*Figure 2.12*, left). Quadrilateral and hexagonal equilateral nets, however, can be transformed into a broad spectrum of synclastic and anticlastic shapes. They are only limited by the maximum rotation of the mesh angles (***Bach and Kullmann 1975***).

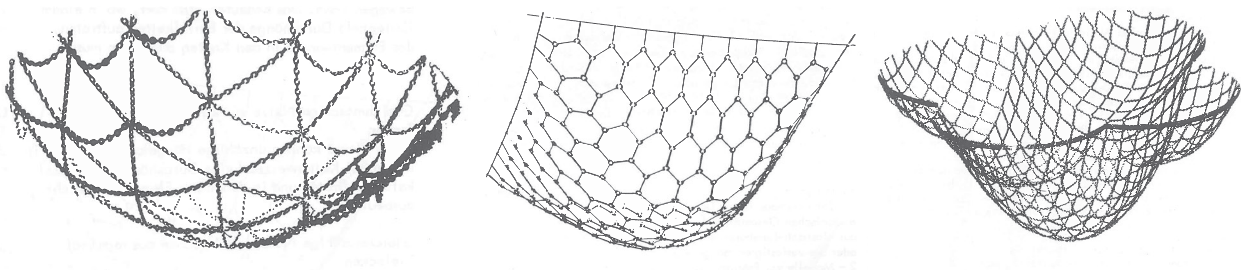

Figure 2.12 *Triangular, hexagonal and quadrilateral chain models with equilateral edges (**Hennicke 1974, pp. 43, 45, 85**).*

A more recent publication by ***Garg et al. (2014)*** looks at a computational approach to adapt Chebyshev nets to complex freeform surfaces to create wire mesh designs.

The research uses the **formula of Hazzidakis** (*1879*),

$$\int_D K(u,v)dA = 2\pi - \sum_{i=0}^{3} \alpha_i \qquad (2.1)$$

which states that the total curvature of a rectangular patch D of a Chebyshev net is equal to 2π minus the sum of its four interior angles α_i. In other words, if the total curvature of a surface is larger then 2π (the curvature of a semisphere), it is impossible to cover this patch with an aligned Chebyshev net without self intersection of the interior angles (compare *Figure 1.10* and *Figure 1.30*).

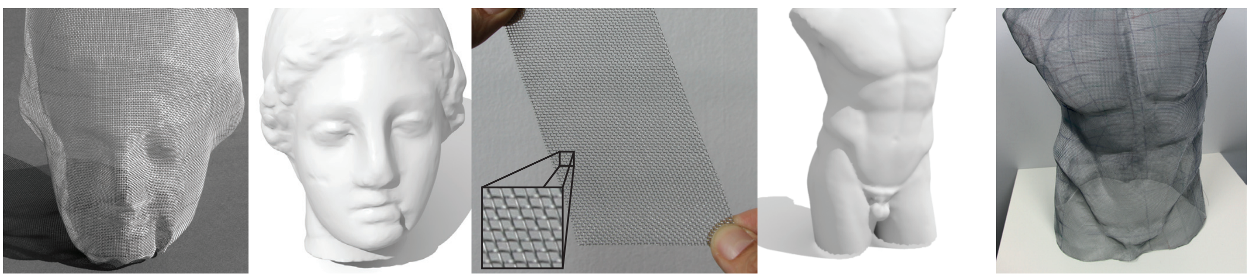

Figure 2.13 *Wire mesh designs made from interwoven material (**Garg et al. 2014**).*

Repetitive Nodes

There are a few methods which achieve a constant mesh angle while accepting a varying kink between faces, such as the Lobel meshes presented above.

Connecting the centre point of each triangle in such a network creates a dual, hexagonal network with regular angles of 120° between the "honeycomb walls" (***Jiang et al. 2014***).[16] Furthermore, all node axes are oriented normal to the surface. This quality is especially useful with respect to multi-layered structures.

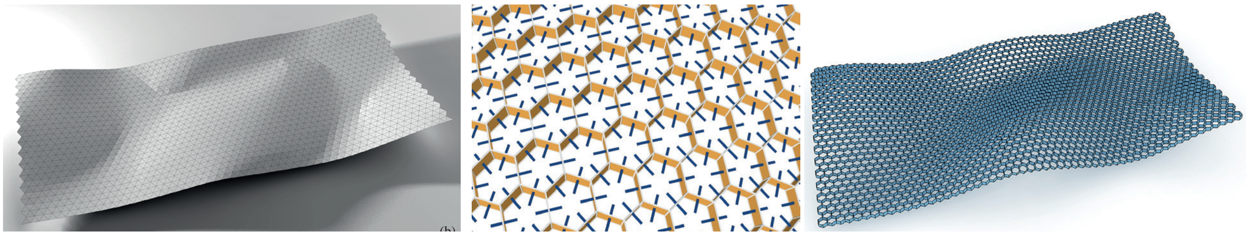

Figure 2.14 *Left: Discrete network from equilateral triangles. Middle/Right: Connecting the centre point of each triangle creates a dual, hexagonal mesh with constant mesh angle, measured in-plane (**Jiang et al. 2014**).*

Node Angles

In their publication on reticulated structures on freeform surfaces, Stephan et al. (***2004***) systematically explain the geometric parameters and related detailing of steel joints in a discrete segmentation. Their definitions are used as a basis of the parametric definitions for discrete segmentations in *Section 3.1*.

Three angles are differentiated – horizontal, vertical and twisting – which define the geometry of any steel node in relation to its centre axis.

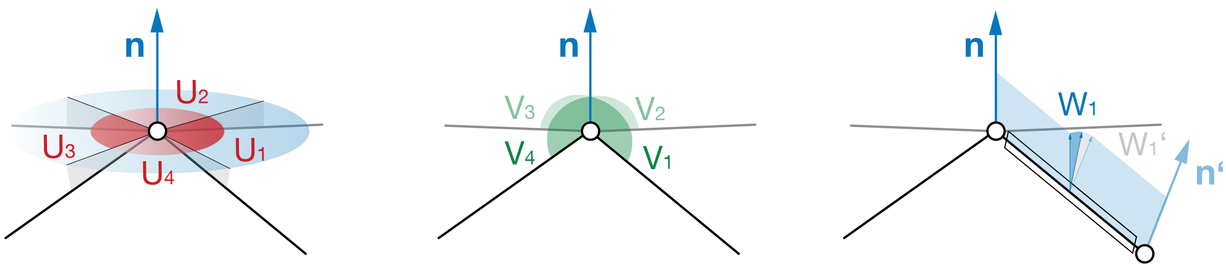

Figure 2.15 *Definition of three node angles U, V and W defining the horizontal and vertical arrangement, and twist at a joint (**ES 2018** based on **Stephan et al. 2004**).*

The horizontal angle (*Horizontalwinkel*) U_i is measured between two adjacent edges projected onto the tangent plane. Stephan describes a general dependency of U_i to the choice of network (hexagonal, quadrilateral or triangular).

The vertical angle (*Vertikalwinkel*) V_i is measured between each edge and the node axis. Stephan mentions a general dependency of V_i with the normal curvature of the surface.

The twisting angle (*Verdrehwinkel*) W_i is measured between the orientation axis of an edge and the plane created by the node axis and the edge. Again, Stephan conjectures a general dependency with the surface curvature.

16 This angle is not equivalent to the mesh angle measured between edges, but equates to its value in projection to the tangent plane. This angle is called the *Horizontalwinkel* by Stephan et al. (***2004***).

Offset Meshes

Creating a mesh offset is not trivial. Two meshes are offset if they are parallel and at constant distance to each other. The offset distance can be measured in between nodes, edges or faces. For triangular meshes, creating an offset mesh is not possible without changing the connectivity of the mesh.[17]
A common goal for quadrilateral and hexagonal meshes is to create a torsion-free, geometric support structure, meaning an arrangement of planar quads connecting the edges of top and bottom offset meshes, such that the edge-quads at a node intersect at a common node axis (**Pottmann et al. 2007b**).

For quadrilateral meshes, differential geometry offers three respective solutions of torsion-free support structures. Circular, conical and edge-offset meshes. They all create planar faces and respectively have a constant node, face and edge distance. They are aligned to the principal curvature direction.

- In a **circular mesh** each face is inscribed in a circumcircle through every corner. Circular meshes may assume any shape and allow a constant node-offset.

- In a **conical mesh** all faces at one node are tangent to a cone of revolution around the node axis. They may assume any shape and allow a constant face-offset.

- An **edge offset mesh** (EO mesh) is best found via its Gaussian image. Here, each face possesses a tangent incircle and all edges at one node are tangent to a cone of revolution around the node axis. This type of mesh, however, is limited to so-called L-isothermic surfaces.

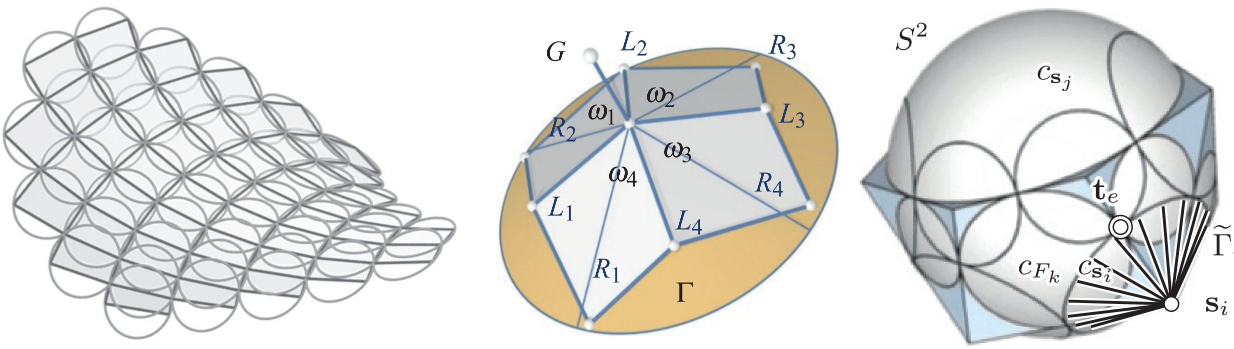

Figure 2.16 *Diagrams showing the requirements of a circular mesh (left) (**Pottmann and Wallner 2008**), a conical mesh (middle) (**Liu et al. 2006**) and the Gaussian image of an edge offset mesh (right) (**Pottmann et al. 2007b**).*

17 Few exceptions, such as spherical meshes or platonic solids, allow a constant offset of triangular meshes.

2.2.2 Smooth Segmentation

The main advantage of smooth segmentation is the simplification of nodes. As all edges and faces are curved, they meet tangentially without any kinks or folds and create planar, traversal nodes.

Smooth Repetitive Moulds

The greatest challenge when constructing smooth segmentations is the fabrication of curved faces. Eigensatz et al. (*2010*) investigate the possibility to classify the faces of a freeform-segmentation into a limited number of “shape proxies”, such as plane, cylinder, paraboloid, torus or “cubic” (meaning freely formed). Each face is first assigned to one of these generic moulds. Afterwards, the best fitting shape is created by individual alignment. By tolerating a slight kink angle between panels, as well as a divergence of the panel-edges and faces from the reference surface, a substantial rationalization can be achieved.

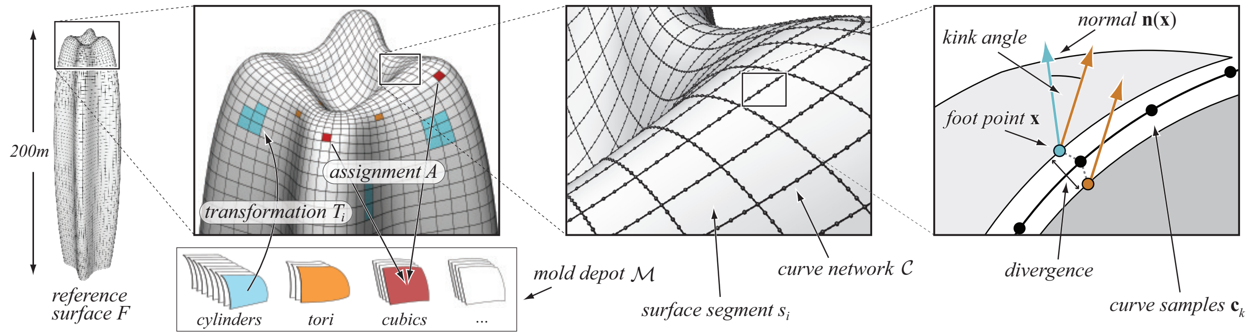

Figure 2.17 *Smooth repetitive moulds. Terminology and variables used in the algorithm by Eigensatz et al. (2010) determining repetitive moulds for the smooth panelization of freefrom surfaces.*

Developable Faces and Edges

A developable building skin can be attained by using a semi-discrete segmentation. The geometric principles are directly related to PQ meshes (*Section 2.2.1*). A linear arrangement of planar quads is nothing else than the discrete representation of a developable strip.

If a discrete, conjugate curve network is subdivided infinitely fine along one direction, it yields a smooth array of developable strips. This method is well documented (***Liu et al. 2006, Pottmann et al. 2008***) and has been implemented in the design of the Eiffel Tower Pavilions, which are constructed with single-curved panels following the principal curvature directions (***Eigensatz and Schiftner 2011***).

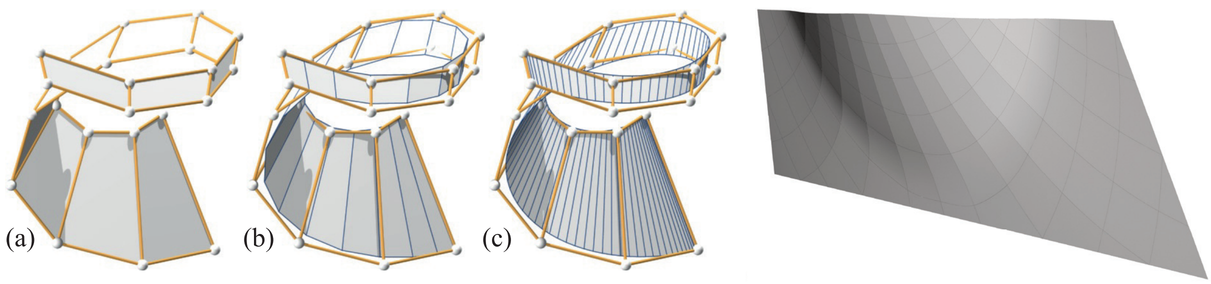

Figure 2.18 *Developable surface strips. Left: A discrete planar quadrilateral strip is refined to approximate a developable strip (**Liu et al. 2006**). Right: The Eiffel Tower Pavilions are an example of such a semi-discrete segmentation (**Eigensatz and Schiftner 2011**).*

For the additional simplification of having straight developments, Pottmann et al. (*2010*) propose a **panelization along geodesic curves**. To obtain a semi-discrete segmentation from nearly geodesic strips with constant width, the reference surface is partitioned separately allowing each pattern to better adjust to the principal curvature directions.

Geodesic curves may also be used to create grid structures from developable strips with straight unrollings. It is, however, difficult to create homogeneous networks from geodesic curves. A hexagonal pattern, e.g., is only possible on surfaces with constant Gaussian curvature.

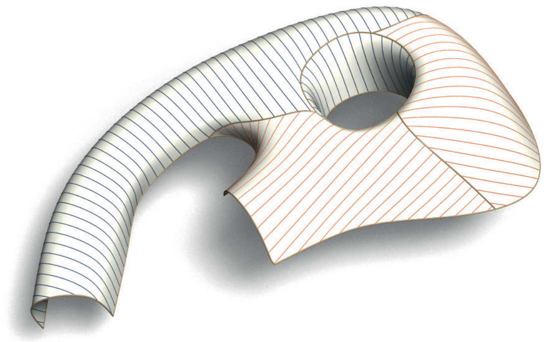

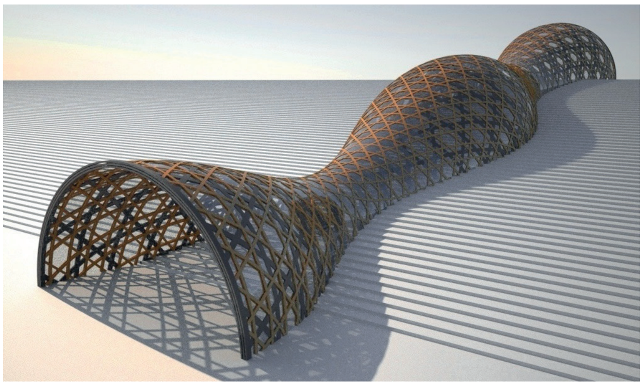

Figure 2.19 *Geodesic patterns on freeform surfaces. Left: A freeform surface is partitioned and then covered in geodesic strips with roughly constant width. Right: A freeform surface is segmented with a smooth tri-hex network approximating geodesic curves (**Pottmann et al. 2010**).*

Circular Arch Structures (CAS)

Disregarding the shape of panels, Bo et al. (***2011***) propose to optimize smooth quadrilateral and hexagonal networks to obtain circular edges and congruent nodes. First, the network is approximated with a discrete mesh. The edges are then computed as individual arcs meeting tangentially at every node. The result is a good approximation of a smooth network via basket arches. To additionally create radius-repetitive arches, Bo et al. propose a network along flow lines of constant curvature k. If the CAS network is aligned to the principal curvature directions, this method allows for congruent, torsion-free nodes in a multi-layered structure.

The cladding of such a CAS network can only be achieved if some kinks are tolerated: "*… there is in general no curvature-continuous surface which contains a given CAS if vertex valences are 4 or higher. This is because the curvatures of the arcs adjacent to a vertex do not match*" (**Bo et al. *2011***).

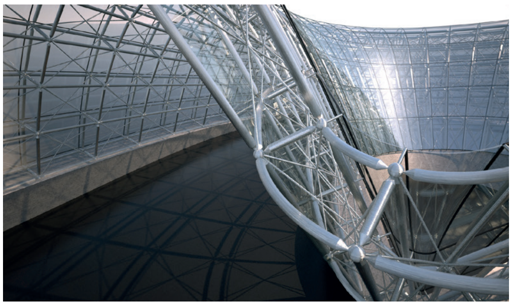

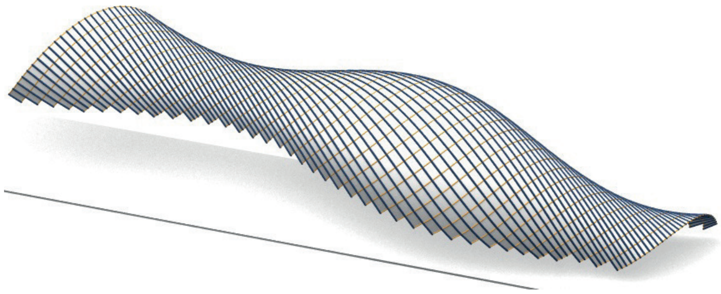

Figure 2.20 *Circular arch structures. Left: A freeform surface is approximated by a double-layered circular arch structure (CAS) with congruent nodes. The network is arranged along the principal curvature directions. Right: A radius-repetitive CAS is possible along flow lines of constant curvature (**Bo et al. 2011**).*

Smooth Offsets

A great potential of smooth segmentations lies in the simplification of multi-layered structures: Any smooth network has a defined offset geometry. If all offset-edges are oriented normal to the surface, the nodes inevitably are torsion-free.

In their paper on curved support structures, Tang et al. (*2016*) investigate the potential of a continuously curved beam layout from developable strips positioned either tangential or orthogonal to a given surface. Based on the three curvatures of a surface-curve τ_g, k_g and k_n (*Section 1.1.3*), Tang et al. analyse the developable properties of principal curvature lines, geodesic curves and asymptotic curves. Only principal curvature lines enable developable strips where rulings remain orthogonal to the guiding curve. Geodesic curves and asymptotic curves allow for straight development as tangential or orthogonal strips. However, their rulings are likely to incline, hindering the modelling process. This behaviour is described as a "*mutual exclusivity of 'good' properties*", as straight developments lead to "*bad*" rulings, and vice versa.
Tang implements further parametric constraints, e.g., the modelling of developable strips along curves of constant normal curvature, which result in a circular development.

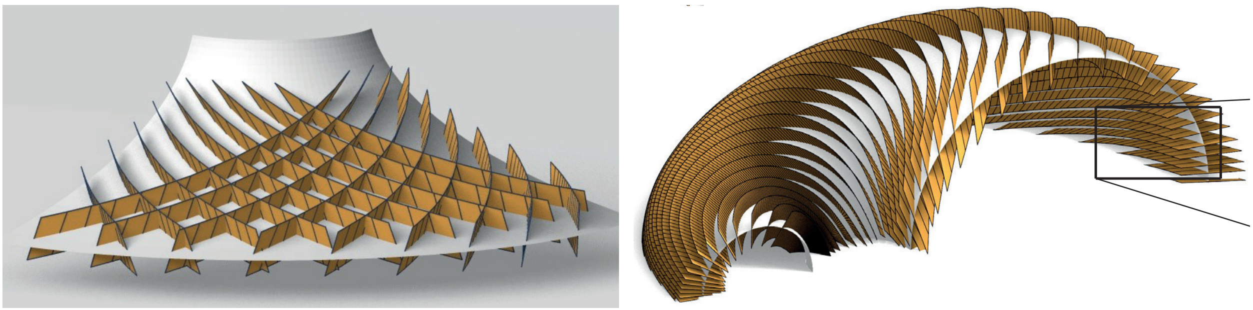

Figure 2.21 *Developable strips on freeform surfaces: Left: A network of developable strips along asymptotic curves. The rulings of strips are not normal to the surface. Right: Strips along constant normal curvature lines result in unrollings with constant radius (**Tang et al. 2016**).*

2.2.3 Conclusion

Geometric investigations focus mostly on discrete meshes. Repetitive faces or nodes can only be achieved if a rough surface or a restricted shape is accepted. Planar faces have been a major focus of research in architectural geometry. An alignment with the principal curvature directions produces most regular panels for quadrilateral and hexagonal networks. The combination of planar quads with equilateral edges has been one of the most succesfully used geometric rationalizations for reticulated gridshells.
Smooth segmentations, on the other hand, have only recently been studied in more detail. Here the focus lies on a simplification of faces either by creating repetitive or developable panelizations. Most recent publications look at the simplification of edges by either designing a constant curvature or using bendable, developable strips. This promising strategy will be investigated further in this thesis.

2.3 Architectural Developments

The development of curved grid structures in architecture is inseparable from the development of lightweight construction. Form-active structures enable a spatial load-transfer as a shell. This has been one of the main motivations to construct curved reticulated structures. However, there are other examples of curved building structures. Especially in modern architecture, freeform façades and curved grillages are a common feature. These structures display a variety of strategies both geometric and constructive to obtain repetitive elements and simplify the fabrication and assembly process.
The following section lists the most relevant examples of curved structural grids and façades. The references are sorted chronologically with regard to the leading planner or the most relevant building and give a short description of their repetitive qualities.

La Bourse De Commerce, in Paris, designed by F.J. Belanger (Architect) and F. Brunnet (Engineer), was the first **transparent rib-cupola**. Other key developments were the greenhouse at Kew Gardens (1845) and the Crystal Palace (1851) in London, as well as the Galleria Vittorio Emmanuele in Milan (1865), all of which use spherical calottes or cylinders with circular or straight beams arranged along the meridian and ring directions (***Schober 2016***).

Figure 2.22 *Early examples of reticulated structures all rely on rotational or cylindrical geometries: (Left to right) La Bourse de Commerce, Paris (**WM 2013**). Greenhouse at Kew Gardens, London (Photo: **Jonas Schikore 2018**). The Crystal Palace, London (**WM 1851**). Galeria Vittorio Emmanuele, Milan (**WM 2014**).*

The early development of lightweight constructions started with the work of **Johann W. Schwedler** and **Vladimir G. Shukhov** in the second half of the 19th century. Their structures mark the beginning of load-bearing gridshells creating a triangulated grid. Both engineers were largely influenced by the need for a simple fabrication and construction process.
Schwedlers reticulated copulas (first built at the Holzmarktstr. 28, Berlin, 1863) are constructed similarly to earlier cupolas along the meridian-curves and horizontal rings of a sphere taking advantage of multiple symmetry-axes. The primary, curved arched beams are connected with a polygonal ring structure and braced diagonally (***Kurrer 2013***).

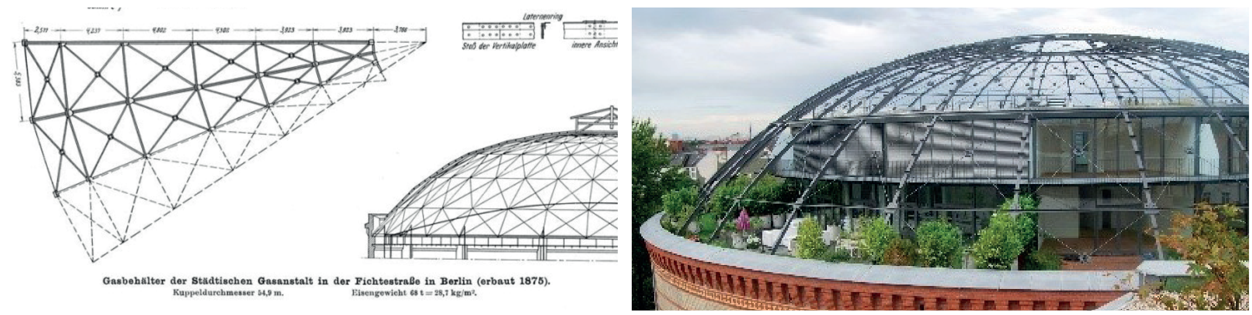

Figure 2.23 *Schwedler Cupola at the Holzmarktstr. in Berlin (**Kurrer and Lorenz 2009**).*

Shukhov expanded the form vocabulary, but remained within well-defined rotational and translational geometries. His famous hyperbolic towers (1896) enable the use of repetitive, straight profiles along the ruling of rotational hyperboloids. In the Nigres Tower at the Oka (looking at the top 5th segment), Shukhov uses standardized 24.8 m long L-profiles (L 100 x 100 x 10), which are twisted by up to 4°/m (a total of 72° degrees) to adjust their orientation to each connection joint (***Beckh 2012***)[18].
The parabolic gridshells in Vyksa (1897) are constructed from repetitive, diagonal arches, translated along a parabola-shaped truss frame. Similarly, to the Nigres tower, Shukhov implies a slight twist of profiles to accommodate a tangent connection at each joint (***Beckh and Barthel 2009***).

Figure 2.24 *Grid structures by Vladimir Shukhov: Left: The hyperbolic Nigres Tower at the Oka (Photo:* ***Matthias Beckh 2007****). Right: The parabolic gridshell in Vyksa (****WM 1897****).*

One of the most prominent historic examples of repetitive structures are the lamella roof systems from the 1920s. **Friedrich Zollinger** and **Hugo Junkers** developed construction systems in timber and steel which were built all over the world. Both systems are based on a rhombic grid on a barrel vault and allow the use of standardized lamellas with repetitive joints (***Tutsch et al. 2017***).

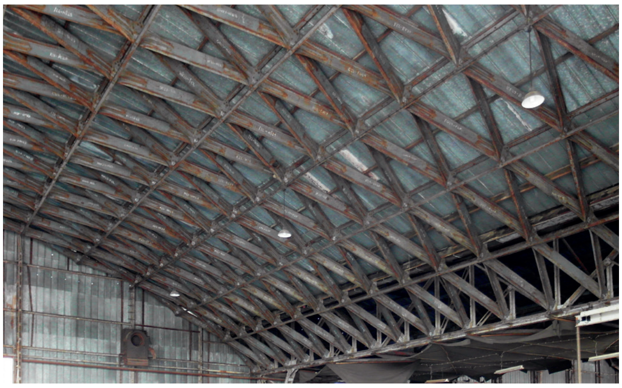

Figure 2.25 *Curved, modular lamella structures. Left: Zollinger Roof of the Marinaforum in Regensburg (Photo:* ***Joram Tutsch 2018****). Right: Steel lamella roof of the airplane hangar in Oberschleißheim by Hugo Junkers (Photo:* ***Joram Tutsch 2018****).*

In 1922, **Walter Bauersfeld** developed the first geodesic dome (*Section 1.4.3*) as the substructure of the Zeiss-Planetarium in Jena. The dome is constructed from 4000 rods comprising of only 50 different lengths. All joints are constructed identically and take up the differences in kink and mesh angle through a circular, notched disc which clamps the groove at the end of each rod (***Krausse 2011; Tornack 2012***).

18 In his dissertation, Beckh (***2012***) simplifies the influence of torsion based on a homogeneous twist (72° / 24.8m = 2.9°/m). The torsion of rulings of rotational hyperboloids is not constant but increases at the "waist-line". The maximal twist between two joints is (18° / 4.5m = 4.0 °/m).

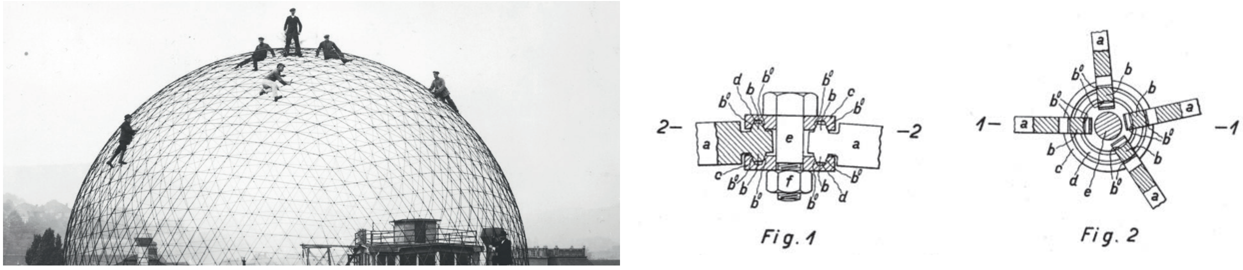

Figure 2.26 Left: The geodesic dome of the Zeiss-Planetarium in Jena ***(Krausse et al. 2011)****. Right: Patent by Bauersfeld and Schmidt showing the adjustable joint detail* ***(Tornack 2012)****.*

Max Mengeringhausen invented the component-based construction system, MERO, in the 1930s. Similarly in 1945, **Konrad Wachsmann** developed the so-called Mobilar Structure for transportable airplane hangars. Even though both techniques were initially designed for non-curved space trusses, the concept of a kit-of-parts was a key development for repetitive construction. Today Mero-TSK International and other companies offer a broad spectrum of standardized joint, bar and façade-elements for the construction of curved surface structures and façades (***Weber 2012***).

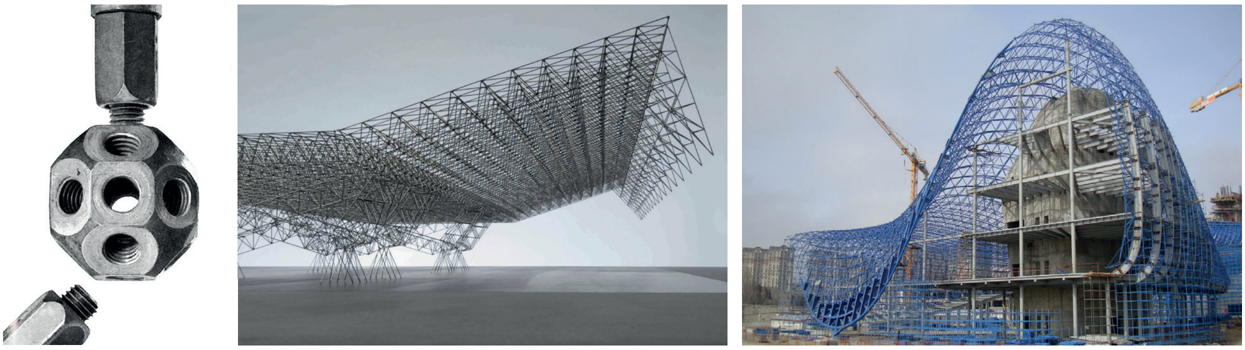

Figure 2.27 Component-based construction systems. Left: The MERO joint ***(Mengeringhausen 1975, p. 65)****. Middle: The mobilar structure by Konrad Wachsmann* ***(Nerdinger 2013, p. 208)****. Right: Spaceframe of the Heydar Aliyev Centre in Baku by Zaha Hadid* ***(Mero 2011)****.*

Richard Buckminster Fuller conducted extensive geometric research on packing and division of spheres. He further developed the geodesic dome, introducing a variety of new construction techniques and patents, which have led him and this building-type to substantial fame. Fuller's work includes the use of new materials, pneumatic and tensegrity structures, folding mechanisms and elastic constructions, and have thus influenced the development of space and shell structures until today (***Krausse and Lichtenstein 1999***). His experimental construction of a bent, geodesic plywood dome in 1957 is one of the first examples of a geometry-based approach to utilize elastic bending to create curved structures (***Lienhard 2014***).

Figure 2.28 Buckminster Fuller developed various techniques to construct geodesic domes, and deliberately employed the elastic deformation of material to ease fabrication. Left: The United States Expo Pavilion 1967 ***(Krausse and Lichtenstein 1999, pp. 424-425)****. Middle: Buckminster with his Dymaxion Car in front of his Fly's Eye Dome* ***(p. 379)*** *Right: Plywood Dome* ***(pp. 380-381)****.*

Félix Candela relied on hyperbolic paraboloids for his design of double-curved, reinforced concrete shells. This allowed him to simplify the formwork construction using only straight planks supported by straight beams. A further example of this geometry is the **Philips Electronics Pavilion of the EXPO 1958** in Brussels by **Le Corbusier and Iannis Xenakis**. Unlike Candela's poured-in-place method, Xenakis used concrete panels which were prefabricated from a simple sand mould, and held together by post-tensioned cables that followed the straight-line geometry of the hypars. Based on this construction process, the Phillips Pavilion can be regarded as one of the first examples of smooth panelization of a double-curved surface (***Sijpkes 2012***).

Figure 2.29 *Hyperbolic paraboloids are used as formwork to create hyperbolic shells or panels. Left: Formwork of the Church „Iglesia de la Medalla de la Virgen Milagrosa" by Félix Candela (**Faber 1965, p. 94**). Middle: Philips Electronics Pavilion at the Expo 1958 (**WM 1958**) Right: Sand mould for the panels of the Philips Pavilion (**Sijpkes 2012**).*

A central figure in the innovation of double-curved structures is **Frei Otto**, who investigated a vast number of natural form-finding and construction methods. His experiments with equilateral chain models have been discussed in *Section 2.2*. The equilateral quad-nets were realized both as tension-only cable networks, as well as compression-only gridshells:
The steel cable-net of the **Olympic Stadium in Munich**, 1972, was prefabricated as a uniform, quadratic net, and pulled into its double-curved geometry. The cables form a discrete, equilateral network with mesh size of 0.75 x 0.75 m. The varying mesh angle is taken up in the overlap joint at each cable intersection (***Bach and Kullmann 1975; Harbeke 1972***).

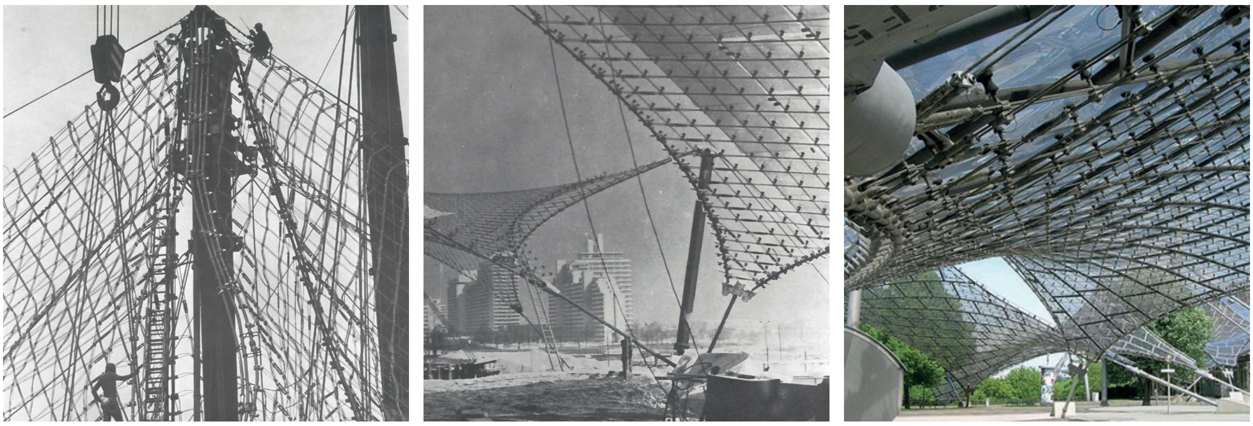

Figure 2.30 *The cable net of the Olympic Stadium in Munich during construction in relaxed and tensioned state (**Harbeke 1972, pp. 129, 132**), and after completion (Photo: **ES 2018**).*

Less noted but as important to the concept of repetitive structures is the **façade paneling of the Munich stadium**. The cable net is clad to a large extent with standardized, square, acryl-glass panels of 2.93 x 2.93 m, which are bent to adjust to the appropriate double curvature creating a seemingly smooth, double-curved façade. This repetition is achieved by accepting a varying gap in between panels.
This seam tolerance not only allowed the simplification of the geometry. It was also necessary to accommodate for the movement and deformation of the structure under varying loads. A flexible neoprene channel closes these gaps, and adapts to movement and tolerances. The roof panels were assembled with stacked seams, similar to a brick pattern. This created simpler joints and helped to adjust the layout of the square panels (***Bach and Kullmann 1975; Harbeke 1972***).

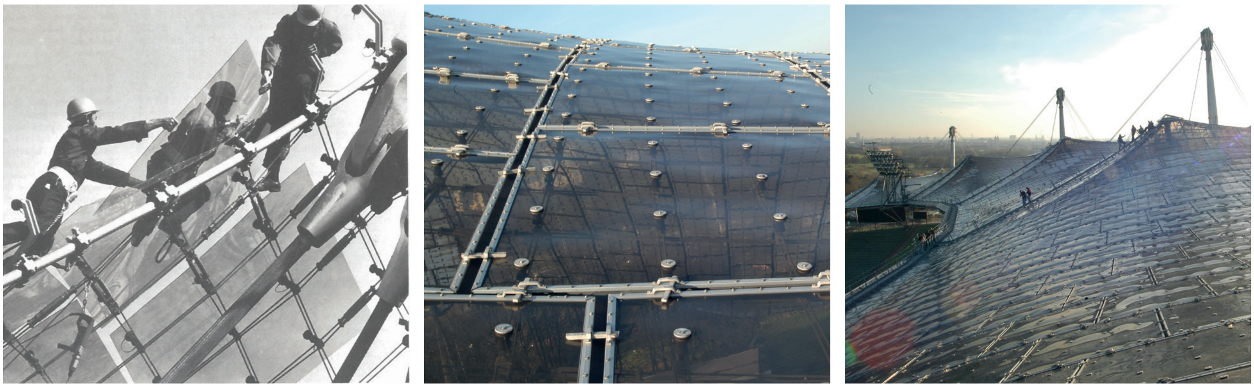

Figure 2.31 *The Olympic stadium in Munich is covered with largely identical acryl-glass panels. During construction (**Harbeke 1972, p. 136**) and after completion (Photos: **ES 2015**).*

The **Multihalle in Mannheim**, 1974, was the first so-called “strained” gridshell which utilized elastic deformation to create a double-curved lattice structure from straight wooden laths. The uniform lattice grid with 0.5 x 0.5 m edge length was assembled flat and subsequently pushed up into the desired geometry. This method creates a smooth quadrilateral network with constant edge length. The hinged joints adapt to the varying intersection angle (***Happold and Liddell, 1975***). The constructive details of the Multihalle in Mannheim will be further discussed in *Section 2.4*.

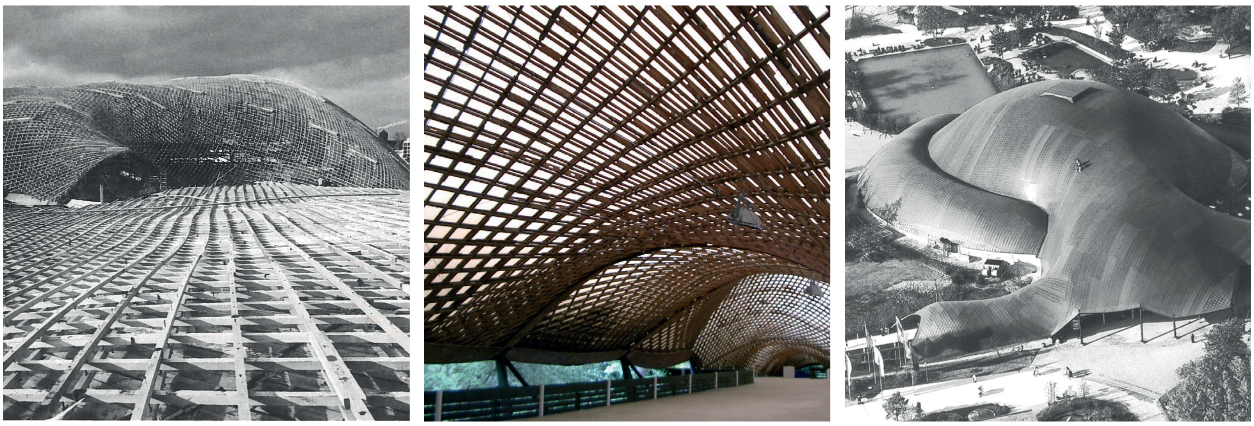

Figure 2.32 *The Multihalle in Mannheim is constructed with a uniform timber lattice. Left: During construction (**Barthel 2005, p. 287**). Middle: Interior View (Photo: **Rainer Barthel 2007**). Right: View from above (**Barthel 2005, pp. 284**).*

The timber gridshell of the **Brinebath in Bad Dürrheim**, 1987, was designed as a smooth quadrilateral network. The layout is designed to approximate the path the principal stress trajectories, creating meridian slope-lines and horizontal rings, most of which display a spatial form. The timber elements were prefabricated individually and assembled on site. The timber grid was braced with two diagonal layers of

laths to create a load-bearing gridshell.
The layout was chosen purely for its structural advantages. However, this segmentation generally results in perpendicular intersections which can be fabricated simply as notch connections (***Wenzel et al. 1987***).

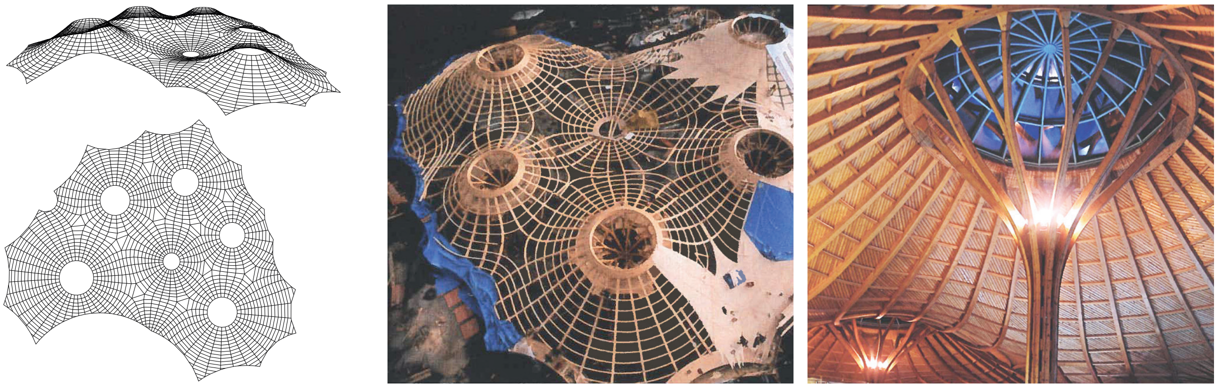

Figure 2.33 *Brinebath in Bad Dürrheim. Left: Network design (**ES 2018** based on **Wenzel et al. 1987**). Middle: Construction Site (**Linkwitz and Veenendaal 2014, p. 150**). Right: Interior view (**p. 142**).*

The **Reticulated Dome in Neckarsulm**, 1989, was designed as an equilateral, quadrilateral network. The dome of 25.2 m diameter and 16.5 m spherical-radius is constructed from 1.0 m long, curved edges and spherical panels. All edge beams are fabricated identically and follow a geodesic path from node to node on the sphere with a constant curvature radius of 16.5 m. Similarly, the spherical glass panels have a constant double curvature and could be produced with the same spherical mould.
Schober differentiates the mesh angle (*Maschenwinkel*) measured between two adjacent edges, and the geodesic angle (*Knickwinkel*) which measures the deviation from a traversal node. Both angles are variable within this structure, but are taken up by the adaptable joints.
Two butt-straps are connected by a central bolt permitting a rotation of 90° - 65° to adjust the *Maschenwinkel*. The edge beams are connected via two bolts, one with a tight fit, the other with an elongated hole, to allow for the additional deviation of the *Knickwinkel* (***Schober 2016***).

Figure 2.34 *Joint, interior and façade of the Reticulated Dome in Neckarsulm (**SBP 1990**).*

The geometric contributions of **Schlaich and Schober** on translational meshes have been discussed in the previous section (*Section 2.2.1*). The **House for Hippopotamus at the Berlin Zoo**, 1997, is a built example of such a mesh. It was designed as two separate parabolic translational meshes which are connected with an anticlastic, non-uniform network. This central grid acts as a transition from one translational mesh to the other. The two domes are built entirely from 1.2 m long rods and planar glass panels (***Schober 2002***). The varying mesh and kink angles at each node were fabricated individually within the splice-connector joints (***Stephan et al. 2004***).

Figure 2.35 *Exterior view and geometry of the translational gridshell of the House for Hippopotamus, Berlin Zoo (**Schober 2002**).*

Frank Gehry is a pioneer in digital design for architecture. His software company, Gehry Technologies, developed modelling tools for developable surfaces and geometry rationalization, simplifying the supporting structure and façade panelling of freeform surfaces. Gehry widely applied the use of single-curved, rectangular panels of glass and steel which can be bent to fit the building geometry. The Fondation Louis Vuitton in Paris specifically employed the use of identical flat panels of 1.5 x 0.4 m which were vacuum moulded into their individual curvature (***Shelden 2002; Mathewson and Gehry 2007***).

Figure 2.36 *Gehrys designs use developable surfaces. Left: Walt Disney Concert Hall, Los Angeles (**WM 2012**). Middle: Weatherhead School of Management in Cleveland (**Shelden 2002, p. 323**). Right: Fondation Louis Vuitton in Paris (Photo: **Fred Romero 2008**).*

An example of both simplified geometry and façade construction is the canopy of the **Strasbourg Train Station**, 2006, designed by Duthilleul in cooperation with RFR engineering. The double-curved glass façade is designed as a toroidal form, producing cylindrical glass elements with only four different radii of curvature. Instead of using hot-bent panels, the curved glass elements were bent elastically and laminated to fix their form (***Kassnel-Henneberg 2010; Januszkiewicz and Banachowicz 2016***).

Figure 2.37 *Strasbourg Train Station. The toroidal façade is constructed from cylindrical glass panels (**SE 2006**).*

The **Kogod Courtyard Roof**, 2007, in Washington DC is a freeform surface. Here, the quadrilateral panels are constructed as a scaled, discontinuous skin to allow for planarity. The steel structure, on the other hand, is optimized to create nearly torsion-free nodes. As a result, adjacent edges meet approximately in a common node axis, which is, however, not necessarily normal to the design surface (***Jiang et al. 2013***).

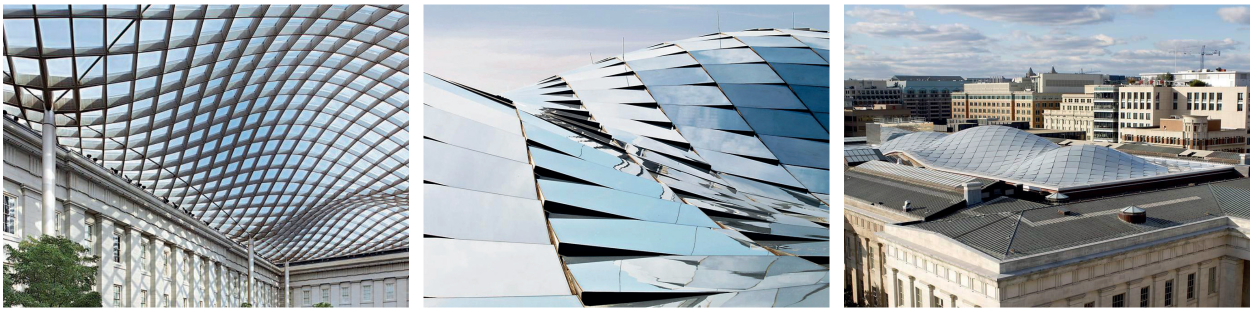

Figure 2.38 *The Kogod Courtyard Roof in Washington DC. The façade is scaled to allow for planar panels (**FP 2007**).*

The **Yas Viceroy Hotel**, 2009, in Abu Dhabi follows a similar strategy of "scaling" the façade and optimizing the node orientation. A subdivision routine creates nearly torsion-free joints. The node axes follow the rulings of developable strips orthogonal to the design surface (***Wang et al. 2013; Pottmann et al. 2015***).

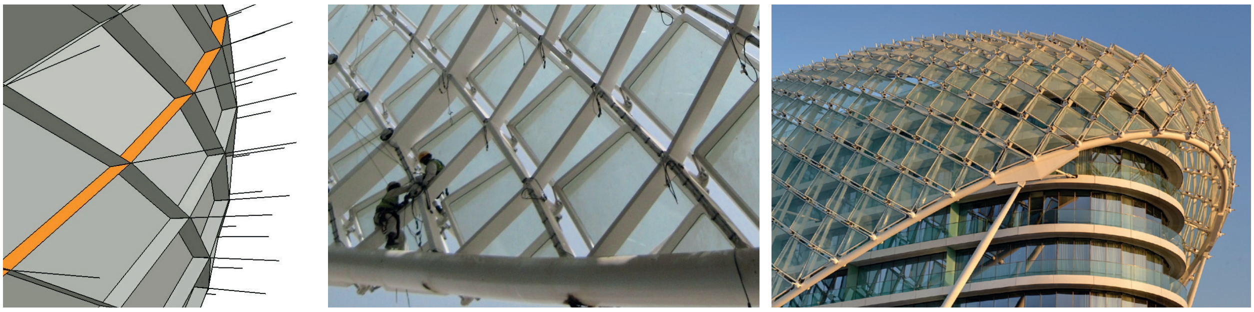

Figure 2.39 *The Yas Viceroy Hotel in Abu Dhabi. The façade structure is optimized for torsion-free nodes (**Pottmann et al. 2015; SBP 2009**).*

A pragmatic way to create torsion-free edges and nodes is by enforcing a vertical beam layout, as was done at the **Metrosol Parasol**, 2011. The design surface is chopped vertically into a regular, quadrilateral 1.5 x 1.5 m pattern in plan. In this case, any relation of beam- and surface-orientation is given up. The beams are fabricated as continuous, flat profiles with variable height. The nodes vary in height but have consistent vertical axes and congruent intersection angles in plan. This design method leads to substantial distortion of the network in areas of steep inclination. Here the vertical height of beams and nodes increases drastically (***Schmid and Fischer 2010***).

Figure 2.40 *The Metrosol Parasol in Seville uses a vertical, orthogonal beam layout (**MPA 2011**).*

The smooth segmentation of the **Centre Pompidou in Metz**, 2010, by Shigeru Ban, was designed with the same method by vertically projecting a homogeneous (tri-hex) pattern onto a reference surface. The network shows extreme distortion in areas where the surface is steep. The orientation of edges and nodes, however, is aligned with the surface, and has a constant offset distance. The network is constructed from four interlaced layers of continuously curved timber beams. Similar to the Brinebath in Bad Dürrheim, all beams have a spatial geometry and needed to be prefabricated individually. The smooth segmentation allows for planar, traversal joints (***Kockelkorn 2008***).

Figure 2.41 *The Centre Pompidou in Metz. The tri-hex network is constructed from individually curved timber elements (**SBA 2010**). Right: The tri-hex network was projected onto the design surface (**ES 2018** based on **Kockelkorn 2008**).*

The smooth network of the **Eiffel Tower Pavilions**, 2014, is aligned towards the principal curvature directions enabling nearly torsion-free edges and developable faces. The curved mullions could thus be prefabricated from flat strips of steel. The façade was rationalized further and constructed with cylindrical panels, with only slight kinks and discontinuities at the vertical joints (***Schiftner et al. 2013***).

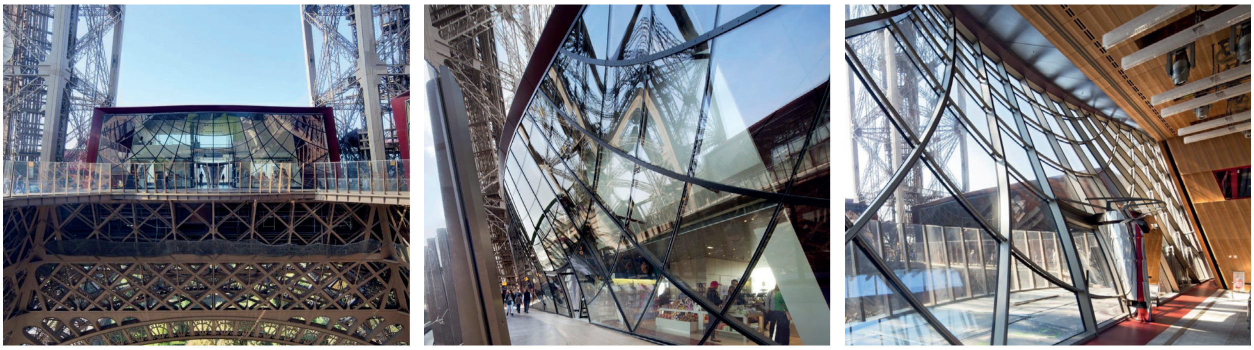

Figure 2.42 *The Eiffel Tower Pavilion in Paris. The network follows lines of principal curvature. This simplifies the geometry of both steel structure and glass panels (**MR 2014**).*

Conclusion

Historically, the shape of reticulated structures has been either cylindrical or spherical, with few exceptions of other traditional surfaces, such as rotational or translational geometries. In particular double-ruled surfaces (such as rotational hyperboloids or hyperbolic paraboloids) have been used to create double-curved structures from straight profiles.

A drastic liberation of design shapes was initiated by Frei Otto and progressed with the development of computer-aided modelling tools. This sparked the development of various digital design and fabrication techniques.

Today, we can observe a diverse combination of discrete and smooth networks for load-bearing structures and façades. Additional to geometric rationalizations, adaptable construction techniques (using tolerances, hinges and deformation) open up further possibilities to simplify building parts.

2.4 The Multihalle in Mannheim

The geometric advantageous of the Multihalle in Mannheim have been briefly discussed in *Section 2.3*. The following review takes a closer look at the assembly and construction details used in this strained timber gridshell. The construction method of the Asymptotic Gridshell, inspired by this paradigm, will be presented in *Chapter 6*.

Assembly

Frei Otto's gridshells utilize elastic deformation to create a double-curved lattice structure from straight wooden laths. The lattice grid is assembled flat and held together by pinned joints. The combined flexibility of elastic laths and scissor joints allows this grid to take on virtually any shape within the permissible bending radii and node range (see *Section 5.1.3* on smooth equilateral quad networks).
The structure is erected using multiple support "stamps", which push the grid up and determine the desired double-curved shape. During this deformation process, the square grids are transformed into varying parallelograms. The final geometry is secured by tightening the joints, fixing the quadrilateral network along the support-edges, and bracing the diagrid with diagonal steel cables.

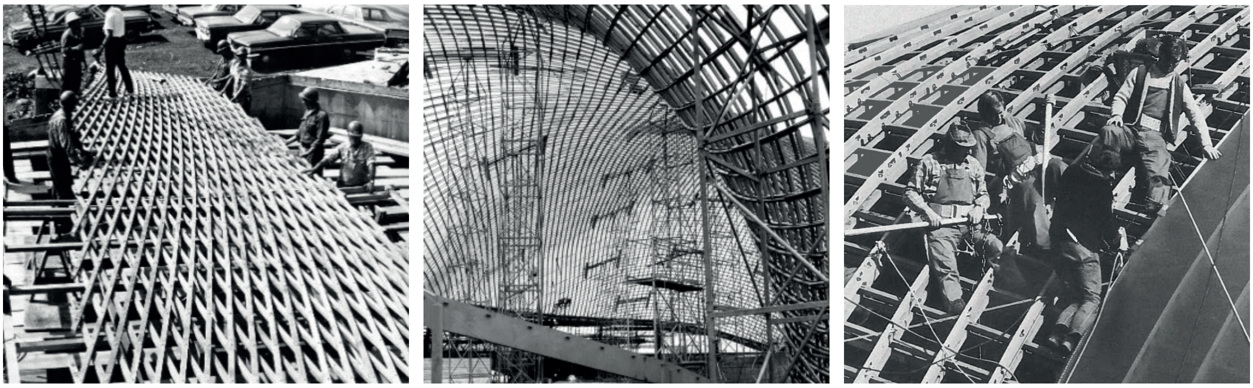

Figure 2.43 *Construction process of the Multihalle in Mannheim. Left: The lattice grid is assembled flat (**Glaeser 1978, pp. 59**). Middle: The grid is erected with scaffolding „stamps" (**Glaeser 1978, pp. 60**). Right: The facade is installed (**Barthel 2005, p. 287**).*

Details

The elastic erection process called for slender laths and flexible joints. At the same time a high stiffness in-plane and out-of-plane was necessary to prevent buckling and deflections. It was achieved in-plane through the rigid supports and diagonal steel cable ties, and out-of-plane through the joint connections and additional shear blocks.
The following three details – typical grid joint and ties, shear couplings, and supports – show commendable solutions for a strained gridshell.

Typical grid joints and ties. The 50 x 50 mm timber laths were connected with a central bolt allowing for an in-plane rotation during the erection process. To activate the additional stiffness of the double-layered grid, shear forces had to be transmitted at every node. This requirement was opposed by the need for a sliding joint (long hole) to accommodate the variation of edge length at the top and bottom layers, thus prohibiting the use of mechanical connectors. The shear stiffness was achieved by introducing high clamping forces using a spring and bolt, which created sufficient friction.
The rotational stiffness of the joints, as well as the diagonal stiffening effect of the PVC skin, proved to be too low to brace the structure. However, a significant in-plane stiffness was essential to the load-bearing behaviour. Consequently, a pair of 6 mm steel cables was installed at every sixth diagonal axis (at 4.5 m distance), and was fixed at every node to transmit the high tension forces (***Burkhardt 1978, p. 112***).

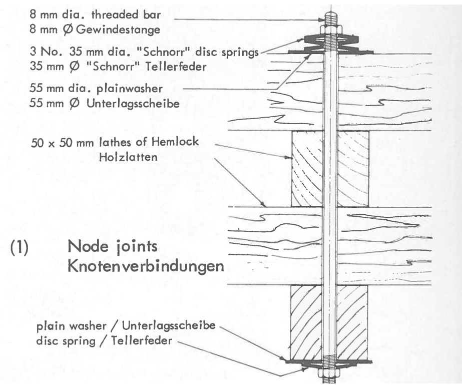

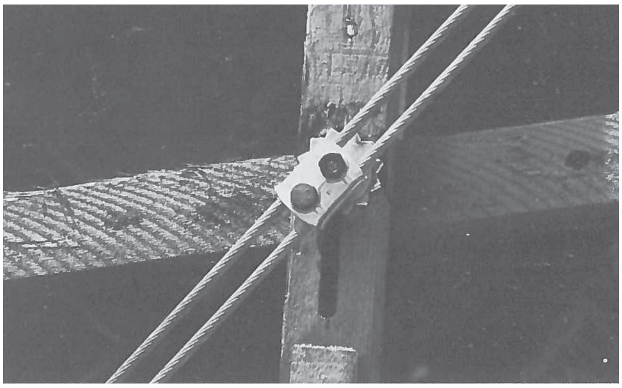

*Figure 2.44 Typical grid joint and diagonal cables of the timber gridshell (**Burkhardt 1978, p. 112**).*

Shear couplings. Due to the high axial load in some areas of the grid, the out-of-plane shear stiffness needed to be increased. This was achieved by adding blocking pieces between the top and bottom laths. At each shear connection, two wedges were adjusted to the right offset and clamped with three bolts and springs to create the necessary friction (***Burkhardt 1978, p. 114***).

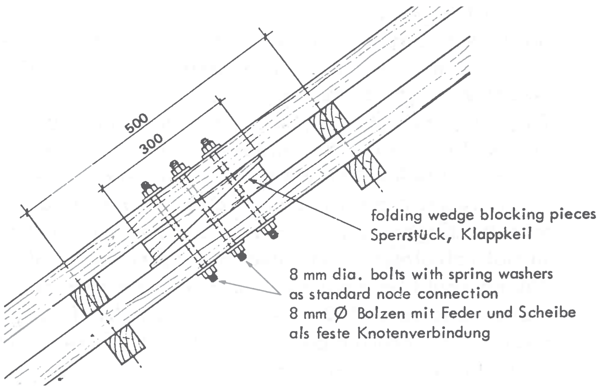

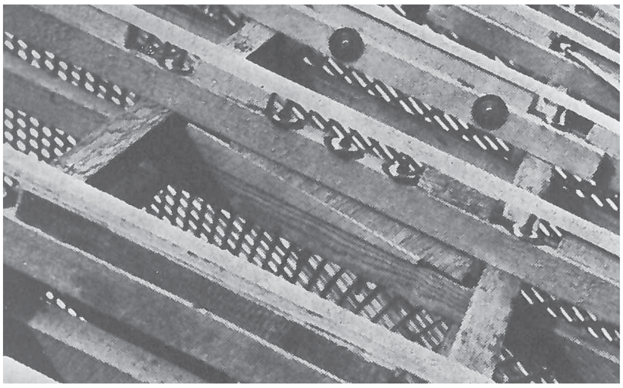

*Figure 2.45 Detail of shear blocks connecting the top and bottom layers (**Burkhardt 1978, p. 114**).*

Supports. The Multihalle in Mannheim displays multiple boundary situations, such as cable supports, walls and arches. At the lower horizontal supports, the timber lattice is simply bolted onto a curved plywood board, which in turn is held by individual brackets fabricated to the correct angle. The brackets experience a bending moment due to the eccentric connection and are bolted rigidly onto a horizontal concrete wall (***Burkhardt 1978, p. 117***).

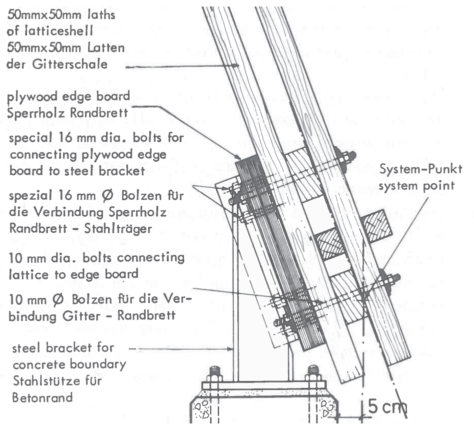

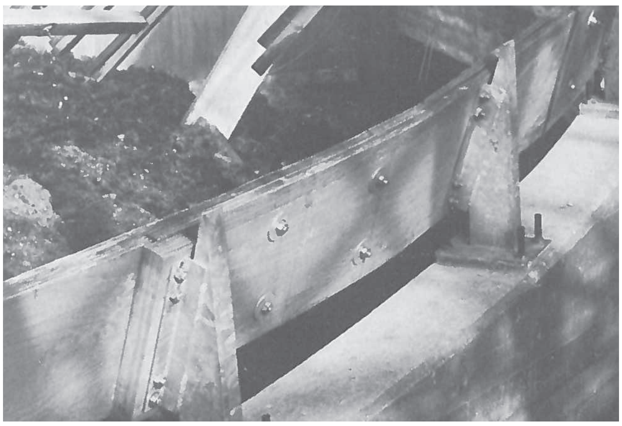

*Figure 2.46 The horizontal supports are adjusted with individual brackets (**Burkhardt 1978, p. 117**).*

PART II
REPETITIVE STRUCTURES

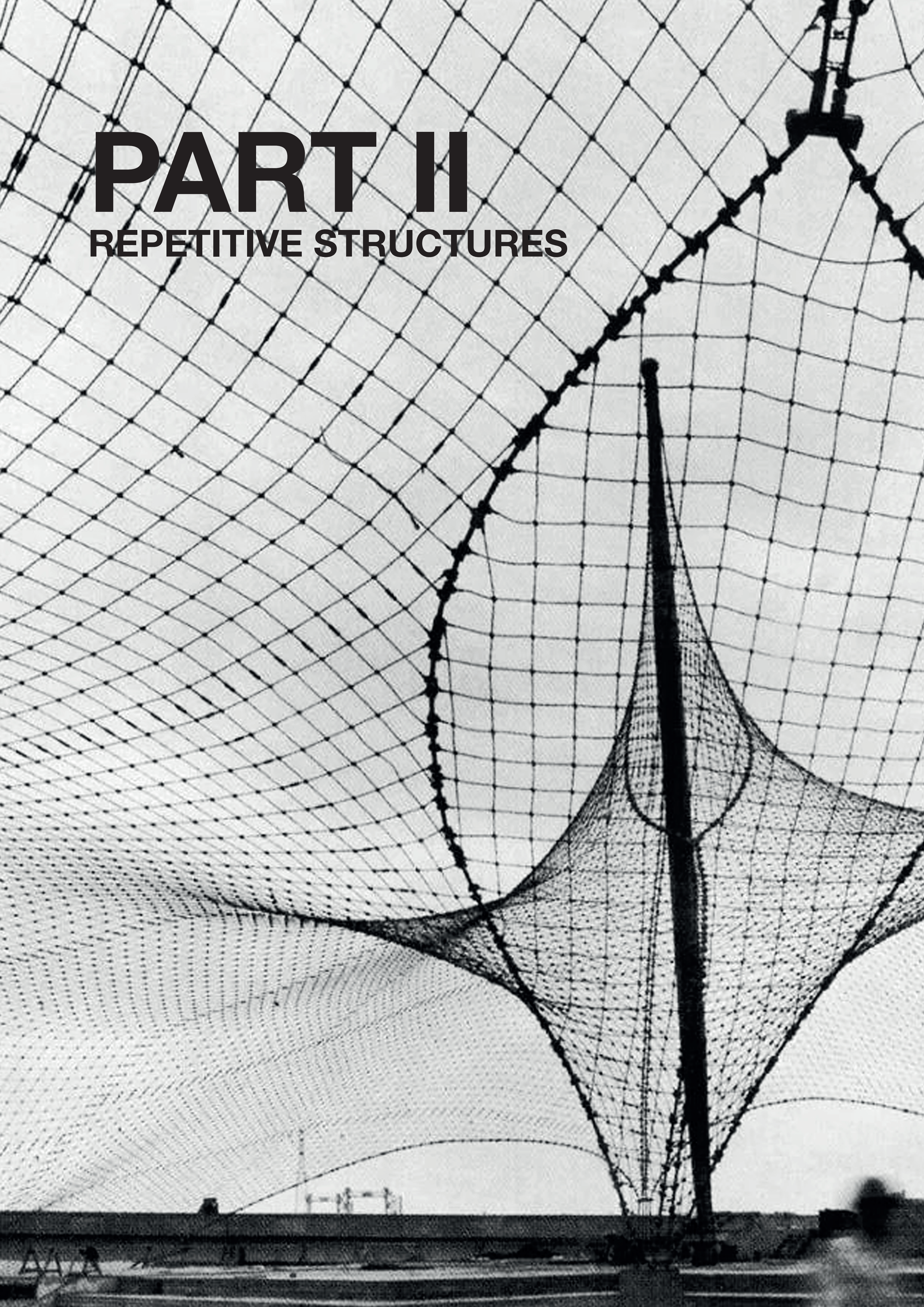

3 Theoretical Framework

In order to classify and quantify repetition within double-curved networks, a novel theoretical framework is created which separately lists geometric parameters and constructive criteria. The framework is used in subsequent investigations to analyse and design repetitive structures.

- *Section 3.1* describes the geometric parameters of networks. It is separated into smooth and discrete segmentations, and lists their parametric dependencies.

- *Section 3.2* introduces constructive criteria which create identical building parts by diverging from, or adapting to, the geometric reference. We focus on deformation as a strategy to construct smooth segmentations, and list requirements for the correlation of curvature and deformation of beams.

- *Section 3.3* discusses further criteria of repetition, such as precision, extent, choice or relevance of parameters in order to avoid misinterpretations.

- Finally, in *Section 3.4* all strategies to attain repetitive parts are concluded.

Figure 3.1 *Cable net of the German Pavilion, Expo1967 in Montreal during construction (**Wilhelm and Otto 1985**).*

3.1 Geometric Parameters

The segmentation of a surface results in three geometric entities: nodes, edges and faces. Each entity is defined by a combination of parameters. We distinguish between smooth and discrete segmentations (Section 1.3.1) as they lead to varying parameter sets. The parameters are described and illustrated for quadrilateral networks, as these are of predominant interest for this thesis. They can, however, be applied to any other network. If a parameter is kept constant throughout the structure, this parameter is fully repetitive.

The parameters examined in this thesis are selected to explain the geometric effects of repetition. Further parameters focusing on specific detail solutions, such as the thickness of a profile or the diameter of a joint, are not relevant for this comparison.

Multi-layered structures. The parameters aim to include the design of so-called multi-layered structures. In this case, the network is offset creating two layers of corresponding nodes, edges and faces. Each node in a multi-layered structure is represented by an axis connecting the top-node to the bottom-node. The edges become two-dimensional strips, or quads, connecting the top-edge with the bottom edge. Each face has a parallel offset face. If all nodes are torsion free this is called a geometric support structure.

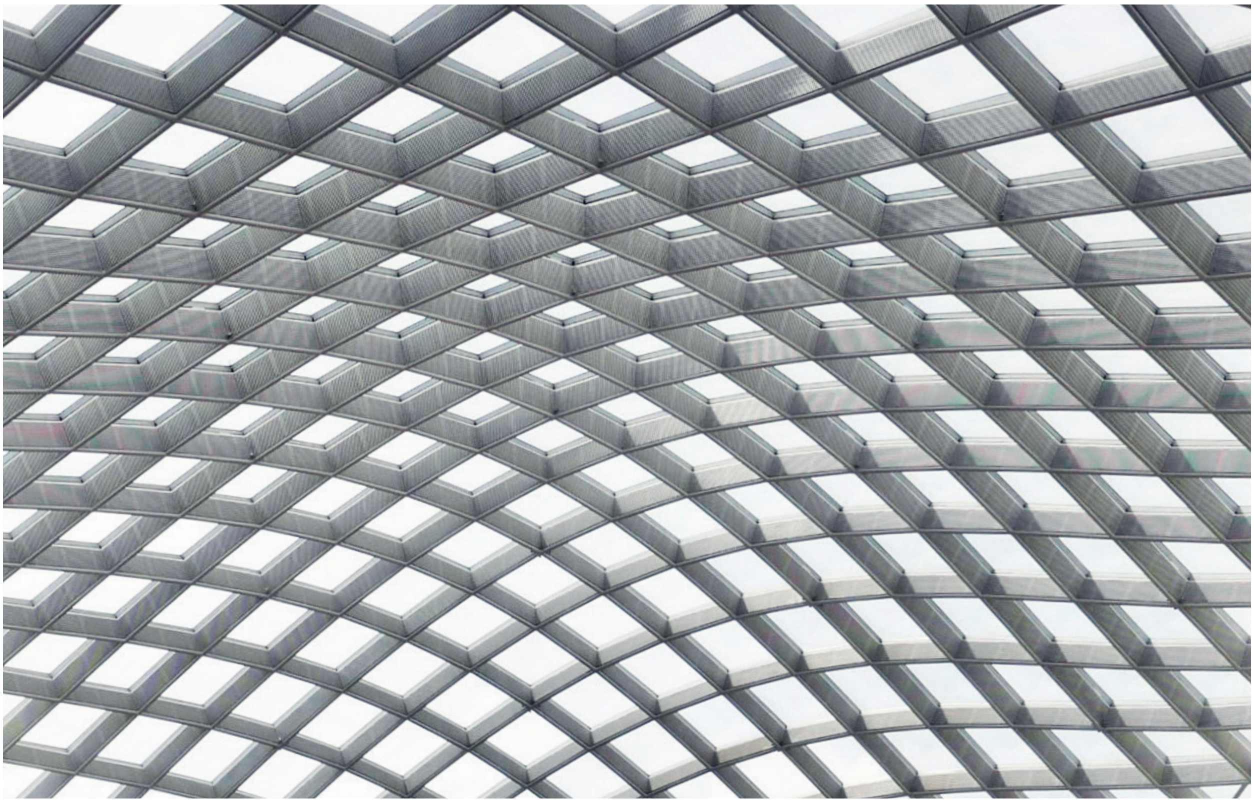

Figure 3.2 *The Kogod Courtyard in Washington DC representing a so-called geometric support structure (Photo:* ***Maja Schling Martin 2018****).*

The following section first lists the parameters for smooth segmentations, then discrete segmentations. For each segmentation, the impact of multi-layered structures is explained separately. The two parameter sets are combined to give a complete overview of parameters for any hybrid, multi-layered network. Finally, the dependencies within the set of parameters will be presented.

3.1.1 Parameters of Smooth Segmentations

Smooth segmentations are the closest network representation of a surface.

Nodes. The nodes are locally planar and can simply be described by their **mesh angles** ω_i measured between two adjacent edges. If all segmentation edges are continuous (quadrilateral and triangular networks), the nodes are also traversal and can be defined by one **intersection angle** ι. The intersection angle is dependent on the network type (quadrilateral = 90°, triangular = 60°, hexagonal = 120°) and its distortion.

Edges. The edges are defined by their length and curvature:
The **edge length** l is measured along the edges from node to node. In a smooth, multi-layered network, the edge length at top and bottom vary depending on the normal curvature.
The curvature of the edges is differentiated into **normal curvature** k_n, **geodesic curvature** k_g, and **geodesic torsion** τ_g in relation to the orientation of the reference surface (*Section 1.1.3*).[19]
Naturally, the general **curvature** k and **torsion** τ of a curve can be measured independently (*Section 1.1.1*). This curvature is relevant when using circular profiles (with no defined orientation) for construction.

Faces. The faces of a smooth network are shaped like any surface (*Section 1.2*) and cannot be described simply. We can compare their **shape** (by looking at surrounding edges and mesh angles) and **Gaussian curvature** K. Single curved faces can be compared through an isometric mapping (*Section 2.1.1*) if developable deformations (as defined in *Section 3.2.3*) are considered.

Offset. The **offset distance** o is simply measured between top and bottom at all entities. It is constant in a smooth segmentation (provided the offset distance is smaller than the minimal curvature radius of the surface). In a smooth, multi-layered network, the shape and curvature of the top and bottom face correspond with respect to the offset distance.

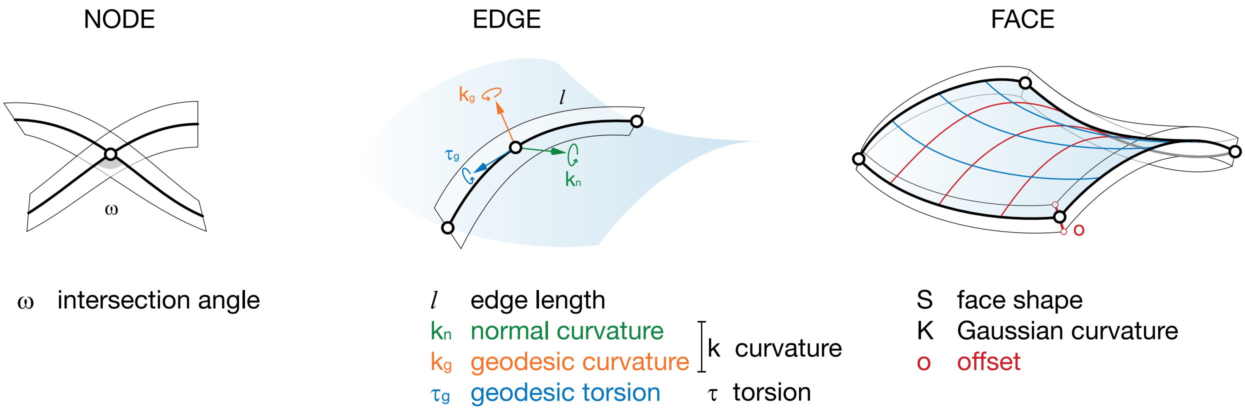

Figure 3.3 *Parameters of a smooth segmentation (**ES 2018**).*

19 If the edge-orientation is not aligned with the surface, these curvatures may be measured around the local x, y and z orientation, as k_x, k_y and k_z. In this thesis we focus on networks which consistently align edge and surface orientation.

3.1.2 Parameters of Discrete Segmentations

In a discrete mesh, all curves become polylines, thus shifting the complexity to the nodes. The discretization naturally creates tangential discontinuities (*Section 1.3.1*) of both curves and faces.

Nodes. The angles at a node are measured differently in various publications. This description is based on ***Stephan et al.*** (*2004*) and ***Schober*** (*2016*), and aims to illustrate the dependencies between smooth and discrete segmentations. There are three node angles in a discrete segmentation which are directly related to the three curvatures of a respective smooth segmentation.[20] They are measured in relation to the node axis and its corresponding tangent plane:

- The **normal angle** α measures the deviation of each edge from the tangent plane at the node. It is related to the normal curvature of the network.
- The **geodesic angle** β measures the deviation of each edge from a traversal node within the tangent plane. It is related to the geodesic curvature of the network.
- The **torsion angle** γ measures the deviation of subsequent node axes within the normal plane of their connecting (straight) edge. It is related to the geodesic torsion of the network.

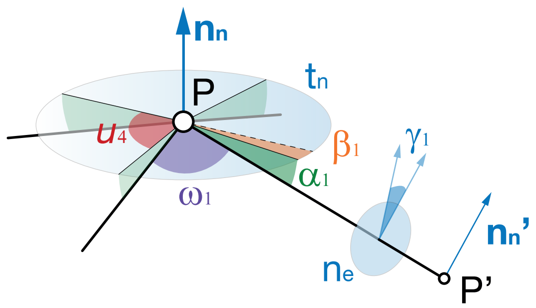

Figure 3.4 *The node angles α, β, γ and ω are measured in relation to the node axis and tangent plane in a discrete segmentation (**ES 2018**).*

Together with the initial intersection angle ι there are four independent angles that illustrate the behaviour of a discrete node. However, the intersection angle ι can only be measured in a traversal node (i.e., in smooth segmentations). We thus use the mesh angle ω, measured between two adjacent edges, in our following parameter sets. It is dependent on α, β and ι, and is the most common angle to describe a node arrangement.[21]

Stephan (*2004*) describes three angles necessary to define the fabrication of a joint: His *Vertikalwinkel* V and *Verdrehwinkel* W measure the same behaviour as the α and γ. His *Horizontalwinkel* U combines the information of the intersection angle ι and its geodesic deviation β. It simply measures the mesh angle between two adjacent edges as a projection onto the tangent plane at the node.

Schober (*2016*) describes the *Vertikalwinkel*, *Verdrehwinkel* and *Maschenwinkel,* equivalent to α , γ and ω, to define a joint. Additionally, in his description of the Reticulated Dome in Neckarsulm, he mentions the deviation from a traversal node as *Knickwinkel,* equivalent to β.

ι	β	α	γ
U		V	W
ω			

Table 3.1 *Hierarchical diagram of node angles. The angles α, β, γ and ω are selected for comparison (**ES 2018**).*

20 We will thus name these angles after the curvature they are related to.
21 If α and β are zero, then $\omega = \iota$.

Edges. The edges in a discrete mesh are defined as straight lines of length l. In a multi-layered structure, the edge-quads of a geometric support structure have a trapezoidal geometry. The edge lengths on top and bottom are related to the normal angle at the adjacent nodes.

Faces. The face shape in a discrete mesh can be deduced by the values of l and ω of the surrounding edges and nodes. A common topic of investigation is their planarity, which is measured separately as the deviation of surrounding nodes from a plane. If P = 0, the face is planar.
Some publications additionally list the kink angle ν which measures the tangential discontinuity between two adjacent faces. It is measured in the normal plane of the edge. This relation is, however, inscribed in the normal angle α, and will not be listed separately in this thesis.

Offset. The offset distances in a discrete mesh are variable for node-offset, edge-offset and face-offset, and need to be measured individually. The planarity of a face is inherited by the offset face.

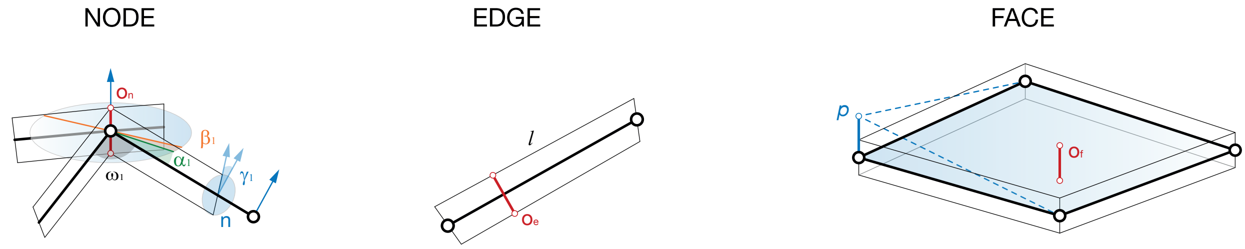

ω_i mesh angle
α_i normal angle
β_i geodesic angle
γ_i torsion angle
o_n node offset

l edge length
o_e edge offset

S face shape
P planarity
o_f face offset

Figure 3.5 *Parameters of a discrete segmentation (ES 2018).*

3.1.3 Combined Parameters

Many built solutions combine characteristics of both smooth and discrete segmentations and can only be described with a combination of all parameters.

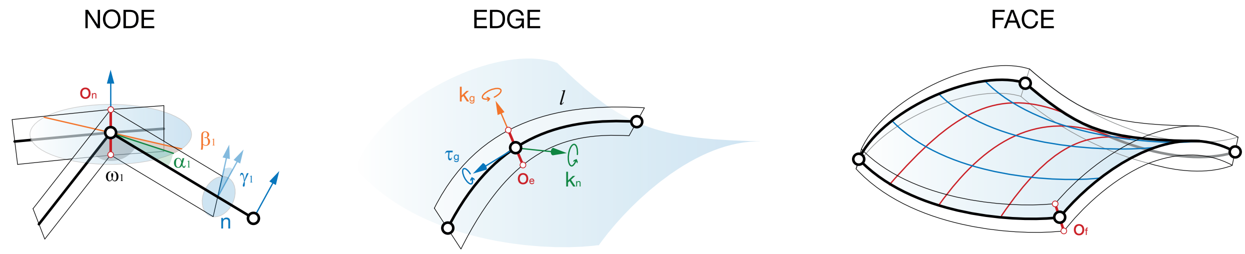

ω_i mesh angle
α_i normal angle
β_i geodesic angle
γ_i torsion angle
o_n node offset

l edge length
k_n normal curvature
k_g geodesic curvature
τ_g geodesic torsion
o_e edge offset

k curvature
τ torsion

S face shape
K Gaussian curvature
P planarity
o_f face offset

Figure 3.6 *All parameters of both smooth and discrete segmentation are combined in one set (ES 2018).*

This set of parameters will be used in the following investigations to analyse repetitive nodes, edges and faces. The parameters are listed in a standard table:

NODE					EDGE					FACE		
ω / ι	α	β	γ	o_n	l	k_n	k_g	τ_g	o_e	S	K/P	o_f

Table 3.2 *Standard table of repetitive parameters (**ES 2018**).*

Fairness

Some optimization tools introduce additional "fairness" parameters to favour meshes of smooth or homogeneous appearance. The mesh-optimizer Evolute for example, defines a parameter which minimizes the curvature of each polyline in a mesh (***Hammerberg 2012***). This creates a continuous progression of mesh edges and reduces the kinks between faces, a quality which is often preferred by designers.
In the subsequent inductive study (*Section 5.1*), this continuity c – measured as the angle between subsequent edges – will be used to induce fairness. Additionally, the fairness will be assessed qualitatively based on specific criteria of the design network.

3.1.4 Terminology and Dependencies

Terminology

Certain terms used in geometric descriptions indicate specific parameter values:

- '**Equilateral**' describes a constant edge length in a network.

- Nodes are described as '**regular**', meaning a constant mesh angle ω or '**planar**', meaning a constant normal angle α of zero.

- Continuous edges create '**traversal nodes**' with the property:
  $\omega_1 = \omega_3$ and $\omega_2 = \omega_4 = 180° - \omega_1$ (for quadrilateral segmentation)
  $\omega_1 = \omega_4$ and $\omega_2 = \omega_5$ and $\omega_3 = \omega_6 = 180° - \omega_1 - \omega_2$ (for triangular segmentations)

- '**Torsion-free nodes**' describe the property of a constant zero torsion angle, $\gamma = 0$.
  One way to identify/install this property are equal sums of opposite angles:
  $\omega_1 + \omega_3 = \omega_2 + \omega_4$ (in a quadrilateral segmentation)

Dependencies of Smooth Segmentations

The majority of parameters in a multi-layered smooth segmentation are determined. If the offset is constant and all edges are continuous and oriented normal to the surface, the following relationships can be expected:

- All normal angles are zero: $\alpha = 0°$
- All geodesic angles are zero: $\beta = 0°$
- All torsion angles are zero (i.e., the nodes are torsion-free): $\gamma = 0°$
- All mesh angles are traversal: $\iota = \omega_1 = \omega_3$ and $\omega_2 = \omega_4 = 180° - \omega_1 = 180° - \iota$.
- Node-, edge- and face-offset are identical: $o_n = o_e = o_f = o$

The curvature values k_n and k_g are derived by projecting the curvature vector of **k** onto the tangent-plane and the tangent-normal plane of the curve. Their relation is expressed as follows:

$$k = \sqrt{{k_n}^2 + {k_g}^2} \tag{3.1}$$

Dependencies of Discrete Segmentation

In a discrete segmentation, the edges are straight and do not lie within the surface. The edge orientation is usually defined as the vector sum of the normalized vectors of the adjacent nodes (***Stephan et al. 2004, p. 564***). The curvature and torsion of discrete edges is zero.

Dependency of Curvature and Node Angles

If we imagine a smooth network on a surface, and a discrete network connecting the same nodes with straight edges, then both networks follow the same layout:
Within the smooth segmentation, the curvature is continuously measurable along the edges, while within a discrete segmentation the curvature is concentrated at the nodes. The three curvatures and respective node angles are related. The dependencies can be described by the "formula for discrete curvature" (***Pottmann et al. 2007a, p. 227***).

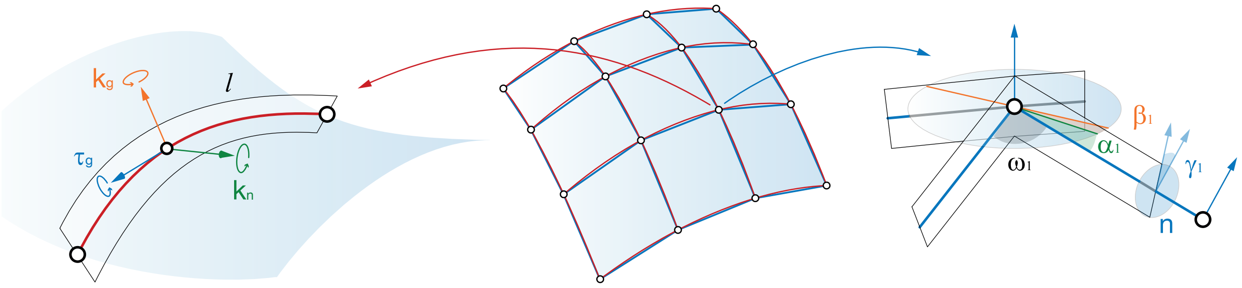

Figure 3.7 *The same network can be modelled as smooth or discrete segmentation (**ES 2018**).*

- The normal curvature k_n is related to the normal angle α_i with respect to the corresponding edge length:

$$k_n \approx \frac{2 \sin \alpha_i}{l} \tag{3.2}$$

- The geodesic curvature k_g is related to the geodesic angle β_i with respect to the corresponding edge length:

$$k_g \approx \frac{2 \sin \frac{\beta_i}{2}}{l} \tag{3.3}$$

- The geodesic torsion τ_g is related to the torsion angle γ_i at the node with respect to the corresponding edge length:

$$\tau_g \approx \frac{\gamma_i}{2l} \tag{3.4}$$

These equations give an approximation of the average edge curvature at each node. They are dependent on the resolution of the network. A finer grid (with smaller edge length) will produce more accurate results. Calculating the average of two subsequent edge-lengths additionally increases the precision.

3.2 Constructive Criteria

The review of architectural structures (*Section 2.3*) showed examples in which standardized parts are used for variable geometric situations. A hinged joint for example, can flexibly adjust to any angle within its rotation range. Such “constructive rationalizations” can be separated into **tolerances** (i.e., positional discontinuities (*Section 1.3.1*)) which deviate from the geometric segmentation, creating a discontinuous model, and adaptations, which **deform** or **hinge** a building part to fit the geometric situation (***Schiftner et al. 2013***).

The constructive criteria are an important part of our analysis of repetition. A sufficient tolerance, deformation or hinge within the construction may validate a variable geometric parameter (*Section 4.1*).

3.2.1 Tolerances

Some degree of tolerance is incorporated in every construction to provide clearance between parts. This accounts for the movement of the structure or allows for variable precision in fabrication and assembly. These tolerances can be deliberately increased to reduce the variety of individual parts. While nodes and edges require more precise fabrication, tolerances are used extensively to allow for repetitive façade panels. Some façades use large elastic seams or even a separate substructure to enable a substantial tolerance and achieve repetitive or planar panels.

Figure 3.8 *Tolerances in architectural construction. Left: Longholes at the outer laths of the Multihalle in Mannheim allow a variation in length (**Burkhardt 1978**). Middle: The panelling of the Olympic Stadium in Munich uses in-plane tolerances which are realized as elastic neoprene joints (**Harbeke 1972**). Right: The glass façade of the Kogod Courtyard is designed with out-of-plane tolerances to obtain planar panels (**FP 2007**).*

Tolerances create a gap (or overlap) between building parts either in-plane, as illustrated by the Neoprene seams of the Olympic Stadium in Munich, or out-of-plane, as illustrated by the scaled glass façade of the Kogod courtyard.

Tolerances are considered in our analysis of repetition by allowing a variation of the specific length or shape parameter. Identifying the magnitude of a tolerance provides an important insight into the design and construction process of an existing structure. Often, further building parts are necessary to bridge the accrued gaps.

NODE					EDGE					FACE		
ω / ι	α	β	γ	o_n	l	k_n	k_g	τ_g	o_e	S	K/P	o_f
					tolerance					tolerance		

Table 3.3 *Parametric impact of tolerances. Tolerances most commonly validate a variable geometry of face shape or edge length. (**ES 2018**).*

3.2.2 Hinges

Hinges are used primarily to enable a specific structural behaviour without restraints and avoid undesired bending moments in beams. They are located at the nodes of a network and facilitate the rotation of edges around a given axis. They allow for an individual adjustment of joints to a variable node geometry.

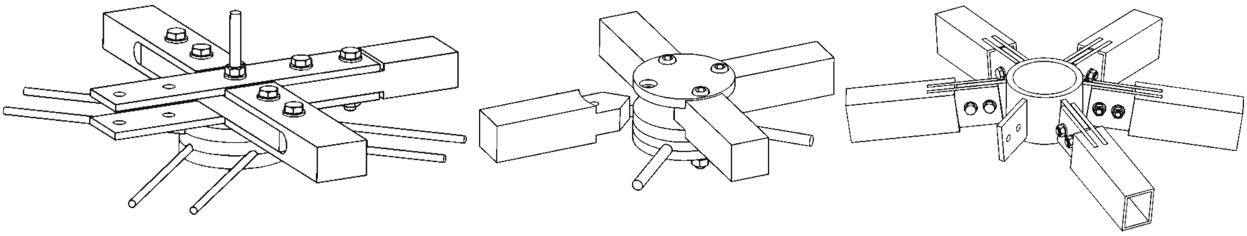

Figure 3.9 *Three hinged joints. Left: Laschenknoten SBP-2 offering an adjustment to the intersection angle ι. Middle: Laschenknoten HEFI-1 with some tolerance of the geodesic angle β. Right: Laschenknoten POLO-1 with vertical buttstraps. This could be used to accommodate variable normal angles α (**Stephan et al. 2004**).*

Hinges are considered in our analysis of repetition by allowing a variation of a specific angle parameter. The type and magnitude of angle give valuable insight into the specific detailing of this joint.

NODE					EDGE					FACE		
ω / ι	α	β	γ	o_n	l	k_n	k_g	τ_g	o_e	S	K/P	o_f
hinge	hinge	hinge	hinge									

Table 3.4 *Parametric impact of hinges. Hinges validate a variable geometry of node angles (**ES 2018**).*

3.2.3 Deformation

'Deformation', in this context, refers to a planned elastic bending or twisting of a beam or panel, with the goal to simplify the construction process. Other deformations caused by self-weight or external loads are referred to as "deflections".

Deformation is used for beams and façade panels to adjust to the desired curvature of edges or faces. It is considered in our analysis of repetition by allowing a variation of specific curvature parameters. The type and magnitude of curvature indicate how the building part is deformed. This information is decisive when choosing the appropriate profile and material. It will be discussed in more detail in *Section 3.2.4*.

Figure 3.10 *Deformation in architectural construction. Left: Multihalle Mannheim. The timber laths are bent and twisted into the curved geometry (Photo: **Rainer Barthel 2007**). Middle: The ICD/ITKE Research Pavilion 2010. The timber lamellas are bent around their weak axis, normal to the design shape (**ICD 2010**). Right: IAC Headquarters, New York. The glass panels are warped on site into a curved geometry (**Millard 2015**).*

NODE					EDGE					FACE		
ω / ι	α	β	γ	o_n	l	k_n	k_g	τ_g	o_e	S	K/P	o_f
						deform.	**deform.**	**deform.**			**deform.**	

Table 3.5 *Parametric impact of deformation. Deformation validates a variable geometry of curvature of edges or faces (**ES 2018**).*

Geometric Differentiation

As the term 'deformation' describes any strain (compression or tension) of material it is necessary to give a more precise **geometric differentiation** in order to be able to model and compare deformed elements. For design and modelling purposes, we therefore distinguish between two kinds of deformation for one or two-dimensional objects (curves and surfaces).

Developable Deformation. Commonly, in geometric modelling, deformation is only considered if the slender panel or lamella is transformed into a developable geometry (*Section 1.2.1*). This ensures that the two-dimensional object does not undergo any geometric streching or shearing.
A deformation is thus called 'developable' if it follows an isometric mapping, as explained in *Section 2.1.1*. This means that the curve or surface may change its shape without changing its length (and area), angles or Gaussian curvature.

One-dimensional edges that are subject to developable deformation may be considered congruent if they have the same length. Similarly, a two-dimensional face or strip which is subject to developable deformation may change its shape, but maintain its edge length, area, proportion and Gaussian curvature. This is only possible for single-curved (K = 0) surfaces.
Double-curved surfaces cannot change their shape without changing their Gaussian curvature and are thus not considered for developable deformations. Similarly, a flat panel or lamella cannot be twisted or formed into a double-curved shape in any other way if only developable deformations are allowed.

Physically, developable deformations result in bending stress, depending on the curvature and the section modulus (W_Z or W_Y) of the material. For slender lamellas or panels the latter can be derived simply by the thickness t and the elasticity E of the material. These mechanical implications will be discussed in the case study in *Section 6.3.2*.

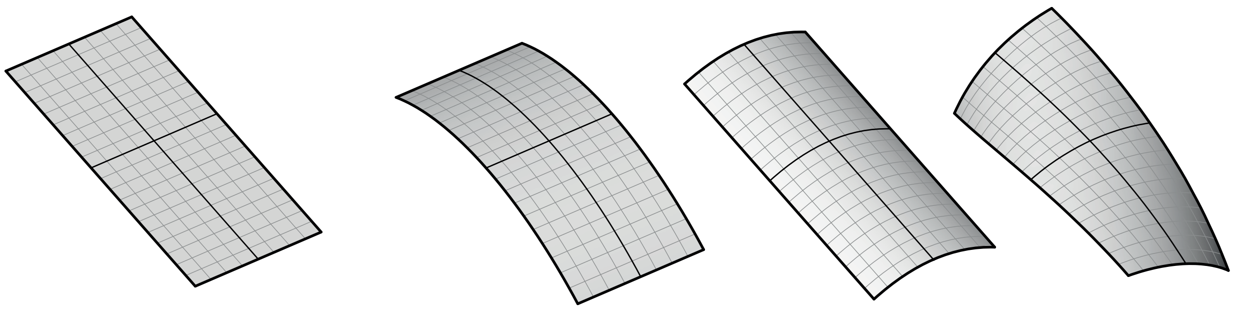

Figure 3.11 *Developable deformation. A flat panel or lamella can be bent around its long or short axis, or even warped diagonally, and maintin a developable geometry, i.e., not undergo change in length, angle or double curvature (**ES 2018**).*

Non-developable Deformation. Any strain exceeding developable deformation is considered 'non-developable'. Such non-developable deformation thus allows a slight change of length within the panel or lamella. Two-dimensional objects such as faces or strips may, e.g., be twisted or buldged to subtly change their double curvature. The repetitive geometry of such elements needs to be analysed individually based on their shape, proportion and material properties.
Physically, non-developable deformations are expected to create additional stress due to strain which

cannot be derived simply from the material thickness. Again, these mechanical implications will be discussed on the basis of the case study in *Section 6.3.2*.

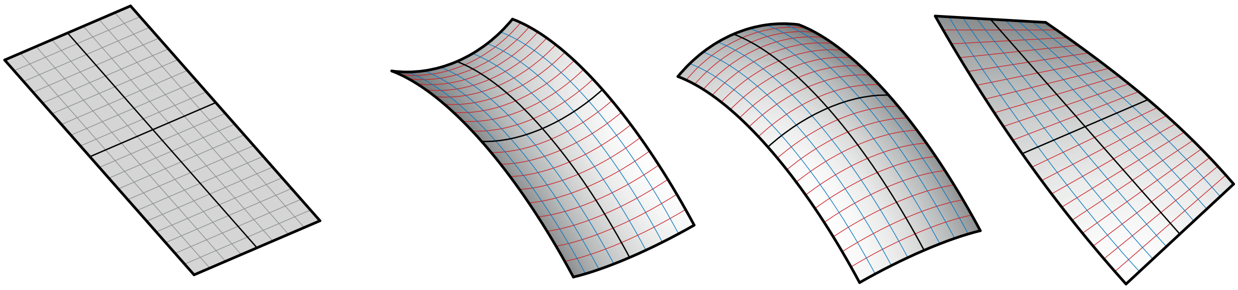

Figure 3.12 *Non-developable deformation. If the panel/lamella is bent into a double-curved shape, such as an anticalstic or synclastic surface, the Gaussian curvature does not stay constant. Even twisting a lamella leads to double curvature and an elongation of fibers (ES 2018).*

Deformation in Built Structures

When analysing built structures, the interpretation of a one or two-dimensional object becomes unclear as even the thinnest rod has a thickness. In our analysis of repetition, panels and lamellas are seen as two-dimensional objects, circular or double-symmetrical rods are seen as one-dimensional objects. Their deformations are thus considered 'developable' if all requirements are fulfilled.

Finally, it must be said that any physical deformation is reliant on material properties and profile dimensions. When designing a repetitive structure with deformation, threshold values, such as maximal normal or shear stress, must be defined to limit the accepted bending radii or torsion.

3.2.4 Curvature and Deformation

To be able to correlate the curvature of curves on a surface (τ_g, k_n and k_g) with the structural deformation of beams (κ_x, κ_y and κ_z), we must clarify the geometric relationship of the geometric model and the built structure.
The following three requirements have to be fulfilled:

- The beams must be curved continuously and follow the smooth design network.

- The profiles must be continuously oriented upright (along the normal vector) to align with the Darboux frame.

- The beams must be initially straight and bent elastically so that their deformation corresponds to their curvature.

If all requirements are satisfied, the profile orientation (defined by the **x**, **y** and **z** axes) corresponds to the Darboux frame (defined by the three vectors **t**, **u** and **n)** of the reference surface-curve. Similarly, the expected deformation κ_x, κ_y and κ_z of the structural profiles can be regarded equivalent to the geometric curvatures τ_g, k_n and k_g, of the surface curves.

$$
\begin{aligned}
\mathbf{t} &\equiv \mathbf{x}; \qquad & \tau_g &\equiv \kappa_x; \\
\mathbf{u} &\equiv \mathbf{y}; \qquad & k_n &\equiv \kappa_y; \\
\mathbf{n} &\equiv \mathbf{z}; \qquad & k_g &\equiv \kappa_z;
\end{aligned}
\tag{3.5}
$$

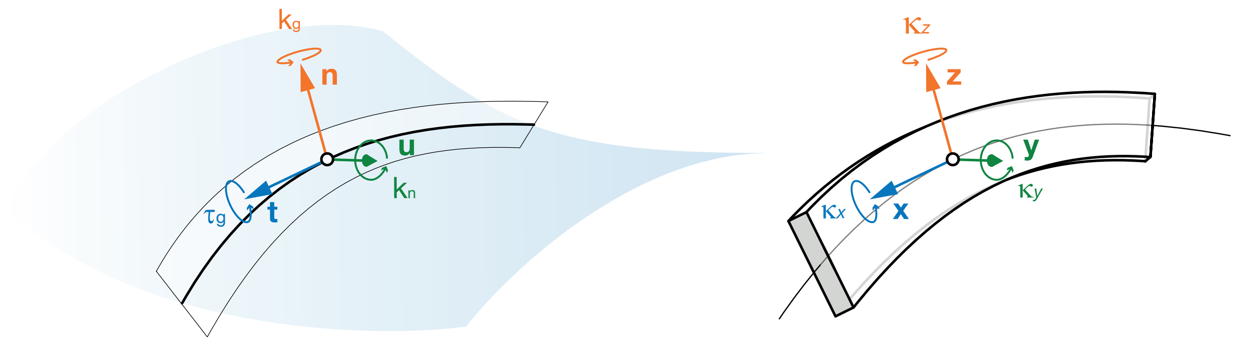

***Figure 3.13** Corresponding parameters of curvature and deformation (ES 2018).*

This relationship allows for a direct analysis of deformation via the curvature radius of the reference geometry. It is used in our analysis to classify the deformation of networks in *Section 4.2*, it is taken as a basis for the study of curvature-related networks in *Section 5.4*, and is implemented in the case study to deduce the residual stresses of bent lamellas in *Section 6.3.2*.

3.3 Additional Criteria

Even though we have defined a set of geometric parameters and constructive criteria, there still remains a large potential for misinterpretation when classifying repetitive structures. The following section lists additional criteria to clarify and complete the author's understanding of repetition.

Extent. The repetition of elements might not be enforced throughout the whole structure. We therefore distinguish between **full repetition**, which is only valid if all instances of a certain parameter are identical throughout the whole structure, and partial repetition. The quality of **partial repetition** can be quantified by the number of equivalence classes and the number of congruent elements in each class. If not stated otherwise, our studies focus on fully repetitive solutions.

Exeptions. Even if a parameter is fully repetitive, there are possible exceptions in a structure which call for individual fabrication. This is often the case along the **boundaries** of a network. Here the beams and panels are trimmed to fit the bespoke boundary and need to be fabricated individually. Another exception are **singularities** within a homogeneous pattern which create nodes of varying mesh angles. Such exceptions are regarded a side effect and have no influence on the parametric assessment.

Precision. Repetition is often approximated through optimization to achieve almost identical elements. The constructive tolerances, described in *Section 3.2*, are a driver for such an approximate search. This tolerance has a blurring, or softening effect on the solution spectrum of forms and segmentations. It is therefore crucial to specify the precision of measurements in any comparative analysis or design study.

Choice. The specific construction technique may alter the choice of parameters to compare in a structure. It might, e.g., be useful to keep a constant overall length of beams (see Shukhov's hyperbolic towers), rather than comparing the specific distances between nodes. While this kind of parameter selection is valid and necessary, our subsequent investigations focus primarily on the parameters specified in *Section 3.1*.

Relevance. Looking at specific built structures, it becomes apparent that not every parameter or entity listed in *Section 3.1* might be relevant. For example, analysing an open cable network does not need any consideration of face shape. Even though a geometric assessment might be possible, it would be misleading and incomplete, as the constructive criteria cannot be judged. Therefore, we will only judge those elements that are present in an existing structure.

Eccentricities. The constructive use of eccentricities can be utilized to simplify joints and create repetition. The most prominent examples are reciprocal structures which allow for the use of identical rods, intersecting tangentially at variable angles and distances. This topic is rich from both a geometric, as well as structural, point of view. However, eccentricities are not a focus of this investigation.

Dimensioning. Even though an element might be geometrically repetitive, it may not be fabricated identically as the specific load-bearing behaviour might call for differently sized elements. Especially in the construction of gridshells, the stresses within the grid varies greatly and often leads to a varying dimensioning of the beams. This thesis is focused on the geometric properties of grid structures and does not evaluate the stress-related variation of elements.

3.4 Strategies to Achieve Repetition

Based on the review of repetitive structures, in combination with the geometric and constructive parameters, the following strategies to obtain repetition have been observed:

Geometric Strategies

In-plane Network Adjustment. The most obvious strategy to create repetition is to design and adjust the network of a surface. Network adjustment refers to the deliberate movement of edges or nodes within the uv-coordinates of the target surface (i.e., in-plane adjustment) without creating a discontinuous network. For instance, using equilateral edges successfully adjusts a network and creates repetition independently of the shape or other strategies.
In-plane adjustment, however, is limited in its possibilities to create repetition. One of the most successful methods of in-plane adjustment is the alignment of the network with the principal curvature directions.

Out-of-plane Network Adjustment. In contrast to the in-plane adjustment, the out-of-plane adjustment refers to the deliberate movement of edges away from the target surface while keeping a continuous network. In case of discrete segmentation, this kind of adjustment may create a **rough (i.e., non-smooth) surface**. It is a powerful strategy and can create full repetition if a sufficient out-of-plane (proximity) tolerance is allowed.

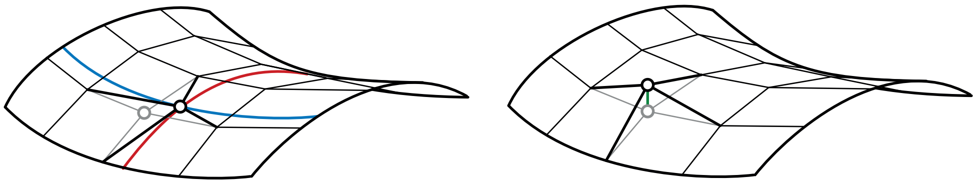

Figure 3.14 Networks can be adjusted in-plane and out-of-plane. This strategy maintains a continuous smooth or polyhedral network (ES 2017).

Shape Adjustment. Shape adjustment can be seen as an extreme out-of-plane adjustment with the requirement of maintaining a smooth surface. In built structures, this is the most prominent strategy to achieve repetition with varying impact on design freedom. While a sphere or cylinder are **predefined shapes,** a translational mesh or minimal surface leaves the designer with a **shape spectrum** to design within.

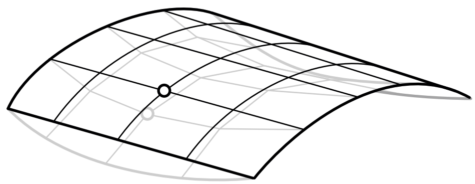

Figure 3.15 Shape adjustments are the most common strategy to achieve repetition (ES 2017).

Shape adjustment may obtain element repetition for various reasons:

- A symmetrical shape creates repetition. In a spherical geometry, e.g., the Schwedler cupola, the point symmetry allows for a repetitive use of meridian curves and horizontal circles.

- A simplified curvature aids repetition. The constant Gaussian curvature of a sphere allows for a repetition of node angles, edge- and face-curvature. In single curved shapes, the additional advantage of isometric mapping applies, allowing the use of, e.g., equilateral triangles in a discrete segmentation, or repetitive elements exhibiting developable deformation in a smooth segmentation.

- Traditional surfaces (*Section 1.2.1*) generally incorporate repetition within their surface definition. While ruled surfaces offer the use of straight, continuous edges, rotational and translational surfaces offer the use of planar quad faces if the network is aligned to the profile and path curves.

Constructive Strategies

The constructive criteria listed in *Section 3.2* can also be understood as strategies to create repetition:

Tolerances. In contrast to the network adjustments listed above, tolerances result in a discontinuous surface. Tolerances have been implemented both in geometric (Repetitive Moulds, *Section 2.2.2*) and practical investigations (the acrylic glass panels of the Olympic Stadium in Munich, *Section 2.3*). For the investigation of repetition, tolerances have a rather blurring effect, as they allow for geometrically imprecise solutions.
We can distinguish an **in-plane tolerance**, creating gaps or overlaps between tangent panels, or an **out-of-plane tolerance**, which creates a scaled appearance.

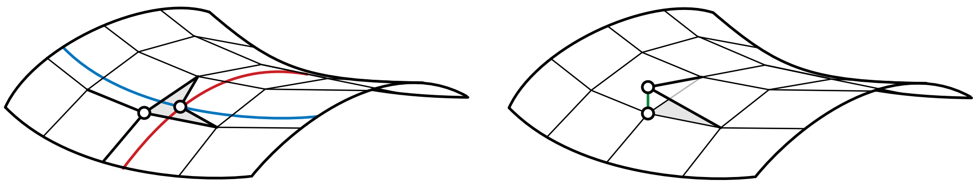

Figure 3.16 *Tolerances cause a positional discontinuity of the network, either in-plane or out-of-plane (ES 2017).*

Hinges. Hinges are a constructive adaptation enabling repetitive parts for a variable geometry. They enable nodes to adapt to variable angles without creating a discontinuous segmentation. They are used in both discrete and smooth segmentations.

Deformation. Deformation is a constructive adaptation to enable edges and faces to adjust to a variable curvature without creating a discontinuous segmentation. They are used to adjust edges and faces in a smooth segmentation, or non-planar faces in a discrete segmentation.
We distinguish between **developable deformation** and **non-developable deformation** (*Section 3.2.3*).

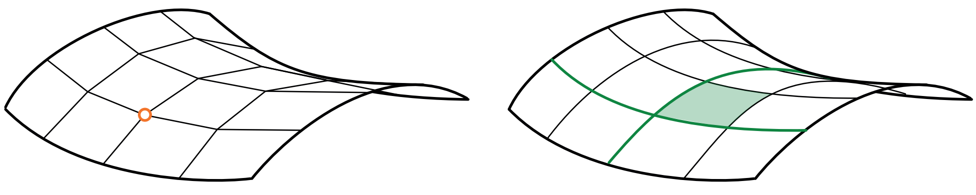

Figure 3.17 *Hinges allow a simplification of joints. Deformation may create curved edges or faces (ES 2017).*

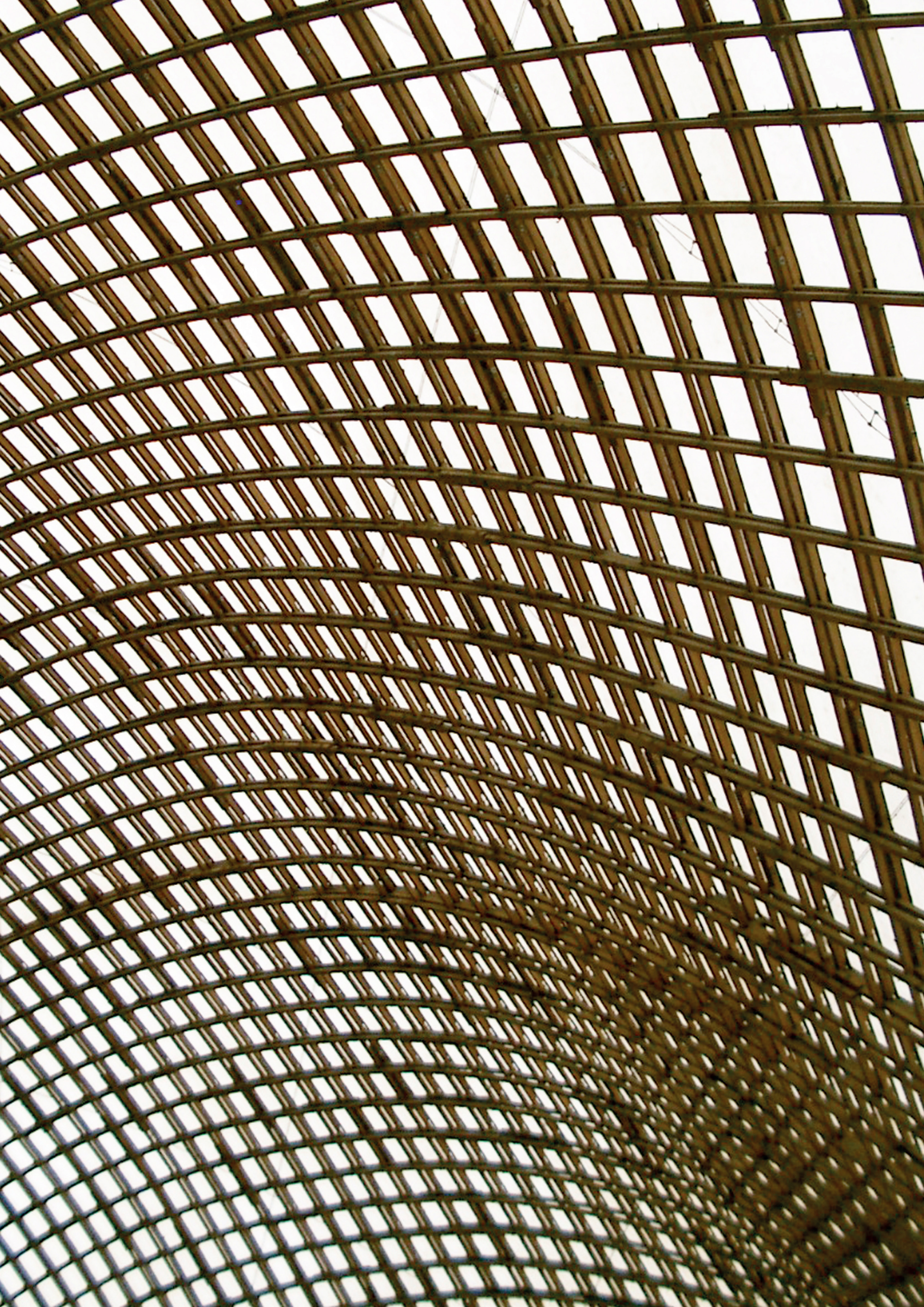

4 Analysis of Repetition

The theoretical framework formulated in *Chapter 3* will be used in this chapter to analyse repetitive structures.
This analysis not only reveals repetitive parameters, but also draws a relationship between geometry and construction: Any parameter variation must be considered in the construction process, either by fabricating individual parts, or by utilizing tolerances, hinges or deformation during assembly. The analysis concludes by identifying applied strategies and thus gives insight into the design and planning process.
This analysis is applied to the projects of the literature review. A comparative overview illustrates which kind of repetition has been investigated so far – and how it was achieved.
Finally, as impulse for future investigations, all possible parameter combinations of smooth segmentations are deduced systematically.

- *Section 4.1* introduces the general workflow to assess the geometric and constructive parameters of a given structure.

- In *Section 4.2* this process is used to quantitatively examine three selected projects: The Multihalle in Mannheim, the Reticulated Dome in Neckarsulm and the Eiffel Tower Pavilions in Paris.

- *Section 4.3* presents an overview of existing structures based on a qualitative analysis and discusses the use of strategies.

- As an impulse for further investigations, a table of all possible repetitive, smooth structures is presented in *Section 4.4*.

Figure 4.1 *Timber lattice of the Multihalle in Mannheim (Photo:* ***Rainer Barthel 2007****).*

4.1 Workflow

The analysis of repetition is separated into the following six steps:

1 Assessment of shape and segmentation
In a first step the shape and segmentation, as well as any specific geometric qualities, of the structure are classified.

2 Analysis of geometric parameters
Based on the classification of surface and network, it is possible to identify the qualitative properties of the network geometry, and label each parameter as either repetitive, variable or irrelevant. A quantitative geometric analysis can even go further and define the precise values/spectrum of each geometric parameter.

3 Review of constructive criteria
Next, we identify tolerances, hinges or deformations used within the construction and attribute them to specific geometric parameters.

4 Superimposition of results
By superimposing both geometric and constructive results, a complete analysis of the repetitive properties is created. Comparing each constructive criterion with its respective parameter values provides a conclusion on the detailing requirements of building parts.

5 Checking additional criteria
Any additional criteria of repetition are discussed, highlighting exceptions or particular properties of the specific project.

6 Insights and strategies
Finally, we summon all insights gained through the geometric and constructive analyses and identify strategies used to obtain repetitive parts.

Qualitative and Quantitative Analysis

In *Section 4.2*, three selected projects are analysed quantitatively. In this case, the values of each instance of parameter are measured in a digital model of the structure. For this purpose, the network geometries were either obtained from the planner (Reticulated Dome in Neckarsulm: Geometry provided by Hans Schober, SBP; Eiffel Tower Pavilions: Geometry provided by Alexander Schiftner, Evolute GmbH), or remodelled based on the literature available (Multihalle in Mannheim). Unfortunately, the data available is not always complete and some personal judgement was required during the modelling process.
A detailed survey of the existing structure could produce more precise measurements. This, however, is not the goal of this research.

In *Section 4.3*, an overview of repetitive structures is given based on the qualitative analysis. In this case, only the classification of surface and network, as well as the data provided in publications, are used in order to judge if parameters are variable or constant without giving precise measurements.

4.2 Analysis of Selected Projects

In the following section three existing smooth networks – the Multihalle in Mannheim, the Reticulated Dome in Neckarsulm and the Eiffel Tower Pavilions in Paris – are used representatively for a quantitative parametric analysis.

4.2.1 Multihalle in Mannheim

The grid structure of the Multihalle in Mannheim was form-found through a uniform, quadrilateral hanging chain-model. The structure itself is constructed as a smooth network of elastically bent timber laths. The PCV-coated membrane façade is not considered in this analysis. A digital 3D model of the network was created, based on the information available. This approximate model is, however, not sufficiently accurate, to derive the parameter values for ω, k_n, k_g and τ_g.

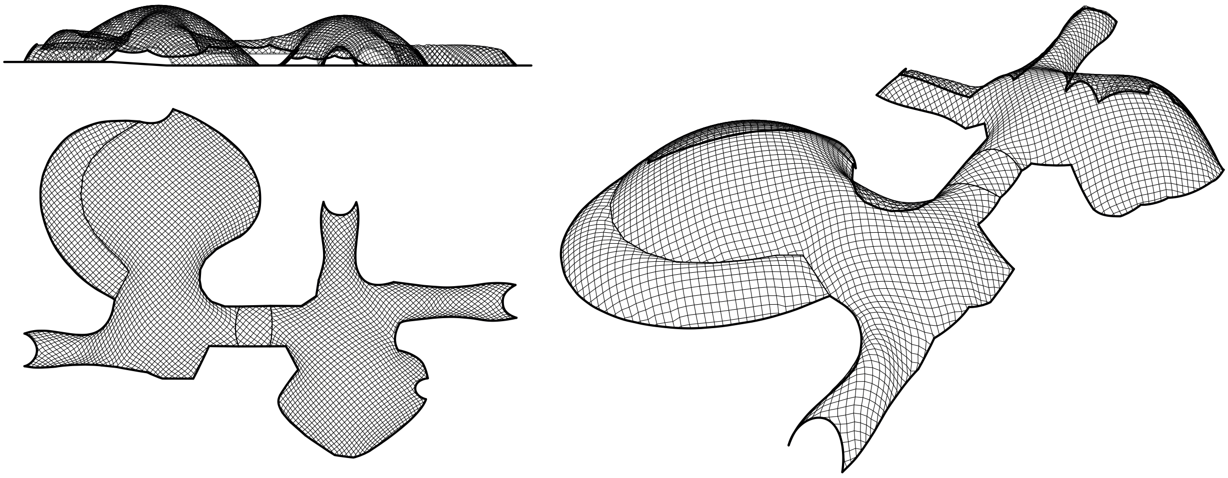

Figure 4.2 *Approximate network-model of the Multihalle in Mannheim (**ES 2018**).*

Geometric Parameters

The funicular structure follows the typical parametric behaviour of a smooth network, resulting in a simplification of nodes and, in this case, repetitive edges. All other parameters, such as the intersection angle, curvature values and face-shape are variable. Due to the multi-layered structure, a varying length of the outer layers of laths was considered.

NODE					EDGE					FACE		
ω / ι	α	β	γ	o_n	l	k_n	k_g	τ_g	o_e	S	K/P	o_f
variable	0°	0°	0°	0.2 m	0.75 m ± 3 cm	variable	variable	variable	0.2 m	-	-	-

Table 4.1 *Repetitive and variable geometric parameters of the Multihalle in Mannheim (**ES 2018**).*

Constructive Criteria

The multi-layered structure is constructed with long holes, allowing the outer laths to slide and adjust to the varying length (*Figure 2.44, right*). The joints are hinged around their z-axis (following the definition of *Figure 3.13*) allowing an adaptation to the varying intersection angles. The laths are constructed from slender, double-symmetric profiles allowing a deformation in all three axes to adapt to the varying curvature k_n , k_g and τ_g.

NODE					EDGE					FACE		
ω / ι	α	β	γ	o_n	l	k_n	k_g	τ_g	o_e	S	K/P	o_f
hinge	-	-	-	-	- tolerance	deform.	deform.	deform.	-	-	-	-

Table 4.2 *Constructive criteria of the Multihalle in Mannheim (**ES 2018**).*

Superimposition

Superimposing the results of the geometric and constructive analyses shows that all parameters are either constant or validated though a constructive criterion. The main structural grid can thus be constructed with repetitive building parts. (With a sufficiently accurate model, the precise range of all parameters would be given, and thus create insight on the maximal rotation of hinges and the minimal bending radii of laths.)

NODE					EDGE					FACE		
ω / ι	α	β	γ	o_n	l	k_n	k_g	τ_g	o_e	S	K/P	o_f
hinge	0°	0°	0°	0.2 m	0.75 m ± 3 cm	deform.	deform.	deform.	0.2 m	-	-	-

Table 4.3 *Superimposition of geometric and constructive parameters of the Multihalle in Mannheim (**ES 2018**).*

Additional Criteria

Exceptions can be observed along all boundaries where varying trims and supports call for bespoke constructive solutions. The quadrilateral grid is assembled in two layers in which one family of laths passes the other tangentially. This creates an eccentricity of 5 cm. The 50 x 50 mm profiles are used homogeneously throughout the structures. To increase the load-bearing capacity, some areas use four layers of laths or shear blocks which connect the top and bottom layers.

Conclusion

Apart from the equilateral design, the simplistic detailing of this complex shape is heavily dependent on constructive strategies. The joints are hinged and the outer laths are equipped with long holes to allow for a flexible adjustment of geometric variations. The main driver of repetition is the use of elastic deformation during assembly. Due to the three varying curvature parameters, the laths must be constructed from double-symmetric profiles to allow a deformation around all profile axes. This limitation leads to necessary structural developments using additional layers and shear-blocks to stiffen this strained load-bearing grid.

4.2.2 Reticulated Dome in Neckarsulm

The Reticulated Dome in Neckarsulm was designed as an equilateral (1.0 x 1.0 m), quadrilateral network on a spherical geometry. The edges are curved and follow the geodesic paths between nodes.

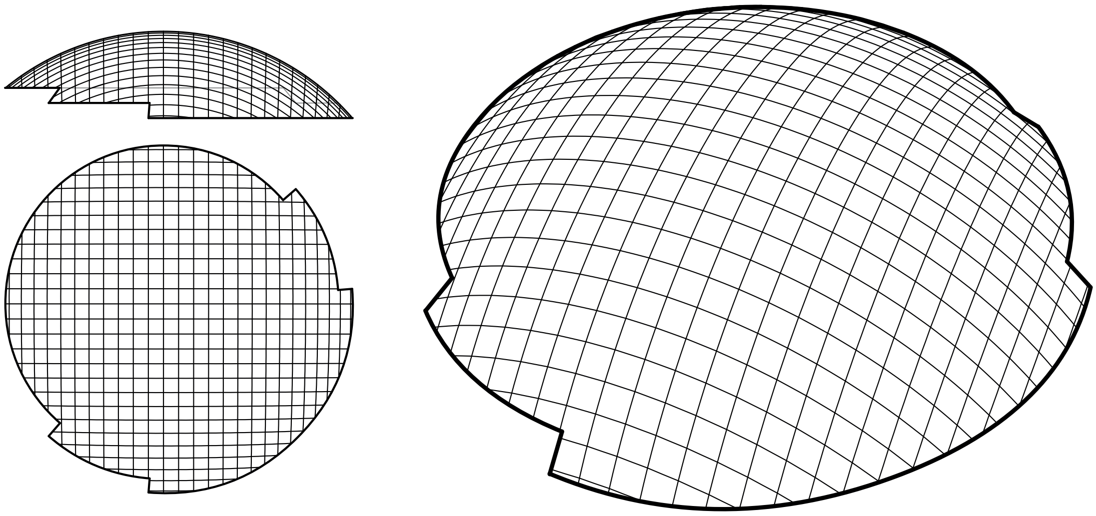

Figure 4.3 *The network of the Reticulated Dome in Neckarsulm (**ES 2018**, Geometry verified with **Schober 2018**).*

Reviewing Geometric Criteria

The equilateral network causes a high variation of mesh angles. The spherical geometry allows for a constant curvature of faces and edges. The smooth segmentation simplifies the node angles such that α and γ are zero. A peculiarity of this network is the varying geodesic angle, creating a discrete progression in-plane, and enabling a vanishing geodesic curvature of edges (*Figure 4.4*). It illustrates how node angle and edge curvature are interchangeable and may achieve the same curvature. This correspondence is decribed mathematically in *Section 3.1.4*. A similar effect is described in *Section 5.1.3* for smooth hexagonal networks with constant edge length on a sphere.

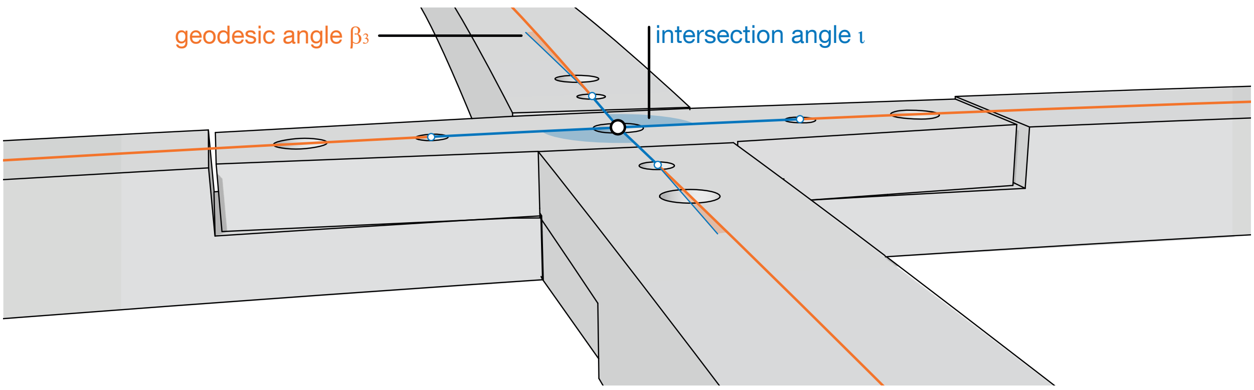

Figure 4.4 *Close-up of the hinged joint at the Reticulated Dome in Neckarsulm. The intersection and geodesic angles are taken at seperate hinges (**ES 2018**).*

NODE					EDGE					FACE		
ω / ι	α	β	γ	o_n	l	k_n	k_g	τ_g	o_e	S	K/P	o_f
48 - 132°	**0°**	**0-3°**	**0°**	**4 cm**	**1.0 m**	**1/16.5 m**	**0**	**0**	**4 cm**	**variable**	**spherical r =16.5 m**	-

Table 4.4 *Repetitive and variable geometric parameters of the Reticulated Dome in Neckarsulm (**ES 2018**).*

Reviewing Constructive Criteria

The grid structure is assembled from standardized curved edges with rectangular steel profiles of 60 x 40 mm. The traversal splice connectors are all identical and adjust to a varying intersection angle via their z-axis (following the definition of *Figure 3.13*). Furthermore, the edges are connected through one fixed and one long hole and allow for an additional varying geodesic connection angle. The façade panels have a varying shape, but constant spherical curvature.

Figure 4.5 *Building parts and assembly of the Reticulated Grid in Neckarsulm (Schober 2016).*

NODE					EDGE					FACE		
ω / ι	α	β	γ	o_n	l	k_n	k_g	τ_g	o_e	S	K/P	o_f
hinge	-	hinge	-	-	-	-	-	-	-	-	-	-

Table 4.5 *Constructive criteria of the Reticulated Dome in Neckarsulm (ES 2018).*

Superimposition

Superimposing the results of the geometric and constructive analyses reveals a full repetition of all parts. Furthermore, the table gives a precise measurement of the angle variation at the joints. While the mesh angles call for a substantial hinge of up to 42°, the geodesic angle was solved simply with a larger hole with up to 3° variance.

NODE					EDGE					FACE		
ω / ι	α	β	γ	o_n	l	k_n	k_g	τ_g	o_e	S	K/P	o_f
48 - 132° hinge	0°	0-3° hinge	0°	4 cm	1.0 m	1/16.5 m	0	0	4 cm	variable	spherical r =16.5 m	-

Table 4.6 *Superimposition of geometric and constructive parameters of the Reticulated Dome in Neckarsulm (ES 2018).*

Additional Criteria

Exceptions of repetition appear along all boundaries where varying trims and supports call for bespoke constructive solutions. The structure is covered with spherical glass panels, which could be fabricated with the same mould but had to be cut individually to fit the variable outline shape. The network is laid out symmetrically creating four similar quadrants.

Conclusion

The gridshell in Neckarsulm achieves a high level of repetition through its restricted spherical shape, equilateral network and hinged joints. The edges are laid out along geodesic paths resulting in a vanishing geodesic curvature. They are thus only curved along their constant normal curvature. The varying intersection angle and geodesic angle are taken up separately within each joint.

4.2.3 The Eiffel Tower Pavilions

The surface and network of the Eiffel Tower Pavilions form a smooth, quadrilateral segmentation which is aligned roughly with the principal curvature directions, simplifying the fabrication of glass panels and mullions.

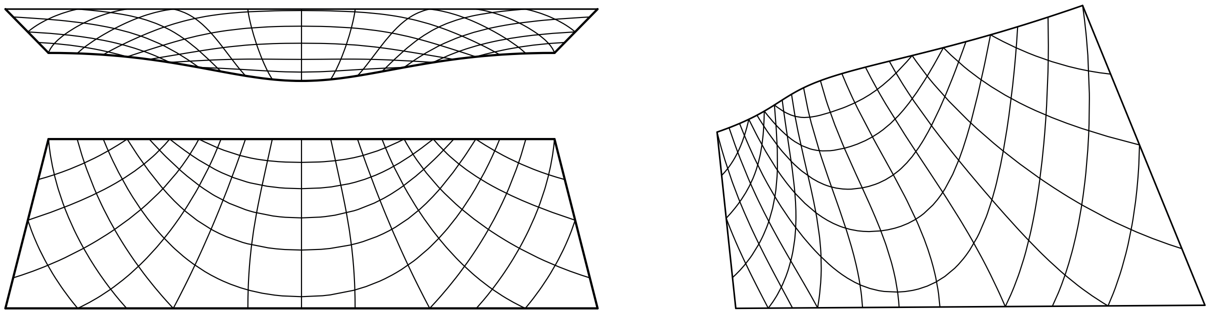

Figure 4.6 *Network of the Eiffel Tower Pavilions in Paris (**ES 2018**, Geometry by **Evolute 2011**).*

Reviewing Geometric Criteria

The vertical steel beams are continuous and create traversal nodes with no variation in normal, geodesic or torsion angles. All edges display both normal and geodesic curvature. The alignment with the principal curvature directions results in a low geodesic torsion, a prerequisite for developable edges and faces. A constant, orthogonal intersection angle (which is usually a property of principal curvature networks) was not pursued in this design.

NODE					EDGE					FACE		
ω / ι	α	β	γ	o_n	l	k_n	k_g	τ_g	o_e	S	K	o_f
70 - 104°	0°	0°	0°	c	0.7- 2.6 m	0 - 1/7 m	0 - 1/6 m	0 -1/24 m	c	variable	develop.	-

Table 4.7 *Repetitive and variable geometric parameters of the Eiffel Tower Pavilions (**ES 2018**).*

Reviewing Constructive Criteria

By considering a slight tangential and positional discontinuity along the mullions, the faces could be rationalized further to be constructed from only cylindrical panels. All other geometric variations are fabricated individually to fit.

NODE					EDGE					FACE		
ω / ι	α	β	γ	o_n	l	k_n	k_g	τ_g	o_e	S	K/P	o_f
-	-	-	-	-	-	-	-	-	-	-	tolerance	-

Table 4.8 *Constructive criteria of the Eiffel Tower Pavilions (**ES 2018**).*

Superimposition

Superimposing the results of the geometric and constructive analyses reveals a high parametric variance. All structural members and façade panels were fabricated individually. Nonetheless, the network optimization greatly simplified the fabrication of vertical mullions. Each box section was cut from flat metal strips which were bent and welded to take on their three-dimensional shape. Similarly, the cylindrical shape of glass panels significantly lowered their fabrication costs.

NODE					EDGE					FACE		
ω / ι	α	β	γ	o_n	l	k_n	k_g	τ_g	o_e	S	K	o_f
70 - 104°	0°	0°	0°	c	0.7- 2.6 m	0 - 1/7 m	0 - 1/6 m	0 -1/24 m	c	variable	cylindrical tolerance	-

Table 4.9 *Superimposition of geometric and constructive parameters of the Eiffel Tower Pavilions (**ES 2018**).*

Additional Criteria

The quadrilateral network is trimmed along all boundaries creating some triangular panels. The design surface is symmetrical along their central axis allowing for a repetition of panels on either side.

Conclusion

The Eiffel Tower Pavilions are an example of post-rationalization (***Schiftner et al. 2013***) of a freeform surface. The façade geometry was optimized to facilitate the use of cylindrical panels and developable edges within the permissible tolerances. This method results in a comparatively low geodesic torsion. All other parameters are variable and call for an individual fabrication of building parts.

4.3 Overview of Repetitive Structures

In the following section two overviews of repetitive structures are presented. The first table illustrates existing structures and compares their repetitive qualities and strategies. The second table gives an impulse for future investigations by deducing all possible parametric combinations for a subset of smooth parameters.

4.3.1 Existing Projects

The existing projects presented in the literature review (*Chapter 2*) were analysed qualitatively. *Table 4.10* gives an overview of their parameter repetition and strategies used, and thus illustrates a more general behaviour of repetitive structures.

The projects are separated into theoretical and built examples, and further sorted by segmentation and shape. The parameters of each project are labelled as 'x' (variable), 'c' (constant), '0' (vanishing) or '–' (not relevant), without specifying precise values (*Table 4.11*). In some cases, abbreviations are used to clarify a specific geometric quality. Each value is also colour-coded to indicate the specific strategy used to achieve repetition.

Analysis

The table illustrates parameters and strategies used in repetitive structures. In the following, we highlight some general principles that become apparent through this chart:

Geometric investigations are merely a first step towards creating repetitive parts. This is visualized by the reduced use of strategies in the upper section of *Table 4.10*. Even if some parameters remain variable, only construction planning will determine if these parameters need to be fabricated individually or if they can be validated through tolerances, hinges or deformation.
Built structures on the other hand, display a more complete analysis. If the planning documentation shows enough detail, we can assess the geometric and constructive criteria, and thus judge the complexity of fabrication.

It is noteworthy that constructive strategies can be implied within geometric investigations: The publications on Shape Proxies (***Eigensatz et al. 2010***), e.g., implement tolerances in the planning process. Similarly, the investigations on developable strips by Tang et al. (***2016***) suggest a use of developable deformation for the construction process.

Network Adjustment. Choosing a discrete segmentation naturally eliminates the curvature of edges and may create planar faces. Smooth segmentations, on the other hand, simplify the node angles, and create a constant offset value. Consequently, a clustered parameter repetition can be observed in the respective groups.

Hybrid segmentations (e.g., the Reticulated Dome in Neckarsulm) combine properties of discrete and smooth segmentation. Here, the distribution of repetitive parameters and related strategies is more varied. It is common in discrete geometric optimizations to allow minimal out-of-plane adjustments to achieve, for example, torsion-free nodes or planar faces, as was done for the investigations on conical, edge-offset and circular meshes. This is less common for smooth segmentations which are foremost created on a reference surface. The publication on "Circular Arch Structures" is an exception. Here the edge curves were optimized to create congruent nodes and circular arches, but allow a deviation from the reference surface.

Authors	Geometric investigations			ω	α	β	γ	o_n	l	k_n	k_g	τ_g	o_e	S	K	o_f
				NODE					EDGE					FACE		
Huard et al. 2015	Voxel Mesh	polyhedral	discrete	c	c	c	0	c	c	-	-	-	c	c	P	c
Huard et al. 2015	Lobel Mesh	developable		c	x	x	x	x	c	-	-	-	x	c	P	c
Jiang et al. 2014	Hexagonal Dual	developable		x	x	c	0	c	x	-	-	-	x	x	x	x
Schober 2016	Translational Mesh	translational		x	x	c	c	x	c	-	-	-	x	x	P	x
Singh, Schaefer 2010	Equivalence Classes	free		pa	x	x	x	x	pa	-	-	-	x	pa	P	x
Troche 2008	Planar Hexagons	free		x	x	x	x	x	x	-	-	-	x	x	P	c
Pottmann et al. 2007b	Conical Mesh	free		x	x	x	0	c	x	-	-	-	x	x	P	x
Pottmann et al. 2007b	Edge Offset Mesh	free		x	x	x	0	x	x	-	-	-	c	x	P	x
Pottmann et al. 2007b	Circular Mesh	free		x	x	x	0	x	x	-	-	-	x	x	P	c
Tang et al. 2016	Geodesic Developable Strips	free	smooth	t	0	0	0	c	x	x	0	x	c	x	x	c
Tang et al. 2016	Principal Curvature Dev. Strips	free		c	0	0	0	c	x	x	x	0	c	x	x	c
Tang et al. 2016	Asymptotic Developable Strips	free		t	0	0	0	c	x	0	x	x	c	x	x	c
Bo et al. 2011	Circular Arch Structures	free		c	0	0	0	c	x	pa		-	c	-	-	
Eigensatz et al. 2010	Shape Proxies	free		-	-	-	-	-	-	-	-	-	-	proxies		c
Schling (see *Section 5.2*)	Smooth, Rectangular Panelistion	free		-	-	-	-	-	-	-	-	-	-	c	x	c

Designer	Architectural developments			ω	α	β	γ	o_n	l	k_n	k_g	τ_g	o_e	S	K	o_f
				NODE					EDGE					FACE		
Hugo Junkers	Junkers Lamella Roof	cylindrical	discrete	c	c	c	c	c	c	-	-	-	c	c	P	c
Friedrich Zollinger	Zollinger Lamella Roof	cylindrical		c	c	c	c	c	c	-	-	-	c	c	P	-
Strozyk 2011	Wooden Textiles	polyhedral		c	x	x	x	-	c	-	-	-	-	c	P	c
Walter Bauersfeld	Geodesic Dome	spherical		pa	pa	pa	pa	c	pa	-	-	-	c	pa	P	c
Jörg Gribl, SBP	House for Hippopotamus, Berlin	translational		?	?	?	c	x	c	-	-	-	x	x	P	x
Otto, Behnisch, Schlaich	Cable Net, Munich	free		x	x	x	x	-	c	-	-	-	-	x	-	-
Foster + Partners	Kogod Courtyard	free		?	?	?	?	?	x	-	-	-	x	x	P	x
Asymptote, SBP	Yas Viceroy Hotel	free		?	?	?	0	c	x	-	-	-	x	x	P	x
Johann Schwedler	Schwedler Cupola	spherical	hybrid	pa	pa	pa	0	c	pa	c	0	0	c	pa	c	-
Kohlmeier + Bechler	Reticulated Dome in Neckarsulm	spherical		x	0	x	0	c	c	c	0	0	c	x	c	c
Agence Moatti-Rivière	Eiffel Tower Pavilions	free		c	pa	0	0	c	x	x	x	0	c	x	0	c
Buckminster Fuller	Plywood Dome	platonic solid	smooth	c	0	0	0	c	c	c	0	0	c	c	0	c
Frank Gehry	Fondation Louis Vuitton	developable		c	0	0	0	c	c	x	0	0	c	c	0	c
Duthilleul	Strasbourg Train Station	toroidal		c	0	0	0	c	pa	x	0	0	pa	c	0	c
Vladimir Shukhov	Hyperbolic Towers	HP-surface		t	0	0	0	c	pa	0	0	x	c	x	x	c
Vladimir Shukhov	Vyksa Gridshells	parabolic		t	0	0	0	c	pa	c	0	x	c	x	x	c
Schling (see *Chapter 6*)	Asymptotic Gridshell	minimal		c	0	0	0	c	x	0	x	x	c	x	x	c
Frei Otto	Multihalle in Mannheim	funicular		t	0	0	0	c	c	x	x	x	c	x	x	c
Jürgen Mayer	Metrosol Parasol	free		t	0	0	0	x	x	vertical			x	x	x	x
Geier+Geier	Brinebath, Bad Dürhheim	free		pa	0	0	0	c	x	x	x	x	c	x	x	c
Shigeru Ban	Centre Pompidou, Metz	free		x	0	0	0	c	x	x	x	x	c	x	x	c
Otto, Behnisch, Schlaich	Olympic Stadium, Façade	free		-	-	-	-	-	-	-	-	-	-	c	x	c

Table 4.10 *Qualitative parametric analysis of the examples listed in Chapter 2 (ES 2018).*

Creating a rough surface is used exclusively with discrete segmentations. The two examples - Voxel Mesh and Wooden Textiles - show how this strategy can either lead to full geometric repetition or be validated by hinged connections in a built prototype.

Shape Adjustment. The restriction of shapes is the prevalent strategy used in built structures. Predefining a shape is most successful with cylinders, spheres and platonic solids, and is often sufficient with no need for other strategies (e.g., Junker's lamella roof). Using a shape spectrum, on the other hand, leaves more design freedom and is often used in combination with constructive strategies, such as hinges or deformation (e.g., House for Hippopotamus at the Berlin Zoo).

Constructive Adaptation. As expected, the constructive strategy of hinges is only used with respect to the angular parameters of nodes. They can be found in both discrete and smooth segmentations, and also in combination with deformation.
Deformation, on the other hand, is only used with respect to curvature parameters of edges and faces. The Multihalle in Mannheim, the Gridshell in Vyksa, and the Hyperbolic Towers, bend or twist linear beams to obtain the curved geometry. The edges are interpreted here as one-dimensional elements, and are thus listed as developable deformations.
The Plywood Dome by Buckminster Fuller uses slender panels which are elastically deformed within a single-curved geometry. The Eiffel Tower Pavilions, the Fondation Louis Vuitton and the Strasbourg Train Station harness similar geometric rules of developabilty to simplifying the production process. However, the panels are prefabricated, which is why the strategies appear as 'individual fabrication'.
There are three examples – the acrylic glass panels of the Olympic Stadium in Munich, the study on smooth, rectangular panelization (presented in *Section 5.2*) and the Asymptotic Gridshell (presented in *Chapter 6*) – which deliberately deform flat elements into a double-curved geometry. These examples are highlighted as non-developable deformations.

Constructive Tolerances. The use of tolerances create ambiguous geometric parameters, resulting in a mostly undefined analysis. However, their potential to achieve repetition is high. For this reason, tolerances have been implemented in both theoretical and practical examples.

Individual Fabrication. Modern designs, such as the Brinebath in Bad Dürrheim and the Centre Pompidou in Metz, create smooth segmentation by individually fabricating each curved beam. This strategy is supported by the increasing possibilities of digital fabrication. Nonetheless, the construction process can be made more efficient by optimizing even a single parameter. This is common for façade-rationalizations, as in the Fondation Louis Vuitton and the Strasbourg Train Station. By creating developable face geometries, the glass panels can be fabricated without individual moulds.
Another trend is looking at the simplification of edge curvature. This was done at the Eiffel Tower Pavilions. By minimizing the geodesic torsion of edges, the mullions can be fabricated from planar strips of metal.

Geometric strategies	**Constructive strategies**	**Parameters**
in-plane adjustment	tolerance	x = variable
out-of-plane adjustment	hinge	c = constant
rough surface	developable deformation	- = not relevant
predefined shape	non-developable deformation	? = unknown
shape spectrum	not relevant	t = traversal node
	individual fabrication	P = planar face
		pa = partial repetition

Table 4.11 *Legend for Table 4.10 (ES 2018).*

Further Potentials

This overview of repetitive structures naturally poses the question: Which other combination of strategies have already been realized and what further applications are worth investigating?
It gives rise to a multitude of further research questions, such as:

- Can extreme out-of-plane tolerance be used to simplify smooth segmentation?
- Can deformation be applied to nodes? Can hinges be applied to edges?
- What are the potentials of deformation and tolerance for the construction of double-curved building envelopes?
- How can limited curvature parameters benefit the construction of strained gridshells?

Some of these questions are part of future research, others are addressed in the following chapter.

4.4 Deduction of Possibilities

The theoretical framework can also be used to systematically deduce all possible solutions for repetitive structures. Starting with a fully repetitive system, such as a platonic solid, we can "loosen" one parameter at a time and investigate the possible geometric freedom. Such systematic deduction is easier said than done. Often, the parameters of edges, nodes and faces are interdependent, and only lead to design freedom if released simultaneously. Furthermore, the possible combinatorics of 13 parameters, would require 8192 separate investigations, many of which have no valuable outcome.

To tackle this problem, we propose a focus on subsets of parameters.
In *Table 4.12* we only look at the immediate edge and node parameters for a smooth segmentation without considering offset and face geometry. This leaves us with five parameters: The intersection angle, the edge length, and the three curvature parameters. Based on this reduced number of parameters, we can create a chart for repetitive, smooth segmentations with only 32 possible combinations. Of course, this reduced chart does not describe all the geometric effects, but it renders the possibility to assign initial solutions and, subsequently, investigate the behaviour of further parameters.

We have added into this chart all solutions which are discussed in this thesis. Some of these solutions might only be one of many options. Others might need to be refined more accurately. This conjecture should be understood as an impulse for future investigations.

NODE						EDGE						FACE			Smooth networks
ω	α	β	γ	o_n		l	k_n	k_g	τ_g	o_e		S	K	o_f	
c	-	-	-	-		c	c	c	c	-		-	-	-	Rhombic network on a cylinder (Zollinger) (Section 2.3) Platonic solids projected onto their circumsphere (Section 5.3.6)
x	-	-	-	-		c	c	c	c	-		-	-	-	Geodesic Chebyshev net on a sphere (Reticulated Dome, Neckarsulm, Section 4.2.2)
c	-	-	-	-		x	c	c	c	-		-	-	-	
c	-	-	-	-		c	x	c	c	-		-	-	-	
c	-	-	-	-		c	c	x	c	-		-	-	-	
c	-	-	-	-		c	c	c	x	-		-	-	-	
x	-	-	-	-		x	c	c	c	-		-	-	-	Geodesic network on a sphere (Section 5.4.2)
x	-	-	-	-		c	x	c	c	-		-	-	-	
x	-	-	-	-		c	c	x	c	-		-	-	-	Asymptotic curves on a pseudosphere (Section 5.4.2)
x	-	-	-	-		c	c	c	x	-		-	-	-	
c	-	-	-	-		x	x	c	c	-		-	-	-	
c	-	-	-	-		x	c	x	c	-		-	-	-	Meridian curves and parallel circles on a sphere (Schwedler Cupola) (Section 2.3)
c	-	-	-	-		x	c	c	x	-		-	-	-	
c	-	-	-	-		c	x	x	c	-		-	-	-	
c	-	-	-	-		c	x	c	x	-		-	-	-	Regular, smooth network on a developable surface (Section 5.1.3)
c	-	-	-	-		c	c	x	x	-		-	-	-	
x	-	-	-	-		x	x	c	c	-		-	-	-	
x	-	-	-	-		x	c	x	c	-		-	-	-	Curved network in the plane (Section 5.4.2)
x	-	-	-	-		x	c	c	x	-		-	-	-	Network of rulings on a hyperbolic paraboloid or rotational hyperboloid (Hyperbolic Towers of Shukhov) (Section 2.3)
x	-	-	-	-		c	x	x	c	-		-	-	-	
x	-	-	-	-		c	x	c	x	-		-	-	-	
x	-	-	-	-		c	c	x	x	-		-	-	-	
c	-	-	-	-		x	x	x	c	-		-	-	-	Principal curvature networks on freefrom surfaces (Section 5.4.2)
c	-	-	-	-		x	x	c	x	-		-	-	-	
c	-	-	-	-		x	c	x	x	-		-	-	-	Constant normal curvature network on a CMC surface (Section 5.5.7)
c	-	-	-	-		c	x	x	x	-		-	-	-	
x	-	-	-	-		x	x	x	c	-		-	-	-	Principal curvature networks on freefrom surfaces (Section 5.4.2)
x	-	-	-	-		x	x	c	x	-		-	-	-	Network of geodesic curves on a freeform surface (Section 5.4.2)
x	-	-	-	-		x	c	x	x	-		-	-	-	Asymptotic network on an anticlastic surface (Section 5.4.2)
x	-	-	-	-		c	x	x	x	-		-	-	-	Smooth Chebyshev net on a freeform surface (Section 5.1.3)
c	-	-	-	-		x	x	x	x	-		-	-	-	Principal curvature network, gradient network, principal stress network (Section 1.4.4)
x	-	-	-	-		x	x	x	x	-		-	-	-	Any smooth network on a freeform surface

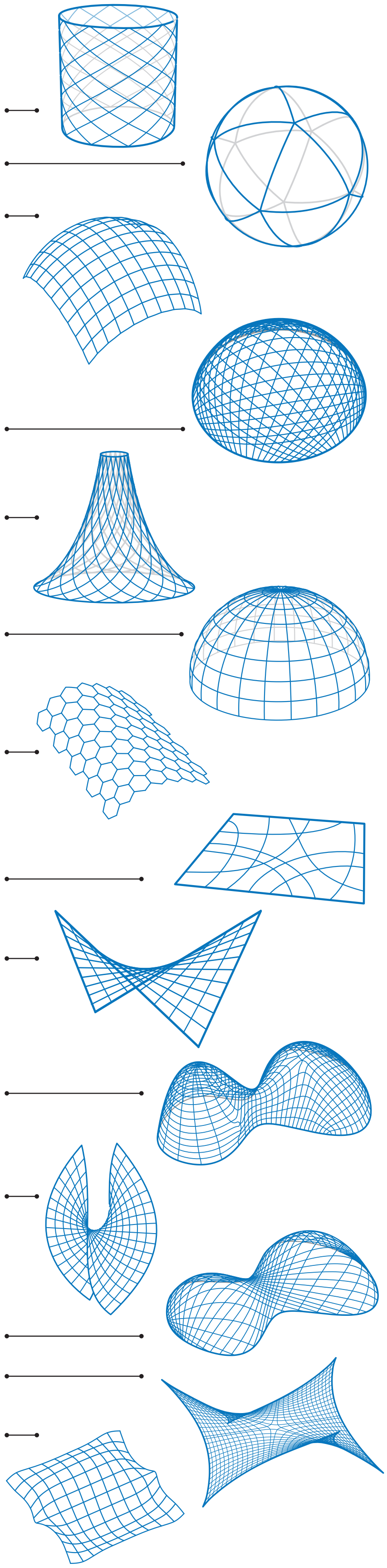

***Table 4.12** Overview of all possible geometric parameter combinations for smooth segmentation, based on a limited set of parameters disregarding offset and face geometry (ES 2018).*

5 Studies on Repetition

This chapter presents five constitutive studies which investigate selected sets of parameters to explore the morphological behaviour of repetitive networks. The studies gradually focus on smooth segmentations and specifically investigate the use of deformation and its effect on design freedom.

There are three methods used in the investigations:
The first two studies (*Section 5.1* and *Section 5.2*) use an inductive approach to generate network samples and analyse their geometric behaviour. *Section 5.3* uses a method of research by design, focusing on aspects of construction and aesthetics. Finally, *Section 5.4* and *Section 5.5* use a deductive approach to define geometric dependencies of curvature and develop a novel design method.

- *Section 5.1* investigates the morphology of triangular, quadrilateral and hexagonal networks for both discrete and smooth segmentation.

- *Section 5.2* investigates a smooth panelization with repetitive, rectangular faces focusing on the effects of deformation and tolerance.

- *Section 5.3* investigates the experimental design of repetitive structures through physical prototypes.

- *Section 5.4* deduces an overview of smooth networks, drawing a relationship between their parameters of curvature and the elastic behaviour of beams. One particular curve type, asymptotic curves, are chosen for further investigation as they show promising characteristics for the design and construction of strained gridshells.

- In *Section 5.5*, a novel design method is developed using asymptotic curve networks on minimal surfaces. The geometrical requirements of surface, network and edge-strips are defined and implemented to illustrate the design spectrum of this repetitive structure.

Figure 5.1 *Experimental design by Eleonora Velluto. Modular gridshell during construction (Photo: **ES 2016**).*

5.1 Inductive Study of Network Morphology

This inductive experiment digitally investigates the morphology of networks by testing their ability to adjust to various shapes under specific parameter constraints. We deliberately choose a small subset of parameters (l, ω and P) to enable a comparison of discrete and smooth segmentations of quadrilateral, triangular and hexagonal networks.

NODE					EDGE					FACE		
ω / ι	α	β	γ	o_n	l	k_n	k_g	τ_g	o_e	S	K	o_f

Table 5.1 *Table of active parameters for the inductive study of network morphology (**ES 2018**).*

We discuss the digital workflow in *Section 5.1.1* and subsequently examine discrete (*Section 5.1.2*) and smooth (*Section 5.1.3*) networks. The final *Section 5.1.4* gives a comparison of both examinations and draws a conclusion on general geometric principles of repetitive networks.

5.1.1 Digital workflow

Each network is first modelled in plane as regular uniform tessellation. Subsequently, the network is pulled onto a predefined surface while a selection of parameters are held constant. Once the simulation is complete, the individual parameters, as well as the proximity to the surface are measured. If the selected parameters have remained constant and the mesh has sufficiently adapted the predefined shape, the sample is approved as valid. If the shape and parameters did not converge, the sample is declared invalid. Valid and invalid samples are recorded, as they both give valuable insights into the morphological behaviour of the network.

Networks

The networks are first modelled as a flat, uniform grid of approximately 10 x 10 m in size, based on a common circumcircle of radius 0.71 m.[22] The following networks were used:

- Square quadrilateral network of 10 x 10 units with edge length l = 1 m
- Equilateral triangular network of 15 x 9 units with edge length l = 1.22 m
- Regular hexagonal network of 7 x 9 units with edge length l = 0.71 m

Control Parameters

For each network, several parameters can be measured and controlled independently. When comparing the parameters, any value within the given tolerance is considered repetitive.

- Edge length l is measured along the edge.
- Mesh angle ω is measured between adjacent edges.
- Planarity P indicates the maximal distance of vertices to a common face plane.
- Proximity δ indicates the distance of each node to a set target surface.
- Continuity c indicates the deviation of continuous edges from a straight line.
- This parameter is used as a soft criterion in discrete segmentations to foster fair solutions. It is also used for smooth segmentation to induce continuous curves.

22 Even though the study is independent of scale, the model uses meters as its base unit.

Target Surface

There are eight generic shapes which are used as target surfaces for the network samples:

- a general cylinder
- a tangential surface, as an example of a developable surface
- a sphere with a radius of 6 m
- an anticlastic, saddle shape which is modelled as an Enneper minimal surface (degree 2)
- a conoid, as an example of a ruled surface
- a translational surface
- a rotational surface
- a freeform surface

Solutions

All results are colour-coded to indicate their success:

- **Blue** represents a geometric solution which satisfied the predefined goals.
- **Green** represents a solution which satisfies all predefined goals, but displays a varying curvature of the edges. This can be interpreted as a developable deformation of one-dimensional elements, as defined in *Section 3.2.3*.
- **Red** represents a solution (either blue or green) which satisfies the predefined goals, but does not satisfy general expectations of network fairness (see below).
- **Grey** represents a trial sample which did not satisfy the predefined goals.

Behaviour and Limitations

Multiobjective Optimization. The transformation is computed in Rhino, Grashopper with the Plugin Kangaroo2 (***Piker 2013***), an interactive physics/constraint solver. It is based on a particle spring solver which iteratively optimizes the geometry of a given network to find the best fitting solution for multiple goals.

It must be said that this kind of non-linear optimization describes a non-convex objective function. It is thus highly dependent on the initialization and may miss the global minimizer. Furthermore, the final solution varies depending on the weighting of each objective, the arrangement and orientation of network and shape, as well as the duration of the optimization process. Even re-computing the exact same settings does not necessarily create the identical numerical result.

However, this software is well suited to experimentally investigate form and structure. It illustrates the general geometric behaviour of repetitive nets and produces valuable results which can be sufficiently reproduced.

Fairness. There are some samples which fulfil all parametric requirements but cannot be used as a representative solution. This is because their general ‘fairness’ is not sufficient. This is caused, e.g., by a wrinkled network, or S-curved edges between nodes.

To prevent these effects, some soft criteria are included that control the network fairness. This is done by setting an additional low weighted objective for constant edge length, continuity or mesh angle. If sufficient fairness cannot be achieved, the sample is colored red. The following criteria are used as an indication of insufficient fairness:

- non-continuous edges:
  · wrinkled edges in a discrete network
  · s-shaped edges in a smooth network
- overlapping or collapsed edges
- irregular non-convex polygons

Alignment. The alignment of network and surface has a decisive influence on the quality and success of the solutions. Especially in respect to planarity (for discrete segmentations) and repetitive nodes (for smooth segmentations), a close alignment to the principal curvature directions is a key feature.
The networks are generally modelled in alignment with profile and path curves of the target surface, and thus have a general alignment with the principal curvature directions.
In some cases of the hexagonal samples, a rotation of the alignment by 90 degrees was tested during the experiment to compare the quality of solutions.

Topology. The networks investigated in this experiment are modelled homogeneously without singularities. This topology cannot change during optimization.

Accuracy. The accuracy of the calculation is limited by the calculation time, the software environment and the solver. The tolerance for all length and angular requirements was set to ± 0.1% of the target value.

Curvature. The curvature of smooth segmentation is modelled discretely by subdividing every edge into four sub-segments. This subdivision has proven to be sufficient in accuracy while maintaining an efficient workflow.

5.1.2 Discrete Segmentations

The first part of this study investigates discrete segmentations.
The following parameter combinations are investigated:

- “Face” enforces congruent faces, based on a constant l, ω and P.
- “Planarity” enforces only P.
- “Planarity + Edge” enforces P and l.
- “Edge” enforces only l.
- “Node” enforces only ω.

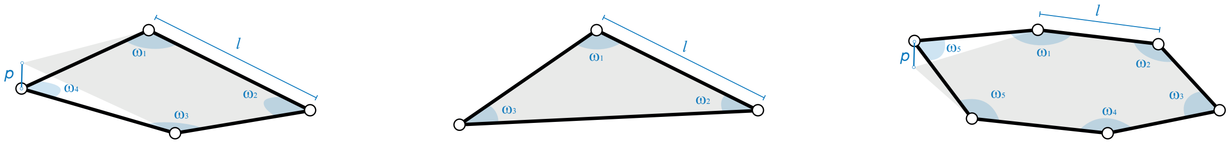

Figure 5.2 *Parameters measured at the discrete quadrilateral, triangular and hexagonal networks (**ES 2018**).*

Quads

Discrete quadrilateral networks (*Figure 5.3*) are versatile and may be adjusted in edge length or intersection angle to fit the enforced repetitive requirements.

Face. Enforcing congruent, square faces is only possible on a general cylinder or a plane. For all other shapes, the sample only approximates the geometry. Depending on how much proximity is enforced, the networks may stray from a cylindrical shape. In the case of the sphere and the anticlastic surface, this results in light folds which allow a closer representation of the target surface.

Planarity. The samples of planar quad meshes tend to align with the principal curvature (PC) directions of the surface. For the cylindrical network this results in a simple parallel assembly. The developable surface triggers a fan-shaped alignment along its rulings. On a sphere the PC-directions are not defined. Here the network approximates the great circles. The solution for the conoid clearly displays the nature of the principal directions – first curved, then straight – illustrating the gradient from double to almost single

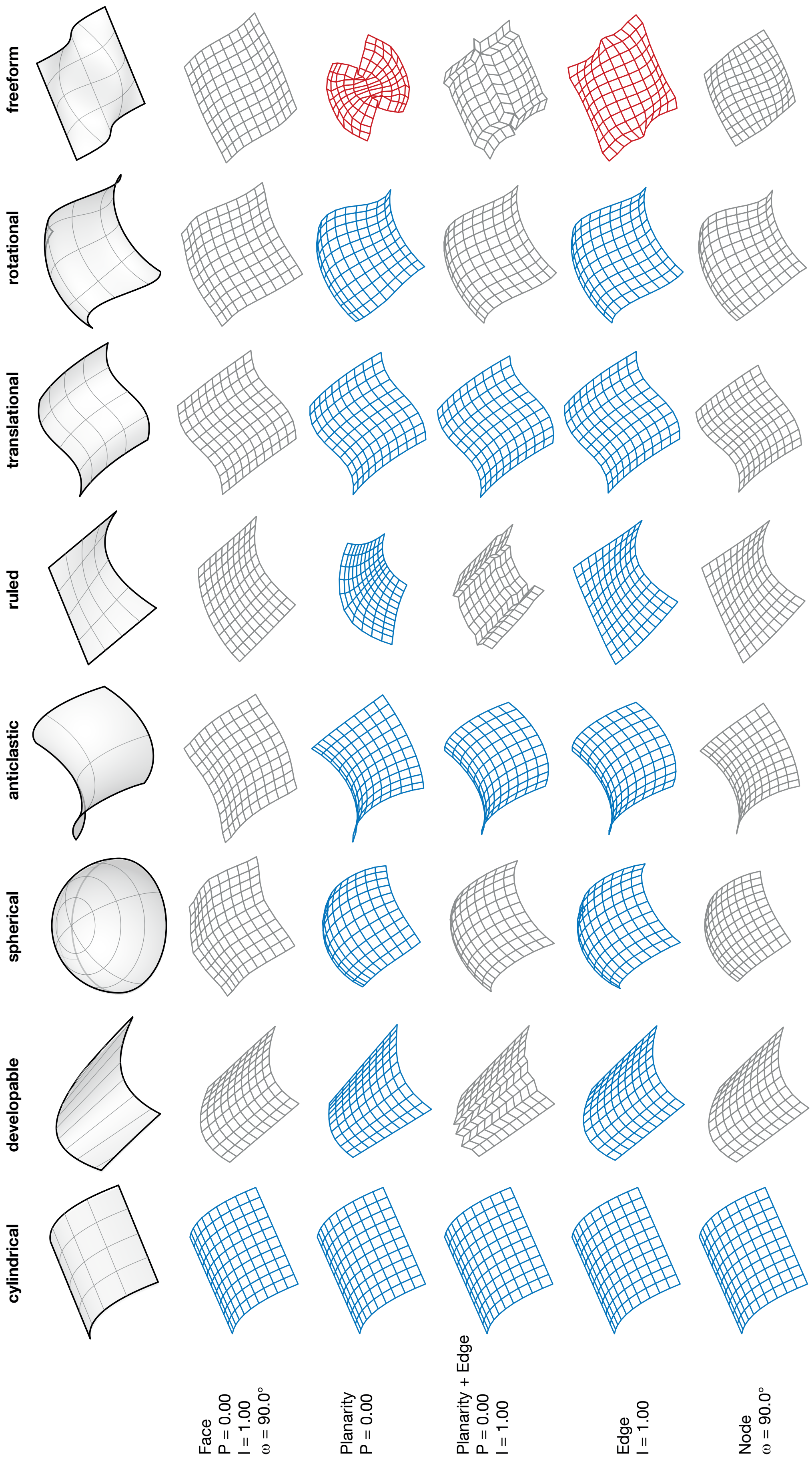

Figure 5.3 *Discrete quadrilateral samples (**ES 2018**).*

curvature. Both translational and rotational surfaces trigger a clean alignment with their generating profile curves. For the rotational surface this creates a strong variation of edge length. A similar behaviour applies to the anticlastic surface.
Even though the solver succeeded in finding a planar solution for the freeform surface, its curvature is too extreme for this grid size (a contraction was avoided by fairness criteria). As a result, overlapping and collapsed edges, wrinkled borders, and non-convex quads corrupt the fairness of this network. In particular, there are two symmetrical locations in which the network overlaps. Here, a singularity would have greatly benefited the layout.

Planarity + Edge. Restricting the planarity and edge length results in translational meshes. This applies to the cylinder, the translational and the anticlastic surfaces. For the latter (which is, strickly speaking, not a translational surface) this is a lucky by-product of its symmetrical geometry and may be the result of the small tolerances of this study. All other shapes cannot find valid solutions. In the case of the sphere, the failed sample displays a great resemblance to the successful edge-enforced sample below, with the only difference that the outermost corners are not capable of wrapping around the sphere.
The invalid freeform sample shows an interesting effect: The quads collapse and create artificial singularities with higher valence at the symmetrical locations mentioned above under Planarity.

Edge. Equilateral, quadrilateral networks can assume virtually any shape. This adaptation distorts the network and creates acute intersection angles especially on shapes with high curvature. This is the case for the sphere and the anticlastic surface where the mesh angles reach their extreme values in the corners. Again, the freeform shape, with its extreme curvature, creates a wrinkled mesh with discontinuous edges along the borders.

Node. A constant mesh angle of 90° results in planar, square panels. A respective network is only possible on a plane or a cylinder where the single curvature can be adopted along parallel folds. Nonetheless, the solver attempts to achieve a constant mesh angle by contracting the samples, exposing them to less curvature.
A side effect of optimizing for constant node angle is planarity which is unintentionally achieved for the samples on the spherical and anticlastic surface. Similar to the Planarity set, a general alignment with the principal curvature directions can be observed.

Triangles

Discrete triangles (*Figure 5.4*) create the most rigid network. Only two groups of triangular networks are tested. The combinations Face, Edge, Node and Planarity + Edge can all be considered in the same set as they all result in rigid, equilateral triangles. Only the Planarity set allows for variable edge length and is thus studied separately.

Equilateral Triangles. Equilateral triangles can only assume developable surfaces, such as the cylinder and the tangential surface. This behaviour is in line with the insights of the literature review (see *Section 2.2.1*, Lobel Meshes). Any other shape triggers kinks and folds similar to the reference project “Wooden Textiles” (***Strozyk 2011***), and thus does not produce valid solutions. The sample for the ruled surface has a comparatively smooth appearance. This is owed to its low double curvature.

Planarity. Triangles are planar by definition. As a consequence, any triangular network, even if projected straight onto a double-curved surfaces inevitably creates planar faces, but does not allow for other parameter repetition. For this setup, the edge length was dampened to create homogeneous and fair meshes.

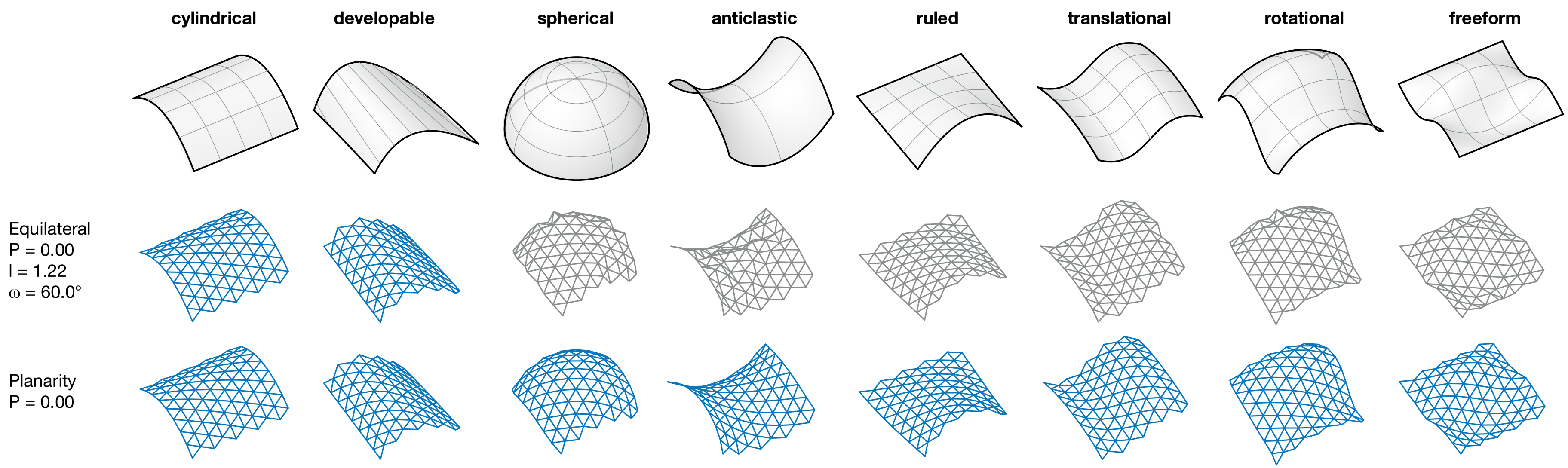

Figure 5.4 *Discrete triangular samples (ES 2018).*

Hexagons

Discrete hexagonal networks (*Figure 5.5*) are flexible. If no fairness objectives are applied to ensure a homogeneous layout, the networks easily distort beyond recognition. This flexibility also enables a great variety of patterns.

Face. Enforcing regular hexagonal faces is only possible in plane as there are no continuous edges acting as folds. Consequently, the samples only approximate the target surfaces. In contrast to the behaviour of the respective quads, the hexagonal samples tend to adapt their geometry by creating a homogeneous, almost spherical geometry.

Planarity. Similar to planar quads, planar hexagons are strongly influenced by the principal curvature direction of a surface. In addition, positive and negative Gaussian curvature induce convex, honeycomb-like or non-convex, mostly bowtie-shaped hexagons. This behaviour is well illustrated in this experiment. For single curved shapes, the hexagons form straight edges aligned with the rulings of the surface, thus creating a brick pattern. For a cylinder this pattern is parallel and regular. For a tangential surface, the pattern fans out along the rulings, causing a variation in edge length.
The spherical and anticlastic shapes enable the most homogeneous convex and non-convex patterns (*Section 2.2.1*). The convex hexagons on the sphere decrease in size towards the boundaries. Inversely, on the anticlastic surface, the bow-tie-shaped hexagons increase in size towards the boundaries.
For the ruled, translational and rotational surfaces, the pattern cleanly depicts the surface curvature morphing from honeycomb to bow-tie shapes. The intermediate areas are most complex, causing an elongation or collapse of edges. The outer corners of the ruled surface sample display a chaotic pattern. This is also the case for the freeform surface which displays the most extreme variation of curvature. In both cases, a finer grid would help to achieve a more homogeneous layout.

Planarity + Edge. Combining planarity and length restriction is only possible on a cylindrical surface where a parallel layout is feasible. In all other cases, the rigid edge length prohibits a smooth adjustment to the surface curvature making planar hexagons impossible. This effect is best illustrated on the anticlastic surface where the edges start overlapping to accommodate the non-convex kink.

Edge. Equilateral, hexagonal networks assume all tested shapes with a smooth, homogeneous appearance. Nonetheless, the double curvature distorts the network. This behaviour is best illustrated by the spherical and anticlastic sample creating condensed, or rather elongated hexagons around their perimeters.

Node. Enforcing a constant angle of 120° between the edges of a hexagonal network inevitably leads to a planar layout. In contrast to triangular and quadrilateral layouts, the hexagons have no continuous edges which would act as folds to allow a developable (for triangular) or at least cylindrical (for quadrilateral) geometry. However, our experiment found a cylindrical solution with a reduced mesh angle. The mesh depicted in *Figure 5.5 (bottom, left)* has a constant length of 0.71 m and a constant mesh angle of 119.87°. Optimizing for constant mesh angles on any double-curved surface leads to partly heavy distortion of the edge length.

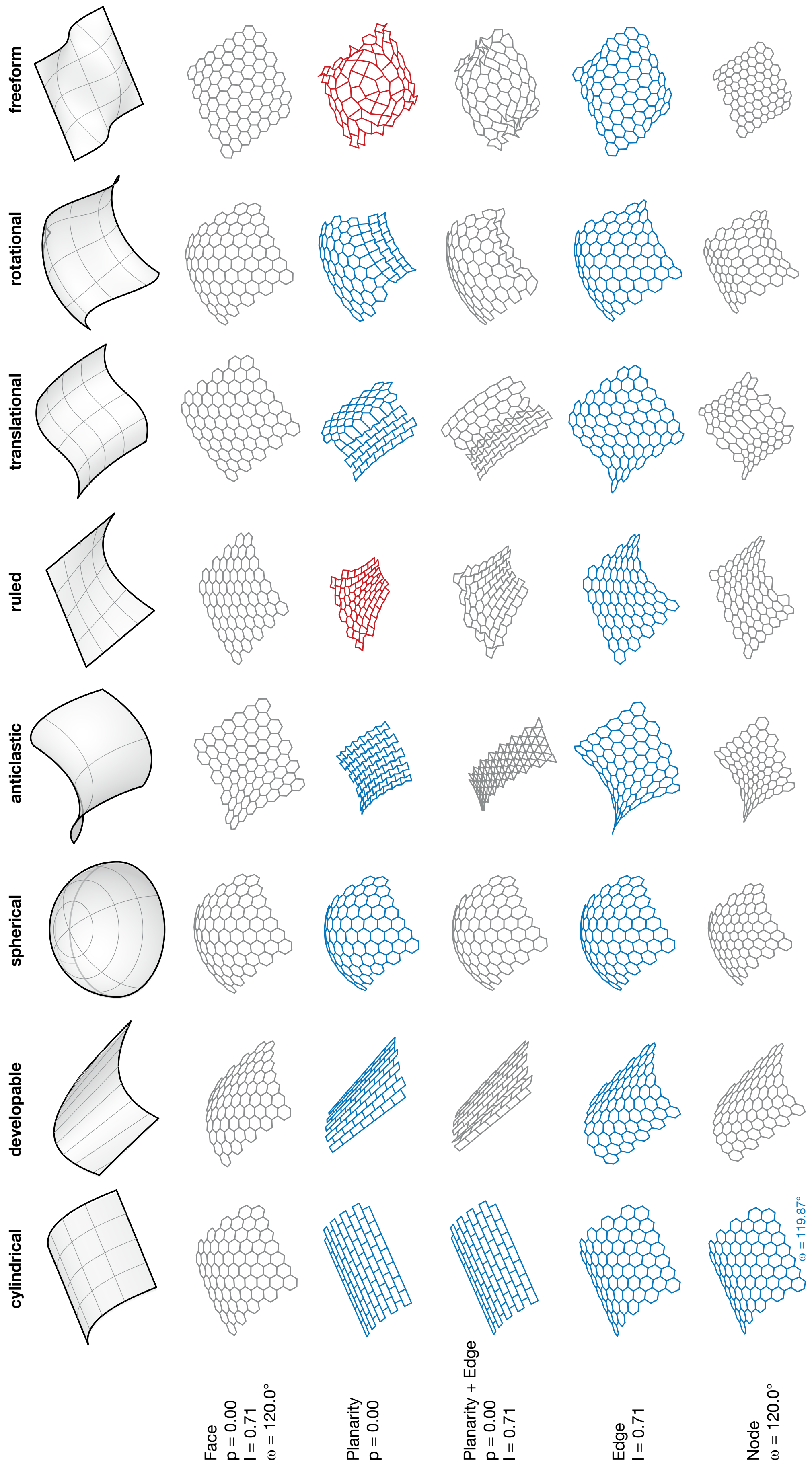

Figure 5.5 *Discrete hexagonal samples (**ES 2018**).*

5.1.3 Smooth Segmentations

The second part of this study investigates smooth segmentations. In this case, the parameter P (Planarity) is not investigated. However, some solutions enable a constant edge curvature k[23]. The following three sets of parameters are investigated:

- "Edge" enforces a constant edge length l.
- "Edge + Node" enforces a constant edge length l and mesh angle ω.
- "Node" enforces a constant mesh angle ω.

The curvature of networks is modelled through a subdivision of each edge into four segments. The edge length is measured along these segments. The mesh angle are measured between the adjacent segments at the nodes. A general continuity of curves is ensured through the continuity c (*Section 5.1.1*) to model a realistic representation of a smooth continuous network.

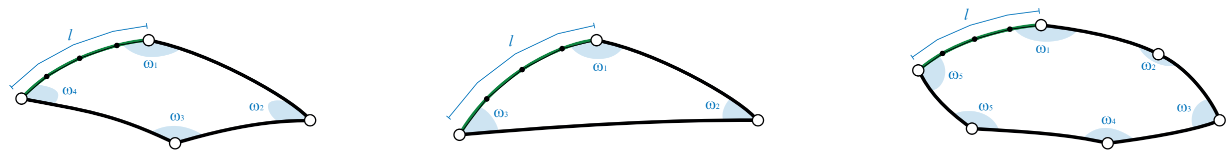

Figure 5.6 *Parameters measured at the smooth quadrilateral, triangular and hexagonal networks (**ES 2018**).*

Fisher-net Effect

Smooth segmentations may adjust to any shape by creating S-curved edges to compensate the variable node distance. This fisher-net effect can be found in quadrilateral, triangular and hexagonal networks. Even though this effect produces geometrically valid solutions, it is interpreted here as having insufficient fairness. Nonetheless, the distribution of S-curves beautifully illustrates the effects of double curvature.

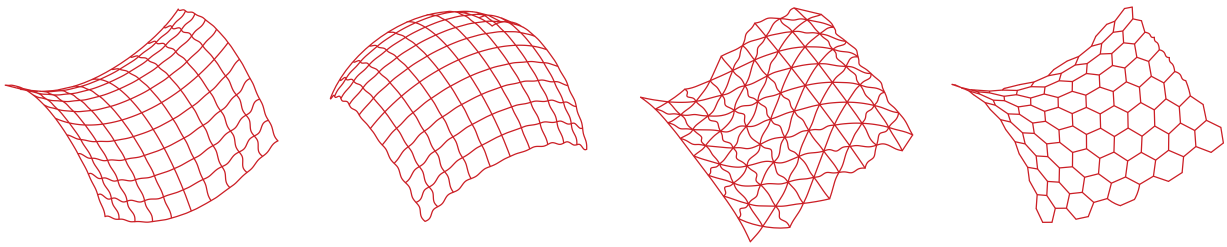

Figure 5.7 *Close-up illustration of the fisher-net effect caused by enforcing constant edge length and mesh angle in smooth segmentations (**ES 2018**).*

Quads

The morphology of smooth quadrilateral networks (*Figure 5.8*) nicely illustrates the reciprocal relationship of edge length and mesh angle. If one is constant, the other must become variable in order to accommodate the distortion of double curvature. Nonetheless, virtually every smooth sample in our experiment produces a geometrically valid solution due to the possibility of creating S-curved edges.

Edge. The behaviour of smooth equilateral quads is virtually identical to the corresponding discrete investigation. The network adjusts to the curvature through a rotation of mesh angles. This effect is most pronounced at the spherical and anticlastic surfaces. A fair network solution was obtained on the freeform surface, but the edges are curved strongly in order to adjust to the double-curved surface.

23 A further differentiation of curvatures (k_g, k_n, τ_g) will be implemented in *Section 5.4*.

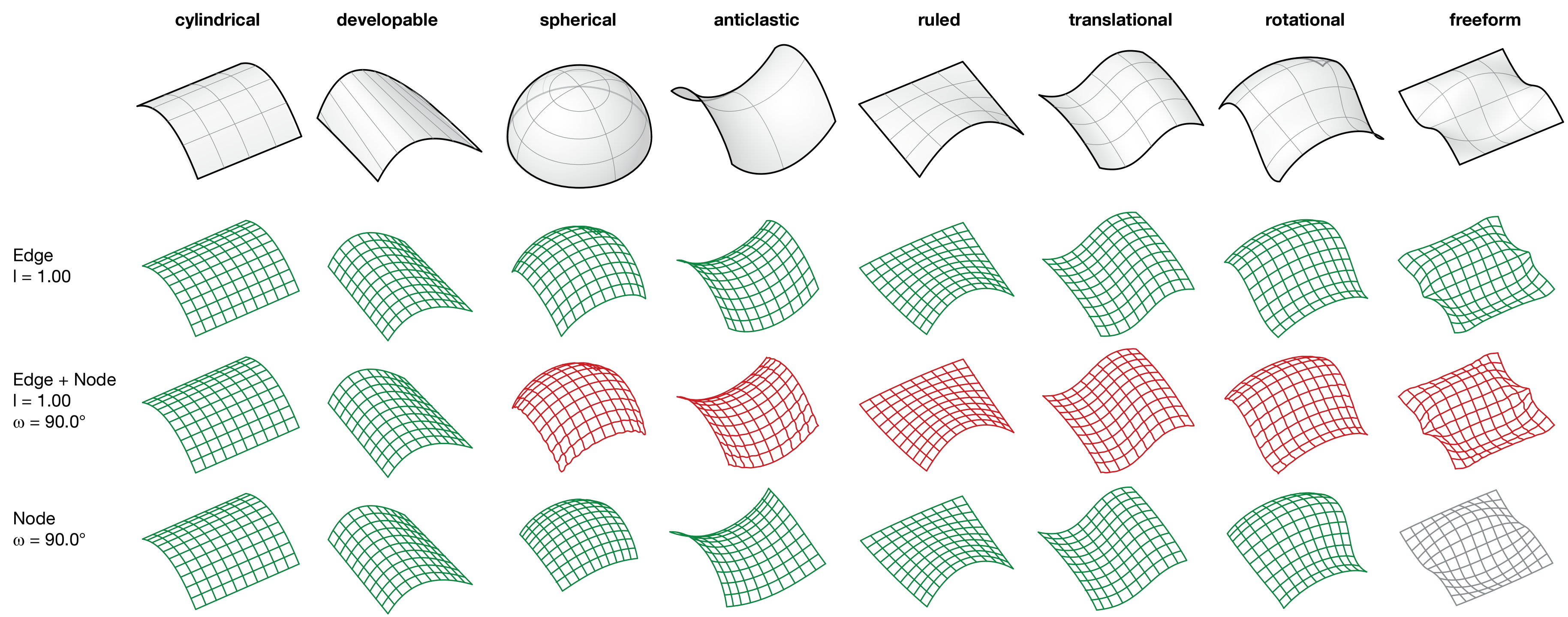

Figure 5.8 *Smooth quadrilateral samples (ES 2018).*

Edge + Node. While in a discrete segmentation (*Section 5.1.2*), the combination of constant edge length and mesh angle created congruent faces and required a planar or cylindrical arrangement, smooth segmentations adjust to any shape by creating S-curved edges between the nodes. The fisher-net effect appears at the outer regions of each sample and is most pronounced at the spherical and anticlastic target surfaces.

Node. Enforcing a constant node angle of 90° within a smooth quadrilateral segmentation is successful in all samples but the freeform surface. This sample did not converge due to the abstract modelling process with four discrete sub-segments. The morphology of networks is similar to the corresponding discrete investigation. An alignment with the principal curvature directions is noticeable, in particular for the rotational and anticlastic samples.

Triangles

Smooth triangular networks (*Figure 5.9*) are similarly restrictive as their discrete siblings. The rigidity of triangular networks results in S-curved edges on any shape other than developable surfaces. This effect is most pronounced when restricting the edge length, but also appears subtly when the mesh angle is restricted. Two samples of the freeform surface did not converge. Again, this behaviour is related to the modelling process with four discrete sub-segments which impedes a constant node angle for highly curved edges.

Hexagons

Smooth hexagonal segmentations (*Figure 5.10*) have a similar solution spectrum to quadrilateral networks. Both constant edges and congruent nodes lead to fair solutions. Only the combination of both results in a subtle fisher-net effect. Again, this illustrates the reciprocal effect of distortion which is either accommodated by the edge length or the mesh angle.

Edge. The behaviour of smooth equilateral hexagons is virtually identical to the corresponding discrete investigation. Adapting the equilateral hexagons to a double curvature causes distortion. This behaviour is best illustrated by the spherical and anticlastic samples, creating elongated hexagons around their perimeters.

Constant Curvature. The spherical hexagonal mesh is the only smooth sample which displays a constant curvature k on all edges, and is thus marked in blue. Because the edges of the hexagonal network are not continuous, i.e., no traversal nodes are enforced, each edge may individually align with the geodesic path between adjacent nodes. On a surface with constant Gaussian curvature (the sphere) this leads to a constant curvature k. A similar effect is possible with equilateral, quadrilateral networks or triangular networks if the continuity of edges was not enforced (*Section 4.2.2*).

Edge + Node. The existing S-curved edges are almost invisible for the Edge + Node parameter combination. The subtlety of this effect asks whether, through some amount of tolerance, a smooth hexagonal network with equilateral edges and congruent nodes could be constructed, defining the shape solely through its edge curvature. A similar solution was achieved for a spherical hexagonal structure within the experimental studies (*Section 5.3.4*).

Node. For the samples with constant mesh angle, the morphology of smooth hexagons also shows great similarities to its discrete pendant. The repetitive nodes are achieved only through an extreme adjustment of edge length. Especially for the translational and rotational surfaces, the enforced mesh angle seems to create a stretching of the network in regions of low double curvature. So far, we cannot pinpoint the cause for this effect.

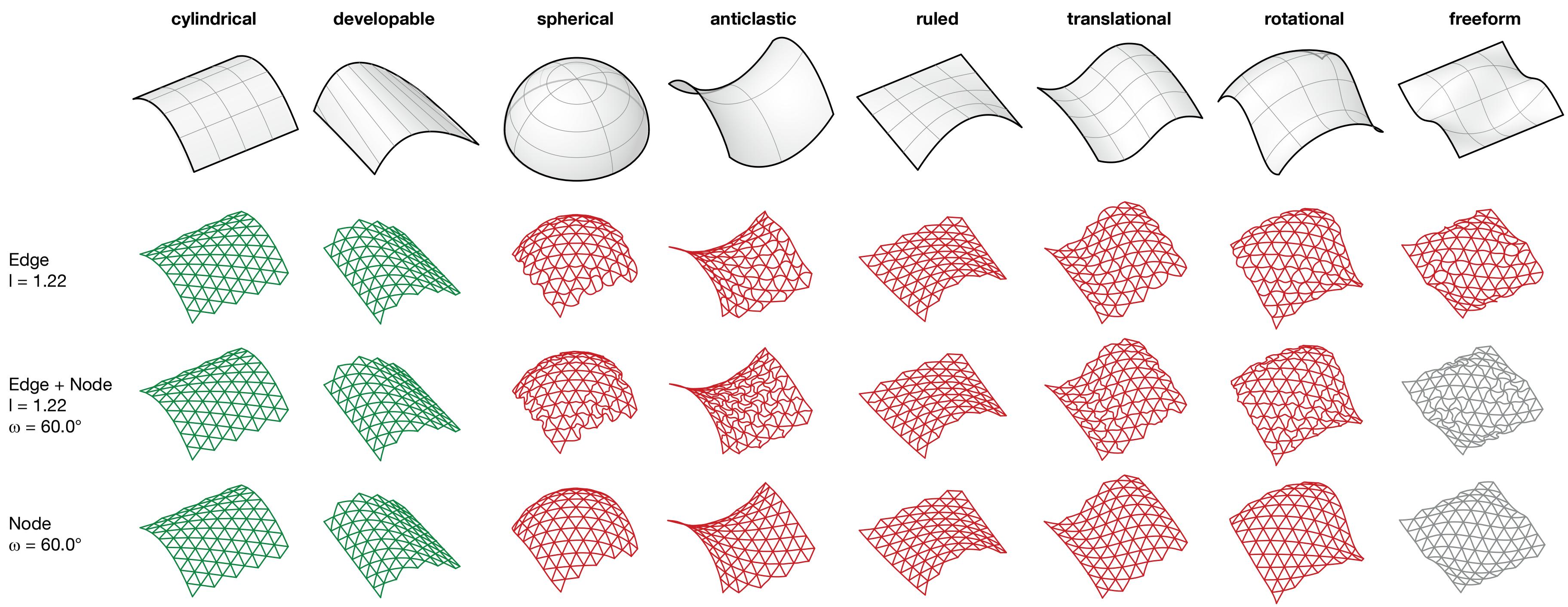

Figure 5.9 *Smooth triangular samples (**ES 2018**).*

5.1.4 Conclusion

The inductive study illustrates the morphological behaviour of triangular, quadrilateral and hexagonal networks for both discrete and smooth segmentations. Even though the samples do not allow a full analysis of all parameters, the various geometrical effects, such as distortion, fairness and alignment, are fundamental to repetitive structures and will continuously occur in further studies.

Networks

The choice of network strongly influences the possible solutions space for repetitive structures. Triangular networks are the most rigid network, offering no repetitive solutions for double-curved shapes other than planarity of faces. However, if a full repetition of faces is intended, triangular segmentations show the highest degree of flexibility due to their triple orientation of folds, and may form any developable shape.
Discrete quadrilateral and hexagonal networks generally allow constant edge length or planar faces on any surface. Quadrilateral networks have the additional possibility to create translational meshes, combining equilateral edges and planarity.
Smooth segmentations may create a regular network (of equilateral edges and congruent nodes) on any developable surface. This is in line with the concept of an isometric mapping (*Section 2.1.1*). All double-curved samples illustrate a reciprocal behaviour of edge length and mesh angle. If both parameters are kept constant, a fisher-net effect will occur.

Alignment

The alignment with principal curvature directions is most promising for both planar networks and networks with constant mesh angle. Ultimately, aligning a network to the surface curvature will trigger the formation of singularities, i.e., a local change of topology. This possibility was not investigated in this study. It would, however, offer further advantages for planar faces and congruent nodes.

Curvature

Considering the curvature of edges as a flexible geometric parameter allows for the adjustment of any network to any shape. However, combining constant edge length and constant mesh angle creates geometrically indeterminate solutions. The samples then display an S-curved shape of edges, which impedes the fairness and would most probably complicate both construction and façade solutions.
Only smooth segmentations allow for congruent nodes. Quadrilateral and hexagonal patterns may achieve this quality on any freeform surface. For triangular networks this option is limited to developable surfaces. In this experiment, only one solution was created which allows for a constant curvature k of all edges. This quality was achieved through a geodesic layout of edges on a sphere.

Fairness and Proximity

The perception of fairness is subjective. Fairness was used in this investigation as a qualitative indication of distortion or irregularities. Similarly, the importance of proximity to a target surface is questionable. Many “failed” discrete samples have a high aesthetic quality. The deliberate investigation of “non-fair” networks without a reference surface presents a versatile and promising field of future investigation. This could be applied to smooth segmentations embracing a fisher-net effect or an undulating surface, or discrete segmentations looking at the design of rough polyhedral meshes, or a combination of both.

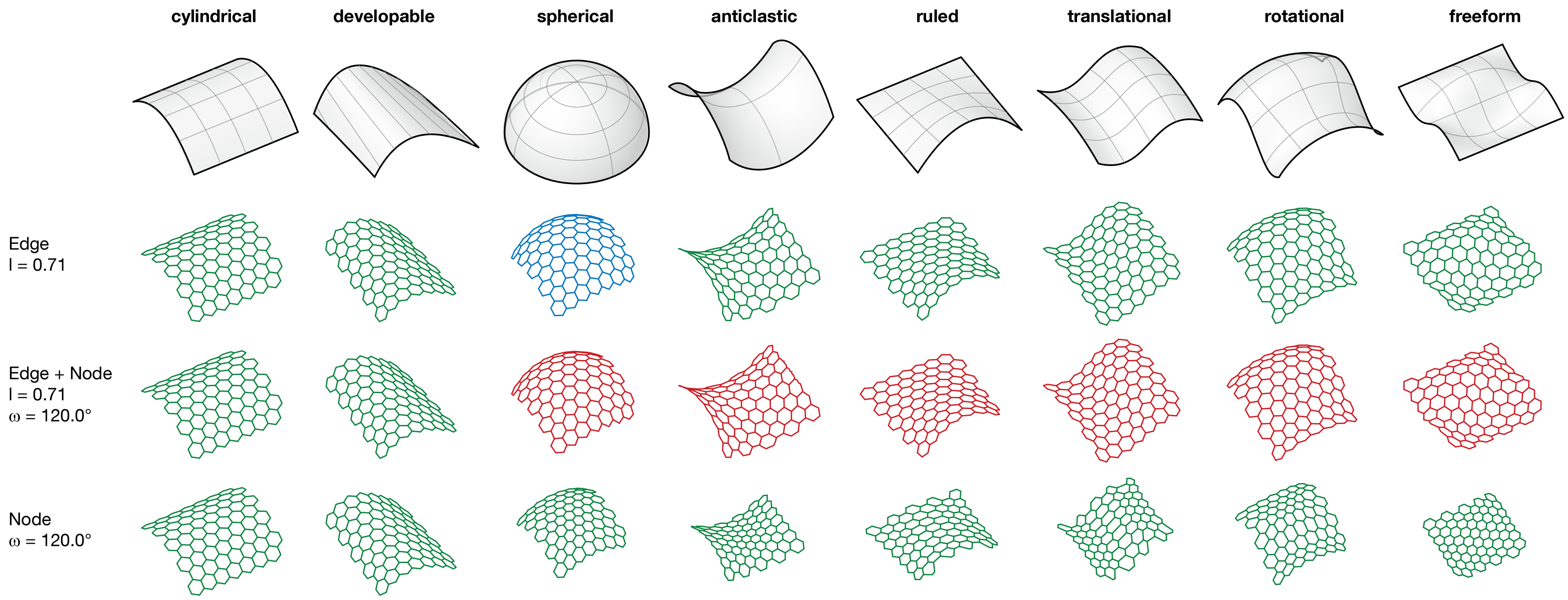

Figure 5.10 *Smooth hexagonal samples (**ES 2018**).*

Distortion and Gaussian Image

Pulling a regular network onto a double-curved shape creates distortion. For equilateral networks, this is expressed by a high variation of mesh angles. Conversely, enforcing a constant mesh angle results in a high variation of edge length. Keeping both mesh angle and edge-length constant results in a **geometrically indeterminate solution**, which is expressed by local "buckling" of edges into an S-shape. This is called the fisher-net effect.

These effects are most pronounced along the outskirts of the networks. The greatest distortion has been observed on the spherical, rotational, freeform and anticlastic surfaces.[24] The intensity of distortions is dependent on the size of the network and the curvature of the target surface.

Such dependencies are well known. The Gaussian curvature itself is nothing but a measurement of the local area distortion between Gaussian image and surface, $K = A_{\text{Gaussian Image}} / A_{\text{Surface}}$.

The total curvature of a geodesic triangle on a doubly curved surface, e.g., equals the deviation of the sum of its angles from π. A similar correlation is true for Chebyshev nets, where the interior angles of a patch is related to its total Gaussian curvature via the formula of Hazzidakis (*Section 2.2.1*).

We conjecture a general correlation of the distortion of a repetitive network (without singularities) with its Gaussian image. We are searching for a value which would indicate the distortion that is to be expected within a repetitive network.

To draw a comparison, we measure the maximum deviation of intersection angles of each smooth, quadrilateral, equilateral network, and analyse its Gaussian map. Next to the total curvature (TC) and the absolute total curvature (ATC), the area of the silhouette of the Gaussian image is measured (i.e., the area of the unit sphere that is touched by the Gaussian image). We call this value the **Gaussian footprint** (GF). It resembles the two-dimensional range of surface orientation.

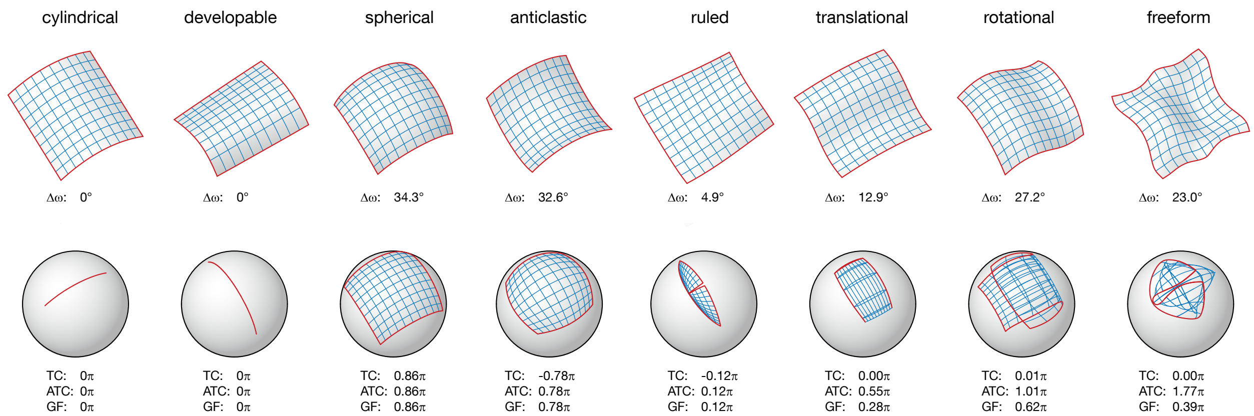

Figure 5.11 *Analysis of the Gaussian image of eight equilateral networks. TC = total curvature, ATC = absolute total curvature, GF = Gaussian footprint (**ES 2018**).*

When comparing the values of curvature and deviation angle, we come to the conclusion that the total curvature is not related to this distortion of networks. The freeform surface, e.g., has zero total curvature, but causes deviations of ω. Similarly, the absolute Gaussian curvature seems to not correspond, as it is extreme for an undulating surface, such as the freeform sample, but causes comparatively little change in mesh angles.

The Gaussian footprint is more informative as its values roughly correspond to the measured effects of angular variation. A more thorough mathematical investigation of this behaviour is a topic for future research.

24 The distortion was measured by comparing the variation of node angles in an equilateral network.

5.2 Inductive Study on Smooth, Rectangular Panelization

This study investigates the use of deformations combined with in-plane tolerances to achieve a smooth layout of standardized panels on double-curved surfaces. It is focused solely on the geometry of faces.

NODE					EDGE					FACE		
ω / ι	α	β	γ	o_n	l	k_n	k_g	τ_g	o_e	S	K	o_f

Table 5.2 *Table of active parameters for the inductive study on smooth, rectangular panelization. The repetitive face-shape is achieved through tolerances; the varying curvature is created by 'non-developable deformations' (**ES 2018**).*

The research was conducted in 2016 in collaboration with Philipp Eversmann, André Ihde and Christian Louter. The project investigated double-curved façades, which are clad with elastically-formed, standardized 1.0 x 2.0 m glass panels. It was published at the IASS 2016 Conference in Tokyo (***Eversmann et al. 2016b***).

The first part of the paper (which is not presented here) focuses on simulating the bending process of 4 mm heat-strengthened glass (HSG). The panels are forced onto a predefined geometry along all four edges while aiming to adhere to a maximum design stress. Through digital and physical experiments, Eversmann and Ihdé define a minimum principal curvature radius of 8.6 m, permissible for the deformation of 4 mm HSG panels. This value was used in the subsequent geometric study (presented here) to investigate the morphological aspects of this construction method.

The peculiarity of this experiment is the deliberate investigation of 'non-developable deformations' (*Section 3.2.3*), which allow the deformation of a flat face into a double-curved shape.

It would seem logical that a flat panel of glass, after bending, would remain a developable (singly-curved) surface. However, the process of bending glass onto curved support frames creates additional elastic strain which allows some deviation from single into double curvature.

Figure 5.12 *Prototype (5 x 4 m) of a double-curved glass façade consisting of 10 rectangular (and initially flat) HSG panels (1.0 x 2.0 m, 4 mm thick) (**Eversmann et al. 2016a**).*

Section 5.2.1 first defines a digital workflow based on abstract assumptions of the panel geometry which ensure an efficient modelling process. This method is used in *Section 5.2.2* to test the behaviour of repetitive layouts in respect to surface curvature, and highlights the effects on seam tolerances. Finally *Section 5.2.3* discusses the design implications and proposes an optimization method for freeform surfaces.

5.2.1 Digital Workflow

Assumptions

To investigate the layout of elastically bent panels on a double-curved surface, it is necessary to efficiently simulate and compare their geometry. Consequently, an abstract modelling process was set up based on the following assumptions:

- The panels will approximate the shape of the target surface provided that the minimal bending radius of 8.6 m is adhered to.
- As the glass panels are aligned tangentially to the target surface, any straight lines on the initially flat panels will be bent along geodesic curves on the target geometry.
- The perimeter and diagonal length of panels will remain constant within the given tolerance.[25]

Assuming that the perimeter and diagonal measurements of panels will remain constant throughout the deformation process, and that the panel will adapt to the target surface, establishes enough information to model their theoretical curved layout without simulating the actual bending process.

3D Modelling

For each panel, four points are projected onto a surface and connected with six geodesic curves (four of which create the perimeter quad, and the other two create the diagonals) to determine the panel size and proportion. These points are iteratively repositioned on the surface until all curves fulfil the predefined length requirements (*Figure 5.13*). The resulting geodesic quad represents the outline of the bent glass panel.

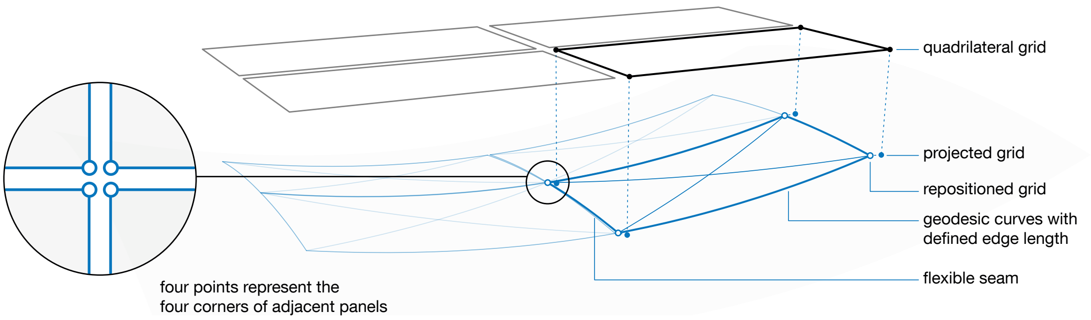

***Figure 5.13** Modelling process: A quadrilateral point grid is projected onto the target surface. The projected grid is then adjusted to fulfil the expected geodesic-length requirements. Additionally, a seam is simulated by modelling each corner of every panel seperately. The resulting four points at each intersection can move independently (**ES 2016**).*

Using this method, any quadrilateral point grid on a surface can be manipulated to represent a potential layout by adjusting the geodesic distance of any point to its eight neighbours (to the expected values of 1.0 m and 2.0 m resp. for the perimeter dimensions, as well as 2.236 m (the square root of 5) for their diagonal dimensions).

For any developable surface, such as cylinders or cones, this process yields a homogeneous, seamless grid of equidistant panels. However, in the case of a double-curved surface, it is impossible for all panels to maintain their edge lengths and proportion, and simultaneously create a seamless layout.

To solve this limitation, a flexible seam is introduced between the panels. The seam is implemented by creating four points at every intersection in a façade grid; each point represents the corner of one of the

25 It is evident that the length requirements cannot remain constant during a transformation from single into double curvature, as this does not qualify as an isometric mapping as defined in *Section 2.1.1*. However, in this experiment, the curvature is limited to a principal curvature radius of 8.6 m. As a consequence, the length-variance remains within the tolerance of 0.1%. The simulated, curved geometry of bent panels represents the closest and most realistic fit of the original panel-geometry. The miniscule change in length may be attributed to non-developable deformation (*Section 3.2.3*).

adjacent panels. These four points can move independently to allow the edges to fulfil the predefined geodesic lengths.

Behaviour and Limitations

Multiobjective Optimization. The digital model is controlled by a particle spring system, Kangaroo 2. The optimization process solves for multiple objectives, such as curve length and surface proximity. The outcome may vary depending on the weighting of each objective, the arrangement and orientation of network and shape, as well as the duration of the optimization process. Even re-computing the exact same settings does not necessarily create the identical result. However, the geometric behaviour is well depicted in this process, and is reproducible.

Simplifications. The geometric study implements an abstract model based on simplified assumptions. This enables the simulation of large panel layouts, but does not consider all physical effects of such a complex bending procedure. The permissible normal and shear stress within the glass are simply expressed as a minimal principal curvature radius.

Alignment. The alignment of the network has a decisive influence on the quality of the layout. All samples in this study are generally aligned with the surface's uv-directions of the target surface. In the case of the "hypar"-surfaces this layout is in line with the principal curvature directions.

Accuracy. The accuracy of the calculation is limited by the calculation time, the software environment and the solver. The tolerance for all length requirements was set to ± 0.1% of the target length.

5.2.2 Morphological Behaviour

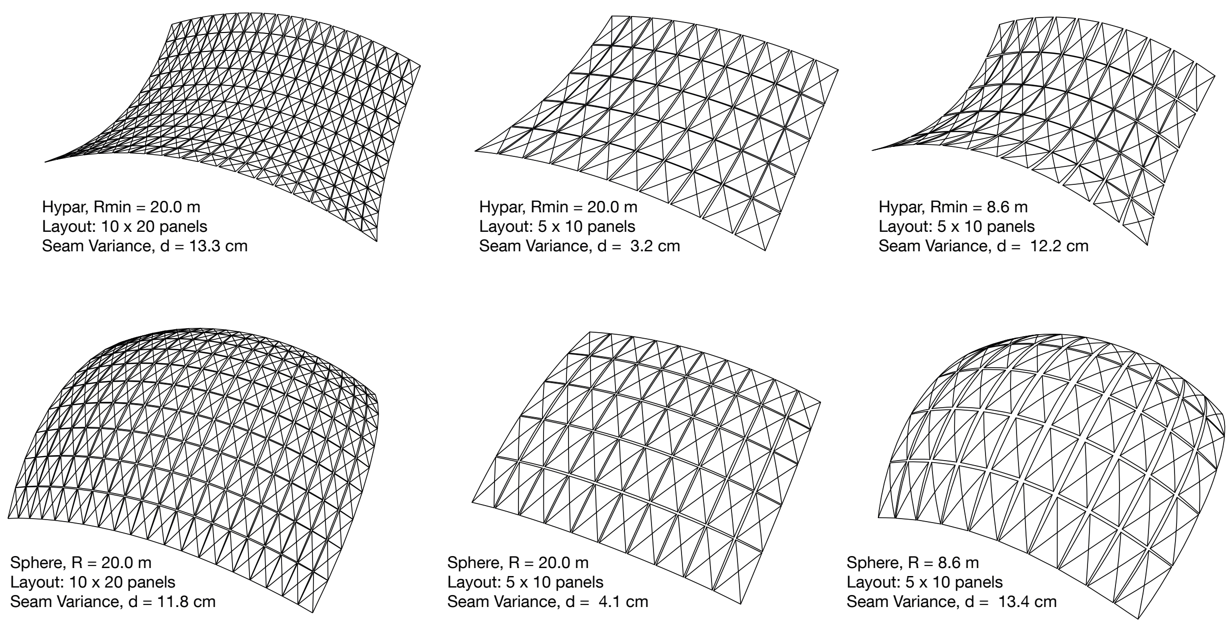

Figure 5.14 *Smooth, rectangular panels on a sphere (bottom row) and a hyperbolic paraboloid (Hypar) (top row). Each panel has a standard format of 1 x 2 m. The seam variance increases with the greater layout extent (left column) and smaller curvature radii (right column). Anticlastic curvature causes a concave seam (top row). Synclastic curvature produces a convex seam (bottom row) (**ES 2016**).*

Curvature, Layout and Seams

The digital workflow is first applied to a sphere and a hyperbolic paraboloid (Hypar) (*Figure 5.14*) – two surfaces with homogeneous positive and negative Gaussian curvature. Any curvature-related effect on the layout are displayed most extremely on these two shapes (as was clarified in the first inductive study, *Section 5.1*). First, we generate a curved panel layout and then we measure the difference in width between the smallest and largest seams. This value is called the seam variance d.

The progression and size of seams throughout the grid is dependent on the curvature, the extent of the layout and the proportion of panels (*Figure 5.20*). On synclastic surfaces, the seams follow a convex, banana-like shape. Anticlastic surfaces produce concave, hour-glass-shaped seams. A greater Gaussian curvature of the target surface induces larger seams in the panelization. Similarly, the layout-extent has an increasing effect on the seams. Rectangular panels generally display wider seams along their long edge.

These characteristics do not come as a surprise. They result from the discrepancy of the surface area when mapping a flat pattern onto a double-curved surface (*Section 1.4.1*). The varying seam-size can be explained mathematically with the help of the Jacobi equation of geodesic curves (***Pottmann et al. 2010, p. 3***).
The example given in *Figure 5.14* illustrates the potential of such a repetitive smooth panelization: A glazed spherical shell of 10 x 10 m with a curvature radius of 20.0 m can be covered using only one single, rectangular glass format if a variance of only 41 mm along the seam is tolerated.

Bulging Effect

The edges of each panel form a geodesic curve along the surface. The panel grid, however, may deviate from a geodesic curve as shown in *Figure 5.15*. Because of this deviation, succeeding glass-edges do not follow a continuous curve. When aiming the view along the seams, we notice the panel edges "bulging" from node to node, creating a cloud-like or serrated edge. In our example, this effect is most pronounced along the boundary (up to 20 mm) and vanishes towards the centre.

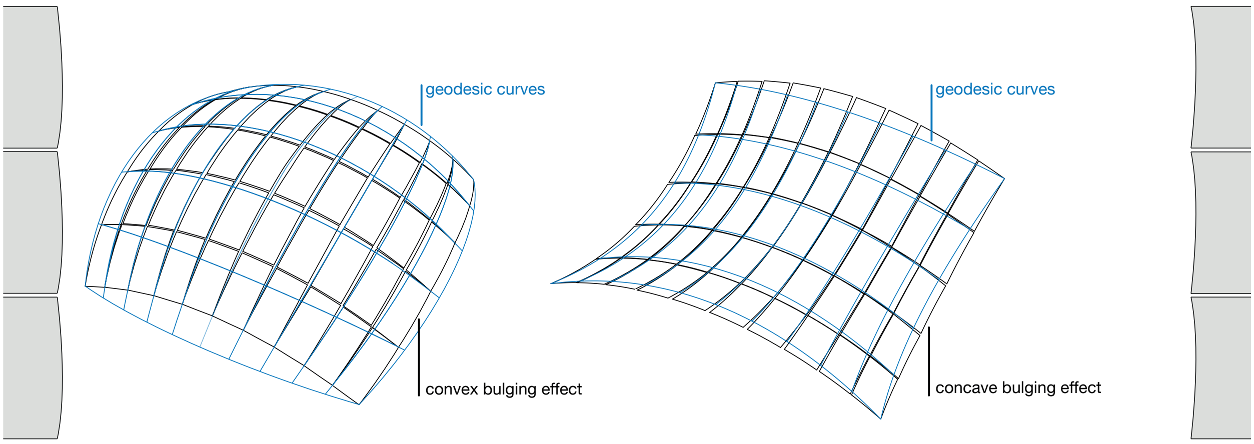

Figure 5.15 *Spherical and hyperbolic layout with minimal principal curvature radius 8.6 m. Shown are the resulting patterns of our panel-fitting routine (black) and geodesics connecting the corner vertices (blue). When deviating from a geodesic curve, the glass edges do not follow a continuous curve. They "bulge" individually from node to node creating a tolerance of up to 20 mm (**ES 2016**).*

Stepping Effect

The tolerance inside the seams can be shifted to only one direction. This property can be useful when designing with a linear substructure. It is achieved by enforcing collinear edges in the other direction, but triggers a stepping effect between panel rows. *Figure 5.16* shows two panelizations of the same target surface with seams oriented in opposite directions. The collinear edges are shifted creating a brick-like pattern. This effect originates from the change in length of each surface strip and is dependent on the variation of curvature in this area.

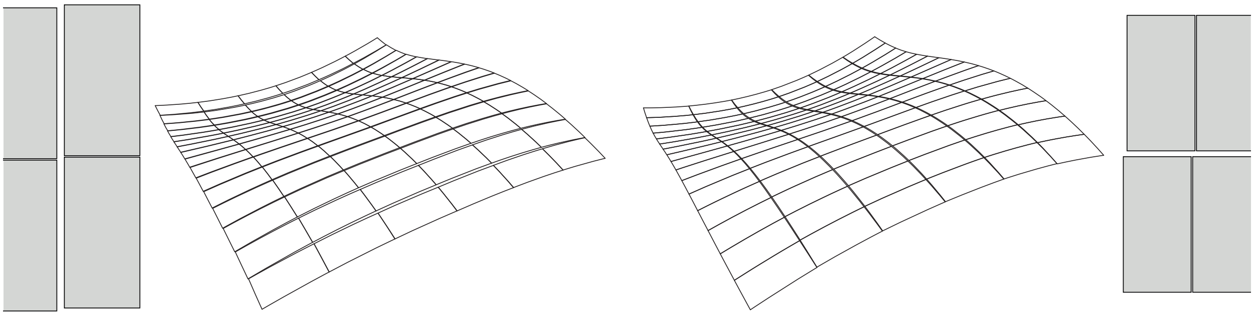

Figure 5.16 *Freeform surface with uni-directional seams. This can trigger a stepping effect transversal to the wider seam (**ES 2016**).*

5.2.3 Freeform Design

To design an appropriate surface for use with bent, rectangular panels, the critical principal curvature radius of 8.6 m has to be respected. This requirement is implemented by analysing the surface throughout its design until no radius violation is detected.

It is our goal to design a freeform surface which displays a high curvature, but a minimal seam variance. Since positive and negative Gaussian curvature have opposing effects on the progression of the seams, we conjecture that distributing positive and negative curvature evenly across a freeform surface would result in smaller seams. The two manual designs (*Figure 5.17*) confirm this assumption.

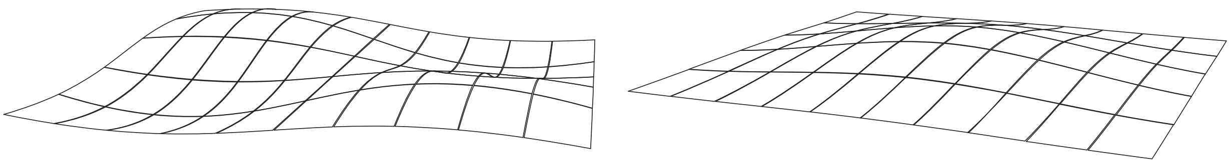

Figure 5.17 *Two manually designed freeform surfaces with 5 x 10 panels: Left: Straight boundaries with local bump, R_{min} = 8.7 m, d = 23 mm. Right: Four alternating hills and valleys, R_{min} = 8.7 m, d = 18 mm (**ES 2016**).*

Surface Optimization

To find a surface shape that maximizes curvature and minimizes seam tolerance, a simple optimization routine is installed using Rhino, Grasshopper and the standard evolutionary solver Galapagos (***Rutton 2010***): A large set of sample surfaces is generated with 5 x 5 control points by randomly varying the z-coordinates of each point. Each sample surface is analysed via a dense point-grid (50 x 50) which is aligned with the rows and columns of the potential panel layout. The following three simple indicators are measured at every point and multiplied within a fitness function:

- k_{SUM} is the absolute sum of all principal curvature radii. This value acts as an indicator for the inverse, absolute total curvature of the surface.
- k_{PEN} is the number of penalties given for any curvature radius below a set value (in this case 8.6 m). This value ensures that the final surface is appropriate for the use of the specific material.
- l_{RANGE} is the difference between the longest and the shortest curve along each direction of the panel layout. This value ensures that each row/column of panels is similar in length, thus minimizing the necessary seam variance. In a sense, it resembles the total curvature of the design surface.

$$\text{Fitness: } F = k_{SUM} * (1 + k_{PEN}) * l_{RANGE}$$

This fitness F is evaluated for each surface sample. Eventually a solution with minimal value F is found[26]. Such a surface has a comparatively high absolute total curvature (within the bounds of the minimal principal curvature radius) and a balanced distribution of surface area. It is optimal for the implementation of curved, rectangular panels, as it results in small seam variations.

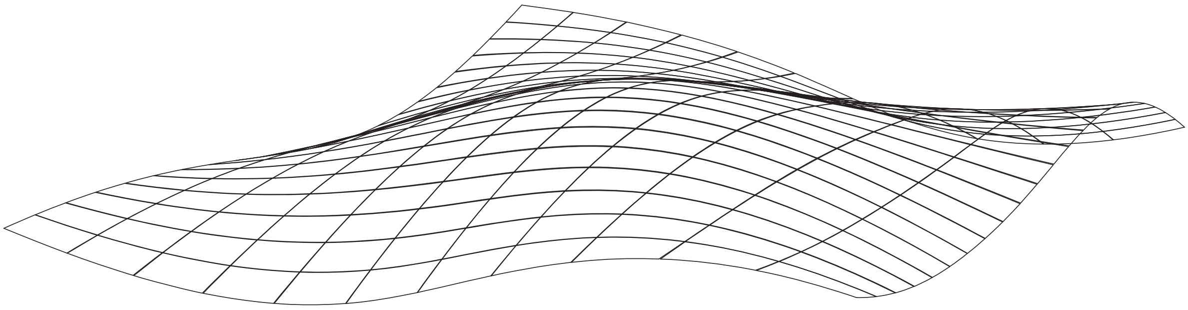

Figure 5.18 *Optimized freeform surface: The algorithm maximizes the surface curvature without violating the minimal principal curvature radius and minimizes the differences of surface length measured along the panel grid. This results in low variation of seams: Layout: 11 x 22 panels, R_{min} = 8.61 m, d = 4.9 cm (**ES 2016**).*

26 More background on the computational process of Galapagos can be found at ***Rutton*** (***2010***).

5.2.4 Conclusion

The combination of tolerances and deformation allows for a smooth panelization of double-curved surfaces with repetitive panels. The possible shape spectrum is dependent on the maximal seam and minimal curvature radius permissible. These factors need to be set by the designer in accordance to the specific construction technique and choice of material.

Seams

The seams take up the natural distortion caused by double curvature. The seam variance is dependent on the curvature and extent of the network. In the case of synclastic curvature, the largest seams are found at the centre of a layout. In the case of anticlastic curvature, the seams increase along the boundaries. Furthermore, a misalignment of seams with geodesic curves leads to a serrated progression of face edges. The implementation of uni-directional seams causes a shift of panels into a brick-like pattern.

Design

The design-surfaces can be optimized for low seam variance and high absolute total curvature by aiming for a constant length for all rows and columns of panels. This optimization process favours undulating surfaces with alternating positive and negative Gaussian curvature.

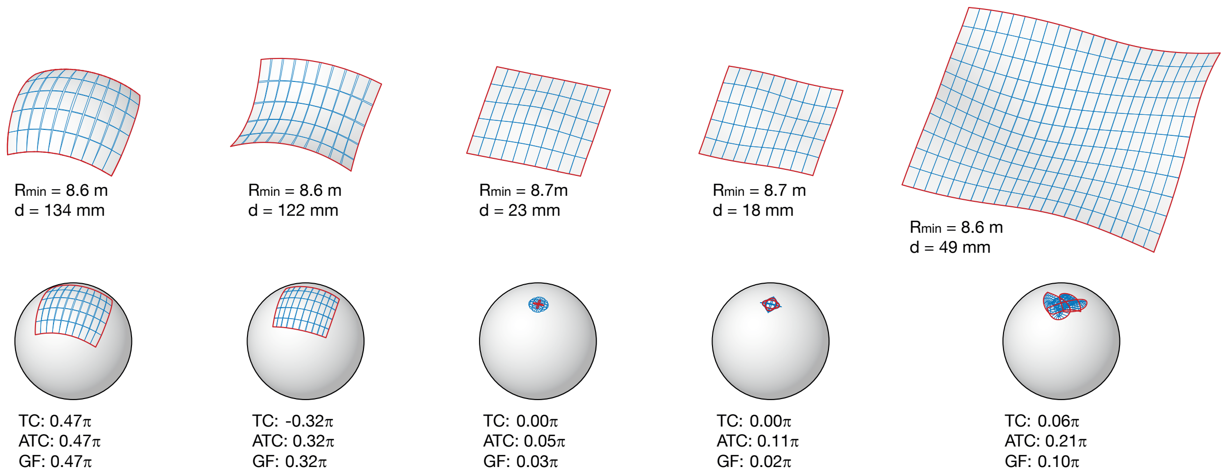

Figure 5.19 *Analysis of the Gaussian image of five panelization layouts. TC = total curvature, ATC = absolute total curvature, GF = Gaussian footprint (ES 2018).*

Distortion

Similar to the comparison of equilateral nets in *Section 5.1*, we conjecture a correlation of the effects of distortion with the Gaussian image. Therefore, we measured the seam variance d and compared it to the total curvature (TC), the absolute total curvature (ATC), as well as the **Gaussian footprint** (GF) (our own measurement of the spectrum of surface orientation, see *Section 5.1.4*).
Both spherical and hypar surfaces create high values for TC, ATC and GF, but also large seam variance. The three freeform examples, on the other hand, create small but folded Gaussian images, with a low total curvature, and comparatively high absolute total curvature.

The Gaussian footprint seems to be the best indicator to predict the intensity of distortion, as its value roughly correlates with the seam variance. A more thorough investigation of this behaviour is a promising topic for future research.

5.3 Experimental Design Studies

Over the course of three years from 2014 - 2016, an annual design studio, Experimental Structures, was conducted at the Chair of Structural Design, TUM, to creatively investigate the use of repetitive parts in the design of double-curved structures. Parts of this study have been published as a technical report in the Bautechnik magazine (***Schling et al. 2014***) and at the AAG 2016 in Zurich (***Schling and Hitrec 2016***).

After an introduction of the course assignment in *Section 5.3.1*, we present six projects from *Section 5.3.2* - *Section 5.3.7* which display various constructive applications of deformation. Each project is analysed parametrically to highlight similarities to earlier studies.
Section 5.3.8 will list observations concerning this parametric behaviour and discuss the importance of distortion for the network shape and construction.

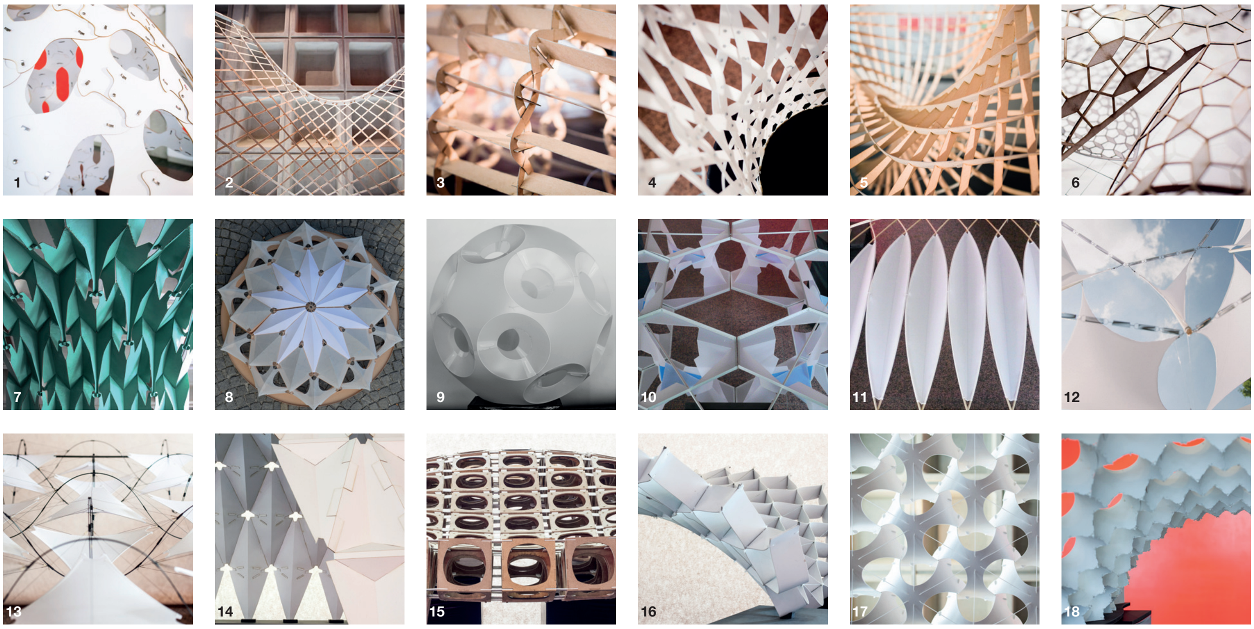

Figure 5.20 *Overview of projects realized in the course of the design studio "Experimental Structures" (Photos:* ***Matthias Kestel 2014*** *and* ***2015, Magdalena Jooß 2016****).*

1 *Eleonora Velluto: Modular Gridshell* **2** *Damiano Tosti: Hypar Gridshell* **3** *Rongguang Na: Reciprocal Gridshell* **4** *Pablo Mollina: Geodesic Gridshell* **5** *Denis Hitrec: Asymptotic Gridshell* **6** *Anna Bosco: Developable Pentagon Gridshell* **7** *Huilian Tang, Bingyu Xu: Folding Origami* **8** *Katrin Fleischer, Corinna Wiest: Deployable Dome* **9** *Jose Maria Arribas, Donald Ottoerson: Curved Folding* **10** *Jeremy Copley, Nick Franz: Snap Through Triangles* **11** *Alessandro Corso, Lukas Kaufmann: Curved Scissors* **12** *Yang Yu, German Rueda: Movable Tensegrity* **13** *Sebastian Huth: Bending Tensegrity* **14** *Miroslava Denina: Folding Vault* **15** *Michal Markusek: Cubic Surface* **16** *David Walsh; Bending Strips* **17** *Quirin Mühlbauer: Hexagonal Bending* **18** *Vitaly Entin: Conic Gridshell*

5.3.1 Course Assignment

The design studio was set up to encourage a “bottom-up” design approach – starting with fabrication and finishing with a design shape – with the goal of investigating form as an emergent property of repetitive construction.
In contrast to common assignments for architects, the students received no list of requirements in respect to site, use or functionality. The design task only required the students to design and build a curved structure from repetitive modules with a span of 2 x 2 m.

The design process was divided into three phases:

- a **research phase**, looking at geometric and structural techniques to fabricate modules

- a **modular design phase**, in which a single unit was developed and analysed for its geometrical and structural properties

- an **assembly phase**, in which the repetitive modules were joined to create a curved surface structure

This process satisfied two goals:

- **Pedagogically**, the studio was directed to engage students in parametric thinking on a physical level. Through iterative developments of physical prototype and active analysis of their parameters, the students developed an understanding of the dependencies of a repetitive module and its related agglomerative surface geometry.

- **Scientifically**, this studio followed the principle of research by design to generate a multitude of creative solutions to a research question. These experimental designs show a broad spectrum of techniques, shapes and structures and thus illustrate the various possibilities to design curvature with repetition.

The students aimed to achieve a symbiosis of fabrication, form and structure, with a strong emphasis on aesthetic design. Their work is thus presented based on these four criteria.

5.3.2 Bending Strips

Module

David Walsh investigated the behaviour of elastic strips. He connected two identical, rectangular plastic sheets on all four corners, and subsequently pulled together the short edges with a cable. As a result, the strips bulge outward creating a smooth, rhombic comb.
By placing the cable eccentrically at the upper edge, a distortion in two directions is obtained: The strips twist, opening the top, and creating a funnel shape in section. Simultaneously, the strips bend downwards, creating a bow-shape in elevation.

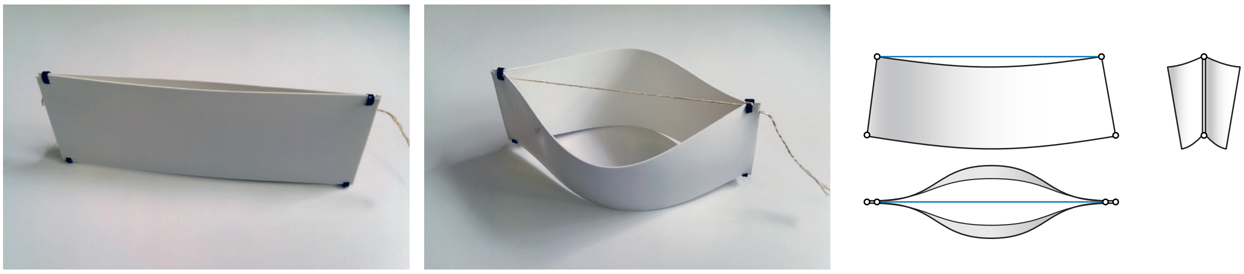

Figure 5.21 *Development of an elastically deformed base module from planar, rectangular strips (ES 2018).*

Assembly and Shape

To assemble this module, long, uniform strips of polysterol were first placed in parallel and connected alternatingly to their left and right neighbour. Then, two families of cables were prestressed in the longitudinal and lateral directions and then tightened at each intersection to ensure a homogeneous waving motion. The bow-shape at each module creates a concave curvature in the longitudinal direction. At the same time, the funnel-shape creates an opposing, convex curvature in the lateral direction.
Consequently, an overall, anticlastic, saddle shape emerges.

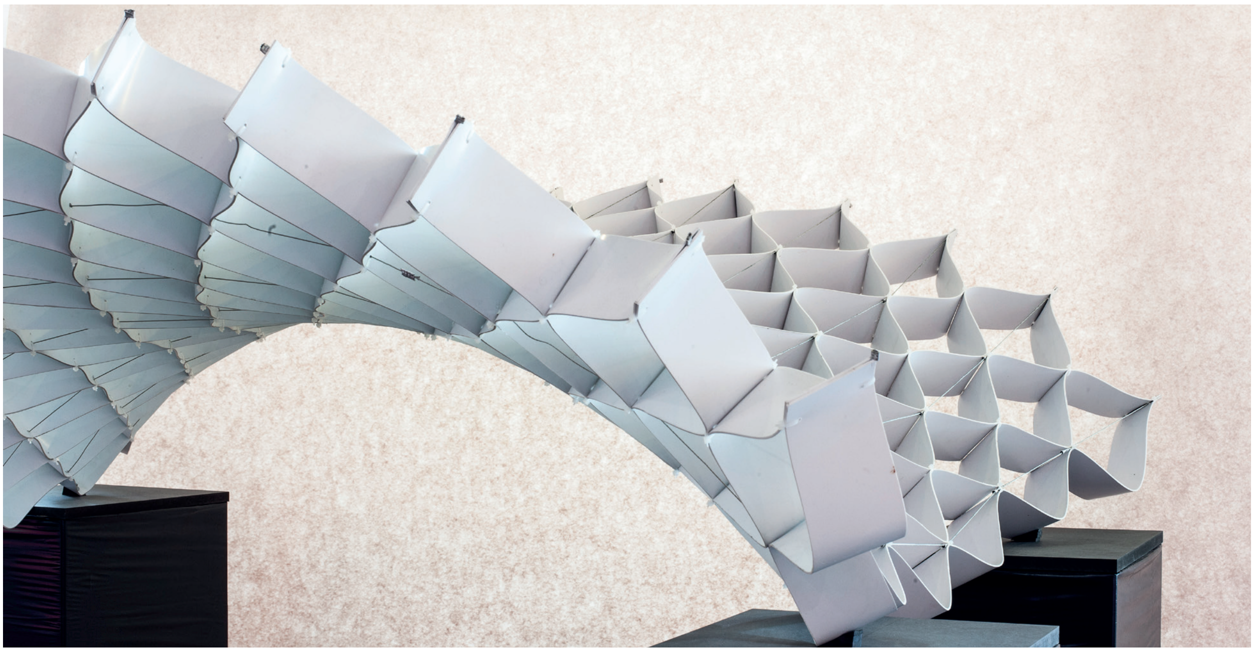

Figure 5.22 *Completed structure, Bending Strips, by David Walsh. The assembly of modules creates a self-supporting sculpture with a negatively curved shape (Photo: **Matthias Kestel 2014**).*

Structure and Aesthetics

The sculpture was assembled from 20 strips of 2 m long and 8 cm high lamellas connected every 28 cm. The lamellas create a curved grillage that is supported vertically and horizontally to aid the load-bearing behaviour of an arch. However, the structure is soft and susceptible to deflections due to the low bending radii, slender lamellas, open boundaries, and point supports.

The smooth anticlastic shape creates a calm and inviting space. The waving motion of lamellas has a natural and pleasant appearance. The slender strips allow for high transparency at a direct view and opacity at an inclined view, and cast an intricate pattern of shadows.

Figure 5.23 *Detail of the structure, Bending Strips. Steel cables on top and bottom induce the deformation and fix the overall shape (Photo:* ***Matthias Kestel 2014****).*

Analysis

The strips are oriented normal to the design surface which impedes a curvature in the normal direction. The rhombic arrangement can be interpreted as a diagonal pattern, in which each diagonal is waving in and out of an asymptotic path. Naturally, this arrangement can only be shaped into an anticlastic form (see *Section 5.4*). The lamella segments are all fabricated equally and the lamellas meet tangentially at every intersection.

The morphological behaviour shows similarities to a smooth quadrilateral network on an anticlastic surface with constant edge length and constant mesh angle (see *Section 5.1.3, Figure 5.8*):

- The strips are naturally shaped in S-curves. This arrangement adjusts to the varying node-to-node distance through a fisher-net effect.

- Due to the negative curvature a gradual distortion of the pattern occurs. The outer units contract and widen to account for the surplus in surface area.

NODE					EDGE					FACE		
ω / ι	α	β	γ	o_n	l	k_n	k_g	τ_g	o_e	S	K	o_f
0°	0°	0°	0°	c	c	0°	deform.	deform.	c	-	-	-

Table 5.3 *Qualitative parametric assessment of the structure, Bending Strips. The strips are interpreted as edges, meeting tangentially at each node (****ES 2018****).*

5.3.3 Cubic Surface

Design Process

Michal Markusek used a 10 x 10 x 10 cm cube as a base module with the goal of constructing a double-curved surface. This posed the challenge to design a variable gap between modules. A standard distance of 2 cm between units was defined which limited the possible inclination angle of two adjacent cubes and thus determined the maximum curvature of the whole sculpture.

__Figure 5.24__ Modules of the structure, Cubic Surface. It is assembled from prefabricated, repetitive Vierendeel cubes (Photo: __ES 2014__).

Markusek designed a double-curved surface with a central hill and two symmetrical valleys on either side. He generated a point grid on this surface which originates at the central apex and reticulates in steps of 12 cm first in the longitudinal, and then in the lateral direction. The grid points mark the centre of each cube which are then positioned normal to the design surface. The tolerance allows each cube to incline without colliding with its neighbours. Once the exact position of each cube is defined, the position of adjacent corners is measured to determine the geometry of ring connectors on top and bottom.

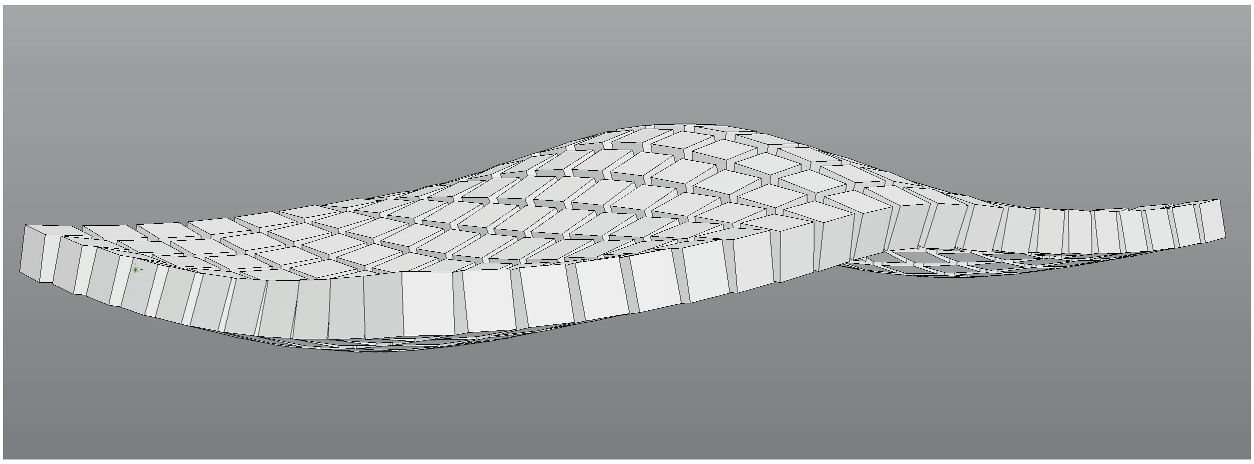

__Figure 5.25__ Digital design model of the Cubic Surface. The cubes are laid out on a double-curved design surface (__ES 2014__).

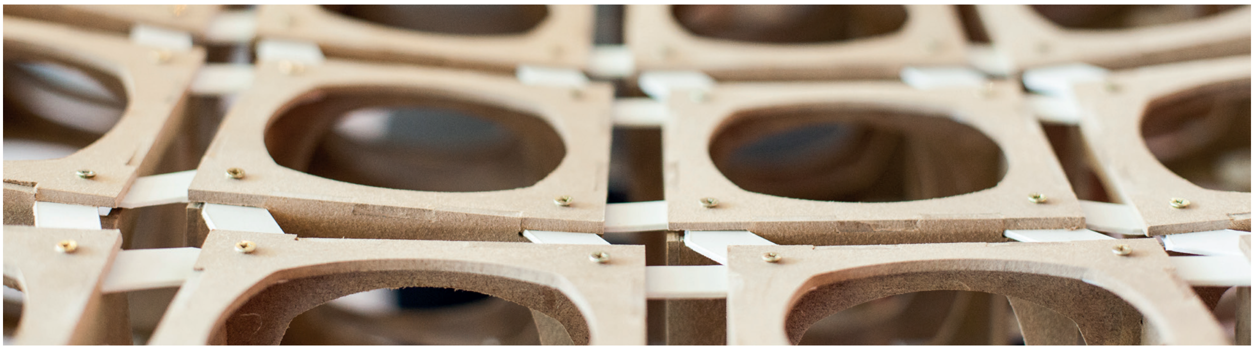

Figure 5.26 Detail of repetitive cubes and individual connection rings (Photo: **Matthias Kestel 2014**).

Connectors

The connection rings are subject to the four geometric effects, all caused by the distortion of the network:

- The ring-edges vary in length due to the convex or concave shape at top and bottom.
- The rings are bent in order to take up the normal angle between cubes.
- The double-curved surface results in a shift of the cubes (similar to the stepping effect described in Section 5.2.2) and creates a sheared geometry of the connection rings.
- Due to geodesic torsion, subsequent cubes are rotated, causing an out-of-plane misalignment of adjacent corners.

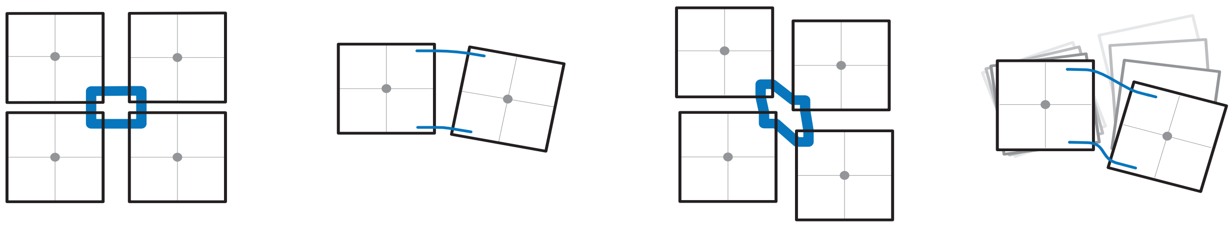

Figure 5.27 Geometric effects of cube connectors. The rings adjust to the distance, angle, shear, and torsion (**ES 2015**).

Pattern

The extent of this distorted system is limited as the shift between cubes steadily increases from the centre outward, ultimately prohibiting a feasible connection between units. The connector rings were unrolled as 2D geometry and cut out with a CNC-mill. The cutting pattern reveals another geometric characteristic: The unrolled connectors create a nearly seamless tessellation, in which the corner angles of four adjacent rings add up to 360°.

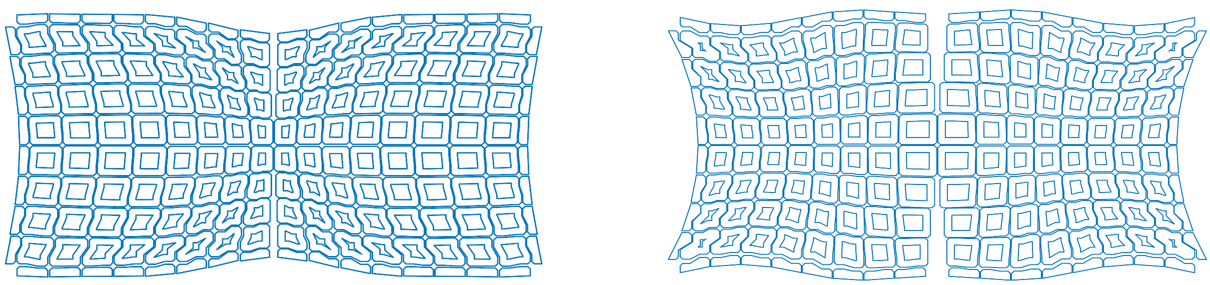

Figure 5.28 Cutting pattern of the cube connectors (Left: bottom layer, Right: top layer). The convex and concave regions of the design surface influence the size of the rings. The shifting of adjacent cubes is most pronounced at the outskirts, especially at the corners of the top layer (**ES 2016** based on **Michal Markusek 2015**).

Structure and Aesthetics

The final sculpture was assembled from 17 x 9 cubes, made of 3 mm plywood, and 352 polysterol rings (1.5 mm), which were bent and folded to bridge the gap and connect to each of the four corners of the adjacent cubes. This curved Vierendeel grillage carries its weight via bending and only needs to be supported vertically.

The contrast between rigid cubes and flexible connectors is graphically emphasized by the change in material. It illustrates the impact of double curvature on an orthogonal grid. The repetitive Vierendeel cubes create a graphical depth.

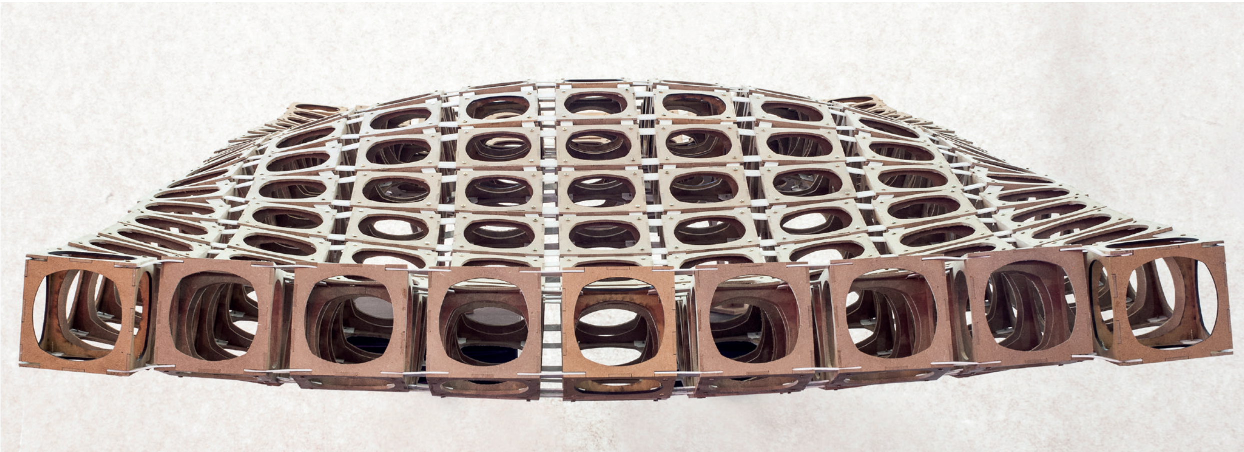

Figure 5.29 *Completed structure, Cubic Surface, by Michal Markusek. The cubes form a rigid girder (Photo: **Matthias Kestel 2014**).*

Analysis

Cubic Surface is an example of a repetitive tiling with tolerance, similar to the inductive study on smooth panelization (see *Section 5.2*):
In this case, the tolerance is used in a multi-layered structure. The concave/convex orientation of curvature has a major influence on the size of the gaps at top and bottom. The hierarchical layout of the underlying point grid in longitudinal and lateral directions results in a stepping effect causing the cubes to shift towards a brick-like pattern. While the middle rows are well aligned with the principal curvature direction, the outer rows display geodesic torsion causing an out-of-plane misalignment of adjacent edges.

NODE					EDGE					FACE		
ω / ι	α	β	γ	o_n	l	k_n	k_g	τ_g	o_e	S	K	o_f
variable	deform.	variable	deform.	c	-	-	-	-	-	tolerance	c / P	c

Table 5.4 *Qualitative parametric assessment of the structure, Cubic Surface. The cubes are interpreted as faces of a quadrilateral network and the rings are interpreted as nodes (**ES 2018**).*

5.3.4 Hexagonal Bending

How can a curved network be formed naturally by its internal stress? Quirin Mühlbauer used a simple 2D concept to develop a 3D structure: When rigidly connecting a series of bent elements in one row with fixed supports, the internal stress naturally pushes the assembly upward.

Figure 5.30 *Two-dimensional concept of the modular elastic design. The moduls are deformed, connected rigidly, and held at horizontal supports. Consequently, the internal stress creates an upwards movement (**ES 2016** based on **Quirin Mühlbauer 2015**).*

This logic can be applied to an elastically bent hexagonal structure, creating restraint stresses in the centre, and a ring of tension along the border. The structure consequently curves upwards to release stress and creates a shallow dome shape.

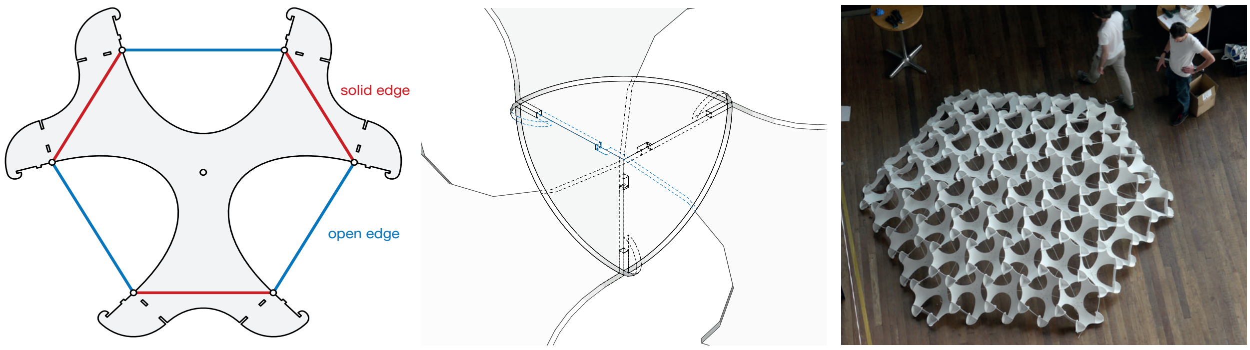

Figure 5.31 *Module, joint and assembly of the structure, Hexagonal Bending (**ES 2016** based on **Quirin Mühlbauer 2015**) (Photo: **ES 2015**).*

Design Development

Mühlbauer developed a star-shaped module based on a hexagonal grid. Three concentric arms branch out to create six connection points. Each point is rigidly interlocked with two further modules. These orthogonal joints enforce an equal distance between all connection points. Consequently, the longer open edges bend into a bowl shape. The assembly creates an equilateral honeycomb system of three-legged blossom-shaped modules connected rigidly on top and bent softly on the bottom.

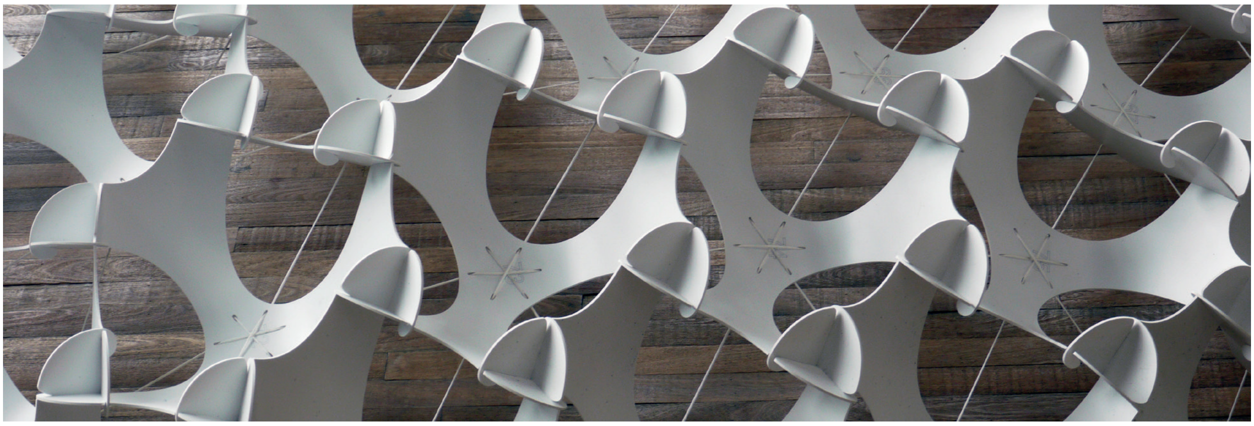

Figure 5.32 *Close-up of the interlocked and bent modules (Photo: **ES 2015**).*

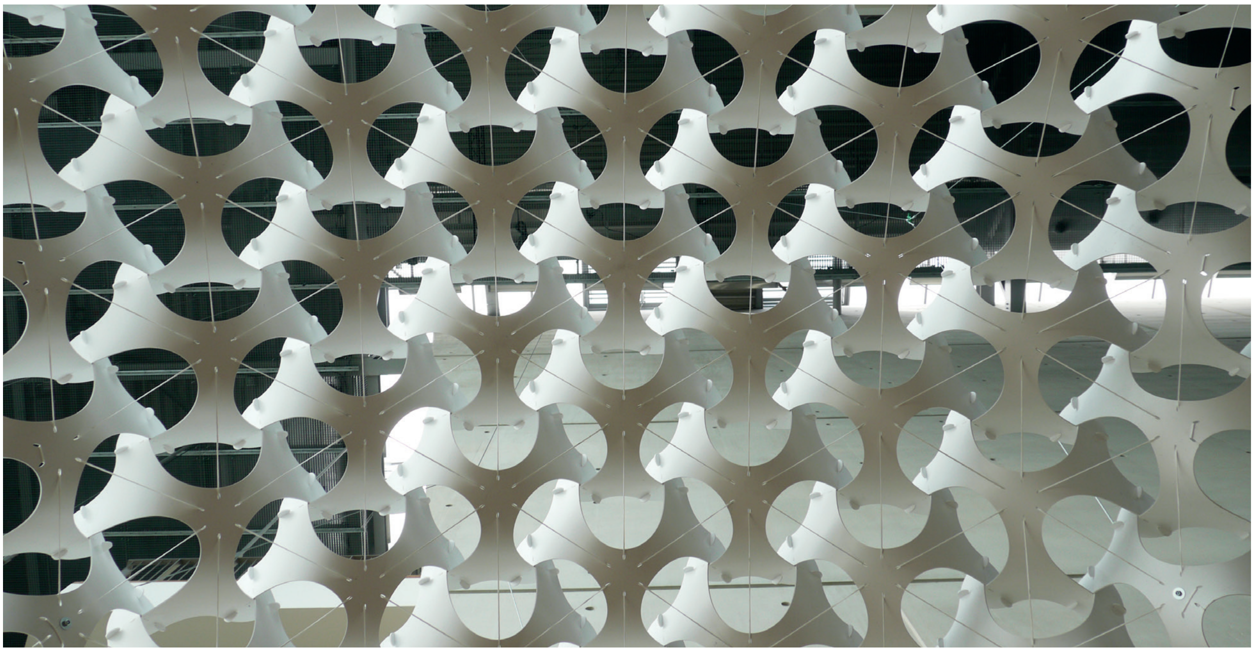

Figure 5.33 *Looking up at the structure, Hexagonal Bending, by Quirin Mühlbauer. The smooth hexagonal modules are overlaid by a clean triangular grid of tension-ties (Photo: **ES 2015**).*

Structure and Aesthetics

This sculpture was exhibited at the IASS[27] Conference 2015 in Amsterdam. The setup consisted of 61 congruent modules cut from 4 mm Forex foam-board which formed a hexagon with five units along each side.

It is remarkable that despite the fully repetitive construction with congruent joints, the sculpture naturally assumes a double-curved dome shape. By adding a set of hexagonal cables to the bottom layer, the structural height of the assembly is activated, creating sufficient stiffness to carry its self-weight over an approximate span of 4 m.

The point symmetry of each connection and the smooth curvature of each module create an optical illusion similar to a graphic of M.C. Escher. The flow of light along the reflective, clean plastic surface adds further quality to this seemingly floating structure. The linear and straight cable-net acts as a regulative layer, like a coordinate system, marking the axis of symmetry.

Analysis

The sculpture follows the principles of a smooth hexagonal network with constant edge length and constant mesh angle on a spherical target surface as described in *Section 5.1.3*. The overall curved geometry is achieved by a gradual distortion of the polygons, which results in a S-shape of the edges along the outer rows of the assembly. Just like in the inductive study, this effect is very subtle due to the low Gaussian curvature.

NODE					EDGE					FACE		
ω / ι	α	β	γ	o_n	l	k_n	k_g	τ_g	o_e	S	K	o_f
120°	c	0°	0°	c	c	deform.	deform.	deform.	-	tolerance	deform.	c

Table 5.5 *Qualitative parametric assessment of the structure, Hexagonal Bending. The modules are interpreted as both edges and faces of a hexagonal network (**ES 2018**).*

27 International Association for Shell and Spatial Structures

5.3.5 Modular Gridshell

The Modular Gridshell by Eleonora Velluto was inspired by the strained timber gridshells of Frei Otto (*Section 2.4*). Similar to Frei Otto's chain models, Velluto relaxed a uniform quadrilateral grid to design a funicular shape with equilateral edges. Velluto used a grid of 18 x 9 units and introduced six supports to create two cupolas with a common arch.

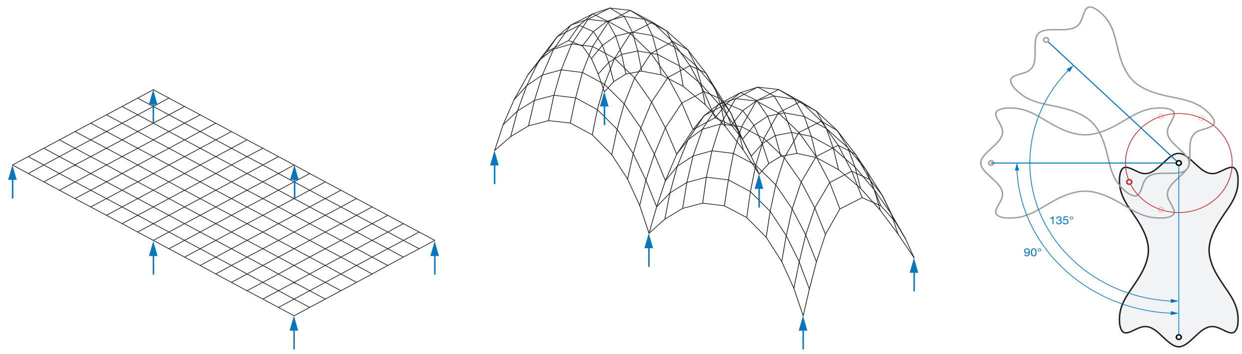

Figure 5.34 *Funicular design process and module geometry of the Modular Gridshell (**ES 2017** based on **Eleonora Velluto 2016**).*

Module

Velluto's goal was to construct this gridshell not from continuous laths with diagonal bracing, but to use identical flat modules, which fulfil both structural functions: transmitting the compression of self-weight, and bracing the system against asymmetric loads. This was achieved by designing a leaf-shaped unit with two kinds of connections.

The primary connection is located on a central axis on both ends of the leaf, resembling the hinge point of the equilateral network. The secondary connection is located on a set radius around the primary nodes, and is emphasized through four arms. This secondary connection allows a coupling of adjacent modules for variable intersection angles (from 45° to 135° degrees) to lock the node rotation and create shear stiffness.

Assembly

The primary joint is inserted first to create a uniform, flat, hinged grid of 9 x 9 units. This network is then hung from four supports to naturally fall into a funicular shape. In the course of this transformation process, the joints rotate to adjust to the double curvature. Once the desired shape is obtained, the secondary connections are inserted, fixing the geometry and creating a stiff shell.

This process is repeated for the second part of the structure. Finally, both shells are inverted and joined, creating a tall, double dome on six supports.

Figure 5.35 *Construction process of the Modular Gridshell. The modules are connected to form a uniform, planar, hinged network. After the net is hung, each joint is fixed with two additional ties (Photos: **ES 2016**).*

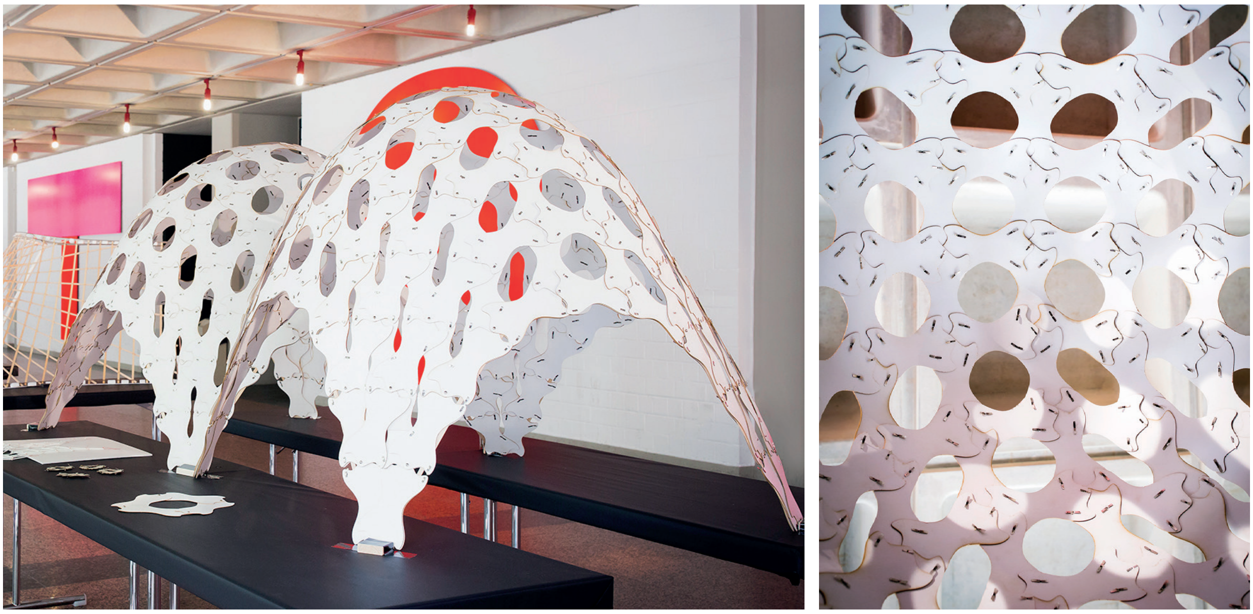

Figure 5.36 *Completed structure, Modular Gridshell, by Eleonora Velluto. Left: Final image of the inverted hanging shape. Right: View up inside the funicular dome (Photos:* ***Magdalena Jooß 2016****).*

Structure and Aesthetics

Simplicity and efficiency are the virtues of this design project. The 162 identical cardboard-units of 1 mm thickness create a shell with comparatively high stiffness. Only the slender supports with little double curvature were strengthened with a second layer of modules to prevent buckling.

The voids between the leaves gradually alter their shape from an almost perfect circle in the apex to an elongated ellipse towards the supports. This intricate pattern s both the geometrically and structural properties of this shell, and simultaneously adds an architectural quality and orientation.

Analysis

The network follows a smooth, geodesic, equilateral, quadrilateral network on a synclastic surface (*Section 5.1.3*) with similar geometric properties to the Reticulated Dome in Neckarsulm (*Section 4.2.2*). In this case, the surface is not spherical, but follows the physical laws of a funicular shape. The modules are deformed into varying normal curvature, but follow geodesic paths. The geodesic curvature itself is taken up at the nodes through a small geodesic angle in-plane. Additionally, the modules are slightly twisted, an almost invisible occurrence, taken up within the “waistline” of each leaf.

NODE					EDGE					FACE		
ω / ι	α	β	γ	o_n	l	k_n	k_g	τ_g	o_e	S	K	o_f
hinge	0	hinge	0°	-	c	deform.	0	deform.	-	-	-	-

Table 5.6 *Qualitative parametric assessment of the structure, Modular Gridshell. The modules are interpreted as edges of a quad network (****ES 2018****).*

5.3.6 Curved Folding

Donald Otterson and Jose Maria Arribas investigated the geometric principles of curved folding. Their basic module is derived from a set of simple model studies.

Geometric Principles

A straight fold produces a flat surface on either side (A). A curved fold creates a concave cone at its inside, and a convex cone on its outside (B). This principle can be repeated along one strip. By alternating the orientation of the curved fold, the resulting single curved surface also alternates its orientation from concave to convex or vice versa (C, D). Expanding this method to hexagonal modules creates consistent concave or convex boundaries surrounding a single curved triangle (E, F). This module has the potential to be designed parametrically and tile a curved surface.

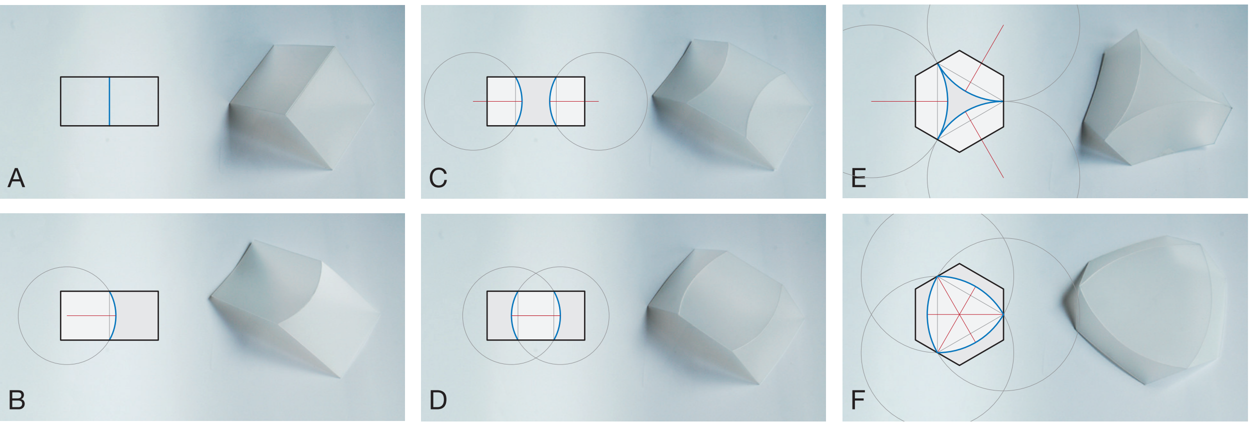

Figure 5.37 *Principles of curved folding for a single, double and triple fold (**ES 2015**).*

Geometric Deduction of the Module

The design objective for Otterson and Arribas was not to create individual modules for a freeform surface, but to use the principle of platonic solids to create a repetitive module for a spherical structure. We can deduce the shape and folds of this unit using two parallel illustrations (*Figure 5.38* - *Figure 5.40*):

- Left: the 3D graphic of platonic solid projected onto its circumsphere
- Right: the 2D plan of the unrolled sheet-geometry for curved folding

The method is explained using a cube: It is defined by the Schläfli diagram {4,3}, where 4 signifies the number of verticies/edges of each square, and 3 is the number of polygons (squares) meeting at each node.

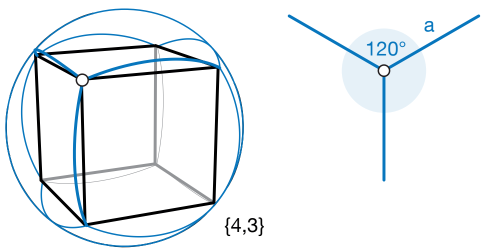

Figure 5.38 *Geometric deduction of the node. Using the Schläfli diagram to generate a 2D node for a curved folding pattern (**ES 2015**).*

The information of one projected corner is mapped onto the plane, thus creating a regular intersection of three edges at a constant angle of 120° and constant edge length a. Each square has four corners which means that this planar node needs to be drawn four times, creating two thirds of a hexagon. This incomplete hexagon is the unrolled representation of one square projected onto the sphere. We deliberately choose a half-edge as the position for the cut (labelled in red).

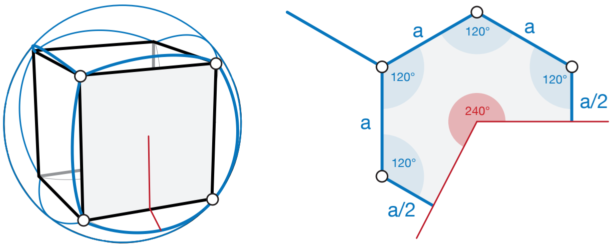

Figure 5.39 *Geometric deduction of the polygon. Mapping the spherical quad onto the plane creates 240° of a regular hexagon (**ES 2015**).*

To be able to fold this shape into the tangential spherical geometry, a circular fold is introduced around the centre of the hexagon. This fold initiates the convex outer cone (tangential to the sphere at the projected edge) and a concave inner cone (directed to the centre of the sphere). To avoid bending the sheet into very small radii, the inner cone is truncated along an offset to the initial circular fold.

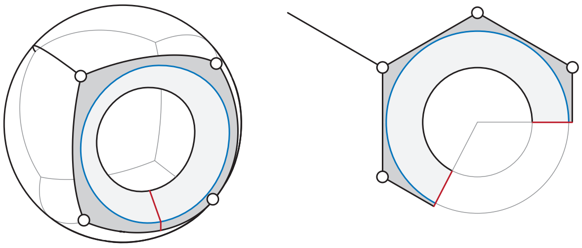

Figure 5.40 *Geometric deduction of the creases. The 2D pattern is used as a layout for the curved-folding structure. The circular creases lie in offsets, tangent to the hexagon. A quadrilateral, conical module can be formed which approximates the sphere (**ES 2015**).*

Platonic Solids

This principle, based solely on the two values of the Schläfli diagram, can be applied to any platonic solid. By multiplying the module by the number of faces, a continuous unrolled pattern for curved folded structures is obtained. This method was verified with simple paper models for each platonic solid.

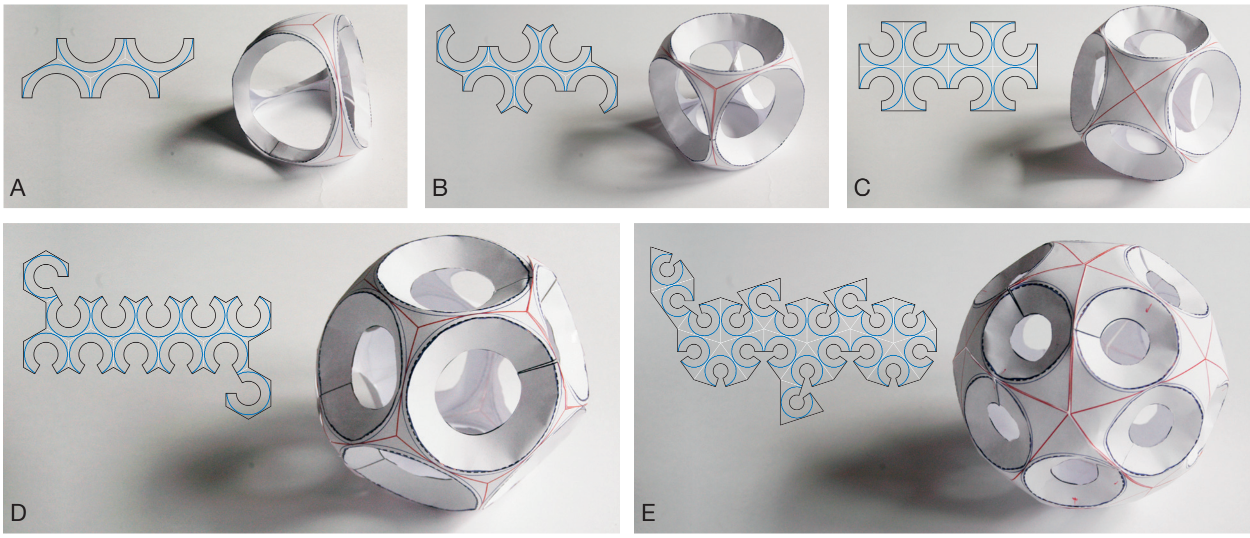

Figure 5.41 *Curved-folding paper models and patterns based on the platonic solids. A) tetrahedron, B) cube, C) octahedron, D) dodecahedron, E) icosahedron (**ES 2015**).*

Structure and Aesthetics

The pattern of the icosahedron was finally implemented at a larger scale by connecting six double-pentagons (adjusting the base module to the available fabrication area of the laser cutter) to form a spherical structure with 1.5 m diameter from 1 mm curved-folded translucent plastic sheets.

The modular structure can be interpreted as a 20-sided icosahedron of triangle-incircles or as a 12-sided dodecahedron of pentagon-stars. The overlapping tangential joints are only visible at second glance. The inner cones not only add aesthetic value to the three-dimensional pattern, they also establish a structural depth and create resilience along the curved folds.
The surface of the pentagons is not mathematically defined. Here, five cones (originating from the surrounding circular folds) merge creating an almost flat shape that is not strictly developable. This behavior can be attributed to slight non-developable deformations.

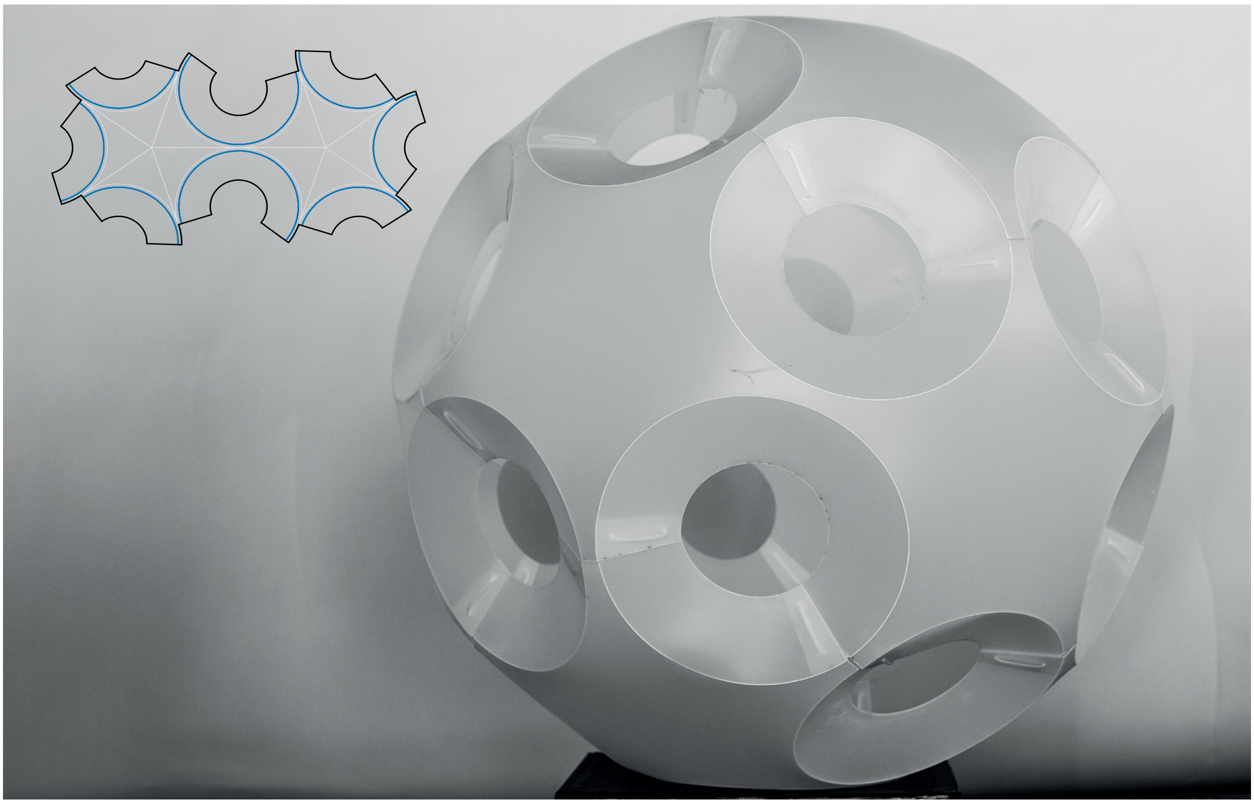

Figure 5.42 *Spherical curved-folding structure based on an icosahedron (Photo:* ***Matthias Kestel 2015****).*

Analysis

The full repetition of segments and joints is owed to the platonic solid underlying the geometry of this sculpture. Each module is deformed from a flat sheet material with predefined, curved folds. The curved sculpture is a compound developable surface approximating a sphere.

NODE					EDGE					FACE		
ω / ι	α	β	γ	o_n	l	k_n	k_g	τ_g	o_e	S	K	o_f
c	c deform.	0°	0°	-	c	c deform.	0	0	-	-	-	-

Table 5.7 *Qualitative parametric assessment of the structure, Curved Folding. The pentagonal modules can be interpreted as nodes or edges (****ES 2018****).*

5.3.7 Asymptotic Grid

The ongoing research on smooth segmentation (*Section 5.4*) was incorporated in the design proposal by Denis Hitrec. In his design for a temporary pavilion, Hitrec first implemented asymptotic curves on a minimal surface. He thus took advantage of the beneficial geometric properties to design a lamella structure with straight unrollings and repetitive, orthogonal nodes. His project was published together with the research and physical models of the author at the AAG[28] 2016 Conference in Zurich (***Schling and Hitrec 2016***).

Surface Design

Hitrec's design shape is based on the periodic minimal surface called Schwarz D. This surface is defined by six edges of a cube. This basic cell can be repeatedly copied and rotated to form an infinitely periodic surface. By clipping this repetitive surface with an inclined block, Hitrec defined the shape for his experimental structure.

Network Design

Hitrec used this trimmed minimal surface to generate a quadrilateral network of asymptotic curves. Because of the use of a periodic surface, the corresponding asymptotic network benefits equally from a high level of repetition. The complete network can be described by the sixth part of the initial cubic cell. In this case, the geometry of only five curve segments holds the information of the complete periodic grid.

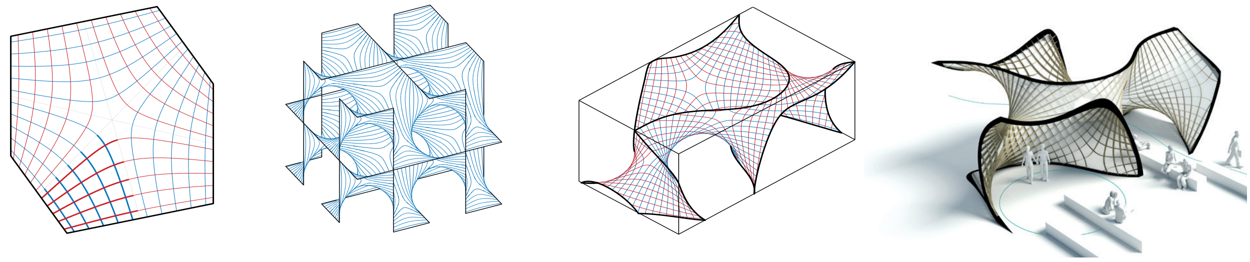

Figure 5.43 *Design implementation of the Asymptotic Grid using a Schwarz D periodic minimal surface (Illustrations:* ***Denis Hitrec 2016****).*

Fabrication and Assembly

The 3D information was translated into simple 2D drawings by marking the node-to-node distance onto straight strips of beech veneer. Hitrec laser cut the strips with repetitive notches which allowed him to interlock them orthogonally. The planar timber boundaries were fabricated separately and combined to create a rigid frame, inside which the lamellas were installed.

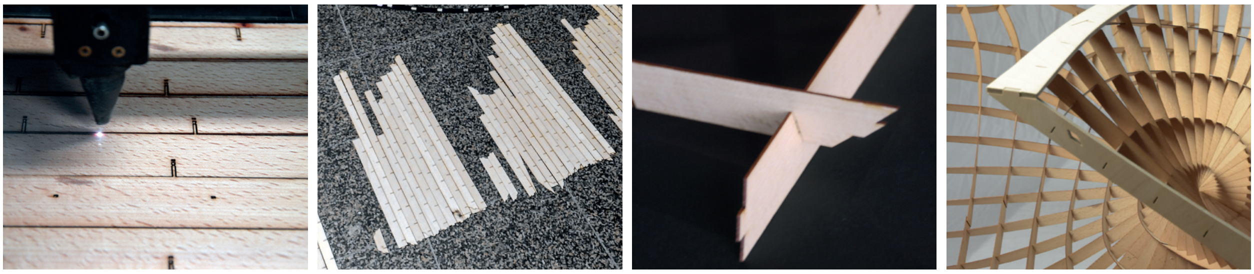

Figure 5.44 *Construction process of the Asymptotic Grid. The timber strips are laser cut straight and assembled within a rigid frame (Photos:* ***Denis Hitrec 2016****).*

28 Advances in Architectural Geometry

Structure and Aesthetics

The timber structure of 2.4 x 1.3 x 1 m has an average mesh size of 8 x 8 cm and a strip height of 24 mm. Even though there is no diagonal bracing, the grid is surprisingly rigid and extremely light. The rigid timber frame supports the grid along the boundaries, allowing for cantilevers at the corners and edges.

Despite the high level of repetition, the pavilion displays a complex and sculptural shape, creating distinct spaces like an archway and a semi-enclosed courtyard. The asymptotic network varies in density and curvature, and thus becomes an important part of the design. The strong timber frame emphasizes both the visual and structural boundary of the structure.

Figure 5.45 *Completed structure of the Asymptotic Grid, by Denis Hitrec. The structure is built from straight strips with exclusively orthogonal nodes (Photo:* ***Denis Hitrec 2016****).*

Analysis

The network follows an asymptotic path of vanishing normal curvature. Each lamella can thus be unrolled into a straight strip. Furthermore, all lamellas meet at 90° degrees. Apart from these geometric properties typical for asymptotic curves on minimal surfaces, the design additionally benefits from a periodic reference surface, creating multiple (invisible) axes of symmetry. The complete grid (with the exception of the boundary trims) consist of only five unique strip segments.

NODE					EDGE					FACE		
ω / ι	α	β	γ	o_n	l	k_n	k_g	τ_g	o_e	S	K	o_f
90°	0°	0°	0°	24 mm	variable	0°	deform.	deform.	24 mm	-	-	-

Table 5.8 *Parametric assessment of the structure, Asymptotic Grid. The table reveals a high quality of geometric repetition (****ES 2018****).*

5.3.8 Observations

This experimental design approach stands in contrast to the theoretical studies presented in *Section 5.1* and *Section 5.2*. It illustrates the broad spectrum of constructive solutions beyond the abstract geometric networks. Nonetheless, each structure can be analysed and compared using the theoretical framework. After the analysis, we will discuss aspects of distortion and its impact on design and construction.

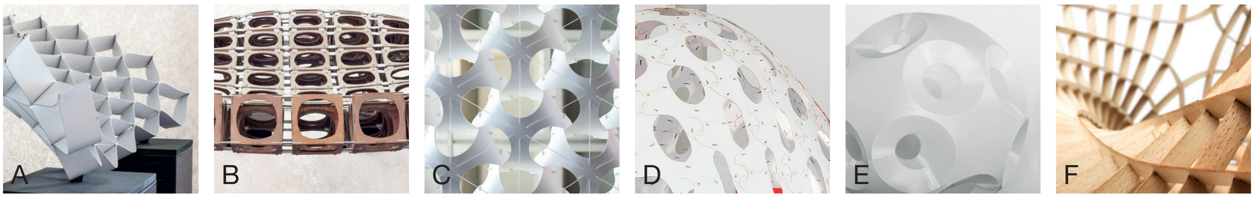

Figure 5.46 *Overview of the six projects presented (Photos: **Matthias Kestel 2014, Magdalena Jooß 2016, Denis Hitrec 2016**)*

		NODE					EDGE					FACE		
		ω / ι	α	β	γ	o_n	l	k_n	k_g	τ_g	o_e	S	K	o_f
A	**Bending Strips**	0°	0°	0°	0°	c	c	0°	deform.	deform.	c	-	-	-
B	**Cubic Surface**	variable	deform.	variable	deform.	c	-	-	-	-	-	tolerance	c / P	c
C	**Hexagonal Bending**	120°	c	0°	0°	c	c	deform.	deform.	deform.	-	tolerance	deform.	c
D	**Modular Gridshell**	hinge	0	hinge	0°	-	c	deform.	0	deform.	-	-	-	-
E	**Curved Folding**	c	c deform.	0°	0°	-	c	c deform.	0	0	-	-	-	-
F	**Asymptotic Grid**	90°	0°	0°	0°	c	variable	0°	deform.	deform.	c	-	-	-

Table 5.9 *Overview of the parametric assessment of the six experimental structures (**ES 2018**).*

Parametric Analysis

Table 5.9 illustrates the geometric and constructive behaviour of all six projects. Listed below are some insights of this parametric analysis:

- Projects A, C, D and E all realize a double-curved structure with identical parts. However, A and C use an additional set of cables with individual lengths to fix the structure. Projects B and F rely on fabricating individual joints/edge-lengths.
- There is a striking parametric similarity between structures A and F, with the only difference that F did not enforce a constant edge length. Both structures combine the use of straight strips, normal to the surface to construct a smooth anticlastic network. This construction technique follows the geometric behaviour (and parametric signature) of asymptotic curves (see *Section 5.5*). While in A this behaviour was stumbled upon experimentally, F deliberately implemented this design method in a systematic process.
- All projects use deformation to achieve repetition. In particular, project C relies heavily on deformation to adjust both edges and faces.
- There are three projects, A, C and E, in which both variables ω and l are constant. Such a constellation immediately causes suspicion as it stands in conflict with the principles of a distorted network (*Section 5.1.4*). A repetition of both edge length and mesh angle (on a doubly curved surface) is only possible if the node-to-node distance is artificially adjusted through an S-shaped deformation of edges (A and C) - or if the network is based on a platonic solid (E).

Distortion

The study on network morphology (*Section 5.1*) has shown that a double-curved network (without singularities) inevitably displays distortion, which comes into effect either through variable edge lengths, or variable mesh angles. This distortion is not merely a morphological occurrence, it is an essential part of the network. It determines the geometry and is crucial to create a rigid structure. The question arises: If the structure is fully repetitive, how is the distortion incorporated? And how is the curved shape determined?

- In project **A**, the distortion is created only by a **deformation** of the individual modules. This deformation can clearly be associated with adjustment of node-to-node distance, creating S-curved edges, while the node angles stay constant. Such a network is considered **geometrically indetermined** and leads to a comparatively soft structure. The shape in A is only determined by a **secondary network** of the cables. These ties vary in length controlling the individual deformation of modules.

- Project **B** uses **tolerances** to accommodate distortion. They are taken up within the connection rings between modules. The **individual joints** simultaneously determine the shape of the structure by fixing the variable distance between faces.

- Similar to A, the distortion in **C** is solely created by a deformation of edges into S-curves. This **geometrically indetermined** network only permits a shallow curvature and results in a soft structure. The dome shape of C is initiated by an **equilibrium of stress** in respect to self-weight and residual stresses of deformation. Similar to A, a **secondary network** of cables is necessary stabilize the structure.

- In **D**, the distortion is realized by **adjustable hinged joints**. This method allows for a greater design freedom and may realize a high double curvature. Furthermore, it offers the possibility to fix the desired shape by locking each joint in its final position.

- The segmentation of **E** follows the regular tessellation of a platonic solid, enabling a full repetition of all elements without distortion. The spherical shape is determined through the **topology** of its network.

- Project **F** is based on an asymptotic curve network which follows the surface curvature and naturally creates singularities limiting distortions. The remaining distortion is incorporated into the design by the **individual fabrication of edge lengths**. However, the nodes are constructed with a slight tolerance and allow for rotation. The rigid frame is thus necessary to determine the shape.

A fundamental insight from these observations is the advantage of incorporating distortion into the design to enable a well-defined shape and a rigid structural system. This is achieved by creating either individual edge length or individual intersection angles, and can be aided by designing with singularities.

5.4 Deductive Study on Curvature and Deformation of Networks

The following section investigates smooth networks with repetitive curvature parameters. By systematically examining all parametric combinations of k_n, k_g and τ_g, specific shapes and network types are deduced which allow for a construction with slender lamellas.
Parts of this study were published in the magazine DETAILstructure in April 2017 (***Schling and Barthel 2017***).

NODE					EDGE					FACE		
ω / ι	α	β	γ	o_n	l	k_n	k_g	τ_g	o_e	S	K	o_f

Table 5.10 *Table of active parameters for the study on curvature and deformation of networks (**ES 2018**).*

This study was inspired by the Multihalle in Mannheim. This strained gridshell fulfils the requirements defined in *Section 3.2.4*, so that the deformation of laths κ_x, κ_y and κ_z, can be considered equivalent to the network curvatures τ_g, k_n and k_g.
In this example, all three curvatures are variable. Consequently, the laths had to be deformed around all three profile axes. This demanded the use of slender, double-symmetric profiles. Understanding this direct dependency of curvature and deformation led to the following research question:

- If one or two of the curvatures τ_g, k_n or k_g are avoided (i.e., kept at a constant value of zero), how does this effect the progression of a curve, the topology and shape of networks, and the choice of profile?

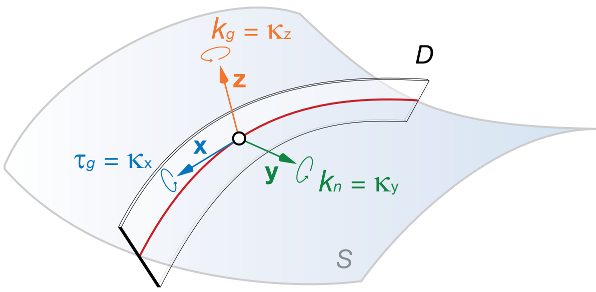

Figure 5.47 *Diagram showing the aligned parameters of curvature and deformation (**ES 2018**).*

We will first discuss the behaviour of each curvature parameter in *Section 5.4.1*, and subsequently present six curvature networks depending on vanishing parameter values in *Section 5.4.2*. We focus on the properties of asymptotic curves and list two more parametric simplifications (equilateral edges and orthogonal nodes) in *Section 5.4.3*.

5.4.1 Curvature Parameters

To better understand the morphology of smooth networks, the distinct properties of each curvature parameter and their influence on the respective curve are observed.

Normal curvature k_n is dependent on the surface curvature and curve direction. It is calculated in respect to the tangent direction of the curve measured as its deviation μ from the principal curvature directions:

$$k_n = k_1(\cos\mu)^2 + k_2(\sin\mu)^2 \quad (5.1)$$

On synclastic surfaces where k_1 and k_2 are positive the normal curvature is never zero.

Geodesic torsion τ_g resembles the twist of a curve and has no influence on the deviation from a straight line. The torsion is unfavourable for developable strips as it leads to an incline of rulings. Similar to k_n, the geodesic torsion is dependent on the principal curvatures and the direction of the curve.

$$\tau_g = \frac{1}{2}\,(k_2 - k_1)\,\sin 2\mu \tag{5.2}$$

On a sphere where k_1 and k_2 are equal, the geodesic torsion is always zero.

Geodesic curvature k_g is independent of the Gaussian curvature and describes the deviation from a straight path within the two-dimensional surface. There is, thus, no mathematical equation relating k_g to the surface-curvature.

5.4.2 Curvature Networks

The properties of curvature can be used to deduce networks with vanishing curvature parameters. For each network, we also describe the quality of developable strips (based on the behaviour of their rulings), which can be modelled either tangentially or orthogonal to the reference surface along each curve. To illustrate these qualities, physical models were built using thin strips of material that are twisted and bent only around their weak axis.

Networks with Only Geodesic Curvature

Curves which display no geodesic torsion or normal curvature have a constant direction of their z-axis. They are planar and permit no curvature of the reference surface. A related network is restricted to a planar surface.
Along these curves, we can model developable strips orthogonal to the surface which have parallel rulings and can be unrolled straight.
Such a network can be built as a planar grillage with curved beams. It can be assembled from straight upright lamellas which are solely bent around their weak axis (z).

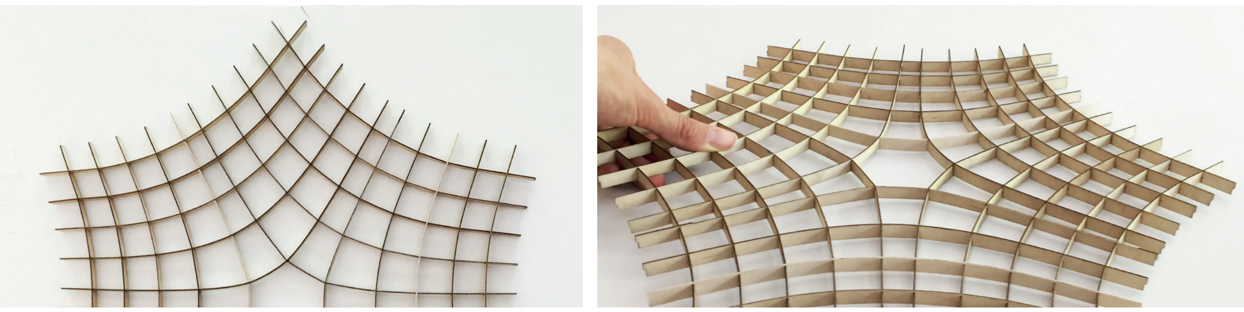

Figure 5.48 *Model of a planar curved grillage. The network displays only geodesic curvature. The lamellas are only bent around their local z-axis (Photos:* ***ES 2018****).*

Networks with Only Geodesic Torsion

Geodesic torsion alone does not cause a curve to change direction. Curves which display no geodesic or normal curvature have a constant direction of the x-axis. They are straight. A network of straight curves only exists in the plane or on doubly ruled surfaces, such as a hyperbolic paraboloid or a rotational hyperboloid.
Such curves are not developable as their rulings are parallel to the curve tangent making a geometric modelling of developable strips impossible.
Such a network can be constructed from straight beams. Due to the continuous torsion, circular profiles are favourable as they do not need to adjust their orientation to the surface. If slender strips of material are

used, the normal orientation must be enforced by twisting the strips around their x-axis, as was done in the physical example.

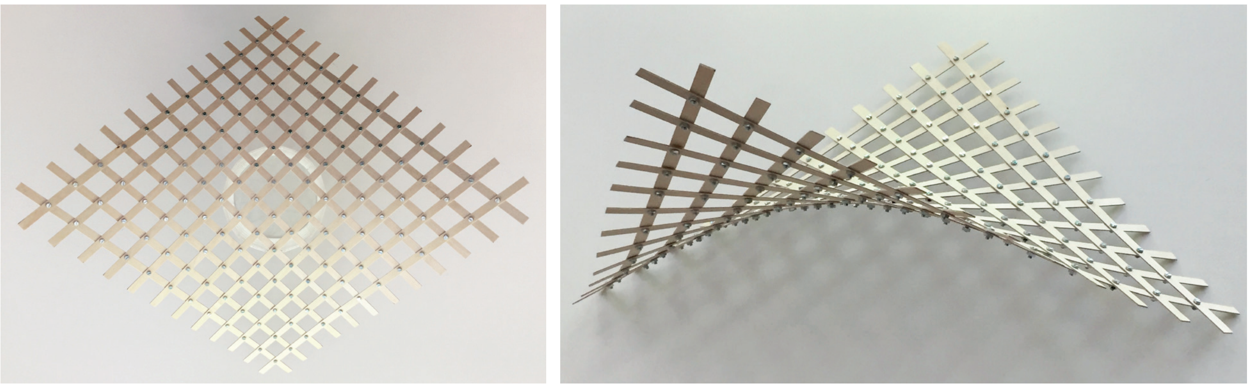

Figure 5.49 *Model of hyperbolic paraboloid. The network displays only geodesic torsion. The lamellas are only twisted around their local x-axis (Photos:* ***ES 2018****).*

Networks with Only Normal Curvature

Curves which display no geodesic torsion or geodesic curvature have a constant direction of the y-axis. These curves are planar and follow the surface curvature. A network of continuous curves is formed by the great circles (geodesic curves) on a sphere.

The rulings of an orthogonal developable strip are oriented normal to the surface which allows clean modelling and circular unrolling. If the strip is oriented tangential to the sphere, the rulings are parallel. The strip can then be unrolled straight.

The respective physical model was constructed from elastically-bent, straight lamellas which lie tangentially to each other.

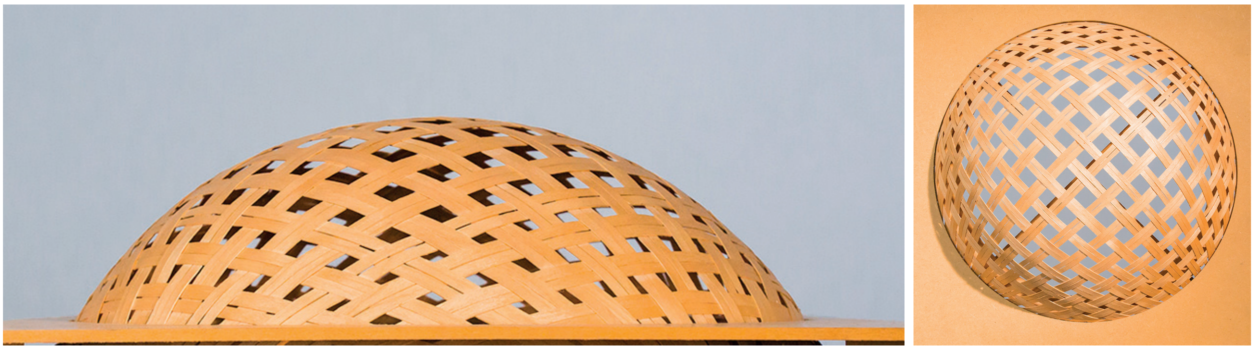

Figure 5.50 *Model of geodesics on a sphere. The network displays only normal curvature. The lamellas are only bent around their local y-axis (Photos:* ***Magdalena Jooß 2016****).*

Networks with No Geodesic Curvature

Geodesic curves have a constant vanishing geodesic curvature. They follow the shortest path between two points on any surface. A geodesic curve is defined by either selecting two points on the surface, or by selecting one point and defining an initial curve direction. A common example for geodesic curves are straight paper strips rolled onto a surface. The paper will inevitably follow a straight path (never turning left or right) along the given surface direction. This property results in limited freedom when designing a geodesic network. Even though the start and end of any curve can be controlled, the path progression cannot be manipulated. On a surface of alternating curvature, geodesic curve networks show large variations in density, scattering on synclastic regions and concentrating on anticlastic regions.

Just like the paper strips, tangential developable strips along geodesic curves can be unrolled straight.

The quality of rulings is dependent on the proportion of normal curvature and geodesic torsion.
A structure along geodesic curves can be assembled from flat lamellas. Their tangential orientation however, has little resistance to external loads and buckles easily.

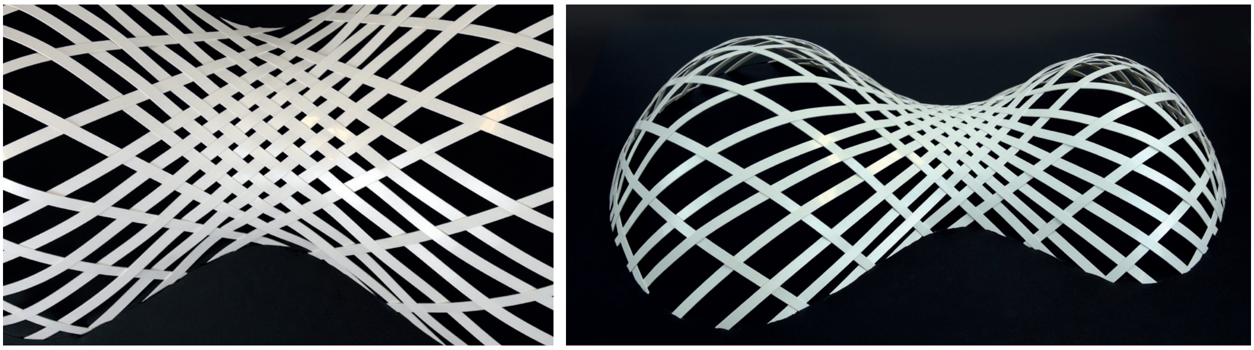

Figure 5.51 Model of geodesic curves on a freeform surface. The network displays no geodesic curvature. The lamellas are not bent around their local z-axis (Photos: ES 2016).

Networks with No Geodesic Torsion

Principal curvature (PC) lines have the property of a constant vanishing geodesic torsion. They are tangent to the "magnetic field" of principal curvature directions (*Section 1.1.3*) creating a quadrilateral network with orthogonal nodes.
A PC line is generated using a digital routine which identifies the PC direction at each subsequent point and iteratively follows this path. The designer cannot influence the direction or progression of the curve. In the case of an umbilical (planar or spherical) surface point, where is constant in all directions, the PC network inevitably exhibits a singularity with a higher or lower valence. The quality of the overall network is dependent on the surface curvature. A homogeneous curvature results in a homogeneous curve layout. Due to the vanishing torsion, PC-networks have very good qualities for both tangential and orthogonal developable strips. The rulings always stand normal to the curve. The unrolled strip however, remains curved in plane. A tangential strip will be curved along the geodesic curvature – an unrolled orthogonal strip displays the normal curvature of its surface curve.

A structure following a PC network can be built from planar strips which are bent around their weak axis and meet perpendicularly at each node. The predetermined network layout with its varying density and singularities can be of high aesthetic quality. However, a limited design freedom has to be accepted.

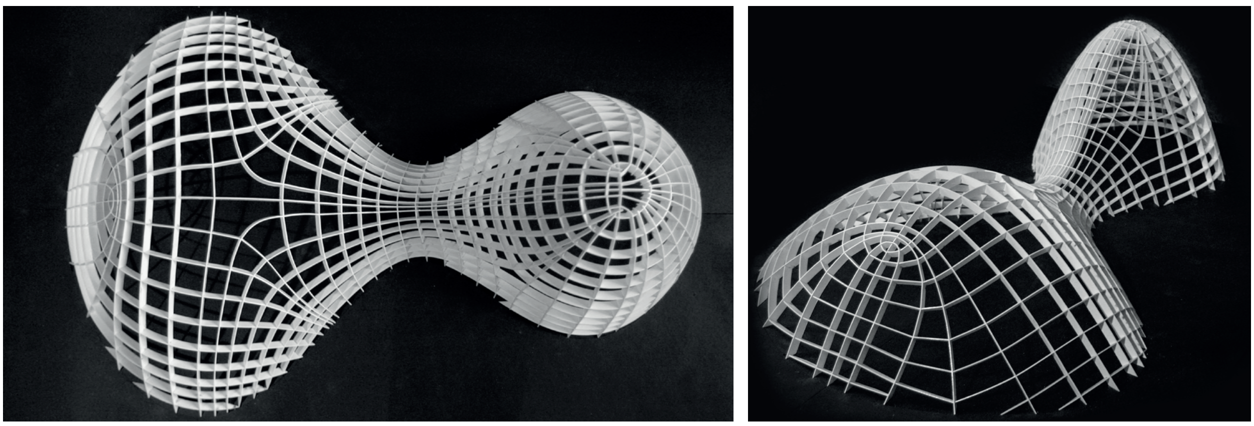

Figure 5.52 Model of principal curvature lines on a freeform surface. The network displays no geodesic torsion. The lamellas are not twisted around their local x-axis (Photos: ES 2016).

Networks with No Normal Curvature

Asymptotic curves define the path along a **constant vanishing normal curvature**. This path only exists on anticlastic regions of a surface. Similar to the PC lines, asymptotic curves are tangent to a magnetic field of asymptotic directions (*Section 1.1.3*) and create a quadrilateral network.

Like PC lines, they can only be generated iteratively by analysing the surface curvature at every point. A designer cannot influence the direction nor progression of asymptotic curves. In the case of an umbilical (planar) surface point where k_n is constant in all directions, the asymptotic network creates a singularity with a higher valence of 6.[29]

Developable strips that are oriented orthogonal to the surface can be unrolled straight. The quality of rulings is dependent on the proportion of normal curvature and geodesic torsion.

A lamella structure following asymptotic curves combines the benefits of straight unrolling and orthogonal orientation. It can be assembled from flat lamellas which are bent (and twisted) only around their weak axis. The orientation of lamellas normal to the surface is beneficial for the structural behaviour because it can transmit external loads via bending.

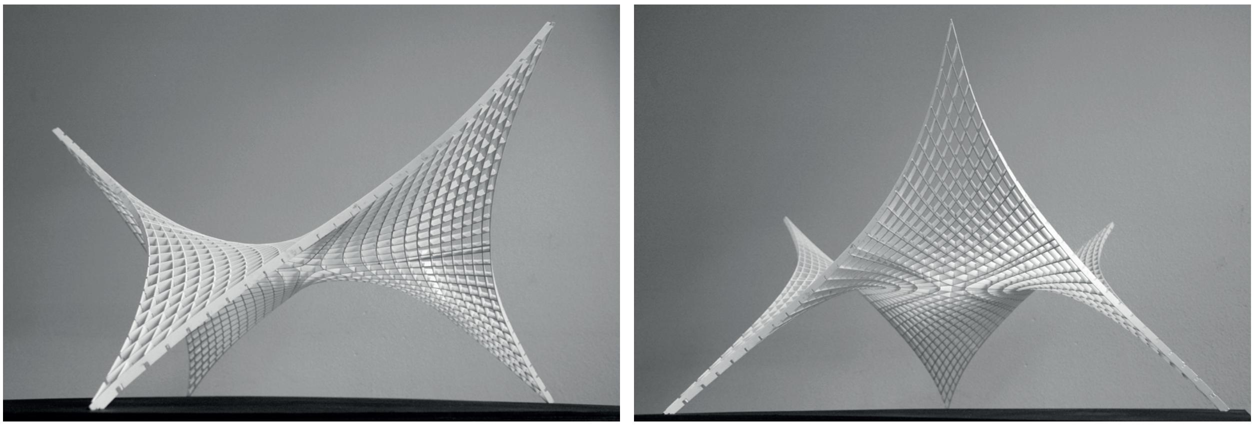

Figure 5.53 *Model of an asymptotic network on an anticlastic surface. The network displays no normal curvature. The lamellas are not bent around their local y-axis (Photos:* ***ES 2016****).*

5.4.3 Asymptotic Networks

Both geodesic curves and principal curvature lines have been successfully used in architectural projects. However, there have been virtually no applications of asymptotic curves for load-bearing structures.[30] This is surprising as asymptotic curves form the only network which combines the benefits of straight unrolling and normal orientation to the surface, thus enabling a simple fabrication and good structural performance. In the following section, we will focus on asymptotic networks and show two additional potentials for creating repetitive parameters, namely, equilateral edges or congruent nodes.

NODE					EDGE					FACE		
ω / ι	α	β	γ	o_n	l	k_n	k_g	τ_g	o_e	S	K	o_f

Table 5.11 *Table of extended parameters for the study on asymptotic networks (****ES 2018****).*

29 There are few exceptions. If a surface is point-symmetric around its singularity, it may exhibit a higher, even valence.
30 The rulings of a hyperbolic paraboloid are a special case of asymptotic curves and have been used in architectural design.

Asymptotic Networks with Equilateral Edges

Asymptotic networks with equilateral edges exist on **surfaces with constant negative Gaussian curvature** and have a constant geodesic torsion (***Wunderlich 1951***).

To build a physical model of such a network, we simply created a uniform grid of lamellas which are hinged at every joint and oriented upright. This grillage can be deformed into any negatively curved network with the above properties.

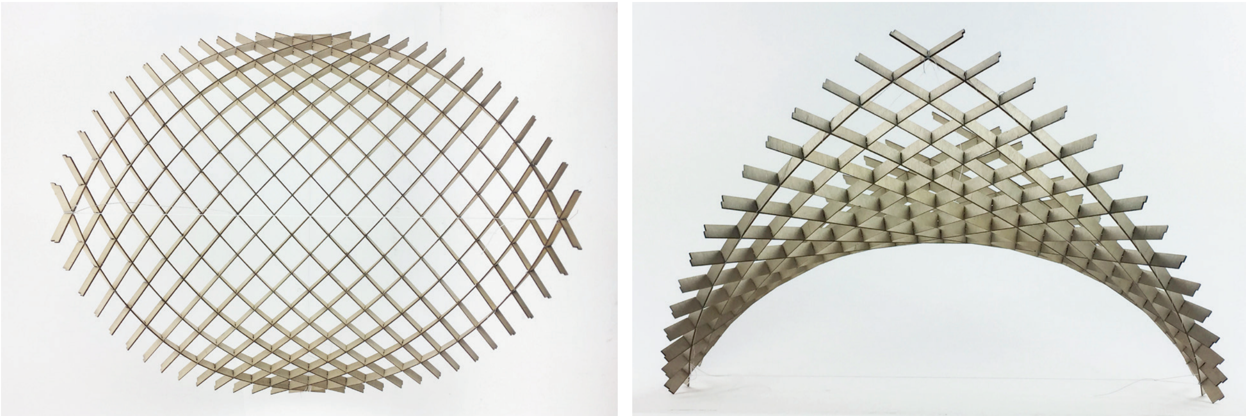

Figure 5.54 *Inductive physical model of an equilateral asymptotic network (Photos:* ***ES 2018****).*

To confirm this behaviour, the same physical modelling process was simulated using an FE-modelling environment (*Figure 5.55, left*). A more common workflow was tested by using a known surface of constant negative curvature, the pseudosphere (*Section 1.2.3*), and generating an equilateral asymptotic network on it (*Figure 5.55, right*). Both digital models display the given parametric properties.

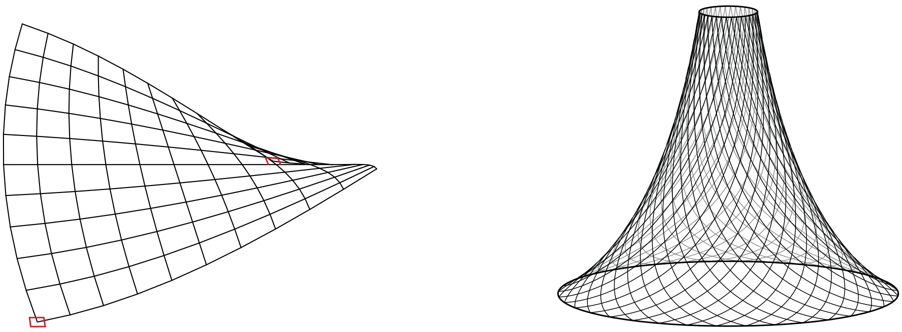

Figure 5.55 *Equilateral asymptotic networks. Left: FEM-simulation, deforming a flat girder into an asymptotic grid (****Jonas Schikore 2018****). Right: Parametric design model on a pseudoshpere (****ES 2018****).*

One particular feature should be mentioned: Equilateral asymptotic networks never display singularities. This is a natural consequence of the constant negative Gaussian curvature of their reference surface. A closer investigation of equilateral asymptotic networks will be part of further research.

Asymptotic Networks with Orthogonal Nodes

Asymptotic networks with a constant intersection angle of 90° exist on **surfaces with constant vanishing mean Gaussian curvature**, i.e., minimal surfaces. This behaviour is well illustrated by the curvature graph (*Section 1.2.2*). The equilibrium of normal curvature determines a regular interval between extreme values and zero-crossings.

A method to model, design and construct asymptotic networks on minimal surfaces will be investigated in the following *Section 5.5* and *Chapter 6*.

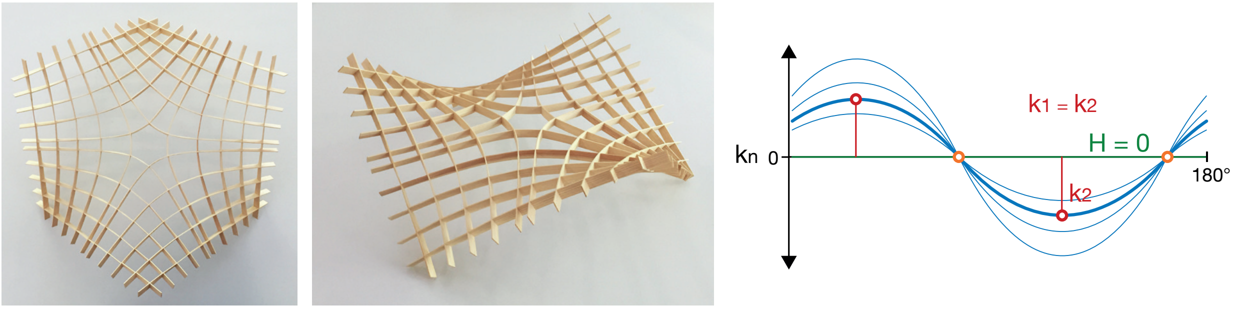

Figure 5.56 *Model of an asymptotic network with congruent nodes. The curvature graph of a minimal surface illustrates the regular behaviour of asymptotic directions (Photos: ES 2018).*

5.4.4 Conclusion

This study illustrates the dependencies of curvature and deformation. It presents possibilities to simplify the construction of double-curved structures by consciously choosing the surface and network depending on the three curvatures of the network, τ_g, k_n and k_g.

Avoiding two curvatures leads to a restriction of shapes, either to the plane (if k_n and τ_g are zero), the sphere (if k_g and τ_g are zero) or a double ruled surfaces (if k_n and k_g are zero).

Avoiding only one type of curvature allows the segmention of any freeform surface, but leads to a restriction of networks to either geodesic curves (if k_g is zero), principal curvature lines (if τ_g is zero) or asymptotic curves (on anticlastic surfaces) (if k_n is zero).

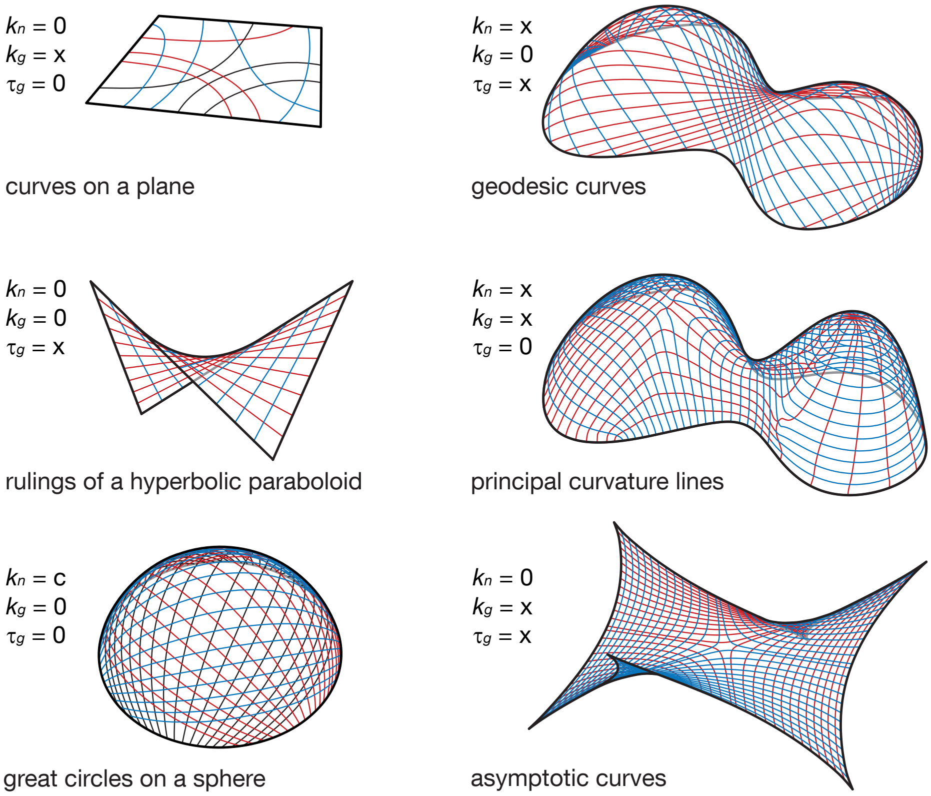

Figure 5.57 *Overview of smooth networks with constant zero curvature values (ES 2018).*

A closer investigation of asymptotic networks presents two additional parametric simplifications, both resulting in a further restriction of the design surface: Equilateral asymptotic networks form surfaces of constant negative Gaussian curvature - asymptotic networks with orthogonal nodes live on surfaces of constant vanishing mean curvature, i.e. minimal surfaces.

5.5 Design Method for Asymptotic Networks on Minimal Surfaces

In the prior study on curvature and deformation of networks (*Section 5.4*) we introduced asymptotic curve networks and their potential to be constructed from straight lamellas oriented normal to the design surface. In this section we investigate the design process of such smooth repetitive networks.
For this purpose, a novel design method is developed which combines the use of minimal surfaces with asymptotic curves to create a network with the additional advantage of repetitive orthogonal nodes. Such a design allows for an elastic assembly of lamellas via their weak axis, and a local transfer of normal loads via their strong axis. Furthermore, the lamellas form a double-curved network, enabling an efficient global load transfer as a shell structure.

The following section is based on the publication "Designing Grid Structures Using Asymptotic Curve Networks" which was published in September 2017 at the Design Modelling Symposium in Paris (***Schling et al. 2017a***).

NODE					EDGE					FACE		
ω / ι	α	β	γ	o_n	l	k_n	k_g	τ_g	o_e	S	K	o_f
90°	**0°**	**0°**	**0°**	**c**	**variable**	**0°**	**deform.**	**deform.**	**c**	-	-	-

Table 5.12 *Parametric signature of asymptotic networks on minimal surfaces (**ES 2018**).*

The method of designing asymptotic networks with orthogonal nodes can be divided into five phases, which will be addressed in subsequent sections:

Section 5.5.1 presents the **surface design** which is focused on a fast and intuitive workflow.
Section 5.5.2 presents the **form-finding** workflow and measures for testing its accuracy.
Section 5.5.3 presents an algorithm to draw **asymptotic curves** on NURBS surfaces.
Section 5.5.4 discusses the challenge of designing a homogeneous **network**.
Finally, *Section 5.5.5* explains the geometry of developable and twisted **strips.**
This design method is tested in *Section 5.5.6* to illustrate the **design spectrum** of surfaces and networks.
Section 5.5.7 presents a **generalization** of this method which was published independently.
Finally, *Section 5.5.8* gives a short **conclusion** of the previous insights.

5.5.1 Surface Design

A minimal surface is the surface of minimal area between any given boundaries. In nature, such shapes result from an equilibrium of homogeneous tension, e.g., in a soap film (*Section 1.2.3*). Such shapes can only be designed by adjusting the boundary edges. For a designer this property is unfamiliar. It takes some experience to understand the geometric behaviour and control such surfaces.
In the initial design phase, a fast and intuitive modelling method is key. The goal is to define the boundary conditions and get instant feedback on the resulting design surface.
The minimal surface can either be approximated through physical models using elastic textiles or soap films, or modelled digitally with fast numeric methods.
More insights on minimal surface shapes and their effects on the asymptotic network are presented in *Section 5.5.6*.

5.5.2 Form Finding

Once the boundary curves are defined, the accurate form is generated digitally by either minimizing the area of a mesh, or finding the shape of equilibrium of tension.

Various tools are capable of performing such optimization on meshes with varying degrees of precision and speed (Surface Evolver, Kangaroo-SoapFilm, Millipede, etc.) (***Brakke 1992***).

The Rhino-plugin TeDa (Chair of Structural Analysis, TUM) provides a tool to model minimal surfaces as NURBS based on so-called isotropic pre-stress fields (***Philipp et al. 2016***).

Both methods, mesh and NURBS, produce sufficiently accurate results if a proper resolution and calculation time is taken into account.

Enneper Surface

Certain minimal surfaces can be modelled via their mathematical definition. This is especially helpful as a reference when testing the accuracy of other tools. We extensively used the parametric representation of an Enneper surface (*Figure 5.58)* as a comparison to determine the accuracy of other tools (***Pottmann et al. 2007a, p. 650***):

$$\begin{aligned} x(u,v) &= 6\,u^2\,v - 2v^3 - 6v \\ y(u,v) &= 6\,u\,v^2 - 2u^3 - 6u \\ z(u,v) &= -12\,u\,v \end{aligned} \tag{5.3}$$

This parametric definition does not only produce mathematically accurate minimal surfaces. The u and v-values also follow the asymptotic directions and can simply be interpolated to draw accurate asymptotic curves (*Section 5.5.3*). Furthermore, the resulting network is isothermal[31], a quality which was also used to test the network design routine (*Section 5.5.4*).

Accuracy

Measuring the total area of competing minimal surface representations is an effective way to compare their overall accuracy. To identify regions of insufficient quality, we analyse the mean curvature and its deviation from zero, or draw asymptotic curves and check the intersection angle. The latter is the decisive requirement for our design method.

5.5.3 Asymptotic Curves

Asymptotic curves cannot be drawn by hand. They require a precise analysis of the reference surface in order to iteratively find the path of vanishing normal curvature.

We developed a custom VBScript for Grasshopper/Rhino to trace asymptotic curves on any anticlastic NURBS-surface based on a routine by Rutton and Gregson (***2016***).

The values and directions of the principal curvatures (k_1, k_2) are retrieved at each point of the surface along this curve. With this information, we calculate the normal curvature k_n for any deviation angle μ from the principal curvature direction.

$$k_n(\mu) = k_1(\cos\mu)^2 + k_2(\sin\mu)^2 \tag{5.4}$$

To find the asymptotic direction, the normal curvature must be zero, $k_n = 0$.

Solving for μ results in:

$$\mu = 2\pi - 2\tan^{-1}\sqrt{\frac{2\sqrt{k_2\,(k_2 - k_1)} + k_1 - 2\,k_2}{k_1}} \tag{5.5}$$

31 A principal curvature network is isothermal if the cells are square in an infinitely fine discretization. Similarly, this asymptotic network has a quality of nearly square cells.

By iteratively measuring μ at each subsequent point and walking along this path, we can draw an asymptotic curve on any anticlastic surface. The algorithm uses the Runge-Kutta method (***Weisstein 2018a***) to average out inaccuracies due to step size. On minimal surfaces, the deviation angle μ is always 45° (due to the bisecting property of asymptotic curves and principal curvature lines).
This computational routine only works on NURBS surfaces. In the case of a mesh, we use EvoluteTools – specifically the command , ExtractCurvatureLines, to find the discrete asymptotic curves.

Accuracy
Both EvoluteTools and the VB-Script were checked for accuracy by comparing their results with the asymptotic network on an Enneper minimal surface. Depending on the high quality of the mesh or NURBS surface and a low step size of the asymptotic-curve-algorithm, a sufficient accuracy was achieved to plan and construct an orthogonal asymptotic grid from straight lamellas.

Properties
It is crucial for a designer to understand the behaviour of asymptotic curves and its dependency on the Gaussian curvature of the surface. The path of asymptotic curves is determined. The designer can merely pick a starting point on an anticlastic surface from which two asymptotic paths will originate. The progression of these paths can best be explained along their remaining curvature parameters:

Geodesic Curvature. The geodesic curvature k_g of asymptotic curves on minimal surfaces is reciprocal to the Gaussian curvature. The higher the Gaussian curvature, the straighter the curves become. When approaching a singularity (a planar point of no Gaussian curvature) the asymptotic curves tend to spread and swerve, increasing the geodesic curvature. Unfortunately, we have not found a mathematical equation describing this relationship.

Geodesic Torsion. The geodesic torsion τ_g of an asymptotic curve correlates directly with the Gaussian curvature. The relationship is determined by the formula (***Tang et al. 2016b***):

$$\tau_g = \frac{1}{2}\,(k_2 - k_1)\,\cdot \sin 2\mu\,, \tag{5.6}$$

where $k_1 = -k_2$ and $\mu = 45°$ thus $\tau_g = k_1$

On a minimal surface, k_1 and k_2 are equal opposites, and μ is 45°. The geodesic torsion τ_g is thus equal to the absolute value of either principal curvature.

With higher Gaussian curvature, more torsion and less geodesic curvature are to be expected.

5.5.4 Network Design
Drawing asymptotic curves on a surface does not necessarily create a homogeneous network. The opposite is the case. Even if the designer picks a regular interval to initiate the asymptotic-curve-routine, the resulting curves (drawn in two directions) will display a heterogeneous pattern unsuitable for architectural design.
To ensure a regular spacing of network curves, we take advantage of the bisecting property between asymptotic curves and principal curvature lines. By alternately drawing each curve and using their intersections as a new starting point, we can create a network with nearly square cells (***Sechelmann et al. 2013***). This is owed to the fact that minimal surfaces are isothermic, i.e., allow for this highly regular segmentation.

With this method we can ensure a homogeneous layout which is not only beneficial for aesthetic reasons, but also improves the structural efficiency of the grid.

Combining both networks, asymptotic curves and principal curvature lines, additionally allows the grid to benefit from both their geometric properties simultaneously for substructure and façade. Subsequently, we can implement efficient façade solutions using tangential developable strips or even planar quads (***Pottmann et al. 2007, p.680***).

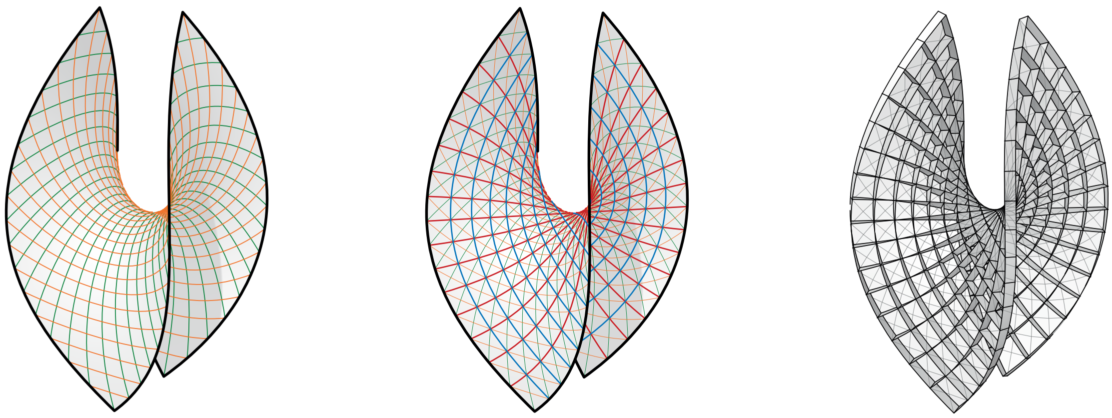

Figure 5.58 *Design process on an Enneper surface. Left: Principal curvature lines. Middle: Isothermal web of principal curvature lines and asymptotic curves. Right: Strip model of the asymptotic network with diagonal bracing (Illustration:* ***Denis Hitrec 2017****).*

Automated Modelling

Implementing this method manually is labour intensive and prone to inaccuracies. There are few routines available which allow for an automated approximation of an isothermal segmentation. We used an existing toolset (Rhino-Grasshopper, Milliped) to reparametrize a mesh and create a quasi-isothermic network along the principal curvature lines. This network is used as the basis for a subsequent generation of the bisecting asymptotic curve network.

Layout and Singularities

The network layout is dependent on the surface curvature. Isothermal networks tend to densify in regions of high Gaussian curvature and spread out in the areas of low Gaussian curvature. This results in the largest cells surrounding the planar singularities.

The singularities are a decisive factor in the grid layout. Their location not only has consequences on the structural and aesthetic quality of the network, it also determines the possible grid size. If all singularities are to be designed identically, e.g., with radial curves, the spacing of the network has to obey a regular interval between them. This logic was used to design the network of the Asymptotic Gridshell (*Section 6.1*).

5.5.5 Strip Geometry

In the final modelling phase, we construct the strip-surfaces along the asymptotic paths. The strips can either be modelled as truly developable surfaces, or as twisted strips normal to the design surface.

Developable Strips

A developable, i.e., singly-curved surface-strip is defined by its rulings. If this strip is orthogonal to a reference surface and follows a surface-curve, its rulings are enveloped by the planes that contain the normal vector **n** and tangent vector **t** of the Darboux frame (*Figure 5.59, left*). The vector of these rulings **r** is dependent on the ratio of geodesic curvature and geodesic torsion. It is calculated via the equation:

$$\mathbf{r} = k_g \mathbf{n} + \tau_g \mathbf{t} \tag{5.7}$$

For asymptotic curves (where $k_n = 0$), k_g is equivalent to k and can simply be measured via the osculating circle.

$$k = \sqrt{k_n^2 + k_g^2} \qquad \text{if } k_n = 0 \qquad \text{then } k = k_g \tag{5.8}$$

To calculate the geodesic torsion, we use *Equation 5.6* (*Section 5.5.4*): $\tau_g = k_1$

The rulings are not necessarily perpendicular to the surface. As a consequence, intersecting two developable strips commonly results in a curved intersection (*Figure 5.59, middle*). Even more, in the case of high Gaussian curvature, the rulings incline dramatically and become parallel to the tangent vector, which makes modelling and construction of a developable strip impossible.

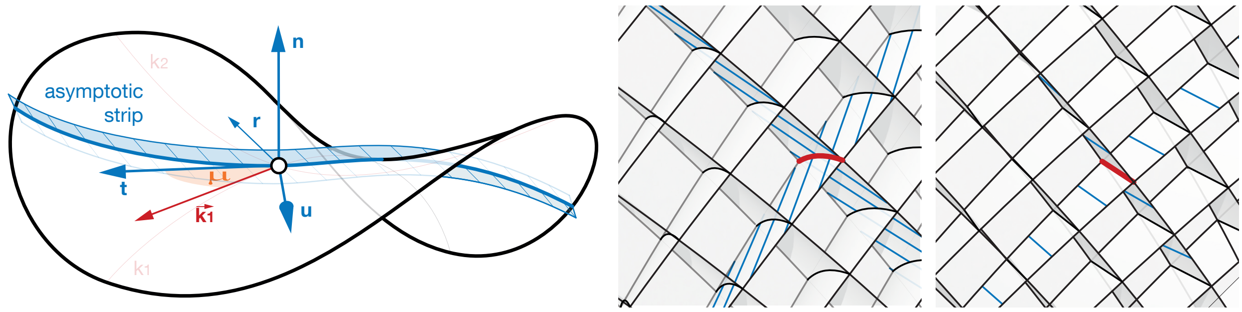

Figure 5.59 *Asymptotic strip geometry. Left: A developable strip along an asymptotic curve, orthogonal to the surface, is defined by rulings* ***r****, which are generally not parallel to the normal vector* ***n****. Middle: This results in curved intersections of developable strips. Right: In our method, the strips are defined by the normal vectors* ***n*** *to ensure straight intersections. Consequently, they are not truly developable, but twisted (****ES 2018****).*

Twisted Strips

We thus propose to model the strip geometry along the normal vectors which allows for straight intersections and a well-defined ruled surface (*Figure 5.59, right*). As a consequence, some twisting of the lamellas needs to be considered during construction. The stresses caused by this twist will be examined in *Section 6.3.2*. This deviation from a truly developable strip is essential to realizing a simplified construction.

Strip Layout

For an elastic assembly the strips can be fabricated flat. The node-to-node distance, measured along the asymptotic curves, is the only variable information needed to produce fabrication drawings. The distances are marked along a rectangle of the desired width. The 3D modelling of strips is only used for visualization.

5.5.6 Design Spectrum

This novel design method was implemented for various minimal surfaces to illustrate the behaviour of the asymptotic network and its singularities (*Figure 5.60*). This study also shows the wide range of possible shapes that can be designed from minimal surfaces.

A minimal surface can be defined by one (A, B), two (C), or multiple (D) closed boundary-curves, with direct impact on the topology and complexity of the surface. Symmetrical properties can be used to create repetitive (C) and periodic (E) minimal surfaces. Asymptotic curve networks benefit greatly from symmetry, both aesthetically and in construction. The Gaussian curvature of the design surface directly influences the geodesic torsion of asymptotic curves, the density of the network and the position of singularities. A well-balanced Gaussian curvature produces a more homogeneous network and thus eases construction.

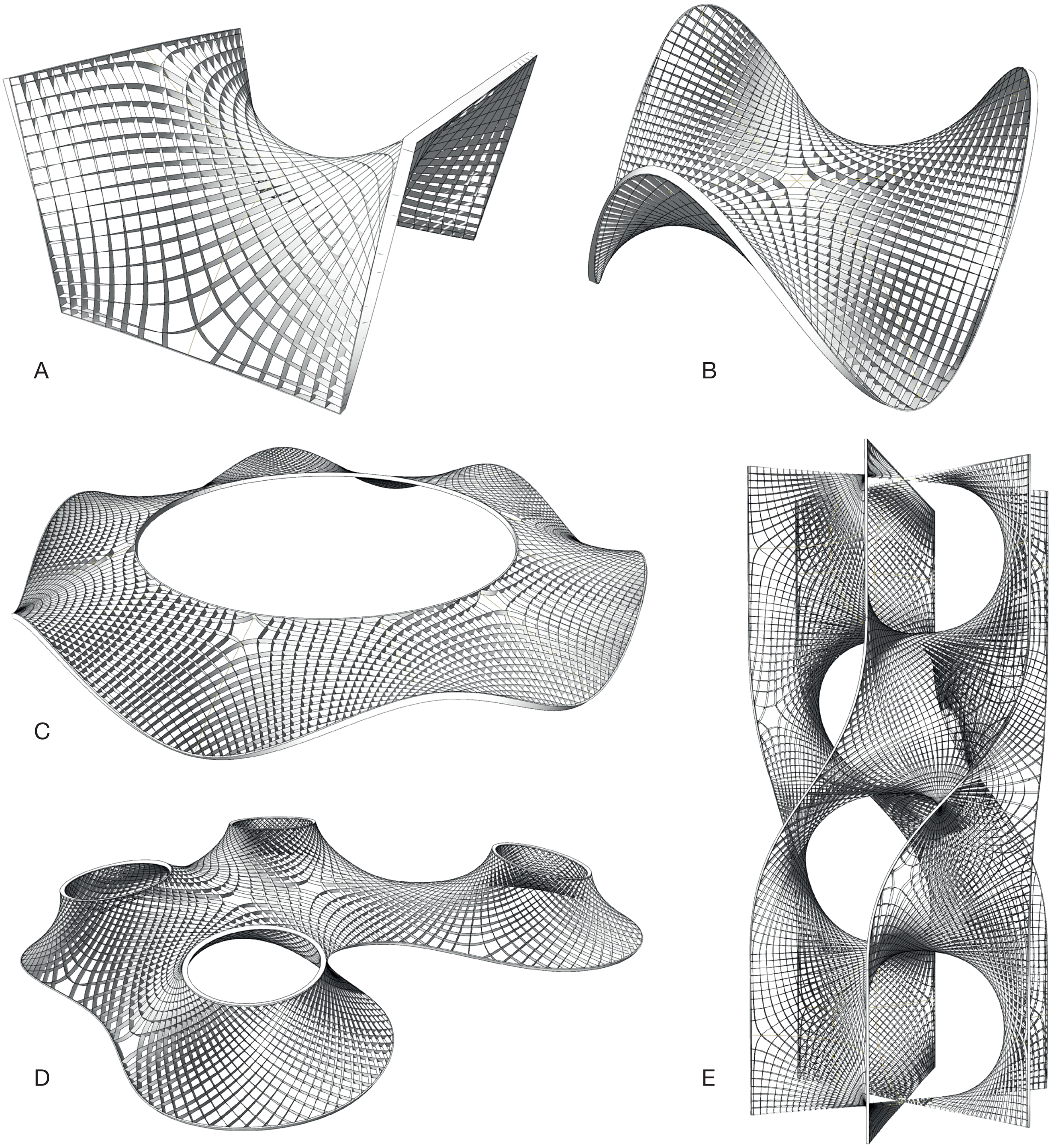

Figure 5.60 *Overview of asymptotic strip networks on minimal surfaces. A) One polygonal boundary creating a saddle-shaped network with singularities located at the boundaries. B) One spatial boundary-curve creating a surface with three high and three low points and a network with central singularity. C) Two curves creating a rotational repetitive network with regular singularities along the planar boundary. D) Multiple boundaries creating a freely designed minimal surface with four high points. E) Variation of a singly-periodic "Sherk's Two Minimal Surface", with six interlinking boundaries (Illustration:* ***Denis Hitrec 2017****).*

Examples shown in *Figure 5.60* display how varying boundary conditions influence the surface and asymptotic network. Boundary-curves may consist of straight lines (A), planar curves (D), or spatial curves (B). This does not only have an effect on the later construction of the edge. Straight lines usually adapt well to the built environment, but are likely to attract singularities (A). Spatial boundaries provide more freedom to design, but increase complexity. A well-integrated boundary can be achieved by modelling a larger surface and "cookie-cutting" the desired shape.

5.5.7 Generalization

Asymptotic networks on minimal surfaces can be understood as a subset of a more general network theory. If the normal curvature of curves must not necessarily be 0, but any constant value, the shape spectrum is expanded to any surface with constant mean curvature.
Such a surface and network follow the simple and intuitive relationship:

$$H_{surface} = k_{n,network} = \text{constant} \tag{5.9}$$

This behaviour is well illustrated by the curvature graph of a CMC surface (*Figure 5.61*).
Constant normal curvature networks are always bisecting the principal curvature lines. The developable strips are not necessarily straight, but have circular unrollings with $r = 1/k_n$. A computational workflow of these networks, including a new discretization as quadrilateral meshes with spherical vertex stars was published in collaboration with Martin Kilian, Hui Wang, Jonas Schikore and Helmut Pottmann at the AAG 2018 Conference (**Schling et al. 2018**).

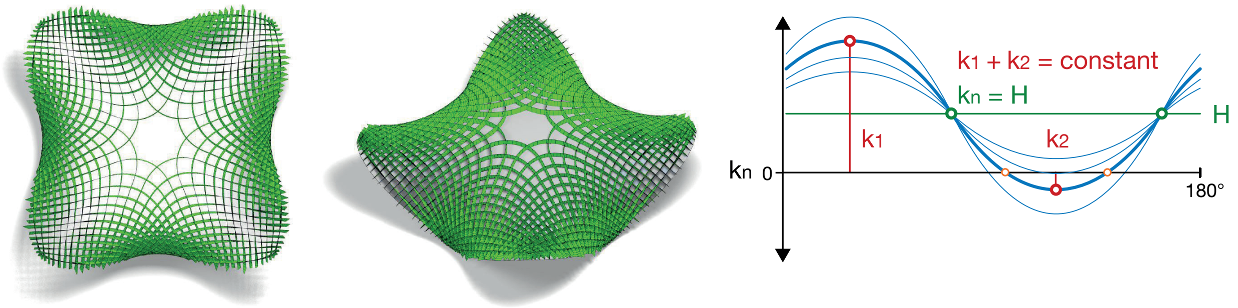

Figure 5.61 *Constant normal curvature network on a constant mean curvature surface. Left: Network on a so-called Ocean reference surface (**Schling et al. 2018**). Right: Diagrammatic curvature graph of a constant mean curvature surface with indicated network directions (**ES 2018**).*

5.5.8 Conclusion

Asymptotic curves on minimal surfaces allow for a high level of repetition simplifying the fabrication and construction process. The structure can be assembled from straight lamellas and identical joints.
Designing such a geometrically optimized structure is heavily dependent on digital tools to enable modelling an accurate minimal surface, drawing accurate asymptotic curves and generating a homogeneous network layout. Similarly, the design freedom is restricted by the natural formation of the surface, the predetermined path of asymptotic curves, and the location of singularities. Despite these restrictions, there is a large design spectrum available to adjust to architectural requirements. We will present a case study, the Asymptotic Gridshell (*Chapter 6*), which illustrates such a bespoke design solution.

PART III
CASE STUDY

6 The Asymptotic Gridshell

The method presented in *Section 5.5* was used to design and construct a large-scale architectural structure, the Asymptotic Gridshell. It was completed in October 2017 for the opening of the Structural Membranes Conference and was used as a venue for the 150th anniversary of the Technical University of Munich in 2018.

Implementing this geometric method in an architectural context called for consideration of all architectural requirements beyond pure geometry, such as site, functionality, safety, construction and load-bearing behaviour. This holistic planning process added numerous insights and is used here as a case study to illustrate the implications of a repetitive design using deformation.

Figure 6.1 *The Asymptotic Gridshell was constructed in October 2017 at the TUM (Photo: **ES 2018**).*

Section 6.1 presents the design process based on the design method developed in *Section 5.5*. A minimal surface is adjusted to the building site (*Section 6.1.1*) and carefully refined to create a beneficial shape for a load-bearing gridshell (*Section 6.1.2*). Subsequently, the curve network is designed by adjusting surface curvature, singularity alignment and density (*Section 6.1.3*).

Section 6.2 presents the construction development of this strained gridshell based on the Multihalle in Mannheim. The use of elastic deformation on a large-scale structure calls for a strategy to ensure stiffness and stability (*Section 6.2.1*). The construction of two prototypes (one in timber and one in steel) further helped to develop an efficient erection process (*Section 6.2.2* and *Section 6.2.3*). The development of joint details reflects these complex requirements (*Section 6.2.4*).
Finally, the fabrication and assembly process of the Asymptotic Gridshell is presented (*Section 6.2.5*).

The load-bearing behaviour is presented in *Section 6.3*. The structural behaviour is interpreted both locally and globally, showing the effects of a grillage and a gridshell (*Section 6.3.1*). The normal and shear stresses are calculated in dependency of the geometric network curvature (*Section 6.3.2*).
An FE-analysis was conducted for construction and approval planning. Its documentation would exceed the research focus of this dissertation. Its content will thus be published separately.

Figure 6.2 *Underneath the Asymptotic Gridshell (Photo: **Martin Ley 2018**)*

Project Team

The project was designed at the Chair of Structural Design, Prof. Dr.-Ing. Rainer Barthel. The research was conducted by Eike Schling (project management) with support of Denis Hitrec (design and modelling) and Jonas Schikore (structural analysis).

The student team during the construction process included Beatrix Huff, Denis Hitrec, Andrea Schmidt, Viktor Späth, Miquel Lloret Garcia and Maximilian Gemsjäger.

The pavillion was constructed in collaboration with the Brandl Steel Construction Company in Eitensheim and the Technisches Zentrum of the TUM, foremost Matthias Müller, the TUM metalsmith.

Financial support was granted by the Department of Architecture and the Architectural Research Incubator /ARI of the TUM, the Dr. Marschall Foundation, as well as the Leonhard-Lorenz-Foundation.

The author’s personal involvement included the complete research and planning process from concept design to construction documents, project management, as well as the installation, supervision and logistics on site.

Publications

The project was published in several conference papers:

- Schling, Eike; Hitrec, Denis; Barthel, Rainer (2017a): Designing Grid Structures using Asymptotic Curve Networks. In Klaas de Rycke et al. (Eds.): Humanizing Digital Reality. Design Modelling Symposium Paris 2017. Singapore: Springer Singapore, pp. 125–140.

- Schling, Eike; Hitrec, Denis; Schikore, Jonas; Barthel, Rainer (2017b): Design and Construction of the Asymptotic Pavilion. In K.-U. Bletzinger, Eugenio Oñate, B. Kröplin (Eds.): VIII International Conference on Textile Composites and Inflatable Structures. STRUCTURAL MEMBRANES 2017. pp. 178–189.

- Schling, Eike; Kilian, Martin; Wang, Hui; Schikore, Jonas; Pottmann, Helmut (2018): Design and Construction of Curved Support Structures with Repetitive Parameters. In Lars Hesselgren, Karl-Gunnar Olsson, Axel Kilian, Samar Malek, Olga Sorkine-Hornung, Chris Williams (Eds.): AAG 2018. Advances in Architectural Geometry. Wien: Klein Publishing, pp. 140–165.

6.1 Design

The design process of the Asymptotic Gridshell closely followed the method described in *Section 5.5*. This section focuses on the findings which are specific to this case study.

In Section *Section 6.1.1*, the architectural requirements of the site are listed. *Section 6.1.2* will present all aspects of the surface design that exceed the purely geometrical parameters. *Section 6.1.3* will address challenges of the network design and its refinement.

6.1.1 Site Requirements

The Asymptotic Gridshell is located at the central campus of the TUM. The building site itself is a west-facing semi-courtyard of approx. 18 x 28 m situated north of the main entrance hall.
This courtyard is designed as a green space for leisure. The landscape of bushes and trees is embedded in elevated islands bound by curved steel rims. Three of these islands create various pathways which connect the two entrances in the northeast and south. Three wide steps bridge the difference in height of approx. 1 m between the courtyard and the main campus.

The design goal was to create an architectural sculpture which matches the scale and form-language of the courtyard, and allows free movement throughout the site. The supports should align with the existing landscape, and the grid structure should incorporate the central island and tree. These complex requirements provided the opportunity to prove the flexibility of this novel design method.

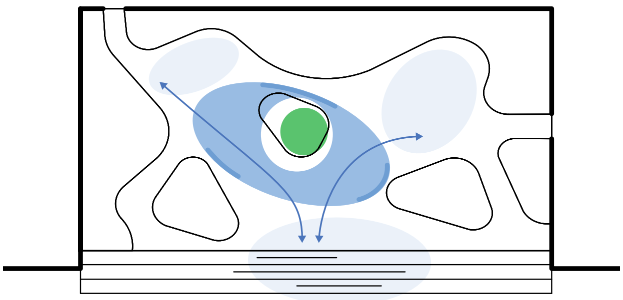

Figure 6.3 *The site requirements called for a well-adjusted design surface encompassing a central tree (**ES 2017**) (Photo: **Felix Noe 2017**).*

6.1.2 Surface Design

The surface design is separated into a concept, and form-finding phase.

During the concept phase, the surface was designed by adjusting only the boundary curves using a fast digital routine to approximate a minimal surface. The real-time manipulation of the shape was key in producing a multitude of design variations, and assessing their visual impact, functionality, support layout and surface area (as a direct indicator of the construction cost).

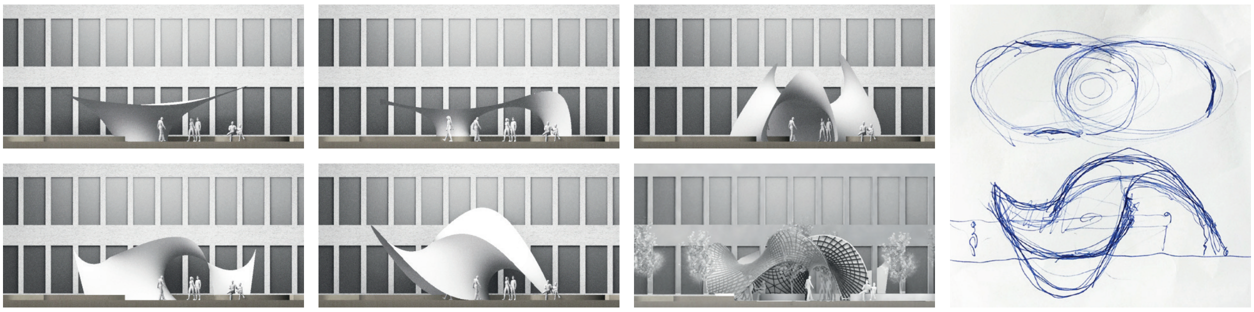

Figure 6.4 *Design iterations and early sketch of the Asymptotic Gridshell (ES 2017).*

A key objective of the concept phase was to find a shape that would benefit the efficient shell-like load-transfer. We deliberately aimed for qualities of a funicular form, such as sufficient double curvature, arch-shaped edges, and well-distributed supports.
While the digital algorithm implemented only the geometric requirement of constant mean curvature, these structural goals were subject to the experience and intuition of the designer.

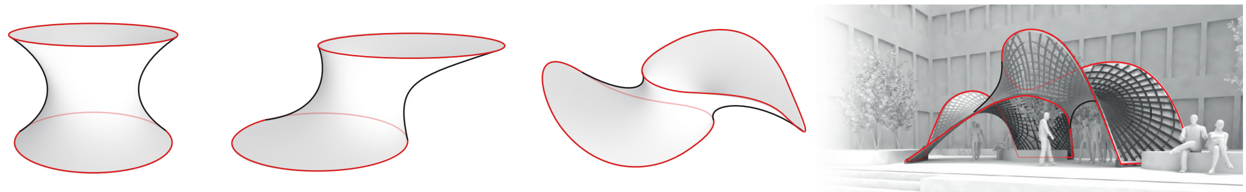

Figure 6.5 *The design shape is derived from a catenoid which is adjusted to fit the site requirements (ES 2017).*

The final design shape is derived from a catenoid – the minimal surface between two circles. By manipulating the position and shape of the two boundary circles, we designed an intricate, mussel-shaped surface with high double curvature and arched-shaped boundaries. Cutting this shape with the horizontal plane generated three curved support lines which nestle well into the site. The catenoidal topology creates a circular oculus around a central island and tree, and opens two archways which allow visitors to move freely throughout the courtyard.

Once the design and boundary curves were defined, the surface was determined more accurately as a mesh and a NURBS surface (*Section 5.5.2*). This process was closely linked to the network design and was conducted repeatedly with small adjustments until the surface curvature and network layout satisfied all aesthetic and structural requirements (defined in *Section 6.3.2*).

6.1.3 Network Design

The network was first designed as an isothermal network of principal curvature lines and later bisected by asymptotic curves at every node. This does not only produce a homogeneous, almost square cell layout. As mentioned in *Section 5.5.4*, aligning the diagonals with the principal curvature direction creates advantages for future façade solutions with single curved or planar quadrilateral panels.

The network layout is directly dependent on the curvature of the surface. A high Gaussian curvature increases the density and torsion of the lamella structure and might prohibit a smooth construction process. Planar surface points, on the other hand, create singularities within the network, and thus have a large impact on the layout and stability of the grid. Both factors were carefully adjusted by controlling the progression of boundary curves, re-computing the surface and testing the new network layout.

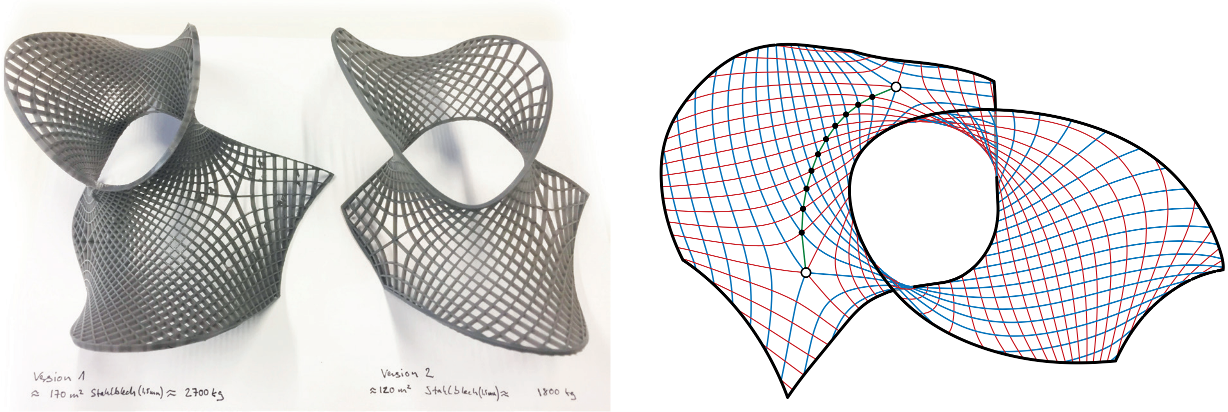

Figure 6.6 *Refinement of surface and network. Left: Two 3D prints testing the network density. Right: Diagram illustrating the alignment of singularities along a common principal curvature line (**ES 2018**).*

In the case of the Asymptotic Gridshell, there are two singularities on opposite sides, east and west of the oculus. To benefit the aesthetic and structural properties of the grid, both singularities are designed identically as traversal nodes connecting six continuous edges. This requirement demanded that the network aligns with both singularities. For this reason, both singularities were arranged on the same principal curvature line. The network density was determined by a subdivision of this connecting axis (*Figure 6.6, right*).

Design Proposal

The final design surface has a circular topology which is the remainder of the catenoid that it is derived from. This property results in an upended shape, flipping the surface from inside to outside. Due to this characteristic, the pavilion was named INSIDE\OUT in media publications.

Figure 6.7 *Visualization of the final design of the Asymptotic Gridshell (Illustration: **Denis Hitrec 2017**).*

6.2 Construction

The repetitive parameters of asymptotic networks on minimal surfaces allow for identical, planar and orthogonal grid joints. The grid can be constructed from straight lamellas, oriented normal to the design surface. They are bent and twisted during construction to account for the geodesic curvature and geodesic torsion of the design network. This large, elastic deformation limits the possible thickness and height of the lamellas (*Section 6.3.2*).
All joints in the structural grid are identical and orthogonal. To activate the load-bearing behaviour of a gridshell, the quadrilateral grid must be able to transmit shear loads in-plane. The grid is thus braced with diagonal steel cables.
The detailing and construction process was informed by the practical solutions of the Multihalle in Mannheim (*Section 2.4*).

Section 6.2.1 discusses a strategy to allow deformation and create stiffness. *Section 6.2.2* and *Section 6.2.3* present the two prototypes (timber and steel) to test the assembly process. *Section 6.2.4* focuses on the developments of joints for the typical grid intersection, singularities, edges, seams and supports. Finally, *Section 6.2.5*, will present the manufacturing of lamellas, the prefabrication of segments and the assembly process on site.

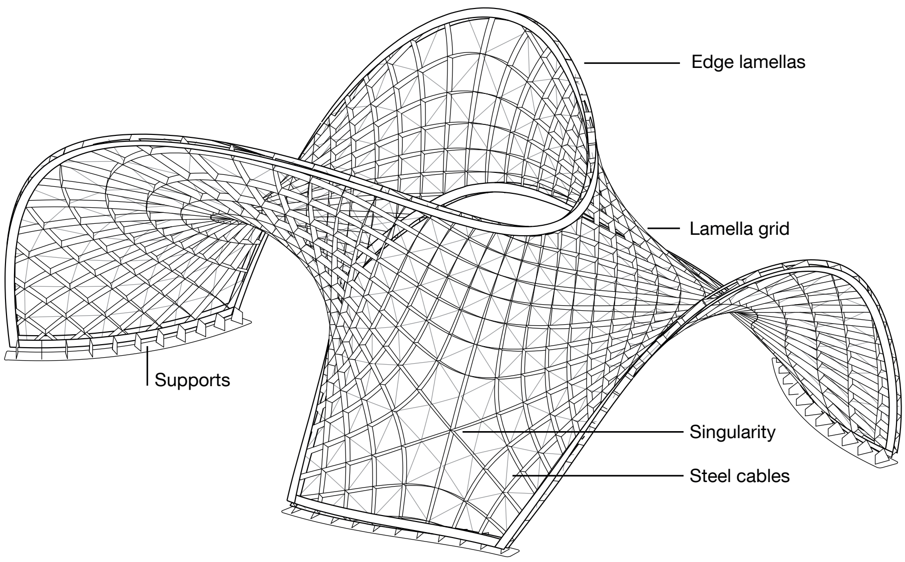

Figure 6.8 *Axonometry of the Asymptotic Gridshell (Illustration: **Denis Hitrec 2017**).*

6.2.1 Deformation and Stiffness

Using the elastic behaviour of a material to construct a curved geometry will always raise the question of deflections and stability under self-weight and external loads. Controlling this by increasing the bending stiffness is not an option if the elements are to be bent elastically into a significantly curved geometry. Lienhard (***2014, p. 141***) calls this discrepancy a "*paradoxon that underlies all bending-active structures*".

The two opposing requirements – elastic deformation and stiffness – can be resolved within the construction by introducing two parallel layers of beams. Each layer is sufficiently slender to be bent and twisted elastically into its target geometry. Once the final geometry is installed, the two layers are coupled with shear blocks in regular intervals to increase the overall stiffness.

This strategy was realized in the Asymptotic Gridshell by installing two slender lamella-profiles of 100 x 1.5 mm each at 25 mm distance. They are coupled naturally at every joint within the dense grid. Additionally, the two layers can be connected with shear couplings in regions close to the supports where normal stresses (due to self-weight) naturally increase. The load-bearing behaviour of this combined profile is dependent on the distance of the two layers, as well as the interval and size of couplings.

Figure 6.9 *View from underneath the pavilion showing the lamellas and cables, as well as a diagonal seam (Photo:* ***Felix Noe 2017****).*

6.2.2 Timber Prototype

This construction method was first tested on a timber prototype. The two asymptotic families of curves were constructed on separate levels (one on top, and one below) using continuous lamellas of 4 mm poplar plywood. The upper and lower level are connected with a square stud of 15 x 15 mm and 80 mm length, enforcing the orthogonal intersection angle.

This rigid connection could only be fitted once all elements were curved in their final spatial geometry. Consequently, each lamella had to be deformed and installed individually between rigid edge beams of 20 mm plywood. The height of these planar, curved beams was determined by their (partly steep) intersection angle with the lamellas, creating a dominant arch-shaped frame. Finally, each pair of lamellas was connected with additional blocks between the joints to increase the overall stiffness. The timber prototype was not yet equipped with diagonal cables and thus carries its self-weight as a curved girder.

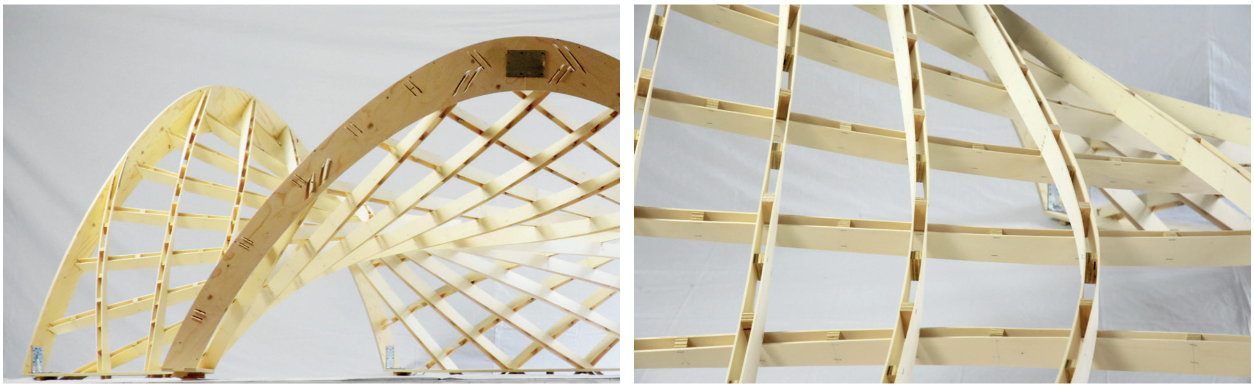

Figure 6.10 *Timber prototype. The lamellas are constructed on separate levels allowing for continuous, uninterrupted profiles. The lamellas were individually fitted between the rigid edge beams and later connected by shear blocks (Photos:* ***Denis Hitrec 2016****).*

6.2.3 Steel Prototype

The second prototype was built from 1.5 mm strips of steel. Here, the two asymptotic families of lamellas are assembled flush on one level. Therefore, the lamellas were prepared with a perpendicular double slot at every joint. The slots define the precise location of intersections and establish a scissor hinge with a stable rotation around the z-axis. This detail allows us to first assemble all the lamellas into a flat grillage and afterwards induce the desired shape through a global deformation.

Figure 6.11 *Assembly process of the steel prototype showing the elastic transformation from flat to curved geometry (Photos:* ***ES 2016****).*

For this purpose, the grillage was placed on a cross-shaped support and was “eased down” and “pushed up” simultaneously (***Quinn and Gengnagel 2014***). During this deformation process, a pair of orthogonal washers were tightened with one bolt at every node, enforcing the 90-degree intersection angle, thus determining the final geometry.

Once the shape was defined, the edges are fitted by attaching bespoke steel strips on top and bottom. This edge-beam is not aligned with the asymptotic grid and thus forms rigid triangles which fasten the final geometry and generate stiffness. Again, no diagonal cables were attached, as the grillage was sufficiently stiff to carry its own weight.

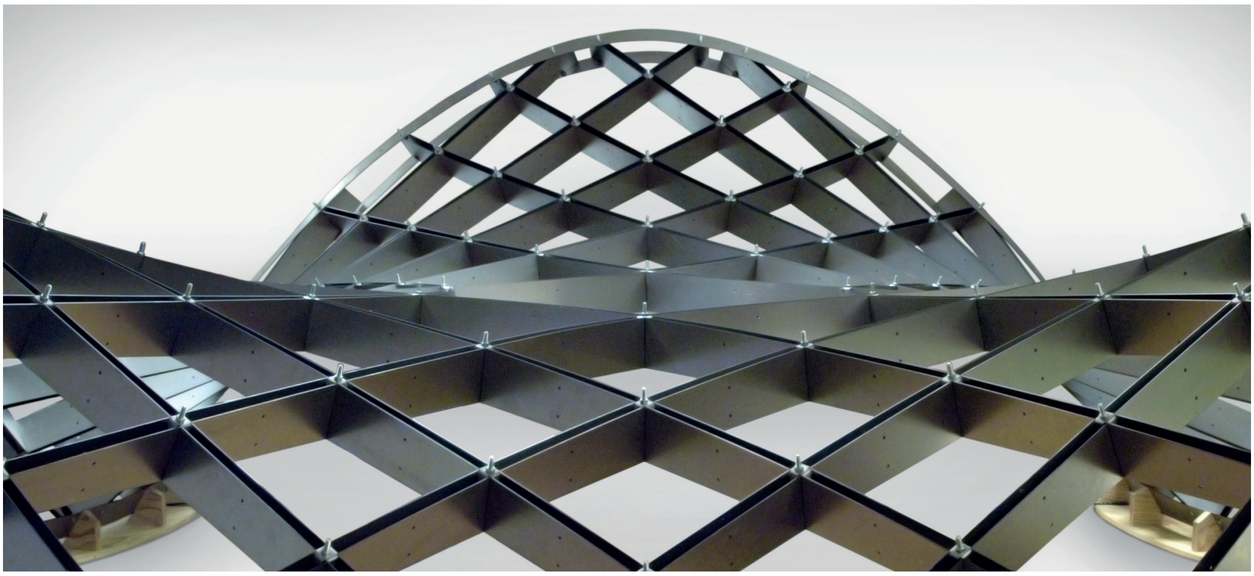

Figure 6.12 *Steel prototype. The lamellas are doubled and coupled to allow for low bending radii and high stiffness (Photo:* ***Tobias Bahne 2016****).*

6.2.4 Joint Development

The construction joints were consistently developed throughout the design process. They were partly built as prototypical joints at a 1:1 scale and later tested within the two prototypes. This helped to assess the aesthetic and practical quality of each solution.

Typical Grid Joint

The typical grid joint is planar and orthogonal with no geometric variation. Nonetheless, the construction process, diagonal bracing and future façade attachment created multiple requirements which were subsequently included in the detailing solutions.

A variety of joints were developed which vary in continuity and number of lamellas, separation of levels and positioning of the diagonal cables (*Figure 6.13*):
The first three proposals (A, B, C) suggested the use of single lamellas to be either welded on site (A), bolted individually (at slight eccentricity) (B), or secured with a bespoke connector and two parallel bolts (C). The use of two parallel lamellas allows for a central connector (D, E). Joint B proposes the use of individual lamella-segments which are folded and bolted at every joint, while joints A, C, D and E realize continuous elements, either by interlocking lamellas through slots (A, C, E) or by arranging them on separate levels (D).
The diagonal bracing can be installed within the slotted lamellas (C) or fixed separately at the top or bottom (E).

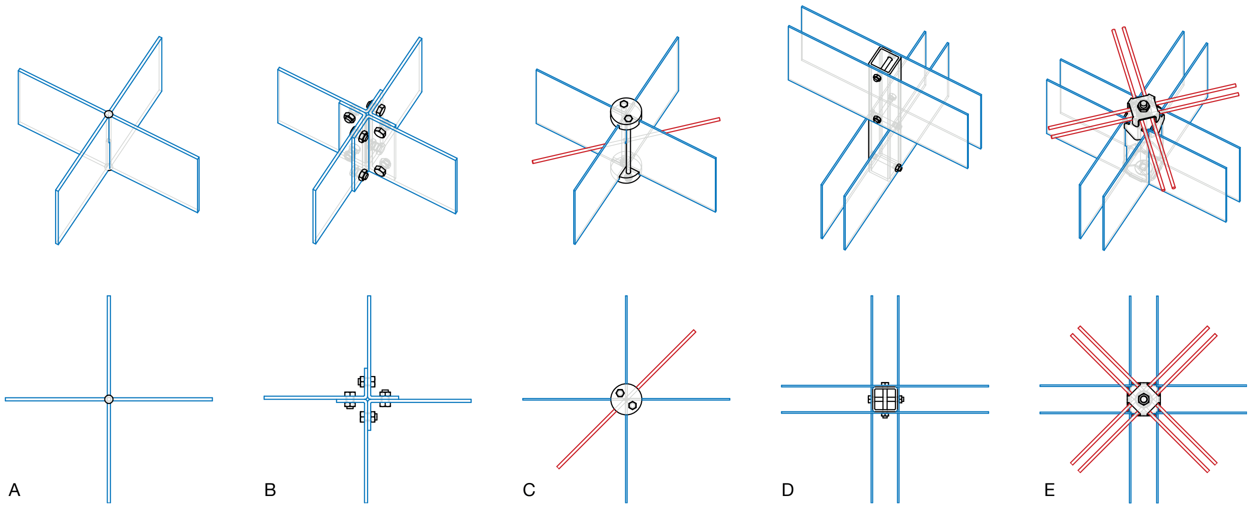

Figure 6.13 *Six proposals for the typical grid joint (**ES 2018**).*

The final joint (E) was first tested in the steel prototype and subsequently chosen for the Asymptotic Gridshell. It is constructed from two layers of lamellas in each direction, interlacing on the same level through perpendicular slots. The slots are double as wide as the thickness of lamellas to allow a rotation of up to 60° during assembly. The lamellas are locked by two star-shaped washers on top and bottom. Another cross-shaped clamp fixes the diagonal cables and keeps them from sliding off. A single carriage bolt and nut are used to fix the lamella and cable connections.

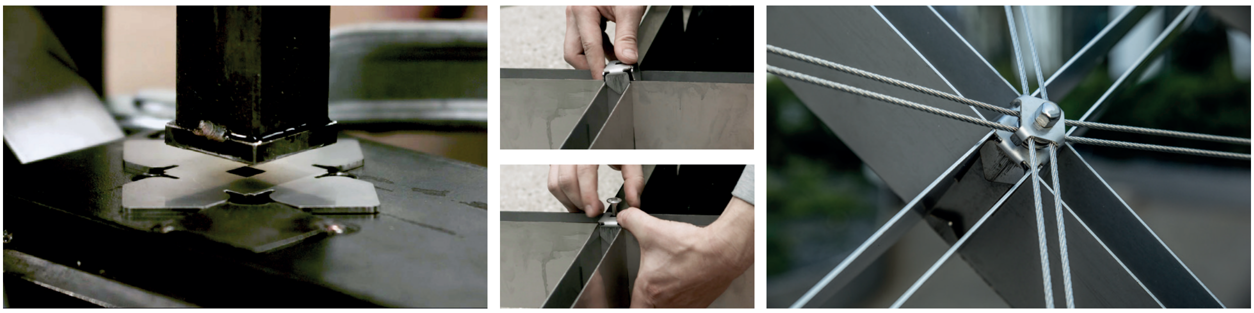

Figure 6.14 *Fabrication and assembly of the typical grid joint (E) (Photos: **Felix Noe 2017**).*

This construction created the following advantages:

- The slotted connection of lamellas generates a **scissor joint** during construction – a prerequisite to enable the global deformation of segments without scaffolding.
- The star-shaped washers allow a fixture of the **90° intersection** and restrict the tolerance of the 3 mm wide connection slots after assembly.
- The single carriage bolt allows a **fast assembly**. The square neck on the underside is held by the square opening of the washer. Thus only one nut per joint must be tightened.
- The **central connection axis** is beneficial for the structural connection of double lamellas as well as the double bracing.
- The two **parallel lamellas** allow the insertion of shear blocks to couple and stiffen the beams. This ensures sufficient rigidity to transmit additional bending and normal stress.
- The joint arrangement results in a **minimalistic appearance** hiding all connecting elements between lamellas. The central bolt, as well as the folded washer and clamp display the structural and functional purpose with minimal effort.

A disadvantage of this construction is the weakening of the lamellas at the joints. On the one hand, this called for special attention during assembly as the lamellas are likely to kink if handled incorrectly. On the other hand, the elastic bending results in a higher curvature and higher bending stress in these areas and promotes buckling.

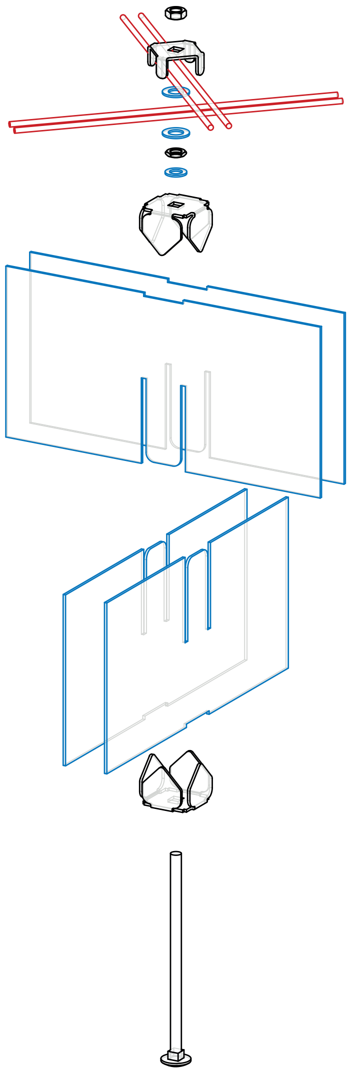

Figure 6.15 *Explosion of the final grid joint (E) (**ES 2018**).*

Singularity Joint
The only exception to the typical grid joint appears at the singularities. Here, six pairs of lamellas meet in a regular hexagonal star. Similarly to the rectangular joints, it is interlaced with slots and fixed by a central carriage bolt. This joint was constructed separately and connected with the lamellas on site.

Seam Connection
The lamellas are fabricated in segments of maximally 4 m in length. They are combined on site by overlapping the lamella-ends between two joints and fixing them with 6 screws. The pavilion was constructed from nine segments, the seams between those segments run diagonally or parallel to the grid. They are almost invisible in the final structure (*Figure 6.9*).

Figure 6.16 *Left: Hexagonal joint for singularities. Right: Seam connecting prefabricated segments (Photos: ES 2018).*

Edge Profiles and Joints

The edges are fitted with curved lamellas at top and bottom, running tangential to the design surface. These edge-lamellas do not follow an optimized path of reduced curvature. They are laser cut individually and later bent and twisted into the required geometry.

The gird-lamellas and cables are connected to these edge profiles. Each pair of lamellas is coupled with a square tube and fixed to the edge-lamellas via a central bolt. The cable loops around a thimble and is secured with a wide washer on top of a carriage bolt. The offset between edge-lamellas is kept constant through a cylindrical tube.

Shear Coupling

The two parallel lamellas are coupled at every grid joint to increase their combined in-plane stiffness. Due to the high axial load in some areas, these compound beams experience additional bending stress. To prevent buckling their bending stiffness needed to be increased. For this purpose, a shear block was planned to be constructed from square tubes (25 x 25 mm) creating an additional coupling of the lamellas between each grid joint. This method turned out to be inefficient for two reasons:

- The tubes were not wide enough to be fixed with multiple screws and could not sufficiently transmit shear forces.
- The curved lamellas tend to buckle between joints. This buckling behaviour is similar to the deflected shape of the well -known Euler Buckling Mode 2. In this case, the shear connection at the central position is ineffective as there is no shear stress at this location.

As a consequence, the square tubes were replaced by wider timber elements to restrict the buckling of lamellas at the most crucial locations.

Figure 6.17 *Left: Edge connections of lamellas and steel cables. Middle: Coupling of lamellas. Right: Each lamella is labeled individually (Photos: ES 2018).*

Supports

The horizontal supports are fabricated individually following the incline and curvature of the grid. The horizontal edge beam is supported in regular intervals by individual brackets taking up the variable incline. The brackets are welded onto a base plate which is curved in the horizontal plane. To prevent the structure from lifting up due to strong winds, the supports were equipped with a 100 mm high border and loaded with gravel, adding approximately 5 kN of weight at every support.

Figure 6.18 *The supports are fabricated individually and filled with gravel to reach the necessary weight against tilting and lifting (Photos: **ES 2017**).*

6.2.5 Construction Process

The Asymptotic Gridshell was constructed in approximately six weeks.
In the first two weeks the stainless steel lamellas were laser cut, labelled and transported to site. Additionally, the star-shaped washers for the typical grid joints had to be cut and folded. During the third and fourth week, nine individually curved segments were prefabricated off site. The final weeks, five and six, were needed to assemble these segments on site, fasten the seam connections, attach the supports and fit the diagonal cables.

Production of Parts

All lamellas are fabricated as flat and straight strips. The edge length of the digital design model are simply marked along the rectangular strips.
The lamellas of the Asymptotic Gridshell were laser cut from rectangular 4 x 2 m steel panels. The rectangular geometry allowed for minimal offcuts and easy transport. The fabrication of washers and clamps was incorporated in the same laser cutting procedure, offering a cost-efficient production of all parts.
The edge-lamellas and supports had to be fabricated individually. The edges were modelled in 3D, unrolled into a flat geometry, and laser cut at the same thickness and width (1.5 x 100 mm) of the standard lamellas. The supports were fabricated separately from 6 mm steel plates. The diagonal steel cables, looping from edge to edge, were tailored to fit the precise length at the top of the lamella construction.

Figure 6.19 *Prefabrication: The straight lamellas are interlocked by hand into flat segments. The segments are then transformed elastically into their designed shape. This erection process follows a compliant mechanism without the need for scaffolding. Nine of these segments were prefabricated individually off site (Photos: **ES 2017, Felix Noe 2017, Andrea Schmidt 2017**).*

Prefabrication

The pavilion was assembled from nine individual segments. The prefabrication process takes advantage of the elastic erection process which was tested with the steel prototype (*Section 6.2.3*).

The lamellas were slotted together by hand to form a flat grillage (*Figure 6.19*). In this state, the lamellas display no geodesic torsion. The intersection angles are not yet constant. The joints are flexible and allow for a scissor movement around their z-axis.

Each planar lamella grillage was placed on a cross-shaped support and then deformed into the desired shape. Unlike other elastic grids (such as the Multihalle in Mannheim) this grillage cannot assume any shape. Instead, its deformation follows a predefined movement. The design shape is determined by enforcing a constant node angle of 90 degrees.

This defined kinetic behaviour is called a compliant mechanism (***Howell 2002***). It enables an elastic erection process without formwork.[32] The geometrical behaviour has been studied and published in (***Schling et al. 2018***). Its detailed mechanical implications will be part of future research.

Assembly

The segments were installed on site in a “top to bottom” process. The two highest segments were first connected on the ground and then hoisted up onto temporary supports. This strategy allowed the construction team to work from the ground and limited the risk of falling. It also lowered the positional tolerances, as all subsequent segments could simply be positioned and attached to the higher central pieces.

After the lamella grid and edges were completed, the supports were attached at each horizontal edge. As a last step, the steel cables were laced at every second diagonal gridline and tightened manually. Only after all cables had been fixed at each node, the supporting scaffolding was slowly released.

The built structure proved to be surprisingly accurate in shape, given that its form is determined to a large degree by the individual deformation of lamellas. The location of supports matched the previously surveyed footprint with a tolerance of only ± 30 mm.

Figure 6.20 *Assembly: The prefabricated segments of up to 400 kg are positioned with a crane, temporarily supported, and bolted together by hand. To activate the structural behaviour of a gridshell, the completed grid is braced diagonally and fixed at supports in the vertical and horizontal directions (Photos:* ***Andrea Schmidt 2017****).*

32 Naturally, the compliant mechanism is subject to gravity and other external loads and needs to be verified by selective measurements.

The Completed Pavilion

The Asymptotic Gridshell is the first architectural structure that utilizes the geometric potentials of an asymptotic network on a minimal surface. The gridshell spans 9 x 12 m and covers an area of approximately 90 m². Its surface weight is approximately 18 kg/m², a total of 1.6 tons.

The steel structure has become an integral part of the Munich campus. The slender lamellas create a gradient shadow with virtually full transparency at a straight view and an almost opaque appearance at an inclined view.

Figure 6.21 *View from the Immatrikulationshalle towards the Asymptotic Gridshell (Photo: **Martin Ley 2018**).*

Figure 6.22 *View underneath the Asymptotic Gridshell (Photo: **Martin Ley 2018**).*

6.3 Load-Bearing Behaviour

Ensuring the structural integrity was a critical driver for the design and construction development. In the following section, two approaches are presented which were used to investigate the load-bearing behaviour of this strained gridshell.

Section 6.3.1 gives a qualitative evaluation of the load-bearing behaviour. The structure is interpreted as both a grillage and a gridshell, considering local and global effects.

Section 6.3.2 investigates the correlation of curvature and deformation. The curvature values of the design-network are used to predict the stresses inside the lamellas due to bending and torsion. The results were used to define minimal curvature radii and maximal twisting, and thus inform the design process.

FE-Analysis

During the planning process, the structural grid was simulated in a Finite Element (FE) environment by Jonas Schikore (Schling et al. 2017b). For this purpose, Schikore developed a novel workflow to incorporate residual stress due to the erection process in the FE-analysis by translating the individual curvature of lamellas into strain loads.
This model was used to calculate deflections and support reactions due to residual stress, self-weight, wind and man loads. The calculations showed that the self-weight of the structure has marginal effects on the stress distribution, which is determined mainly by the residual stress of the erection process. The model verified the stability of the pavilion and was used to obtain planning approval.
The documentation and discussion of the FE-analysis is not part of this thesis.

6.3.1 Qualitative Structural Behaviour

We observed a hybrid load-bearing behaviour of two competing systems: a grillage and a gridshell. The profiles are oriented normal to the surface. Due to the bending stiffness in their strong axis, the grid is able to act as a beam grillage. This bending-stiffness is needed to account for the local planarity of asymptotic networks (due to their vanishing normal curvature) and to stabilize open edges.
At the same time, the strips form a double-curved grid. Bracing this quadrilateral network with diagonal cables and creating fixed supports (in vertical and horizontal directions) activates the form-active behaviour of a gridshell.
Which of the two mechanisms dominates is dependent on the overall shape, supports and loading. The Asymptotic Gridshell was designed with high double curvature and arch-shaped boundaries to promote a shell-like behaviour for gravity load cases.

The elastic erection process results in residual stresses inside the curved and twisted grid elements. Due to the low profile thickness, the initial bending moments stay low and have minor effects on the global behaviour. However, compression of these curved elements increases the bending moment in their weak axis. The strategy of doubling and coupling lamellas is therefore essential to control local buckling. The buckling behaviour is dependent on the grid size as well as the offset distance and coupling interval of parallel lamellas, and was adjusted individually during the construction process.

Generally, principal stress trajectories of a shell constitute the optimal orientation for compression and tension elements in a respective grid structure. The novel design method chooses to follow a geometrically optimized orientation along the asymptotic directions, taking into account an increase of stresses.

6.3.2 Curvature and Deformation

During the early design phases, it was necessary to predict the normal and shear stress caused by the deformation of lamellas, and deduce minimal bending radii and maximal torsion for the design.

In order to correlate the design curvature of a network with the deformation of its building parts, we have defined three requirements (*Section 3.2.4*) that need to be fulfilled in the built structure.

- The beams must be curved continuously and follow the smooth design network.
- The profiles must be continuously oriented upright (along the normal vector) to align with the Darboux frame.
- The beams must be initially straight and bent elastically so that their deformation corresponds to their curvature.

The Asymptotic Gridshell satisfies all three requirements. The continuous and straight lamellas were bent elastically and held upright (normal to the reference surface) at every scissor joint. Therefore, the profile orientation **x**, **y** and **z** can be considered equivalent to the three vectors **t**, **u** and **n**, and the expected deformation κ_x, κ_y and κ_z of the structural element can be regarded equal to the geometric curvatures τ_g, k_n and k_g of the surface curves (*Section 3.2.4*).

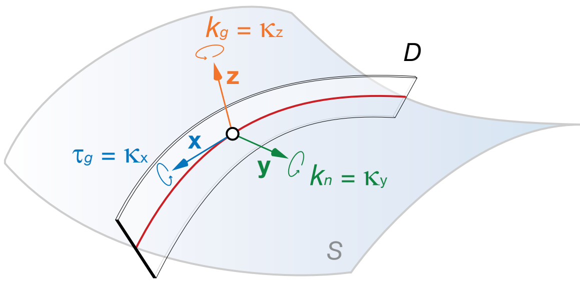

Figure 6.23 *Diagram showing the aligned parameters of curvature and deformation (**ES 2018**).*

Based on this relationship, each curvature can be analysed and used to predict respective stresses due to deformation.

- Due to geodesic curvature, the lamellas are bent around their z-axis. We use the classical beam theory, Euler-Bernoulli, to calculate the normal stress due to bending.

- Due to geodesic torsion, the lamellas are twisted around their local x-axis. Since the cross-section is warp-free, the shear stress is calculated with the Saint-Venant Theory.

- Additionally, the large twist of up to 65°/m causes an elongation/compression of the outermost/central fibres within the lamellas. The normal stress is calculated using the theory of so-called Helix Torsion (***Lumpe and Gensichen 2014***).

When choosing the profile height and thickness, the section modulus is adjusted to the maximum bending and twist in order to keep deformation elastic.

Analysis of Normal Stress due to Bending

We can express the relationship between the curvature k_g and the bending moment M_z of the lamellas based on the bending stiffness $E \cdot I_z$ using the Euler-Bernoulli model.[33]

$$k_g = \kappa_z = \frac{1}{r} = \frac{M_z}{E \cdot I_z} \; [\mathrm{mm}^{-1}] \tag{6.1}$$

This relationship is used to calculate the minimum bending radius r_{min} for lamellas.

$$r_{min} = \frac{E \cdot I_z}{M_{z,max}} = \frac{E \cdot I_z}{\sigma_{y,k} \cdot W_z} = \frac{E \cdot t}{\sigma_{y,k} \cdot 2} \; [\mathrm{mm}] \tag{6.2}$$

$$(\text{where} \quad I_z = \frac{t^3 h}{12} \quad \text{and} \quad W_z = \frac{t^2 h}{6})$$

The equation shows that only the lamella's thickness t is relevant to determine the minimal bending radius. This calculation was used throughout the design process to check for plausibility of curvature and profiles.

Implementation. We determined the minimum bending radius r_{min} for structural steel lamellas with *Equation 6.2* using the following specifications: t = 1.5 mm, $\sigma_{y,k}$ = 235 N/mm², E = 210000 N/mm²

$$r_{min} = \frac{210000 \, \frac{N}{mm^2} \cdot 1.5 \text{ mm}}{235 \, \frac{N}{mm^2} \cdot 2} = 670 \text{ mm} \tag{6.3}$$

The structure was designed with a minimum bending radius of approx. r_{min} = 1060 mm. This corresponds to a max. normal stress due to bending of 148.6 N/mm² (or a material utilization of 63%).

Analysis of Shear Stress due to Torsion

We can express the relationship between the geodesic torsion τ_g and the torsional moment M_T around the x-axis of warp-free profiles based on the Saint-Venant torsional rigidity $G \cdot I_T$, where G is the shear modulus (indicating the shear rigidity of the material), and I_T is the torsional constant (indicating the geometry of the rectangular profile). The twist κ_x is described geometrically in radians as the angle of rotation θ per length l along the lamella.

$$\tau_g = \kappa_x = \frac{M_T}{G \cdot I_T} \left[\frac{\mathrm{rad}}{\mathrm{m}}\right] \tag{6.4}$$

If the maximum allowable shear stress $\tau_{y,k}$ of the material is known, the maximal twist $\kappa_{x,max}$ can be deduced:

$$\tau_{g,max} = \kappa_{x,max} = \frac{M_{T,max}}{G \cdot I_T} = \frac{\tau_{y,k} \cdot W_T}{G \cdot I_T} = \frac{\tau_{y,k}}{G \cdot t} \left[\frac{\mathrm{rad}}{\mathrm{m}}\right] \tag{6.5}$$

$$(\text{where} \quad I_T = \frac{t^3 h}{3} \quad \text{and} \quad W_T = \frac{t^2 h}{3})$$

Again, only the lamella's thickness is relevant to determine the maximum elastic twist.

33 E is the Young's modulus (indicating the material elasticity), and I_z is the second moment of area with respect to the z-axis (indicating the geometry of the rectangular profile with respect to thickness t and height h). The curvature is described geometrically by the reciprocal value of the bending radius r.

Implementation. We determined the maximum twist $\kappa_{x,max}$ with *Equation 6.5* for a structural steel lamella of 1 m length using the following specifications: t = 1.5 mm, $\tau_{y,k}$ = 136 N/mm², *G* = 81000 N/mm²

$$\tau_{g,max} = \kappa_{x,max} = \frac{136\,\frac{N}{mm^2}}{81000\,\frac{N}{mm^2}\cdot 1.5\text{ mm}} \cdot 1000\,\frac{mm}{m} = 1.12\,\frac{rad}{m} \approx 64\,°/m \tag{6.6}$$

The pavilion structure was designed to fully utilize the elastic range due to twisting. This was necessary to allow for the high double curvature of this gridshell.
Following *Equation 5.6* (*Section 5.5.3*), $\tau_g = k_1$, the surface was designed with a maximum principal curvature of 1.12 m^{-1}, which equates to a curvature radius of 0.89 m and a Gaussian curvature of 1.25 m^{-2}.

Analysis of Normal Stress due to Torsion

Calculating normal stress due to extreme torsion is not common. We will first present a purely geometrical explanation of this effect, and subsequently introduce the mechanical theory.

The geodesic torsion of the design network causes a change in length within the geometry of strips. This non-developable deformation (*Section 3.2.3*) was planned to allow for a simplification of nodes and a well-defined geometry of strips (*Section 5.5.5*).
The difference in length Δl within a twisted strip is simply calculated by comparing helix-length l_{helix} and its original length l. The helix-length is linearly dependent on the geodesic torsion τ_g and the radius r = h/2.

$$\Delta l(r) = \sqrt{(\tau_g * l * r)^2 + l^2} - l \tag{6.7}$$

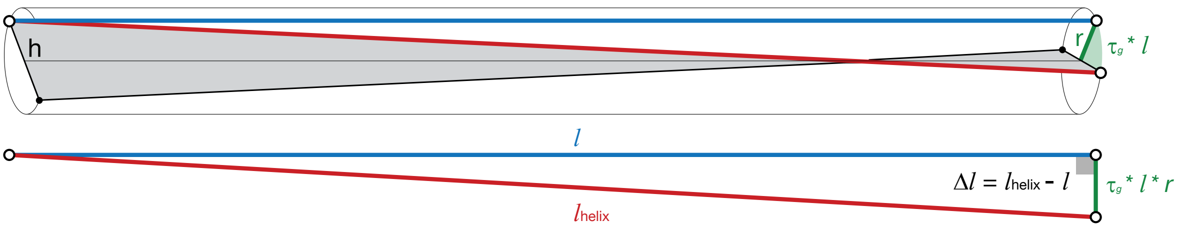

Figure 6.24 *Helix length. The difference in perimeter-length between a twisted and straight strip is dependent on the torsion and the height of the strip (**ES 2018**).*

This simple geometric dependency is used in the so-called theory of Helix Torsion (***Lumpe and Gensichen 2014, pp. 118–124***). The theory provides an equation to calculate strain and normal stress[34] due to extreme twisting. In this case, the difference in length is distributed between outer and inner fibres to create an equilibrium of normal stress throughout the cross-section.

$$\varepsilon_H = \tfrac{1}{2}(r\,\kappa_x)^2 + c_\varepsilon; \qquad \text{with} \qquad c_\varepsilon = -\tfrac{1}{2}\,i_p{}^2\,\kappa_x^2 \tag{6.8}$$

The strain ε_H is distributed along a parabola which is naturally shifted such that its sum (and the sum of normal stresses) at each section are zero. This shift is represented by c_ε. The maximum normal stress $\sigma_{H,max}$ occurs at the outermost fibers and the minimal stress $\sigma_{H,min}$ occurs at the centre of the profile.

34 The strain and normal stress related to Helix Torsion will be labelled as ε_H and σ_H.

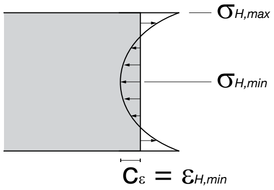

$$\sigma_{H,max} = \frac{1}{2} E \left(\frac{1}{4} h^2 - {i_p}^2\right) {\kappa_x}^2$$

$$\sigma_{H,min} = -\frac{1}{2} E\, {i_p}^2\, {\kappa_x}^2 \tag{6.9}$$

In the case of slender lamellas, where height is much greater than their thickness, h >> t, we can consider $i_p \approx i_y = 1/\sqrt{12} \cdot h$, and simplify the equations:

$$\sigma_{H,max} \approx \frac{1}{12}\, h^2\, \kappa_x^2 \cdot E \;= -2 \cdot \sigma_{H,min} \left[\frac{N}{mm^2}\right]$$

and (6.10)

$$\varepsilon_{H,max} \approx \frac{1}{12}\, h^2\, \kappa_x^2 \;= -\; 2 \cdot \varepsilon_{H,min} \left[\frac{N}{mm^2}\right]$$

The profile thickness is thus eliminated from the equation so that only the lamella height h is relevant to determine the maximum normal stress.

Implementation. We determined the maximum and minimum strain and normal stress caused by torsion using *Equation 6.10*, based on a maximum twist of 64°/m (= 1.12 rad/m), for a structural steel lamella of 100 mm height.

$$\varepsilon_{H,min} = -\frac{1}{24}\,(100\ mm)^2 \left(0.00112\,\frac{1}{mm}\right)^2 = -0.000523$$

$$\varepsilon_{H,max} = -\,2 \cdot\, \varepsilon_{min} \;= 0.001045 \tag{6.11}$$

$$\sigma_{H,min} = \varepsilon_{H,min} \cdot E \;= \;-109.76\,\frac{N}{mm^2}$$

$$\sigma_{H,max} = \varepsilon_{H,max} \cdot E \;= \;219.52\,\frac{N}{mm^2}$$

The maximal normal stress due to torsion almost reaches the permissible stress of $\sigma_{y,k}$ = 235 N/mm². Additionally, a contraction of the lamellas by up to 0.52 mm/m is expected at their most twisted part. This change in length was not considered in the fabrication planning.

The normal stresses due to bending and torsion were not superimposed as their occurrence is reciprocal. If the geodesic curvature is high, the geodesic torsion vanishes and vice versa (*Section 5.5.3*).

Conclusion

This thesis investigates double-curved grid structures with constant geometric parameters.
For this purpose, a holistic theory of repetitive structures was established considering both geometric and constructive criteria. This theory was used to analyse existing structures, investigate the morphology of repetitive networks, and develop a novel method to design and construct strained gridshells.

Results and Insights

The thesis is arranged in three parts and six chapters:

Part I State of the Art

Chapter 1 presents the fundamental theories of geometry relevant for this thesis: The parameters of curvature, classification of surfaces, segmentation and network topology are discussed. We highlight analytical tools, such as the ‘normal curvature graph’ or the Gaussian image, and illustrate the effect of singularities.

In *Chapter 2*, the review of relevant publications in geometry and architecture shows that a repetitive construction is not necessarily based on a repetitive network geometry. Many built examples rely on tolerances, hinges or deformation to adapt identical building parts to variable geometric situations. We focus on the construction of the Multihalle in Mannheim, looking at detailing solutions of this elastically-formed gridshell.

Part II Repetitive Structures

In *Chapter 3*, a theoretical framework for repetitive structures is established using both geometric and constructive criteria.
The separate analysis of smooth and discrete segmentations has proven especially insightful: Comparing their parameter-sets allows the definition of dependencies between the three parameters of curvature of an edge (k_n, k_g, τ_g) in a smooth network, and three respective angles (α, β, γ) at the nodes of a discrete network. Combining both sets establishes a complete table of parameters which can be used to geometrically compare even hybrid networks.
We distinguish tolerances, hinges and deformation as constructive criteria to achieve repetition. Our focus is set on deformation which creates a curved structure from straight or flat building parts. We separate its geometric behaviour into ‘developable deformations’, causing a change in curvature without a change of length or proportion (for one or two-dimensional objects), and ‘non-developable deformations’, which cause additional elongation or compression and may transform a flat element into a double-curved shape. Finally, we define the requirements under which the curvature of edges can be regarded equivalent to the deformation of beams.

In *Chapter 4*, the theoretical framework is implemented to analyse existing structures. The workflow is demonstrated in three examples – The Multihalle in Mannheim, the Reticulated Dome in Neckarsulm and the Eiffel Tower Pavilions in Paris. The quantitative analysis of parameter values not only allows for an identification of repetitive parts, but also gives insights into the detailing of joints or bending radii of beams based on their parametric range of angles and curvature. Furthermore, we can identify geometric and constructive strategies which affect both the design and construction process.

Figure 6.25 *Night view of the Asymptotic Gridshell (Photo: **Felix Noe 2017**).*

The projects presented in the literature review are analysed qualitatively to create an overview of theoretical and practical, smooth and discrete networks. This table allows a broader understanding of common trends and strategies used in repetitive structures.
Finally, a second table systematically deduces all possible parameter combinations of smooth segmentations. It illustrates the potentials for repetitive design and gives incentives for future research.

Chapter 5 investigates the morphology and design of repetitive networks within five consecutive studies:

- The first study (*Section 5.1*) uses an inductive approach to simulate regular networks which are pulled onto various shapes under constant parameter constraints. The experiment illustrates the morphological behaviour of triangular, quadrilateral and hexagonal networks, detects principles of form and distortion, and allows a comparison of discrete and smooth networks.
    - Triangular nets show a geometrical rigidity. Their repetitive solutions are restricted to developable shapes. In contrast, quadrilateral and hexagonal networks are versatile and adjust their layout to various parameter constraints. An alignment with the principal curvature direction is a successful strategy to achieve repetitive solutions.
    - We observe a drastic increase of geometrically valid solutions if the curvature (i.e., deformation) of edges is permitted. However, this flexibility is attained through the occurrence of fisher-net effects, causing a “non-fair” S-curved shape of edges.
    - We conclude that a great potential for repetitive structures lies in the deliberate design of structures which do not fulfil fairness or proximity requirements, creating S-curved edges or undulating / folded surfaces.
    - Finally, we conjecture that there is a correlation between the distortion of a repetitive network (without singularities) and the footprint-area of its Gaussian image.

- The second inductive study (*Section 5.2*) investigates the use of tolerances and deformation to create double-curved façades from standardized rectangular panels. It examines the design workflow of appropriate surfaces and layouts that are limited by minimal curvature radii and aim for minimal seam tolerance. This investigation comes to the following conclusions:
    - With sufficient tolerance, any shape can be constructed from repetitive parts.
    - Non-developable deformations may, to some degree, enable the construction of smooth double-curved skins from flat panels.
    - We describe the general behaviour of seam tolerance, where synclastic regions create convex seams and anticlastic regions create concave seams. Furthermore, if the network is not aligned with geodesic curves, the panel edges show a serrated progression. Enforcing minimal seams along a row of panels causes a stepping effect which shifts adjacent rows into a brick pattern.
    - Again, we conjecture a correlation of the effects of distortion (in this case the seam variance) with the footprint-area of its Gaussian image.

- In our experimental studies (*Section 5.3*), we follow a research-by-design approach using physical prototypes. We present six designs which all use deformation to create double-curved structures from repetitive parts. The subsequent analysis of parameters reveals hidden similarities between structures and illustrates the specific use of deformation. In a final observation, we discuss aspects of distortion and come to the following conclusions:
    - The distortion of a network is not merely a side-effect of curvature, but a crucial factor to design and build double curvature. Designing a network which accommodates distortion (through the topology of a network, the variation of angles or adjustment of edge lengths), allows for a well-defined geometry, and aids an efficient self-supporting structure.

- The deductive study (*Section 5.4*) investigates the dependency of curvature and network, and their potentials for strained grid structures. It reveals the close relationship between the curvatures of surface curves and the shapes and networks which derive from them.
  Combining repetitive curvature parameters with an elastic construction process additionally offers the use of developable or straight strips of material to construct a curved network of beams. Especially promising are asymptotic curves which are able to combine the benefits of straight unrolling and an upright orientation of lamellas. A closer investigation of asymptotic networks reveals two parametric simplifications:
    - Equilateral asymptotic networks live on surfaces of constant negative Gaussian curvature.
    - Asymptotic networks with orthogonal nodes live on surfaces with constant vanishing mean Gaussian curvature (i.e., minimal surfaces).

- Our final study (*Section 5.5*) takes advantage of the geometric properties of asymptotic networks on minimal surfaces to develop a novel design method. We develop a workflow of designing minimal surfaces, finding the paths of asymptotic curves and creating a homogeneous network bisecting principal curvature directions.
  We choose to deviate from a truly developable geometry of strips in order to obtain identical intersections and a well-defined, ruled geometry of strips throughout the structure. As a consequence, some twisting of beams, i.e., non-developable deformations, have to be considered in the construction planning.
  Finally, we illustrate the design spectrum of this novel method and discuss how the boundaries effect the surface, network and singularities.

Part II Case Study

In *Chapter 6* we implement the novel design method developed in *Section 5.5* and present the planning and construction process of an architectural case study, the Asymptotic Gridshell. The project development reveals a multitude of practical and theoretical insights on the design process, the construction, fabrication and assembly, as well as the load-bearing behaviour:

- In *Section 6.1*, we discuss the design process of surface and network. Fulfilling the architectural requirements related to site, functionality and structure is naturally more complex, if the design spectrum is restricted to minimal surfaces and asymptotic networks. In particular, the conception of a beneficial structural form and network to foster the load-bearing behaviour of a gridshell demanded much experience during this phase.

- *Section 6.2* presents the planning, testing and execution of construction. The asymptotic network allows for a simple construction from straight lamellas and orthogonal nodes. To ensure sufficient stiffness a strategy of doubling and coupling lamellas was implemented. This also facilitated an efficient grid-joint with a central connection axis. A novel erection process was developed along two prototypes, one in timber and one in steel. The lamella grid with scissor joints create a so-called compliant mechanism which allows a defined elastic deformation without the need for formwork.

- Finally, the load-bearing behaviour is investigated in *Section 6.3* in three separate approaches:
    - The qualitative evaluation observes a hybrid structural behaviour of both a grillage and a gridshell which is dependent on the shape and support of the structure. The deliberate use of deformation calls for constructive measures to control the buckling of lamellas around their week axis. Finally, the asymptotic directions do not align with the principal stress trajectories of a shell and thus constitute an increase of stress in the grid structure.

- The correlation of curvature and deformation was used to calculate the permissible bending radii and torsion of lamellas, and ensure an elastic behaviour of beams during construction. A special focus was set on the twisting of lamellas. Next to shear stress, which are calculated using the Saint-Venant-Theory, this non-developable deformation causes an elongation of the outer fibres and compression of the inner fibres within the lamellas. This results in normal stresses related to the lamella height, which can be calculated based on the theory of Helix Torsion (***Lumpe and Gensichen, 2014***).

Final Reflections

This thesis combines the knowledge of differential geometry, architecture and structural engineering, and establishes a parametric framework that takes into account both geometric and constructive criteria. This approach allows us to design and build double-curved structures with repetitive parameters.

We systematically investigate the morphology of repetitive networks and uncover dependencies of shape and structure: For example, we correlate the node angles in a mesh to the curvature of edge in a respective smooth segmentation, and define requirements to equate the curvature of a network to the deformation of its beams. We study the behaviour of triangular, quadrilateral and hexagonal nets and create an overview of repetitive, discrete and smooth solutions. One important insight is that the effects of distortion, such as rough meshes or S-curved edges, appear only if both mesh angle and edge length are restricted.

The results not only illustrate the spectrum of repetitive design. They bridge the gap between mathematics and engineering and discover novel design solutions, which purposefully apply elastic deformation to simplify the fabrication and assembly process. We focus on the use of straight, bendable strips to construct strained lamella gridshells and demonstrate the mathematical background and physical application of such designs. Finally, the insights are tested and verified in an architectural structure, the Asymptotic Gridshell. The development of a construction technique and assembly process demonstrate the bandwidth of this research.

Throughout this endeavour we have developed analytical tools, such as the curvature graph to visualize curvature or the Gaussian footprint to detect distortion. Furthermore, we have deduced equations that relate the parameters of curvature to the structural bending and torsion of edges and thus allow an informed design process.

This dissertation is not the final result of our research. Rather it is part of the process and should be used as a driver for further investigations.

Future Research

Throughout the thesis we have encountered multiple domains that call for further investigation. These domains can be separated into purely geometric observations related to the theoretical framework of repetitive structures, structural aspects which investigate the load-bearing behaviour of strained gridshells, and further construction development of our case study.

Geometrical Investigations on Repetitive Structures

- The thorough examination of physical surfaces and their potential to carry repetitive structures is a promising field of future research. Some further steps in this direction have already been addressed in our publication on constant mean curvature surfaces (Schling et al. 2018). Another promising field are equilateral, asymptotic networks on surfaces of constant negative Gaussian curvature.
- The theoretical framework can be used to systematically deduce further parameter combinations for repetitive structures. This research includes not only smooth and discrete, but also hybrid and offset segmentations, offering a vast field of research. The various combination of strategies to achieve repetition could be investigated in a similar way to produce novel design solutions. Furthermore, the deliberate design of “non-fair” networks or polyhedral surfaces, offers great potential for future repetitive designs.
- The analysis of repetitive parameters proved to be very insightful in the investigation of existing structures. This workflow could be used in the analysis of historic structures and help to understand the design and construction process.
- Furthermore, we suggest a mathematical study of the dependency of distortion of networks and their Gaussian footprint.
- Finally, the investigation of eccentricities and their impact on repetitive structure was left open in this thesis and deserves further investigation.

Structural and Interdisciplinary Investigations

- The structural analysis of repetitive structures seems to reveal global principles to do with the network morphology. A sensitivity analysis of smooth and discrete, triangular, quadrilateral and hexagonal networks would give further insights.
- Using the curvature parameters to deduce the residual stress of strained structures has not only proven efficient for the structural analysis. This workflow can also be used for form finding and the simulation of deformation processes.
- Similarly, the investigation of compliant mechanisms within lamella grids holds great potential for future interdisciplinary research. We have already encountered a close overlap of mathematics and engineering in the behaviour of elastically-bent lamellas grids (***Schling et al. 2018***).
- Another interdisciplinary task is the optimization of surfaces for both geometric requirements (such as a minimal surface) and structural performance (like a funicular form), offering to create a new hybrid class of design shapes.

Construction Development

Apart from both geometric and structural domains, we aim to further develop the construction technique of strained lamella gridshells looking at the following aspects:

- Façade solution using planar quadrilateral panels, developable strips or membranes
- Investigation of materials and related construction details
- Constructive solutions and digital fabrication for permanent, large-span constructions

Abbreviations

The following abbreviations are used to shorten the sources of institutions and architecture offices.

AB	Archive Boston
AJN	Atelier Jean Nouvel
AWA	Auer + Weber Architects
FA	Fuksas Architects
FP	Foster + Partners Architects
GA	Grimshaw Architects
ICD	Institute for Computational Design and Construction
MBA	Mario Bellini Architects
MPA	J. Mayer H. and Partner Architects
MR	Moatti Rivière Architecture et Scénographie
NA	Nesbits Auctions
NP	Ney + Partners Architects
SBP	Schlaich Bergermann Partner
SE	Seele GmbH
WM	Wikimedia

Additionally, an abbreviation is used to label illustrations and photos by the author:

ES	Eike Schling

Bibliography

AB (2008): National Aquatics Center Beijing. Photo: Nh Han Guan. Archive Boston. Available online at http://archive.boston.com/bigpicture/2008/07/beijing_2008_preparations_thre.html, checked on 7/31/2018.

Agkathidis, Asterios (2009): Modulare Konstrukte. Analog wird digital. In Asterios Agkathidis (Ed.): Modulare Strukturen in Entwurf und Architektur. Dt. Aufl. Amsterdam: BIS Publishers, pp. 47–50.

AJN (2017): Louvre in Abu Dhabi. Ateliers Jean Nouvel. Available online at http://www.jeannouvel.com/en/projects/louvre-abou-dhabi-3/, checked on 6/4/2018.

Almegaard, H.; Bagger, A.; Gravesen, J.; Jüttler, B.; Šir, Z. (2007): Surfaces with Piecewise Linear Support Functions over Spherical Triangulations. In R. Martin, M. Sabin, J. Winkler (Eds.): Mathematics of Surfaces XII, vol. 4647: Springer (Lecture Notes in Computer Science), pp. 42–63.

AWA (2010): Botanical Garden Shanghai. Auer+Weber+Assoziierte. Available online at http://www.auer-weber.de/de/projekte/details/bauten-im-botanischen-garten-shanghai.html, checked on 6/4/2018.

Bach, Klaus; Kullmann, Ernst (1975): Netze in Natur und Technik. Nets in nature and technics. Stuttgart (IL, 8).

Barthel, Rainer (2005): Frei Otto - das Gesamtwerk. Leicht bauen, natürlich gestalten ; [anlässlich der Ausstellung „Frei Otto - Leicht Bauen, Natürlich Gestalten“ im Architekturmuseum der TU München in der Pinakothek der Moderne vom 26. Mai bis 28. August 2005]. Edited by Winfried Nerdinger. Basel, Boston, Berlin: Birkhäuser.

Barthel, Rainer (2015): Structural Design. Flächen- und Raumtragwerke. Lehrstuhl für Tragwerksplanung.

Beckh, Matthias (2012): Hyperbolische Stabwerke. Suchovs Gittertürme als Wegweiser in den modernen Leichtbau. 1. Aufl. München: Institut f. Intern. Architektur-Dokumentation (Edition Detail).

Beckh, Matthias; Barthel, Rainer (2009): The first doubly curved gridshell structure. Shukhov‘s building for the plate rolling workshop in Vyksa. In Karl-Eugen Kurrer, Werner Lorenz (Eds.): Proceedings of the Third International Congress on Construction History. Brandenburg University of Technology Cottbus, Germany, 20th - 24th May 2009. Berlin: NEUNPLUS 1, pp. 159–166. Available online at http://www.bma.arch.unige.it/pdf/construction_history_2009/vol1/beckh-matthias_layouted.pdf.

Block, Philippe (2009): Thrust Network Analysis. Exploring Three-dimensional Equilibrium. PhD Thesis.

Bo, Pengbo; Pottmann, Helmut; Kilian, Martin; Wang, Wenping; Wallner, Johannes (2011): Circular Arc Structures. In ACM Trans. Graphics 30, #101,1-11. DOI: 10.1145/1964921.1964996.

Brakke, Kenneth A. (1992): The Surface Evolver. In Experimental Mathematics 1 (2), pp. 141–165. DOI: 10.1080/10586458.1992.10504253.

Burkhardt, Berthold (Ed.) (1978): IL13 Multihalle Mannheim. Stuttgart: Krämer (Mitteilungen des Instituts für leichte Flächentragwerke (IL), Universität Stuttgart, 13).

Chebyshev, Pafnuty Lvovich (1878): Sur la coupe des vêtements, „On the cutting of garments“. In Association francaise pour l‘avancement des sciences, pp. 154–155.

Eigensatz, Michael; Kilian, Martin; Schiftner, Alexander; Mitra, Niloy J.; Pottmann, Helmut; Pauly, Mark (2010): Paneling Architectural Freeform Surfaces. In Tony DeRose, Hugues Hoppe (Eds.): ACM SIGGRAPH 2010 papers on - SIGGRAPH ,10. ACM SIGGRAPH 2010 papers. Los Angeles, California, 26.07.2010 - 30.07.2010. New York, New York, USA: ACM Press, p. 1.

Eigensatz, Michael; Schiftner, Alexander (2011): Paneling the Eiffel Tower Pavilions. In Intelligent Glass Solutions: Complex geometries and freeform building envelopes 4, pp. 41–48. Available online at https://www.glassonweb.com/article/paneling-eiffel-tower-pavilions.

Eversmann, Philipp; Ihde, André; Louter, Christian (2016a): Low Cost Double Curvature. Exploratory Computational Modelling, FE-analysis and Prototyping of Cold-Bent Glass. In Jan Belis, Freek Bos, Christian Louter (Eds.): Challenging Glass 5 Conference. Ghent: Ghent University, pp. 81–92. Available online at https://www.researchgate.net/publication/322316886_Low_cost_double_curvature-Exploratory_computational_modelling_FE-analysis_and_prototyping_of_cold-bent_glass.

Eversmann, Philipp; Schling, Eike; Ihde, André; Louter, Christian (2016b): Low Cost Double Curvature. Geometrical and Structural Potentials of Rectangular, Cold-bent Glass Construction. In K. Kawaguchi, M. Ohsaki, T. Takeuchi (Eds.): Proceedings of the IASS Annual Symposium 2016. Spatial Structures in the 21st Century. IASS Annual Symposium 2016. Tokyo: IASS.

FA (2005): New Milan Trade Fair. Fuksas Architects. Available online at http://www.fuksas.com/en/Projects/New-Milan-Trade-Fair-Milan, checked on 6/4/2018.

Faber, Colin (1965): Candela und seine Schalen. With assistance of Max Cetto. München: Callwey.

FP (2007): Smithsonian Institution, Kogod Courtyard in Washington DC. Photo: Chuck Choi Architectural Photography. Foster + Partners. Available online at https://www.fosterandpartners.com/projects/smithsonian-institution-courtyard/#gallery, checked on 7/5/2018.

Fu, Chi-Wing; Lai, Chi-Fu; He, Ying; Cohen-Or, Daniel (2010): K-set tilable surfaces. In ACM Trans. Graphics 29 (4), 44:1-44:6. DOI: 10.1145/1833351.1778781.

GA (2001): The Eden Project / The Biomes in Cornwall. Grimshaw Architects. Available online at https://grimshaw.global/projects/the-eden-project-the-biomes/, checked on 6/4/2018.

Garg, Akash; Sageman-Furnas, Andrew O.; Deng, Bailin; Yue, Yonghao; Grinspun, Eitan; Pauly, Mark; Wardetzky, Max (2014): Wire mesh design. In ACM Trans. Graph. 33 (4), pp. 1–12. DOI: 10.1145/2601097.2601106.

Hammerberg, Kris (2012): Evolute tools Primer. for Rhino. Available online at www.evolute.at.

Happold, Edmund; Liddell, W. Ian (1975): Timber lattice roof for the Mannheim Bundesgartenschau. In Structural Engineer 1975 (53/3), pp. 99–135.

Harbeke, Carl Heinz (Ed.) (1972): Bauten für Olympia 1972 [neunzehnhundertzweiundsiebzig]. München, Kiel, Augsburg = Buildings and facilities for the Olympic Games 1972 [nineteenhundred and seventy-two]. Behnisch & Partner. München: Harbeke.

Hauberg, Jørgen (2012): Research by Design - a research strategy. In Revista Lusófona de Arquitectura e Educação (5), pp. 46–56.

Hazzidakis, Ioannis N. (1879): Über einige Eigenschaften der Flächen mit constantem Krümmungsmass. In Journal für die reine und angewandte Mathematik (88), pp. 68–73.

Hennicke, Jürgen (Ed.) (1974): IL10 Gitterschalen. Sonderforschungsbereich Weitgespannte Flächentragwerke. Stuttgart: Krämer (Mitteilungen des Instituts für Leichte Flächentragwerke (IL), 10).

Howell, Larry L. (2002): Compliant mechanisms. New York: John Wiley & Sons.

Huard, Mathieu; Eigensatz, Michael; Bompas, Philippe (2015): Planar Panelization with Extreme Repetition. In Philippe Block, Jan Knippers, Niloy J. Mitra, Wenping Wang (Eds.): Advances in Architectural Geometry 2014. Cham: Springer International Publishing, pp. 259–279.

ICD (2010): ICD/ITKE Research Pavilion 2010. Institute for Computational Design and Construction. University Stuttgart. Available online at http://icd.uni-stuttgart.de/?p=4458, checked on 7/6/2018.

ICD (2014): Landesgartenschau Exhibition Hall. Institute for Computational Design and Construction. University Stuttgart. Available online at http://icd.uni-stuttgart.de/?p=11173, checked on 6/4/2018.

Januszkiewicz, Krystyna; Banachowicz, Marta (2016): Glass as A Component of Curvilinear Architecture in 21st Century. In Procedia Engineering 161, pp. 1490–1495. DOI: 10.1016/j.proeng.2016.08.615.

Jiang, Caigui; Tang, Chengcheng; Vaxman, Amir; Wonka, Peter; Pottmann, Helmut (2015): Polyhedral patterns. In ACM Trans. Graph. 34 (6), pp. 1–12. DOI: 10.1145/2816795.2818077.

Jiang, Caigui; Wang, Jun; Pottmann, Helmut; Wallner, Johannes; Bompas, Philippe (2013): Freeform Shading and Lighting Systems from Planar Quads. In Christoph Gengnagel, Axel Kilian, Julien Nembrini, Fabian Scheurer (Eds.): Rethinking Prototyping. Proceedings of the Design Modelling Symposium Berlin 2013. Berlin: epubli GmbH, pp. 335–346.

Jiang, Caigui; Wang, Jun; Wallner, Johannes; Pottmann, Helmut (2014): Freeform Honeycomb Structures. In Computer Graphics Forum 33 (5), pp. 185–194. DOI: 10.1111/cgf.12444.

Kassnel-Henneberg, Bruno (2010): Innovative Processes in the All-Glass Sector. In Herwig Barf (Ed.): Innovative Design + Construction: Manufacturing and Design Synergies in the Building Process (DETAIL Development): Detailextra Limited, pp. 75–78.

Kockelkorn, Anne (2008): Zur Kommunikation zwischen Zimmermeistern und CNC-Fräsen. Centre Pompidou Metz, Shigeru Ban. In ARCH+ (189), pp. 72–75. Available online at http://www.archplus.net/home/archiv/artikel/46,2905,1,0.html, checked on 4/16/2018.

Köhler-Hammer, Carmen (2013): ArboSkin. Durable and Recyclable Bioplastics Facade Mock-Up. ITKE. Available online at http://www.itke.uni-stuttgart.de/download.php?id=692, checked on 3/29/2018.

Krausse, Joachim (2011): Das Zeiss-Planetarium. Wissen in Bewegung. 80 Jahre Zeiss-Planetarium Jena. TU Berlin. Available online at https://www.zeitbildraum.tu-berlin.de/fileadmin/f30/Materialseite/Texte/Krausse_DasZeissPlanetariumWissenInBewegung.pdf, checked on 3/29/2018.

Krausse, Joachim; Lichtenstein, Claude (1999): Your private sky. R. Buckminster Fuller. The Art of Design Science. Baden: Lars Müller Publ.

Kurrer, Karl-Eugen (2013): Das Fachwerk erobert die dritte Dimension: 150 Jahre Schwedler-Kuppel. momentum magazin. Available online at https://momentum-magazin.de/de/150-jahre-schwedler-kuppel/, checked on 4/12/2018.

Kurrer, Karl-Eugen; Lorenz, Werner (Eds.) (2009): Proceedings of the Third International Congress on Construction History. Brandenburg University of Technology Cottbus, Germany, 20th - 24th May 2009. Brandenburgische Technische Universität Cottbus; International Congress on Construction History. Berlin: NEUNPLUS 1.

Lienhard, Julian (2014): Bending-active structures. Form-finding strategies using elastic deformation in static and kinetic systems and the structural potentials therein. Zugl.: Stuttgart, Univ., Diss., 2014. Stuttgart: ITKE (Forschungsberichte aus dem Institut für Tragkonstruktionen und Konstruktives Entwerfen, Universität Stuttgart, 36).

Linkwitz, Klaus; Veenendaal, Diederik (2014): Nonlinear Force Density Method. Constraints of Force and Geometry. In Sigrid Adriaenssens, Philippe Block, Diederik Veenendaal, Chris J. K. Williams (Eds.): Shell structures for architecture. Form finding and optimization. London: Routledge, pp. 142–155.

Lipson, Andrew (2002): Andrew Lipson‘s LEGO Page. Available online at http://www.andrewlipson.com/catalan, updated on 4/1/2005.

Liu, Yang; Pottmann, Helmut; Wallner, Johannes; Yang, Yong-Liang; Wang, Wenping (2006): Geometric modeling with conical meshes and developable surfaces. In ACM Trans. Graph. 25 (3), p. 681. DOI: 10.1145/1141911.1141941.

Lobaton, E. J.; Salamon, T. R. (2007): Computation of constant mean curvature surfaces: Application to the gas-liquid interface of a pressurized fluid on a superhydrophobic surface. In Journal of colloid and interface science 314 (1), pp. 184–198. DOI: 10.1016/j.jcis.2007.05.059.

Lobel, Alain (2005): Lobel Frames. Uniformity generating diversity. Available online at http://www.equilatere.net/, updated on 11/20/2005, checked on 11/24/2017.

Ludwig, Matthias; Cook, Peter (1998): Mobile Architektur. Geschichte und Entwicklung transportabler und modularer Bauten. Stuttgart: Dt. Verl.-anst.

Lumpe, Günter; Gensichen, Volker (2014): Evaluierung der linearen und nichtlinearen Stabstatik in Theorie und Software. Prüfbeispiele, Fehlerursachen, genaue Theorie. 1., Auflage. Berlin: Ernst (Bauingenieur-Praxis).

Mathewson, Casey C. M.; Gehry, Frank O. (2007): Frank O. Gehry. Selected works : 1969 to today. Richmond Hill, Ont.: Firefly Books.

MBA (2012): Department of Islamic Arts at the Louvre in Paris. Mario Bellini Architects. Available online at http://www.bellini.it/architecture/Louvre.html, checked on 6/4/2018.

Mengeringhausen, Max (1975): Komposition im Raum. Raumfachwerke aus Stäben und Knoten. Veröffentlichung des Strukturforschungszentrums e.V. Würzburg. Band 1. Wiesbaden: Bauverlag.

Mero (2011): Heydar Aliyev Cultural Center in Baku by Zaha Hadid Architects. MERO-TSK International GmbH & Co. KG. Available online at https://www.mero.de/index.php/en/construction-systems/references-en/36-space-structures/78-heydar-aliyev-merkezi-projekt-baku, checked on 11/16/2018.

Millard, Bill (2015): Bending Glass in the Parametric Age. Enclos. Photo: Waywuwei. Available online at http://www.enclos.com/site-info/news/bending-glass-in-the-parametric-age, checked on 5/7/2018.

MPA (2011): Metropol Parasol. Redevelopment of Plaza de la Encarnacion, Seville, Spain. J. MAYER H. und Partner, Architekten. Available online at http://www.jmayerh.de/19-0-Metropol-Parasol.html, checked on 7/5/2018.

MR (2014): Eiffel Tower Pavilions in Paris. Moatti Rivière Architecture et Scénographie. Available online at https://www.moatti-riviere.com/en/projects/equipment/tour-eiffel-paris, checked on 7/5/2018.

NA (2015): Tractricoid. An early clockwork puck phonograph, with lyre-shaped base and aluminium. Nesbits Auctions Ltd. Available online at https://www.the-saleroom.com/en-gb/auction-catalogues/nesbits-auctions-ltd/catalogue-id-srnes10017/lot-f28f14ff-25e2-46e6-84d8-a54d0096e1e9, checked on 6/4/2018.

Nerdinger, Winfried (2013): Wendepunkt/e im Bauen. Von der seriellen zur digitalen Architektur. Photo: Alexander Lorenzo. München: Institut für internationale Architektur-Dokumentation (Edition Detail).

NP (2011): Glass Roof Dutch Maritime Museum. Ney+Partners. Available online at http://www.ney.be/project/glass-roof-dutch-maritime-museum.html, checked on 6/4/2018.

Piker, Daniel (2013): Kangaroo. Form Finding with Computational Physics. In Archit Design 83 (2), pp. 136–137. DOI: 10.1002/ad.1569.

Pottmann, Helmut (2013): Architectural Geometry and Fabrication-Aware Design. In Nexus Netw J 15 (2), pp. 195–208. DOI: 10.1007/s00004-013-0149-5.

Pottmann, Helmut; Asperl, Andreas; Hofer, Michael; Kilian, Axel (2007a): Architectural geometry: Bentley Institute Press (Architectural geometry). Available online at https://books.google.de/books?id=bIceAQAAIAAJ.

Pottmann, Helmut; Eigensatz, Michael; Vaxman, Amir; Wallner, Johannes (2015): Architectural Geometry. In Computers and Graphics 47, pp. 145–164. DOI: 10.1016/j.cag.2014.11.002.

Pottmann, Helmut; Huang, Qixing; Deng, Bailin; Schiftner, Alexander; Kilian, Martin; Guibas, Leonidas; Wallner, Johannes (2010): Geodesic Patterns. In ACM Trans. Graphics 29 (3). Available online at http://www.geometrie.tugraz.at/wallner/geopattern.pdf.

Pottmann, Helmut; Liu, Yang; Wallner, Johannes; Bobenko, Alexander; Wang, Wenping (2007b): Geometry of multi-layer freeform structures for architecture. In Marc Levoy (Ed.): ACM SIGGRAPH 2007 papers on - SIGGRAPH ,07. ACM SIGGRAPH 2007 papers. San Diego, California, 05.08.2007 - 09.08.2007. New York, New York, USA: ACM Press, p. 65.

Pottmann, Helmut; Schiftner, Alexander; Bo, Pengbo; Schmiedhofer, Heinz; Wang, Wenping; Baldassini, Niccolo; Wallner, Johannes (2008): Freeform surfaces from single curved panels. In : ACM SIGGRAPH 2008. ACM SIGGRAPH 2008. Los Angeles, California, 11.08.2008 - 15.08.2008. New York, New York, USA: ACM Press, 76: 1-10. Available online at http://www.geometrie.tugraz.at/wallner/strip.pdf.

Pottmann, Helmut; Wallner, Johannes (2008): The focal geometry of circular and conical meshes. In Adv Comput Math 29 (3), pp. 249–268. DOI: 10.1007/s10444-007-9045-4.

Quinn, Gregory; Gengnagel, Christoph (2014): A review of elastic grid shells, their erection methods and the potential use of pneumatic formwork. In N.De Temmerman, C.A Brebbia (Eds.): MARAS 2014. Ostend, Belgium, 11-13 June 2014: WIT PressSouthampton, UK (WIT Transactions on The Built Environment), pp. 129–143.

Rutton, David (2010): Evolutionary Principles applied to Problem Solving. using Galapagos. Available online at https://www.grasshopper3d.com/profiles/blogs/evolutionary-principles, checked on 7/31/2018.

Rutton, David; Gregson, Sam (2016): Principal Curvatures.gh. VB-Script. for Grasshopper. Available online at http://www.grasshopper3d.com/forum/topics/principal-curvature-lines-on, checked on 4/3/2018.

Sauer, Robert (1970): Differenzengeometrie. Berlin, Heidelberg: Springer Berlin Heidelberg.

SBA (2010): Centre Pompidou-Metz. Shigeru Ban Architects. Available online at http://www.shigerubanarchitects.com/works/2010_centre-pompidou-metz/index.html, checked on 6/4/2018.

SBP (1990): Neckarsulm. Schlaich Bergermann Partner. Available online at https://www.sbp.de/projekt/freizeitbad-aquatoll-neckarsulm/, checked on 7/5/2018.

SBP (1996): House for Hippopotamus, Zoo Berlin. Schlaich Bergermann Partner. Available online at https://www.sbp.de/en/project/house-for-hippopotamus-zoo-berlin/, checked on 6/4/2018.

SBP (2009): Yas Hotel, Abu Dhabi, VAE. Schlaich Bergermann Partner. Available online at https://www.sbp.de/projekt/yas-hotel/, checked on 7/5/2018.

Schiftner, Alexander; Leduc, Nicolas; Bompas, Philippe; Baldassini, Niccolo; Eigensatz, Michael (2013): Architectural Geometry from Research to Practice. The Eiffel Tower Pavilions. In Lars Hesselgren, Shrikant Sharma, Johannes Wallner, Niccolo Baldassini, Philippe Bompas, Jacques Raynaud (Eds.): Advances in Architectural Geometry 2012. Vienna: Springer Vienna, pp. 213–228.

Schling, Eike; Barthel, Rainer (2017): Experimentelle Studien zur Konstruktion zweifach gekrümmter Gitterstrukturen. Experimental studies on the construction of doubly curved structures: Fachwissen. In Detail structure (01), pp. 52–56. Available online at ISSN (DETAIL): 0011-9571/B2772.

Schling, Eike; Barthel, Rainer; Tutsch, Joram (2014): Freie Form - experimentelle Tragstruktur. In Bautechnik 91 (12), pp. 859–868. DOI: 10.1002/bate.201400086.

Schling, Eike; Hitrec, Denis (2016): Asymptotic gridshell. Physical curvature line analysis. Exhibition. Zurich: Advances in Architectural Geometry (AAG), 9/9/2016.

Schling, Eike; Hitrec, Denis; Barthel, Rainer (2017a): Designing Grid Structures using Asymptotic Curve Networks. In Klaas de Rycke, Christoph Gengnagel, Olivier Baverel, Jane Burry, Caitlin Mueller, Minh Man Nguyen et al. (Eds.): Humanizing Digital Reality. Design Modelling Symposium Paris 2017. Singapore: Springer, pp. 125–140.

Schling, Eike; Hitrec, Denis; Schikore, Jonas; Barthel, Rainer (2017b): Design and Construction of the Asymptotic Pavilion. In K.-U. Bletzinger, Eugenio Oñate, B. Kröplin (Eds.): VIII International Conference on Textile Composites and Inflatable Structures. STRUCTURAL MEMBRANES 2017. Barcelona: International Center for Numerical Methods in Engineering (CIMNE), pp. 178–189. Available online at http://congress.cimne.com/membranes2017/frontal/Doc/Ebook2017.pdf.

Schling, Eike; Kilian, Martin; Wang, Hui; Schikore, Jonas; Pottmann, Helmut (2018): Design and Construction of Curved Support Structures with Repetitive Parameters. In Lars Hesselgren, Karl-Gunnar Olsson, Axel Kilian, Samar Malek, Olga Sorkine-Hornung, Chris Williams (Eds.): AAG 2018. Advances in Architectural Geometry. 1. Auflage. Wien: Klein Publishing, pp. 140–165.

Schmid, Volker; Fischer, Markus (2010): Metropol Parasol Sevilla - ein neues Wahrzeichen für den Ingenieurholzbau. 16. Internationales Holzbau-Forum. Available online at http://www.forum-holzbau.de/pdf_11/pdf_referate_1erepage_ihf2011.pdf, checked on 4/16/2018.

Schober, Hans (2002): Geometrie-Prinzipien für wirtschaftliche und effiziente Schalentragwerke (Teil 1). In Bautechnik 79 (1), pp. 16–24. DOI: 10.1002/bate.200200030.

Schober, Hans (2016): Transparent shells. Form, topology, structure. With assistance of Claudia Schaffert. Berlin: Ernst & Sohn. Available online at http://search.ebscohost.com/login.aspx?direct=true&scope=site&db=nlebk&AN=1133041.

SE (2006): Glass Shell of Strasbourg Railway Station. Seele. Available online at https://seele.com/references/strasbourg-railway-station/, checked on 7/5/2018.

Sechelmann, Stefan; Rörig, Thilo; I.Bobenko, Alexander (2013): Quasiisothermic Mesh Layout. In Lars Hesselgren, Shrikant Sharma, Johannes Wallner, Niccolo Baldassini, Philippe Bompas, Jacques Raynaud (Eds.): Advances in Architectural Geometry 2012. Vienna: Springer Vienna, pp. 243–258. Available online at http://sechel.de/publications/AAG2012Quasiisothermic.pdf, checked on 4/3/2018.

Shelden, Dennis (2002): Digital Surface Representation and the Constructability of Gehry`s Architecture. Phd Thesis. MIT, Cambridge, Massachusetts - USA. Department of Architecture.

Sijpkes, Pieter (2012): An overview of methods to build full-scale architectural complex (mostly double curved) surfaces and structures. McGill School of Architecture. Available online at http://www.arch.mcgill.ca/prof/sijpkes/Downloads/proposal-htmlonly.html, checked on 1/12/2018.

Singh, Mayank; Schaefer, Scott (2010): Triangle surfaces with discrete equivalence classes. In ACM Trans. Graphics 29 (4), p. 1. DOI: 10.1145/1778765.1778783.

Stephan, Sören; Sánchez-Alvarez, Jaime; Knebel, Klaus (2004): Stabwerke auf Freiformflächen. Herrn Dr.-Ing. Herbert Klimke zur Vollendung seines 65. Lebensjahres gewidmet. In Stahlbau (73, Heft 8), pp. 562–572.

Strozyk, Elisa (2011): Wooden-textiles. a material between wood and textile. Available online at https://www.elisastrozyk.com, checked on 12/8/2017.

Strubecker, Karl (1969): Theorie der Flächenkrümmung. 2., verb. Aufl. Berlin: de Gruyter (Sammlung Göschen, 1180/1180a).

Tang, Chengcheng; Kilian, Martin; Bo, Pengbo; Wallner, Johannes; Pottmann, Helmut (2016): Analysis and design of curved support structures. In Sigrid Adriaenssens, Fabio Gramazio, Matthias Kohler, Achim Menges, Mark Pauly (Eds.): Advances in Architectural Geometry 2016. 1. Auflage. Zürich: vdf Hochschulvlg, pp. 8–23. Available online at http://www.dmg.tuwien.ac.at/geom/ig/publications/2016/curvedsupport2016/curvedsupport.pdf.

Tessmann, Oliver (2009): Prozesse zur performativen Geometrie. In Asterios Agkathidis (Ed.): Modulare Strukturen in Entwurf und Architektur. Dt. Aufl. Amsterdam: BIS Publishers, pp. 51–54.

Tornack, Sven (2012): der moderne ingenieurbau der junkers-werke in dessau. zur stellung der metallarchitektur von hugo junkers und seiner werke in der architekturgeschichte. HTWK, Leipzig.

Troche, Christian (2008): Planar Hexagonal Meshes by Tangent Plane Intersection. In Helmut Pottmann, Axel Kilian, Michael Hofer (Eds.): Advances in Architectural Geometry 2008. Vienna, pp. 57–60.

Tutsch, Joram; Hipper, Andreas; Schling, Eike; Barthel, Rainer (2017): Modulare Stahllamellenhallen von Hugo Junkers. Wissenschaftliche Grundlagen für eine denkmalgerechte Instandsetzung. In Bautechnik 94 (3), pp. 161–169. DOI: 10.1002/bate.201600071.

van Ouwerkerk, Marieke (2001): Research by design. International conference, Faculty of Architecture, Delft University of Technology in co-operation with the EAAE/AEEA, November 1 - 3 2000. Delft: DUP.

Wang, J.; Jiang, C.; Bompas, P.; Wallner, J.; Pottmann, Helmut (2013): Discrete Line Congruences for Shading and Lighting. In Computer Graphics Forum 32 (5), pp. 53–62. DOI: 10.1111/cgf.12172.

Weber, Christine (2012): Fritz Leonhardt - ‚Leichtbau - eine Forderung unserer Zeit. Anregungen für den Hoch- und Brückenbau‘. [s.l.]: KIT Scientific Publishing.

Weisstein, Eric (2018a): Runge-Kutta Method. Available online at http://mathworld.wolfram.com/Runge-KuttaMethod.html, updated on 3/26/2018, checked on 3/30/2018.

Weisstein, Eric (2018b): Tractrix. Available online at http://mathworld.wolfram.com/Tractrix.html, updated on 3/26/2018, checked on 3/29/2018.

Wenzel, Fritz; Frese, Bernd; Barthel, Rainer (1987): Die Holzrippenschale in Bad Dürrheim. Entwurf und Konstruktion des Daches über dem Solebad. In Bauen mit Holz 89 (5), pp. 282–287.

Wilhelm, Karin; Otto, Frei (1985): Architekten heute. Portrait Frei Otto. Berlin: Quadriga Verlag J. Severin (Architekten heute, Bd. 2).

WM (1851): Crystal Palace Great Exhibition tree. Wikimedia. Available online at https://commons.wikimedia.org/wiki/File:Crystal_Palace_Great_Exhibition_tree_1851.png, checked on 6/5/2018.

WM (1897): Gridshell in Vyksa by Shukhov ,1897. Wikimedia. Available online at https://commons.wikimedia.org/wiki/File:Double_curvature_steel_lattice_Shell_by_Shukhov_in_Vyksa_1897_shell.jpg, checked on 6/5/2018.

WM (1958): Philips Pavilion, Le Corbusier. Photo: Wouter Hagens. Wikimedia. Available online at https://commons.wikimedia.org/wiki/Category:Philips_Pavilion_of_Expo_1958#/media/File:Expo58_building_Philips.jpg, checked on 8/1/2018.

WM (2004): C60-rods. Wikimedia. Available online at https://commons.wikimedia.org/wiki/File:C60-rods.png, checked on 6/5/2018.

WM (2006): Habitat 67 in Montreal, panorama. Wikimedia. Available online at https://commons.wikimedia.org/wiki/File:Habitat_panorama.jpg, checked on 6/5/2018.

WM (2010): Selfridges in Birmingham. Photo: Pascal Terjan. Wikimedia. Available online at https://commons.wikimedia.org/wiki/File:Selfridges_Birmingham_-_panoramio.jpg.

WM (2012): Walt Disney Concert Hall in Los Angeles. Photo: John O'Neill. Wikimedia. Available online at https://upload.wikimedia.org/wikipedia/commons/8/8c/Walt_Disney_Concert_Hall%2C_LA%2C_CA%2C_jjron_22.03.2012.jpg, checked on 11/16/2018.

WM (2013): Dôme Bourse du Commerce. Wikimedia. Available online at https://commons.wikimedia.org/wiki/File:D%C3%B4me_Bourse_du_Commerce.jpg, checked on 6/5/2018.

WM (2014): Galleria Vittorio Emanuele. Wikimedia. Available online at https://commons.wikimedia.org/wiki/File:Galleria_vittorio_emanuele_(14133651758).jpg, checked on 6/5/2018.

Wunderlich, Walter (1951): Zur Differenzengeometrie der Flächen konstanter negativer Krümmung. In Österreich. Akad. Wiss. Math.-Nat. Abt. IIa 1951 (160), pp. 39–77.

Zimmer, Henrik; Campen, Marcel; Bommes, David; Kobbelt, Leif (2012): Rationalization of Triangle-Based Point-Folding Structures. In Computer Graphics Forum 31 (2pt3), pp. 611–620. DOI: 10.1111/j.1467-8659.2012.03040.x.

Figures

Chapter 1

Chapter 2

Chapter 3

Chapter 4

Chapter 5

Study 5.1

Study 5.2

Study 5.3

Study 5.4

Study 5.5

Chapter 6

Tables

Chapter 3

Chapter 4

Chapter 5